Towards understanding and overcoming the antibiotic resistance conferred by acetyltransferases

by

Jacob L. Houghton

A dissertation submitted in partial fulfillment
of the requirements for the degree of
Doctor of Philosophy
(Medicinal Chemistry)
The University of Michigan
2012

Doctoral Committee:

Assistant Professor Sylvie Garneau-Tsodikova, Chair
Professor David P. Ballou
Professor David H. Sherman
Associate Professor Garry D. Dotson
Research Professor Hollis D. Showalter

2012

To my parents:

"The voice of parents is the voice of gods, for to their children they are heaven's lieutenants."
~William Shakespeare

Acknowledgments

First, I would like to express my sincere gratitude to Professor Sylvie Garneau-Tsodikova not only for guiding my Ph.D. studies but also for being a supportive and caring mentor over the past four years. It was an honor and a pleasure to work under her tutelage. Her tireless work ethic and positive attitude have been an inspiration and motivation in both the good times and the tough times, and these traits are something that I hope to emulate and carry with me throughout my career. Of course, the last four years of research would not have been possible without her monetary support and intellectual guidance for which I could not be more grateful. Professor Garneau-Tsodikova has provided me a blend of intellectual freedom, high expectations, and personal liberty that has molded me into the scientist and person that I am today. She has led by example and taught me what it takes to be a successful scientist and for all of these things, I am forever indebted to her. I could not have asked for a better mentor.

To my committee members- Professors David P. Ballou, Garry D. Dotson, David H. Sherman, and Hollis D. Showalter- I would like to express my utmost appreciation. Your guidance throughout the past four years has been invaluable. The direction you provided has greatly contributed to the success of my Ph.D. studies, and your letters of support were vital to my success in being awarded fellowships to support my research. I could not have asked for a better group of mentors.

The members of Garneau-Tsodikova group have been an invaluable support system, both intellectually and socially. The past four years would not been as productive or enjoyable without them, and it has been a great pleasure to get to know and work with all of them. In particular, I would like to thank Dr. Keith D. Green and Dr. Wenjing Chen, both of whom I have closely collaborated with during my time in the Garneau-Tsodikova laboratory. Thank you to the Garneau-Tsodikova laboratory technician, Dr. Olga E.

Zolova, for keeping us all organized and making our lives easier. To all of the current and past members, thank you for helping me prepare for talks, providing insight into my project, and making work an enjoyable and rewarding experience.

Without the support and collaboration of Dr. Tapan Biswas and Professor Oleg V. Tsodikov, my Ph.D. studies would not have been as fruitful. I appreciate and marvel at their work that provided crystal structures of both CAT and Eis- working with and learning from them was an exceptionally valuable experience. I would also like to express my gratitude to Professor Micha Fridman (Tel Aviv University, Israel), for allowing me to visit his group at Tel Aviv University and teaching me about the synthetic modification, purification, and characterization of aminoglycosides. Without the generosity of Professors Tomasz Cierpicki, Mi Hee Lim, and John J. Tesmer (University of Michigan), all of whom allowed me to use instrumentation in their laboratories, much of my thesis work would have been impossible. I thank Professors David H. Sherman and Philip C. Hanna (University of Michigan, USA) and Paul J. Hergenrother (University of Illinois at Urbana-Champaign, USA) for providing bacterial strains to test our compounds against. Additionally, I would like to thank Professors Timor Baasov (Technion, Israel Institute of Technology, Israel), John S. Blanchard (Albert Einstein College of Medicine, USA), and Juan L. Asensio (Instituto de Química Bio-orgánica General (CSIC), Spain) for their generous gift of the plasmids harboring genes encoding some of the enzymes I used in my research.

I would like to thank all of the great people at Esperion Therapeutics for allowing me to do an internship at their company. I learned a great deal about how small biotechnology companies function and I greatly enjoyed working with them on a daily basis.

Without funding sources, none of this research would have been possible. I would like to thank the Life Sciences Institute and the College of Pharmacy at the University of Michigan start-up fund (S.G.-T.), the United States-Israel Binational Science Foundation (BSF, grant 2008017 and Prof. Rahamimoff Travel Grant, S.G.-T. and M.F.), the Rackham Merit Fellowship (University of Michigan), an American Chemical Society

Division of Medicinal Chemistry Predoctoral Fellowship, an American Foundation of Pharmaceutical Education Predoctoral Fellowship, the Cellular Biotechnology Training Program (special thanks to Margaret Allen as well as Professors. Joel Swanson and Mary O'Riordan), and the National Institutes of Health (NIH) Grant AI090048 (S.G.-T.).

Thank you to all the faculty, staff, and students from the Interdepartmental Program in Medicinal Chemistry for giving me the wonderful opportunity to pursue my doctoral studies at University of Michigan. You provided an intellectually stimulating and rewarding environment, and I am grateful for your mentorship, friendship, and support throughout my time at the University of Michigan.

The transition to Ann Arbor was made much easier thanks to the love and support of my friends- thank you all. In particular I would like to thank Zack Wollack for his unconditional friendship and the Wollack family for being a pillar of support, especially when I could not be with my family during the holidays. Also, I owe a great debt to Dave Campbell for being a great friend over the years and for introducing me to the love of my life. To Katie Decker, my best friend and future wife, you are the best thing to ever come into my life. Through many tough times you stuck with me and I cannot express how much your love and companionship has meant to me over the past five years. You have given me the strength, courage, and love I needed to persevere through the toughest of times- I will be forever grateful.

Finally, I would like to thank my family- this thesis is dedicated to each and everyone one of you who supported me since the day I was born. I would like to thank my grandparents, Robert and Lucille Tvedt, for their unceasing prayers, support, and love, without which I would not be where I am today. Also, my love and gratitude goes out to my grandmother, Constance Houghton, whom I love and miss very much. To my parents, Ronald Houghton and Elizabeth Kahlon, I would like to say that I love you both very much. You taught me the true meaning of love, patience, diligence, and goodness- you have shaped me into the man I am today. Without your love, support, and sacrifice none of this would have been possible. Finally, to my brothers and sisters: Lauren, Jonah,

Hannah, and Josiah, I want to thank you for being a constant source of joy in my life. I hope that someday I inspire you half as much as you have inspired me. I love you all very much.

Preface

This dissertation is comprised of six chapters that describe my Ph.D. studies aimed at understanding and overcoming the antibiotic resistance conferred by acetyltransferases. Chapter one focuses on properties of aminoglycosides (AGs) as antibacterials, the challenges facing their use and development, as well as background on the other antibiotics discussed in this thesis; this chapter was adapted in-part from a review article (**Houghton, J. L.**; Green, K. D.; Chen, W.; Garneau-Tsodikova, S. *ChemBioChem* **2010**, *11*, 880). Chapter two describes the characterization of Eis from *Mycobacterium tuberculosis* (*Mtb*) including NMR and TLC studies of the order and positions modified on various AGs (**Houghton, J. L.**; Chen, W.; Garneau-Tsodikova, S.). Chapter three reports the acetylation of capreomycin (CAP), a cyclic peptide antibiotic used as second-line treatment for tuberculosis (TB), by Eis (**Houghton, J. L.**; Green, K. D.; Mayhoub, A. S.; Garneau-Tsodikova, S.). Chapter four focuses on the synthesis and testing of novel AGs aimed at overcoming antibacterial resistance (**Houghton, J. L.**; Green, K. D.; Garneau-Tsodikova, S.). In chapter five, crystal structures of chloramphenicol acetyltransferase I (CAT_I) in the unbound (apo) form and a chloramphenicol (CAM)-bound complex are reported and compared to CAT_I-fusidic acid (FA) and CAT_{III}-CAM structures to provide insight into the broader substrate preference of CAT_I (Biswas, T.; **Houghton, J. L.**; Tsodikov, O. V.; Garneau-Tsodikova, S. *Protein Science* **2012**, *4*, 520.) Chapter six discusses future directions of the projects, with a focus on further synthesis of novel AGs to combat resistance and progression of methodology to study the kinetics of acetylation by Eis by NMR spectroscopy.

Table of Contents

Dedication ..... **ii**
Acknowledgments ..... **iii**
Preface ..... **vii**
List of Figures ..... **xiii**
List of Tables ..... **xx**
List of Abbreviations ..... **xxii**
Abstract ..... **xxvii**
Chapter
1. Introduction: aminoglycosides (AGs), chloramphenicol (CAM), tuberculosis (TB), and bacterial resistance
1.1. Introduction to AGs 1
1.1.1. AGs 1
1.1.2. AGs' antibacterial modes of action 3
1.1.3. Problems associated with AGs 4
1.1.3.1. Toxicity 4
1.1.3.2. Resistance 4
1.1.3.2.1. Covalent modification of AGs 6
1.1.3.2.2. AG acetyltransferases (AACs) 7
1.1.4. Strategies for developing novel AGs 8
1.1.4.1. Development of novel AGs *via* chemical synthesis 8
1.1.4.2. Development of novel AGs *via* chemoenzymatic methods 11
1.2. Tuberculosis (TB) 13
1.2.1. Anti-TB drugs 13
1.2.2. TB resistance and enhanced intracellular survival (Eis) protein 14
1.2.2.1. Resistance to anti-TB drugs 14

1.2.2.2. Eis 15

1.3. Chloramphenicol (CAM) and CAM acetyltransferase (CAT) 16
1.3.1. CAM as an antibacterial agent 16
1.3.2. Resistance to CAM 17
1.3.2.1. Resistance conferred by CATs 18
1.4. References 19

2. Characterization of regio-promiscuity and regio-versatility of Eis *via* NMR and X-ray crystallography

2.1. Abstract 26
2.2. Introduction 26
2.3. Results: determination of positions of AGs modified by Eis *via* NMR and TLC 28
2.4. Discussion 35
2.5. Conclusions 36
2.6. Materials and instrumentation 37
2.7. Methods 38
2.7.1. Determination of amine positions acetylated by Eis on AMK, KAN, NET, SIS, and TOB 38
2.7.1.1. TLC assays 38
2.7.1.1.1. Control TLCs of AGs mono-acetylated at the 2'-, 3-, and 6'-position by AAC(2')-Ic, AAC(3)-IV, and AAC(6'), respectively 39
2.7.1.1.2. Control TLCs of AGs di-acetylated sequentially by pairwise treatment with AAC(2')-Ic, AAC(3)-IV, and AAC(6') 39

2.7.1.1.3. TLCs of the time course of multi-acetylation of KAN, AMK, NET, SIS, and TOB by Eis 39
2.7.1.2. Mass spectrometry analysis of the multi-acetylated AMK, KAN, NET, SIS, and TOB Eis products 40
2.7.1.3. NMR analysis of the multi-acetylated AMK, KAN, NET, SIS, and TOB Eis products 41
2.7.1.3.1. Di-acetylation of AMK by Eis and NMR analysis of the 3",AHB-di-acetyl-AMK product 41
2.7.1.3.2. Di-acetylation of KAN by Eis and NMR analysis of the 3",6'-di-acetyl-KAN product 49
2.7.1.3.3. Di-acetylation of NET by Eis and NMR analysis of the 2',6'-di-acetyl-NET product 57
2.7.1.3.4. Dual di-acetylation of SIS by Eis and NMR analysis of the 2',6'- and 1/3,6'-di-acetyl-SIS products 65
2.7.1.3.5. Di-acetylation of TOB by Eis and NMR analysis of the 3",6'-di-acetyl-TOB product 78
2.8. References 84

3. Unexpected modification of capreomycin by the *mycobacterial* enzyme Eis

3.1. Abstract 85
3.2. Introduction 85
3.3. Results and discussion 87
3.3.1. Exploration of anti-TB drugs as potential substrates of Eis 87
3.3.2. Regio-specificity of CAP acetylation by Eis_*Mtb* 89
3.3.3. MIC values for CAP against various *mycobacteria* 90
3.4. Conclusions 91
3.5. Materials and methods 92
3.5.1. Materials and instrumentation 92
3.5.2. Determination of Eis_*Mtb* and Eis_*Msm* acetylation activity with anti-TB drugs by UV-Vis assays 92

3.5.3. TLC and LCMS assays showing the conversion of CAP into mono-acetyl-CAP (AcCAP) products 93
3.5.4. Molecular modeling of CAP IB with Eis_*Mtb* 93
3.5.5. Acetylation of CAP by Eis_*Mtb* analyzed by NMR: analysis of the 6'-*N*-acetyl-CAP (AcCAP) products and comparison to the parent compounds 94
3.5.6. Determination of the MIC values for CAP against various *mycobacteria* 101
3.6. References 101

4. Towards the development of novel aminoglycosides *via* chemical modification of known aminoglycosides

4.1. Abstract 103
4.2. Introduction 103
4.3. Results and discussion 105
4.4. Conclusions 112
4.5. Materials and instrumentations 112
4.6. Methods 113
4.6.1. Chemistry 113
4.6.1.1. Preparation of coupling reagents 113
4.6.1.2. General procedure for preparation of *N*-azidoacetyl compounds 114
4.6.1.3. General procedure for preparation of *N*-γ-benzyloxycarbonylamino-α-hydroxybutyric acid (*N*-(CbzAHB)) compounds 116
4.6.1.4. General procedure for hydrogenation reactions 117
4.6.1.5. General procedure for Staudinger reactions 120
4.6.1.6. General procedure for Cbz coupling reactions 121

4.6.2. Mass spectrometry analysis of the acylated AMK, KAN, NET, SIS, and TOB synthetic products 122

4.6.3. Determination of the MIC values against various bacteria 123
4.7. References 124
4.8. Appendix 126

5. The structural basis for substrate versatility of chloramphenicol acetyltransferase CAT_I

5.1. Abstract 133
5.2. Introduction 133
5.3. Results 137
5.3.1. Overall structure of CAT_I 137
5.3.2. Chloramphenicol (CAM) interactions in the active site 140
5.3.3. Fusidic acid (FA) interactions in the active site 142
5.4. Discussion 145
5.5. Materials and methods 147
5.5.1. Expression and purification of CAT_I 147
5.5.2. Crystallization of CAT_I alone and in complex with CAM 148
5.5.3. Date collection and structure determination 148
5.6. References 149

6. Future directions 151

List of Figures

Chapter 1

1.1. The chemical structures of common AGs 2
1.2. The structures of **A.** TOB, **B.** GTC, and **C.** AMK bound to 16S oligonucleotides mimicking the bacterial decoding A-site. Also shown is **D.** the crystal structure of PAR docked into a bacterial A-site oligonucleotide 3
1.3. Illustration of the various mechanisms of AG resistance 5
1.4. Three AMEs and their modified KAN products 6
1.5. The positions of kanamycin B that are acetylated by each of the known AAC enzymes 7
1.6. Synthesis of APR starting from NEA 9
1.7. Synthesis of 6'-*N*-glycinyl-TOB in two steps from TOB 10
1.8. A chemoenzymatic approach to the generation of mono-*N*-acylated AGs as well as homo- and hetero-di-*N*-acylated AGs *via* two sequential acylations by AACs utilizing acyl-CoA as cosubstrates 11
1.9. Commonly used first-line and second-line anti-TB drugs 14
1.10. Illustrations of the X-ray crystal structure of Eis from *Mtb* depicted in **A.** hexameric form and **B.** monomeric form with CoA bound in one monomer (PDB: 3R1K) 16
1.11. Structure of CAM 16
1.12. Modifications causing resistance to CAM by **A.** CAT, **B.** a nitroreductase, and **C.** CPT 18

Chapter 2

2.1. The di-acetylation of KAN by Eis 30
2.2. The di-acetylation of AMK by Eis 31
2.3. The di-acetylation of NET by Eis 32
2.4. The multiple di-acetylations of SIS by Eis 34

2.5. The di-acetylation of TOB by Eis 35
2.6. Mass spectra of Eis-AG reaction products studied in this work 40
2.7. ^{1}H NMR of AMK in D_2O at pH 3 (400 MHz). The full spectrum is shown in panel **A** and the expansions in panels **B-E** 43
2.8. gCOSY of AMK in D_2O at pH 3 (400 MHz) 44
2.9. zTOCSY of AMK in D_2O at pH 3 (400 MHz) 44
2.10. ^{1}H NMR of 3",AHB-di-acetyl-AMK in D_2O at pH 3 (400 MHz). The full spectrum is shown in panel **A** and the expansions in panels **B-E** 45
2.11. gCOSY of 3",AHB-di-acetyl-AMK in D_2O at pH 3 (400 MHz). The inserts show portions of the spectrum more clearly 45
2.12. ^{1}H NMR of 3",AHB-di-acetyl-AMK in 9:1/H_2O:D_2O (600 MHz). The full spectrum is shown in panel **A** and the expansions in panels **B-F** 47
2.13. zTOCSY of 3",AHB-di-acetyl-AMK in 9:1/H_2O:D_2O (600 MHz). The full spectrum is shown in panel **A** and the expansion showing the amide protons coupling to the protons at the 1-, 3"-, and AHB-positions in panel **B.** A red box in panel **A** indicates the portion of the spectrum expanded and shown in panel **B**. In panel **B**, the coupling of the amide protons at the 1-, 3"-, and A3 of the AHB-positions are indicated by turquoise, green, and blue boxes, respectively 48
2.14. ^{1}H NMR of KAN in D_2O at pH 3 (400 MHz). The full spectrum is shown in panel **A** and the expansions in panels **B-D** 51
2.15. gCOSY of KAN in D_2O at pH 3 (400 MHz). The insert shows a portion of the spectrum more clearly 52
2.16. ^{13}C NMR of KAN in D_2O at pH 3 (100 MHz). The full spectrum is shown in panel **A** and the expansions in panels **B-D** 52
2.17. gHSQC of KAN in D_2O at pH 3 (400 MHz). The insert shows a portion of the spectrum more clearly 53
2.18. gHMBC of KAN in D_2O at pH 3 (100 MHz) 53
2.19. ^{1}H NMR of 3",6'-di-acetyl-KAN in D_2O at pH 3 (400 MHz). The full spectrum is shown in panel **A** and the expansions in panels **B-E** 54

2.20. gCOSY of 3",6'-di-acetyl-KAN in D_2O at pH 3 (400 MHz). The insert shows the amide protons coupling to the protons at the 3"- and 6'-positions 55
2.21. ^{13}C NMR of 3",6'-di-acetyl-KAN in D_2O at pH 3 (100 MHz). The full spectrum is shown in panel **A** and the expansions in panels **B-D** 55
2.22. gHSQC of 3",6'-di-acetyl-KAN in D_2O at pH 3 (400 MHz)..... 56
2.23. gHMBC of 3",6'-di-acetyl-KAN in D_2O at pH 3 (100 MHz). The insert shows the carbonyl carbons coupling to the protons at the 3"- and 6'-positions..... 56
2.24. ^{1}H NMR of NET (9:1/H_2O:D_2O, pH 8, 25 mM KH_2PO_4) (400 MHz). The full spectrum is shown in panel **A** and the expansions in panels **B-E** 59
2.25. gCOSY of NET (9:1/H_2O:D_2O, pH 8, 25 mM KH_2PO_4) (400 MHz) 60
2.26. zTOCSY of NET (9:1/H_2O:D_2O, pH 8, 25 mM KH_2PO_4) (400 MHz)..... 60
2.27. ^{1}H NMR of 6'-acetyl-NET Eis reaction mixture (9:1/H_2O:D_2O, pH 8, 25 mM KH_2PO_4) (400 MHz). The full spectrum is shown in panel **A** and the expansions in panels **B-E** 61
2.28. gCOSY of 6'-acetyl-NET Eis reaction mixture (9:1/H_2O:D_2O, pH 8, 25 mM KH_2PO_4) (400 MHz). The insert shows the amide protons coupling to the protons at the 6'-position 62
2.29. zTOCSY of 6'-acetyl-NET Eis reaction mixture (9:1/H_2O:D_2O, pH 8, 25 mM KH_2PO_4) (400 MHz) 62
2.30. ^{1}H NzMR of 2',6'-di-acetyl-NET Eis reaction mixture (9:1/H_2O:D_2O, pH 8, 25 mM KH_2PO_4) (400 MHz). The full spectrum is shown in panel **A** and the expansions in panels **B-E** 63
2.31. gCOSY of 2',6'-di-acetyl-NET Eis reaction mixture (9:1/H_2O:D_2O, pH 8, 20 mM KH_2PO_4) (400 MHz). The insert shows the amide protons coupling to the protons at the 6'- and 2'-positions 64
2.32. zTOCSY of 2',6'-di-acetyl-NET Eis reaction mixture (9:1/H_2O:D_2O, pH 8, 25 mM KH_2PO_4) (400 MHz) 64
2.33. ^{1}H NMR of SIS (9:1/H_2O:D_2O, pH 8, 25 mM KH_2PO_4) (400 MHz). The full spectrum is shown in panel **A** and the expansions in panels **B-D** 68
2.34. gCOSY of SIS (9:1/H_2O:D_2O, pH 8, 25 mM KH_2PO_4) (400 MHz) 69
2.35. zTOCSY of SIS (9:1/H_2O:D_2O, pH 8, 25 mM KH_2PO_4) (400 MHz)..... 69

2.36. ^{1}H NMR of SIS (9:1/H_2O:D_2O, pH 3) (400 MHz). The full spectrum is shown in panel **A** and the expansions in panels **B-D** 70
2.37. gCOSY of SIS (9:1/H_2O:D_2O, pH 3) (400 MHz) 71
2.38. zTOCSY of SIS (9:1/H_2O:D_2O, pH 3) (400 MHz) 71
2.39. ^{1}H NMR of 6'-acetyl-SIS Eis reaction mixture (9:1/H_2O:D_2O, pH 8, 25 mM KH_2PO_4) (400 MHz). The full spectrum is shown in panel **A** and the expansions in panels **B-D** 72
2.40. gCOSY of 6'-acetyl-SIS Eis reaction mixture (9:1/H_2O:D_2O, pH 8, 25 mM KH_2PO_4) (400 MHz) 73
2.41. zTOCSY of 6'-acetyl-SIS Eis reaction mixture (9:1/H_2O:D_2O, pH 8, 25 mM KH_2PO_4) (400 MHz) 73
2.42. ^{1}H NMR of a mixture of two di-acetylated SIS products (9:1/H_2O:D_2O, pH 3) (400 MHz). The full spectrum is shown in panel **A** and the expansions in panels **B-D** ... 74
2.43. gCOSY of a mixture of two di-acetylated SIS products (9:1/H_2O:D_2O, pH 3) (400 MHz) 75
2.44. zTOCSY of a mixture of two di-acetylated SIS products (9:1/H_2O:D_2O, pH 3) (400 MHz) 75
2.45. ^{1}H NMR of a mixture of two di-acetylated SIS products (9:1/H_2O:D_2O, pH 8) (400 MHz). The full spectrum is shown in panel **A** and the expansions in panels **B-D** ... 76
2.46. gCOSY of a mixture of two di-acetylated SIS products (9:1/H_2O:D_2O, pH 8) (400 MHz) 77
2.47. zTOCSY of a mixture of two di-acetylated SIS products (9:1/H_2O:D_2O, pH 8) (400 MHz) 80
2.48. ^{1}H NMR of TOB (9:1/H_2O:D_2O, pH 8, 25 mM KH_2PO_4) (500 MHz). The full spectrum is shown in panel **A** and the expansions in panels **B-D** 80
2.49. gCOSY of TOB (9:1/H_2O:D_2O, pH 8, 25 mM KH_2PO_4) (500 MHz) 81
2.50. zTOCSY of TOB (9:1/H_2O:D_2O, pH 8, 25 mM KH_2PO_4) (500 MHz) 81
2.51. ^{1}H NMR of 3'',6'-di-acetyl-TOB Eis reaction mixture (9:1/H_2O:D_2O, pH 8, 25 mM KH_2PO_4) (500 MHz). The full spectrum is shown in panel **A** and the expansions in panels **B-E** 82

2.52. gCOSY of 3",6'-di-acetyl-TOB Eis reaction mixture (9:1/H_2O:D_2O, pH 8, 25 mM KH_2PO_4) (500 MHz) 83
2.53. zTOCSY of 3",6'-di-acetyl-TOB Eis reaction mixture (9:1/H_2O:D_2O, pH 8, 25 mM KH_2PO_4) (500 MHz) 83

Chapter 3

3.1. Structures of anti-TB drugs tested against Eis proteins in this study. CAP = capreomycin; STR = streptomycin; INH = isoniazid; PZA = pyrazinamide; CIP = ciprofloxacin. 87
3.2. Confirmation of mono-acetylation of CAP by Eis from *Mtb* and *Msm.* **A.** Scheme showing the acetylation of CAP by Eis from *Mtb,* **B.** TLC showing the mono-acetylation of CAP. **C.** UV-Vis assay confirming the mono-acetylation of CAP by Eis from *Mtb* and *Msm*. **D.** Confirmation of mono-acetylation by LCMS. **E.** Michaelis-Menten kinetics of the acetylation of CAP by Eis from *Mtb*..... 88
3.3. Docking of CAP in the binding pocket of Eis from *Mtb* showing **A.** CAP and AcCoA bound to Eis from *Mtb* and **B.** the potential for acetylation at either amine of the β-lysine side-chain 90
3.4. ^{1}H of CAP in 9:1/H_2O:D_2O (500 MHz). The full spectrum is shown in panel **A** and the expansions in panels **B-D**..... 95
3.5. gCOSY of CAP in 9:1/H_2O:D_2O (500 MHz)..... 96
3.6. zTOCSY of CAP in 9:1/H_2O:D_2O (500 MHz)..... 96
3.7. gHSQC of CAP in 9:1/H_2O:D_2O (500 MHz)..... 97
3.8. ^{1}H of 6'-*N*-acetyl CAP in 9:1/H_2O:D_2O (500 MHz). The full spectrum is shown in panel **A** and the expansions in panels **B-D** 98
3.9. gCOSY 6'-*N*-acetyl CAP in 9:1/H_2O:D_2O (500 MHz)..... 99
3.10. zTOCSY of 6'-*N*-acetyl CAP in 9:1/H_2O:D_2O (500 MHz) 99
3.11. gHSQC of 6'-*N*-acetyl CAP in 9:1/H_2O:D_2O (500 MHz) 100

Chapter 4

4.1. The structures of AGs that were synthetically modified to generate novel AGs in this study 104

4.2. Synthesis of coupling reagents (**1-3**) used in this study 105

4.3. **A.** Representative synthetic scheme illustrating the preparation of the 6'-*N*-azidoacetyl compounds (**4-8**). **B.** Representative synthetic scheme illustrating the conversion of 6'-*N*-azidoacetyl compounds **4-6** to the respective 6'-*N*-glycinyl compounds **9-11** by catalytic hydrogenation. **C.** Representative synthetic scheme illustrating the conversion of 6'-*N*-azidoacetyl compounds **7** and **8** to the respective 6'-*N*-glycinyl compounds **12** and **13** by Staudinger reaction 106

4.4. **A.** Representative synthetic scheme illustrating the preparation of the 6'- and di-*N*-(CbzAHB) compounds (**14-16**) from TOB or KAN. **B.** Representative synthetic scheme illustrating the conversion of 6'- and di-*N*-(CbzAHB) compounds **14-16** to the respective 6'- and di-*N*-(CbzAHB) compounds **17-19** by catalytic hydrogenation 110

4.5. Representative synthetic scheme illustrating the preparation of the *N*-Cbz compounds (**20-22**) 111

4.6. ^{1}H of *O*-(CbzAHB)-*N*-hydroxysuccinimide (**2**) in $CDCl_3$ (400 MHz) 126

4.7. ^{1}H of *O*-Cbz-*N*-hydroxyphthalimide (**3**) in $CDCl_3$ (400 MHz) 127

4.8. ^{1}H of 6'-*N*-glycinyl-TOB (**9**) in 9:1/H_2O:D_2O (400 MHz) 127

4.9. ^{1}H of 6'-*N*-glycinyl-KAN (**10**) in 9:1/H_2O:D_2O (500 MHz) 127

4.10. ^{1}H of 6',AHB-di-*N*-glycinyl-AMK (**11**) in 9:1/H_2O:D_2O (500 MHz) 128

4.11. ^{1}H of 6'-*N*-glycinyl-SIS (**12**) in 9:1/H_2O:D_2O (400 MHz) 128

4.12. ^{1}H of 6'-*N*-glycinyl-NET (**13**) in 9:1/H_2O:D_2O (400 MHz) 129

4.13. ^{1}H of 6'-*N*-AHB-TOB (**17**) in 9:1/H_2O:D_2O (500 MHz) 129

4.14. ^{1}H of 6'-*N*-AHB-KAN (**18**) in 9:1/H_2O:D_2O (500 MHz) 130

4.15. ^{1}H of 6',1-di-*N*-AHB-KAN (**19**) in 9:1/H_2O:D_2O (500 MHz) 130

4.16. ^{1}H of 6'-*N*-Cbz-TOB (**20**) in 9:1/H_2O:D_2O (500 MHz) 131

4.17. ^{1}H of 6'-*N*-Cbz-KAN (**21**) in 9:1/H_2O:D_2O (500 MHz) 131

4.18. ^{1}H of 6'-*N*-Cbz-AMK (**22**) in 9:1/H_2O:D_2O (500 MHz) 132

Chapter 5

5.1. Chemical structures of **A.** CAM and FA. **B.** Acetylation of CAM by CATs..... 134

5.2. Sequence alignment of CAT_I, CAT_{II}, and CAT_{III} enzymes from various bacteria (EC = *Escherichia coli*, YP = *Yersinia pestis*, KP = *Klebsiella pneumoniae*, SM = *Serratia marcescens*, SF = *Shigella flexneri*, PM = *Proteus mirabilis*, HI = *Haemophilus influenzae*, SE = *Salmonella enterica*, VS = *Vibrio sp.*, BC = *Bacillus cereus*, BA = *Bacillus anthracis*, SP = *Streptococcus pneumoniae*, EF = *Enterococcus faecium*, LM = *Listeria monocytogenes*, SA = *Staphylococcus aureus*, CD = *Clostridium difficile*, CB = *Clostridium botulinum*, and CT = *Clostridium tetani*). Important residues in the active site that are either conserved or non-conserved (vary) between CAT_I and CAT_{III} are indicated by red and blue circles, respectively. Residues involved in CAM and FA binding are marked by orange and yellow circles, respectively. 136

5.3. **A.** Overall fold and trimeric organization of CAM-bound form. The strands of the β-sheets comprising the central scaffold are marked. The CAM molecule and its molecular surface are shown in blue. **B.** A close-up view of the active site at the interface of two monomers in CAT_I-CAM structure. Substrate binding residues of the binding monomer and catalytic monomer are colored in green and orange, respectively. A few highly conserved residues involved in catalysis are marked in red. **C.** A representative view of one of the CAT_I active sites. The violet mesh clearly defining the CAM molecule (blue sticks) is Fo-Fc omit electron density generated without the CAM in the model and contoured at 3σ. **D.** A zoomed in view of the active site shown in panel **C**, depicted in a slightly different orientation. **E.** A schematic view of residues of the CAT_I active site and their interactions with CAM. Hydrogen bonds and hydrophobic contacts are marked by black dashed lines and the grey hashed lines, respectively. The color coding is consistent with that of panel **B** 140

5.4. **A.** Close-up views of interactions of FA with active-site residues of CAT_I. and **B.** Close-up views of interactions of FA with active-site residues of CAT_{III} (quadruple mutant). **C.** Schematic views of interactions of FA with CAT_I. **D.** Schematic views of interactions of FA with CAT_{III} (quadruple mutant)..... 145

List of Tables

Chapter 2

2.1. R_f values of mono- and di-, acetylated AGs by the AAC(2')-Ic, AAC(3)-IV, AAC(6'), and Eis proteins 28
2.2. Mass analysis of AGs acetylated by Eis 40
2.3. Proton chemical shifts determined for AMK and 3",AHB-di-acetyl-AMK 42
2.4. Proton chemical shifts determined for KAN and 3",6'-di-acetyl-KAN 50
2.5. Carbon chemical shifts determined for KAN and 3",6'-di-acetyl-KAN 50
2.6. Proton chemical shifts determined for NET and 6'-acetyl-NET 58
2.7. Proton chemical shifts determined for NET and 2',6'-di-acetyl-NET 58
2.8. Proton chemical shifts determined for SIS and 6'-acetyl-SIS 66
2.9. Proton chemical shifts determined for SIS and 6',2'-di-acetyl-SIS as well as 6',3 or 1-di-acetyl-SIS 67
2.10. Proton chemical shifts determined for TOB and 3",6'-di-acetyl-TOB 79

Chapter 3

3.1. MIC (μg/mL) values for CAP against *mycobacteria* 91
3.2. Proton chemical shifts determined for CAP IA and 6'-*N*-acetyl-CAP IA (AcCAP IA) 100
3.3. Proton chemical shifts determined for CAP IB and 6'-*N*-acetyl-CAP IB (AcCAP IB). 101

Chapter 4

4.1. Antibacterial activity of AGs against Gram-negative bacteria: MIC values (μg/mL) determined by double dilution. 108

4.2. Antibacterial activity of AGs against Gram-positive bacteria: MIC values (μg/mL) determined by double dilution 109
4.3. Antibacterial activity of AGs against various *mycobacteria*: MIC values (μg/mL) determined by double dilution 109

Chapter 5

5.1. X-ray diffraction data collection and refinement statistics for apo-CAT_I and CAT_I-CAM structures 138

List of Abbreviations

AG	Aminoglycoside
AAC	Aminoglycoside *N*-acetyltransferase
ABK	Arbekacin
Ac	Acetyl
AcCoA	Acetyl coenzyme A
ADP	5'-Adenosine diphosphate
AHB	1-*N*-(S)-α-hydroxy-γ-amino-*n*-butyryl
AIDS	Acquired immune deficiency syndrome
AME	Aminoglycoside-modifying enzyme
AMK	Amikacin
ANT	Aminoglycoside nucleotidyltransferase
APH	Aminoglycoside phosphotransferase
APR	Apramycin
AST	Astromicin
ATP	Adenosine triphosphate
BUTA	Butirosin A
BUTB	Butirosin B
CAM	Chloramphenicol

CAN	Cerium ammonium nitrate
CAP	Capreomycin
CAT	Chloramphenicol acetyltransferase
Cbz	Chlorobenzyloxycarbonyl
CIP	Ciprofloxacin
CoA	Coenzyme A
CPT	Chloramphenicol *O*-phosphotransferase
Cys or C	Cysteine
D	Dimension
DBK	Dibekacin
DCC	Dicyclohexylcarbodiimide
DEPT	Distortionless enhancement by polarization transfer
DNA	Deoxyribonucleic acid
DOS	Deoxystreptamine
DTNB	5,5'-dithiobis-(2-nitrobenzoic acid)
E. coli	*Escherichia coli*
EDTA	Ethylenediaminetetraacetic acid
Eis	Enhanced intracellular survival
EMB	Ethambutol
eq	Equivalent
EtOAc	Ethyl acetate
FA	Fusidic acid
GCN5	General control non-derepressible 5

GEN	Gentamicin
Gly or G	Glycine
GNAT	GCN5-related *N*-acetyltransferase
gCOSY	Gradient correlation spectroscopy
gHMBC	Gradient heteronuclear multiple bond correlation
gHSQCAD	Gradient heteronuclear single-quantum coherence
GTC	Geneticin
GTP	5'-Guanosine triphosphate
HCl	Hydrochloric acid
HEPES	4-(2-hydroxyethyl)-1-piperazineethanesulfonic acid
HIV	Human immunodeficiency virus
HYG	Hygromycin
INH	Isoniazid
KAN	Kanamycin A
KOH	Potassium hydroxide
LB	Luria-Bertani
LCMS	Liquid chromatography mass spectrometry
LIV	Lividomycin
Lys or K	Lysine
MDR	Multidrug-resistant
Me	Methyl
MeOH	Methanol
MES	2-(*N*-morpholino)ethanesulfonic acid

MIC	Minimum inhibitory concentration
Msm	*Mycobacterium smegmatis*
Mtb	*Mycobacterium tuberculosis*
MRSA	Methicillin-resistant *Staphylococcus aureus*
MXF	Moxifloxacin
NaCl	Sodium chloride
NEA	Neamine
NEO	Neomycin B
NET	Netilmicin
NH_4OH	Ammonium hydroxide
Ni-NTA	Nickel-nitrilotriacetic acid
NMR	Nuclear magnetic resonance spectroscopy
NTP	Nucleotide triphosphate
O/N	Overnight
OD	Optical density
PAR	Paromomycin
PCR	Polymerase chain reaction
pdb	Protein data bank
PLZ	Plazomicin
ppm	parts-per-million
PTC	Premature termination codon
PURGE	Presaturation utilizing relaxation gradients and echoes
PZA	Pyrazinamide

R_f	Retention factor
RIB	Ribostamycin
RMP	Rifampicin
RNA	Ribonucleic acid
rt	Room temperature
S. aureus	*Staphylococcus aureus*
SDS-PAGE	Sodium dodecyl sulfate-polyacrylamide gel electrophoresis
SIS	Sisomicin
spp.	Species
SPT	Spectinomycin
STR	Streptomycin
TB	Tuberculosis
THF	Tetrahydrofuran
TLC	Thin layer chromatography
TOB	Tobramycin
Tris-HCl	Tris(hydroxymethyl)aminomethane-hydrochloride
VRE	Vancomycin-resistant *enterococci*
VIO	Viomycin
WHO	World health organization
XDR	Extensively drug-resistant
zTOCSY	z-Filter total correlation spectroscopy

Abstract

Aminoglycoside (AG) antibiotics have been widely applied to the treatment of bacterial infections since the discovery of streptomycin, the first drug successfully applied to treatment of tuberculosis (TB). The bactericidal properties of these carbohydrate natural products are attributed to their ability to bind to the prokaryotic ribosome at the decoding A-site of the 16S rRNA, in a fashion that disrupts the cells ability to properly produce proteins and eventually leads to the death of the affected cell. Having enjoyed over 60 years of clinical success, AGs have encountered problems with bacterial resistance, as is eventually the case with all antibiotics. While there are several mechanisms by which bacteria may evade the activity of AGs, the covalent chemical modification of the AG structure by AG-modifying enzymes (AMEs) is the most common and poses the largest threat to the future use of AGs as antibacterial agents. Chloramphenicol (CAM), another natural product with excellent antibacterial properties, suffers from a similar resistance problem. The modification of CAM by CAM-modifying enzymes such as chloramphenicol acetyltransferase (CAT), reduces its affinity for the prokaryotic 50S ribosome, its cellular target, rendering it inactive. This dissertation focuses on the acetyltransferases that confer resistance to antibiotics, discussing progress towards understanding and overcoming a major hurdle in our ability to combat bacterial infections.

Our laboratory recently reported the unusual regio-versatility of the AG *N*-acetyltransferase (AAC), Eis, from *Mycobacterium tuberculosis* (*Mtb*). We used NMR spectroscopy to determine the order, number, and regio-specificity of the acetylations carried out by Eis. We found that Eis not only acetylates multiple positions, but that the order and positions of the acetyltations vary based on the particular AG scaffold studied. Furthermore, Eis is capable of acetylating amines that have never been reported with any other AAC. Those results caused us to investigate other anti-TB drugs in order to determine if it was possible that Eis could cause resistance across drug classes. We found

that capreomycin (CAP), a cyclic peptide antibacterial agent used as a second-line treatment for TB infections, could also be acetylated by Eis.

Using our knowledge of AMEs, we sought to develop novel AGs with improved/maintained activity and the ability to avoid modification by AMEs. A series of molecules that incorporated 6'-*N*- and 1-*N*-glycinyl/AHB groups was synthesized and tested against a number of bacterial strains. These synthetic studies and the knowledge gained regarding Eis will serve as a guide to the development of novel AGs targeting *Mtb* and other pathogens, which are difficult to treat with known antibiotics.

Additionally, we determined the first X-ray crystal structure of CAT_I with its natural substrate, CAM, bound in the active site, along with a structure of the unbound form of CAT_I. Comparison to a structure with fusidic acid (FA) bound in the active site and the previously well-characterized CAT_{III} with CAM bound allowed for a deeper understanding of the broader substrate preference of CAT_I. Though CAM is seldom used in many developed countries due to problems with toxicity, the need for effective antibiotics may soon outweigh the risks, and we hope that the insights provided in our studies may one day aid in the development of novel CAM analogs that overcome the toxicity and resistance problems encountered by CAM itself.

Chapter 1

Introduction: aminoglycosides (AGs), chloramphenicol (CAM), tuberculosis (TB), and bacterial resistance

1.1. Introduction to AGs

1.1.1. AGs

Since the discovery of penicillin in 1928, a variety of antibiotics including aminoglycosides (AGs), chloramphenicol (CAM), β-lactams, fluoroquinolones, among many others, have been discovered and applied clinically towards the treatment of one of the many growing number of bacterial infections. AGs (Fig. 1.1) in particular are being extensively studied in order to find new molecules or derivatives of existing scaffolds that may overcome the current resistant pathogens as well as prevent or slow the development of novel resistant pathogens.

AGs were first established as antibiotics in the 1940s with the discovery of streptomycin (STR), the first drug successfully applied to the treatment of tuberculosis (TB). Since then, AGs have enjoyed widespread application as chemotherapeutic agents in the treatments of many types of bacterial infections, including those associated with both Gram-positive and Gram-negative pathogens.[1] Additionally, kanamycin A (KAN) and amikacin (AMK) are both second-line drugs currently used to treat TB and multidrug-resistant TB (MRD-TB), although STR, the first therapy used against TB infections, is no longer used. In addition to being used for antibacterial purposes, the application of AG-based compounds in the treatment of HIV has been the focus of many research efforts in recent years due to their affinity for RNA.[2-10] Yet another potential use for AGs is in the treatment of genetic diseases caused by premature termination codons (PTCs), which have been linked to over 1800 genetic disorders.[11-18] However, no AGs are currently approved for these indications in the United States.

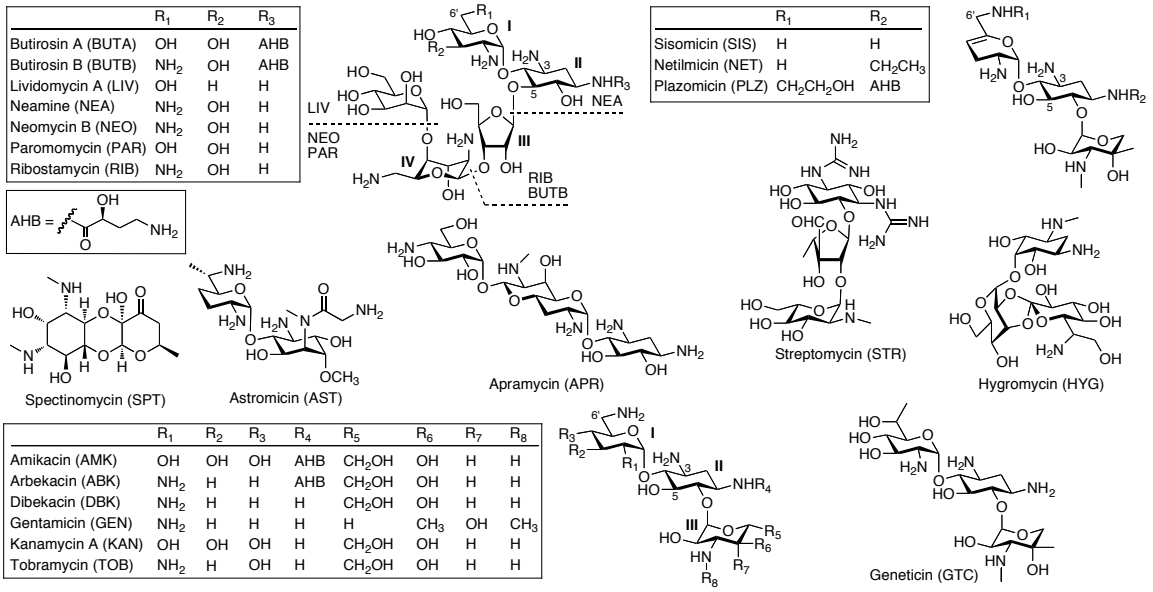

Fig. 1.1. The chemical structures of common AGs.

AGs, and most other antibiotics isolated from bacterial species, arose in response to selective pressure from, presumably, another bacterial species. As such, the antibacterial agents of this class were designed by Nature as very potent RNA binding agents, which leads to some toxicity in mammals, and, consequently, apprehensive use in many places around the world. In addition, as with many other classes of antibiotics, heavy use in the treatment of bacterial infections has caused many strains of bacteria to become resistant to normal doses of AGs. This resistance often occurs *via* the production of AG-modifying enzymes (AMEs), though other mechanisms exist. In order to circumvent the issue of antibiotic resistance as it applies to AGs, many scientists have taken on the intricate task of synthesizing AG derivatives, including synthetically modified AGs, AG dimers, and AG-biomolecule conjugates. Efforts aiming to create better AGs have utilized several new strategies including chemoenzymatic modification, selective modification of amine or hydroxyl groups, as well as the coupling of antibiotics, both AGs as well as other classes of drugs, by synthetic or semi-synthetic methods. The scientific community's understanding of these compounds and their effect on biological systems is increasing rapidly and significant effort is being put forth in order to solve these problems.

1.1.2. AGs' antibacterial modes of action

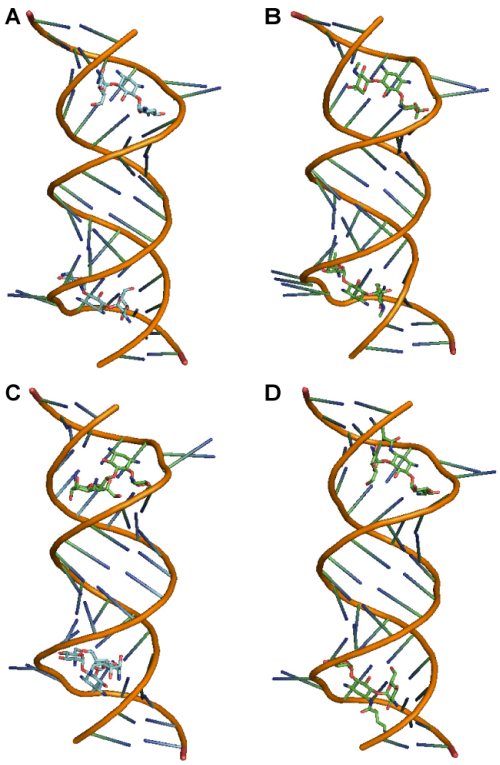

Fig. 1.2. The structures of **A.** TOB, **B.** GTC, and **C.** AMK bound to 16S oligonucleotides mimicking the bacterial decoding A-site. Also shown is **D.** the crystal structure of PAR docked into a bacterial A-site oligonucleotide. These images illustrate the 'flipped-out' conformation of the residues displaced upon binding of AGs to the decoding A-site.

After decades of study, the modes of action of AGs have been well characterized. It was discovered in the late 1980s that their molecular target is the 16S rRNA subunit of the 30S bacterial ribosome.[19] While alternative modes of binding have been seen with various AG derivatives,[20] as determined by biochemical[21-24] and structural[25-28] (X-ray and modelling) studies, in general, the interactions of AGs with three unpaired adenine residues in the decoding loop displace non-complementary adenines and lock them into a so-called 'flipped-out' orientation similar to that observed during mRNA decoding. Additionally, some AGs interfere with translocation *via* stabilization of the 70S subunit, by strengthening the interactions between the 50S and 30S subunits. These interactions stabilize the 70S complex, leading to faulty translocation of tRNAs, which may arise from the AGs' ability to interact with specific sites of the 16S rRNA.[29] The interactions of AGs with the eukaryotic ribosome serve to reduce the fidelity of translational processes by reducing the ability of the ribosome to discriminate between the proper mRNA•tRNA complexes, leading to the accumulation of truncated or non-functional proteins in the bacterial cells and eventually cell death.

Two types of interactions have been shown to facilitate binding of AGs to their targets: (1) the electrostatic interactions that occur between the positively-charged amino groups of the AG and the negatively-charged phosphate backbones of the RNA target, which are

the most important,[30] and (2) the hydrogen bonds that are formed between the amino and hydroxyl groups of both the RNA bases and AGs. Both types of interactions combine to form an intricate network of contacts between the RNA and AGs that results in very tightly bound complexes that are prone to decreased translational fidelity.[31-34]

1.1.3. Problems associated with AGs

1.1.3.1. Toxicity

One of the primary obstacles preventing more widespread use of AGs as long-term treatment for genetic, viral, or microbial issues is the inherent toxicity associated with non-specific binding to RNA. The primary risk factors for AG-induced toxicity include the duration, dosage, and frequency of therapy, the patient's age, the patient's liver and kidney health, and drug-drug interactions with other potential nephrotoxic agents.[35,36] Toxicity and selectivity are two intertwining issues associated with targeting RNA, due to the fact that RNA is important in all forms of life.[24,33,37-41] In general, AGs with fewer amino groups on the scaffold will show less toxicity, and the same is true of AGs with lower relative basicity of their existing amino groups, notably the 2'-amine.[42,43]

Nephrotoxicity, from drug compounds damaging the kidneys is generally reversible upon halting therapy in the case of AGs. Ototoxicity, in contrast to nephrotoxicity, is mostly irreversible. There are two types of ototoxicity: vestibular toxicity and cochlear toxicity. AGs toxicity may lead to a temporary vestibular hypofunction or permanent high-frequency hearing loss.[44] The permanence of AGs ototoxicity, which is the result of degeneration of hair cells and neurons in the cochlea, remains one of the primary obstacles in AG based therapies.[44-54] Very recently, Böttger and co-workers discovered that the AG apramycin (APR) is not ototoxic.[55]

1.1.3.2. Resistance

There are three mechanisms of bacterial resistance to AGs and more than one of the above mechanisms may be simultaneously active, leading to complex resistance problems. One mechanism of bacterial resistance to AGs is the reduction of the intracellular concentration of AGs due to alteration of the bacterial outer membrane (Fig.

1.3), decreasing drug transport into the cell and/or increasing the activity of active efflux systems. It is thought that three steps are involved in the uptake of AGs into bacterial cells. The first step is the adsorption of the poly-cationic AG to the surface of bacteria by electrostatic interactions with the negatively charged portions of biomolecules found on the outer cell membranes of bacteria.[56-59] In numerous cases, changes in membrane components involved in interactions with AGs are associated with increased levels of resistance.[57-66] The two subsequent absorption steps are oxygen dependent. For this reason anaerobic bacteria are intrinsically resistant to AGs,[67] and mutations in ATP synthases involved in these processes can cause decreased susceptibility to AGs.[68]

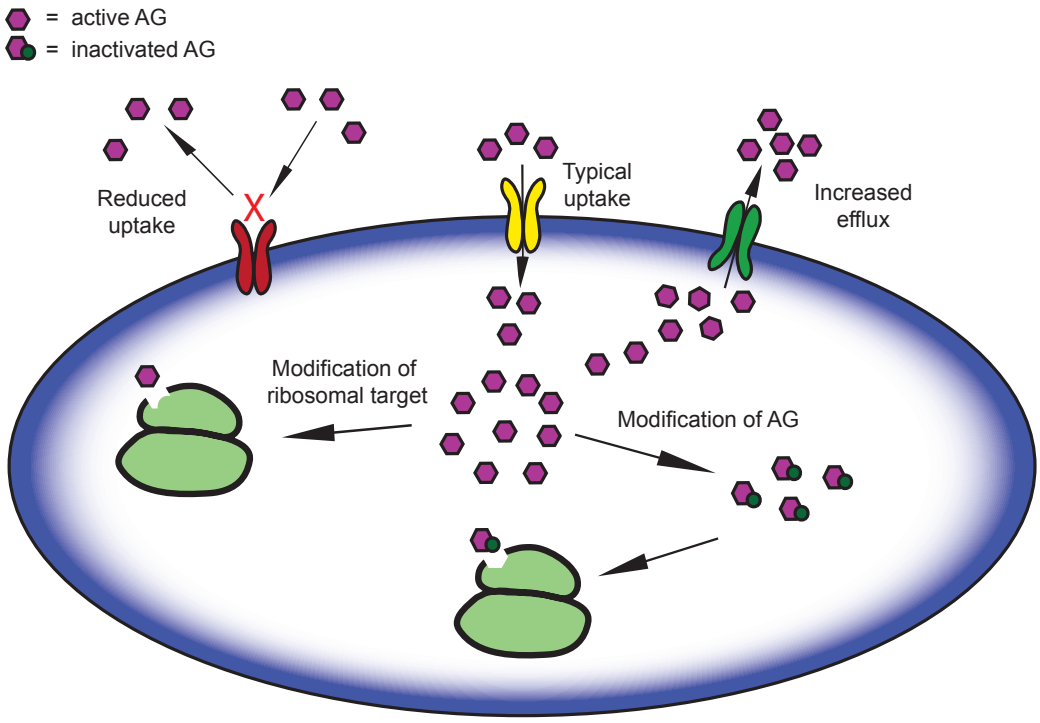

Fig. 1.3. Illustration of the various mechanisms of AG resistance.

Another resistance mechanism involves the alteration of the 16S RNA of bacterial 30S ribosomal subunit by mutation or methylation of the AG binding site (Fig. 1.3). Many AG-producing organisms are capable of expressing rRNA methylases, which are able to methylate the 16S rRNA.[69,70,71,72] Resistance to AGs resulting from a mutation of the ribosomal target has also been found in clinical isolates of *Mycobacterium tuberculosis* (*Mtb*).[73] In general, the modifications carried out by these enzymes occur in two highly

conserved regions, resulting in decreased affinity of the AG for its oligonucleotide partner such that the compounds are no longer effective.[24]

1.1.3.2.1. Covalent modification of AGs

Although AGs often target the 16S rRNA, the most common cause of AG resistance is not conferred by alteration of this target, owing to the highly preserved function of the rRNA across genera. Rather, the most common mechanism for bacterial resistance arises from the covalent modification of AGs by AMEs expressed by resistant strains (Fig. 1.3), which evolved from enzymes involved in normal cellular metabolism. Most modifications take place at the 1-, 3-, 2'-, and 6'-amino groups and the 3'-, 4'-, and 2''-hydroxyl groups.[74] There are three classes of AMEs: ATP-dependent AG nucleotidyltransferases (ANTs), ATP (and/or GTP)-dependent AG phosphotransferases (APHs), and AcCoA-dependent AG acetyltransferases (AACs) (Fig. 1.4), which are grouped according to the positions of the AG they modify. There are four ANTs, seven APHs, and four AACs (AAC(1), AAC(3), AAC(2'), and AAC(6')). An additional AAC, the enhanced intracellular survival (Eis) protein, has been shown to confer AG resistance in *Mtb*.[75]

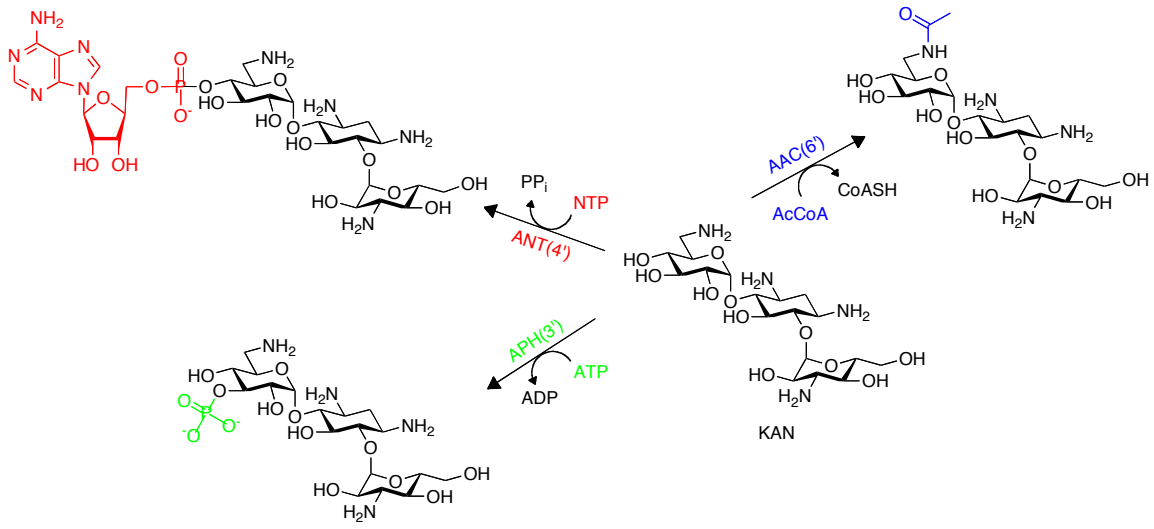

Fig. 1.4. Three AMEs and their modified KAN products.

There are also many bi-functional enzymes including AAC(6')/APH(2"),[74,76,77] ANT(3")-Ii/AAC(6')-IId,[78] AAC(3)-Ib/AAC(6')-Ib',[79] and AAC(6')-30/AAC(6')-Ib'[80] that are capable of modifying numerous positions, and in some cases are capable of two types of modification. The various sites of modification demonstrated with kanamycin B are shown in Fig. 1.5.

1.1.3.2.2. AG acetyltransferases (AACs)

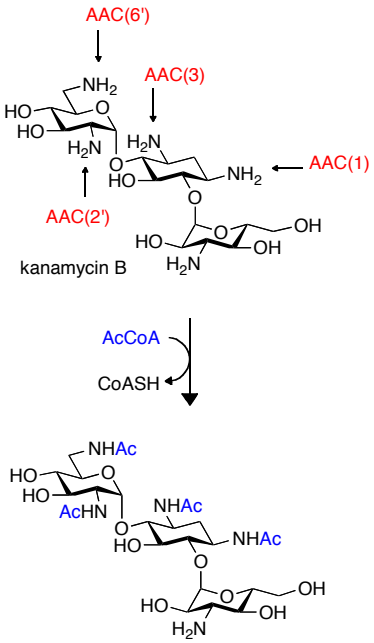

Fig. 1.5. The positions of kanamycin B that are acetylated by each of the known AAC enzymes.

Over 50 members of the AAC family have been identified. These enzymes catalyze the AcCoA-dependent *N*-acetylation of AGs. They modify the 1- and 3-amino groups of the central 2-deoxystreptamine (2-DOS) ring (Fig. 1.5) and the 2'- and 6'-amino groups of the 6-deoxy-6-aminoglucose ring (Fig. 1.5). Two AAC(1) enzymes have been found in *E. coli* and *actinomycetes* strains, but their clinical importance is minor due to the fact that their occurrence is extremely rare and neither has been reported in dangerous pathogenic bacterial strains.[81,82]

The AACs that acetylate at the 2'-amino group are all chromosomally encoded and, interestingly, mutations in the *aac*(2')-Ia gene may cause increased levels of peptidoglycan *O*-acetylation, suggesting that peptidoglycan acetylation may be the original physiological function of the enzyme. The chromosomally encoded *Mtb* AAC(2')-Ic was shown, in contrast to some other AACs, to be active against AMK and KAN, both of which contain a 2'-hydroxyl group, suggesting that this enzyme may also catalyze *O*-acetylation.[83]

The 6'-amino group plays an important role in rRNA binding as probed by the structural analysis of bound AGs to the 30S ribosomal subunit[84,85] and, unsurprisingly, is the target of one of the major classes of AMEs, the AAC(6') sub-family, which consists of more

than 25 members. Interestingly, a recently discovered variant of AAC(6'), the AAC(6')-Ib-cr, has been shown to be able to modify AGs as well as fluoroquinolones.[86] It seems likely that the steady increase in the clinical use of ciprofloxacin (CIP) during the 1990s has generated selective pressure for this variant.[87]

The AAC(3) sub-family is one of the largest AME families of enzymes and includes four major types, I-IV, based on the AG resistance profile. The AAC(3)-I from *Serratia marcescens* was the first AAC whose 3D structure was determined.[88,89] The enzyme-CoA complex determined at 2.3 Å allowed for identification of the interactions between the enzyme and the product. Unfortunately, there is no structure of AAC(3) with bound AG substrate available at this time.

1.1.4. Strategies for developing novel AGs

1.1.4.1. Development of novel AGs *via* chemical synthesis

Nature has evolved a number of very potent classes of antibacterials that effectively kill bacteria, and AGs are no exception. Owing to the difficulties associated with the synthesis of complex carbohydrates such as AGs, chemical synthesis remains a relatively ineffective tool in the total synthesis of large quantities of AG from basic chemical building blocks. This fact was evidenced in the early work on AGs reported by Hannesian and co-workers on a number of modified AGs, and it is still evident today.[90-93] The steps required to manipulate saccharide rings into the correct protection states is often staggering. Their synthesis, starting from grams or kilograms of starting materials, often provide only enough of the final product to test for minimum inhibitory concentration (MIC) and toxicity. In fact, the overall yields of syntheses of many types of complex molecules are often very low, and AGs are no exception.

Many reported syntheses of AG derivatives begin with the protection and hydrolysis of neomycin B (NEO) to generate the neamine (NEA) core common to many many AGs, leaving the 5-hydroxyl group of the 2-DOS ring open for derivatization.[94-96] This type of strategy often requires more than 20 steps,[97] so, even when starting with a known AG scaffold, the chemical modification can be quite tedious. An example in which APR was

synthesized from NEA is illustrated, highlighting key steps, in Fig. 1.6.[98] Some solutions to these problems have been found, such as syntheses that start from a known AG to produce novel compounds in few steps. Even though solutions like this are often specific to a particular problem or only lead to a small number of novel compounds, the progress made has been substantial.

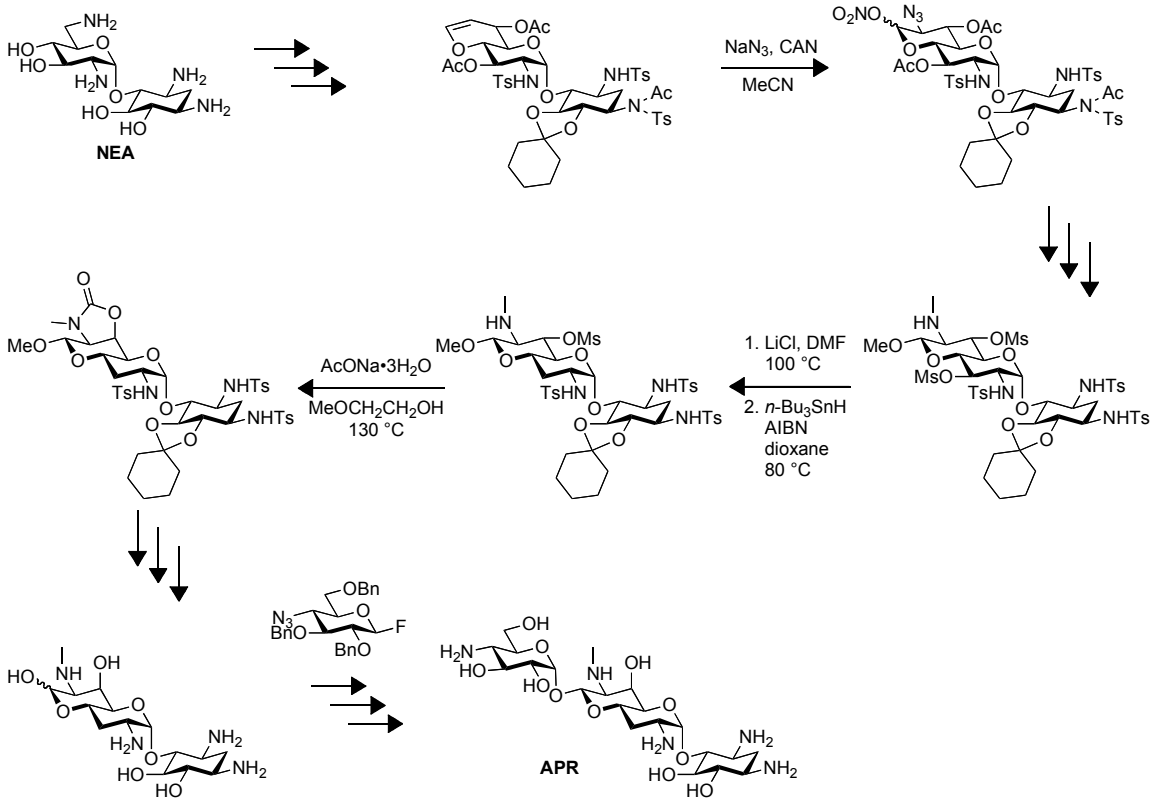

Fig. 1.6. Synthesis of APR starting from NEA.

One alternative to multi-step protections and deprotections involves metal chelation directed reactions as used by Nudelman *et al.*[17] In this example, zinc was used to preferentially protect the amino group at the 1-position. Afterwards they were able to preferentially react the *N*-1-position with γ-aminohydroxybutyric acid (AHB). After several more steps the novel PAR derivative, NB54, was generated. NB54 was found to suppress PTCs better than GEN, PAR, and its non-AHB containing counterpart NB30, while also proving less toxic than PAR and GEN.[17]

The appending of various chemical functionalities to known AGs is another popular strategy aimed at developing improved AG-based drugs. An increasing number of biochemical and structural studies have correlated the incorporation of the AHB at the *N*-1-position of the 2-DOS ring, common in many AGs, with an improved antibacterial profile.[27,99] Interestingly, the acyl moiety lowers the pK_a of the *N*-1 nitrogen atom, and this alteration of the *N*-1 nitrogen of compounds such as AMK, butirosin B, and others, significantly enhances the binding of ring II to RNA. Additionally, the ammonium on the terminus of the AHB group provides another favorable interaction with a backbone phosphate.[100] As a result of these observations, current strategies for increasing the antibacterial activity of AGs involve the incorporation of AHB or functionalized acyl groups to the scaffold of known AGs, a strategy that has produced results and shown enormous promise. A good example is the next-generation AG derived from sisomicin (SIS), ACHN-490 (Plazomicin, (PLZ)), which has shown very promising results against a number of bacterial strains that pose public health threats. PLZ incorporates an AHB at the *N*-1-position of SIS.[101-103]

The incorporation of a number of other functionalized acyl groups to the amines of known AGs has proven a successful strategy for overcoming bacterial resistance and maintaining/or improving antibacterial activity. In contrast to other syntheses of AG derivatives, the incorporation of a 6'-*N*-glycinyl group to AGs has showed promise, and may be accomplished in only two steps (Fig. 1.7).[104] MIC studies of 6'-*N*-glycinyl-TOB with bacterial strains harbouring AMEs showed that the compound could avoid the activity of AMEs while maintaining similar activity to the parent compound against the same strains that did not have the AMEs.

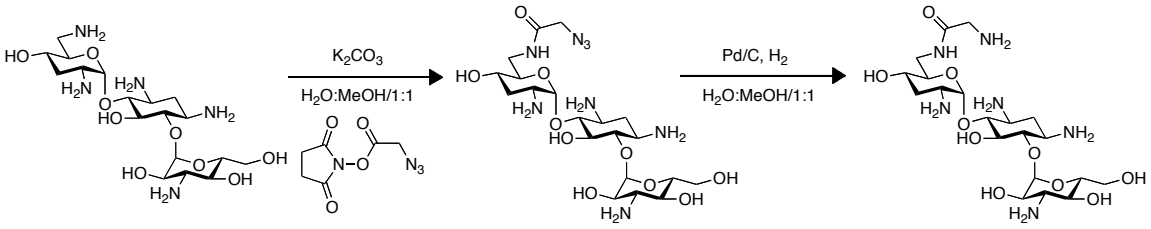

Fig. 1.7. Synthesis of 6'-*N*-glycinyl-TOB in two steps from TOB.

The sensitivity to modification of natural AGs and the difficulty of enhancing compounds that Nature has spent thousands of generations optimizing has been well established. There is precedence in the literature that suggests potency, selectivity, and the ability to overcome resistance may be achieved by synthetically modifying known AGs, though it is rarely easy to control or predict. Nonetheless, many efforts have quite successfully yielded active compounds, and knowledge in the field continues to grow.

1.1.4.2. Development of novel AGs *via* chemoenzymatic methods

Recently it has been shown that chemoenzymatic methods hold great promise in generating large libraries of compounds. Generating large amounts of compound chemoenzymatically can be challenging. However, using these methods, enough compound can be produced for initial testing to help decide which compounds are worth pursuing synthetically, expediting the process of novel AG development significantly. There are also many other techniques currently being developed or already in practice that will allow for a simplified approach which is less time consuming and more efficient than the classical synthetic methods for developing novel AGs.

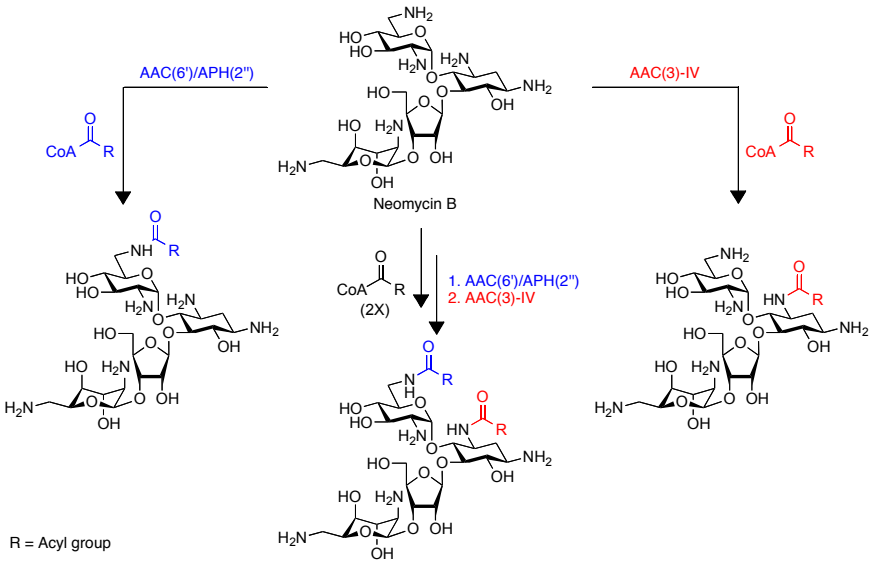

Fig. 1.8. A chemoenzymatic approach to the generation of mono-*N*-acylated AGs as well as homo- and hetero-di-*N*-acylated AGs *via* two sequential acylations by AACs utilizing acyl-CoA as cosubstrates. R groups accepted include, but are not necessarily limited to acetyl-, *n*-propionyl-, 4-bromo-thiophene-2-carbonyl-, 6-fluoro-picolinyl-, glycinyl-, and malonyl-CoA.

While it is clear that *N*-acetylation of AGs by AACs evolved as a mechanism of resistance in bacteria, there have been many reports of *N*-acylated AGs, both natural and semi-synthetic, that show a retention or even improvement in activity.[105-107] *N*-acetylation by AACs is a common means of deactivation in bacteria that results in decreased efficacy of the AG. However, the semi-synthetic *N*-acylation with groups other than the normal acetyl has resulted in highly potent AGs, as mentioned in the preceding sub-section. Adopting this approach led to the development of AMK by *N*-1-acylation of KAN with AHB,[105] and arbekacin, which was produced by a combination of 3',4'-dideoxygenation and *N*-1-acylation.[106] While these advancements in AGs are exciting, the synthesis of the compounds is subject to the previously discussed pitfalls, making it difficult to generate a large number of novel compounds quickly and efficiently. Current strategies aimed at circumventing this particular problem include the application of enzymes to regio-specifically acylate an amine on the AG scaffold.

Our laboratory recently reported a methodology which utilizes AACs and unnatural acyl-CoA analogs to chemoenzymatically generate *N*-acylated AGs (Fig. 1.8).[107] Two AACs, (AAC(6')/APH(2") and AAC(3)-IV) were utilized, and both enzymes showed diverse substrate promiscuity towards a number of AGs as well as acyl-CoA derivatives. The method allows for the generation of mono-*N*-acylated AGs as well as homo- and hetero-di-*N*-acylated AGs in quantities sufficient to screen each analog's antibacterial potential. Thus, it is possible to decide which of the novel compounds show promising activity that is worth investigating on a larger scale all the while avoiding an arduous chemical synthesis that leads to a dead end.

Baasov and co-workers reported a similar, yet distinct chemoenzymatic approach to the development of novel acylated AG derivatives in 2008. They applied recombinant enzymes involved in butirosin biosynthesis to selectively acylate the *N*-1-position of a series of 2-DOS containing pseudo-di and trisaccharide AGs using a synthetic acyl donor.[108] Similarly, Llewellyn and Spencer recently used the enzymes responsible for synthesizing butirosin B in *Staphylococcus aureus* to generate AMK and neokacin from

NEO.[109] As is the case when applying AACs to chemoenzymatically alter AGs, this method greatly reduces the synthetic workload required to make such compounds *via* purely synthetic methods.

1.2. Tuberculosis (TB)

Causing 1.4 million deaths globally in 2010, TB is the second leading pathogen-related cause of death,[110] and the most common cause of death among immuno-compromised people living with HIV/AIDS.[111-115] Although as much as a third of the global population may be infected with TB,[110] in most cases (~90%), the infection remains dormant and may never lead to a life-threatening infection.[116] The global distribution of *Mtb* infection, latent or otherwise, is very skewed towards developing countries, especially those in which relatively large portions of the populations are immuno-compromised.[117] TB primarily affects the lungs and pulmonary function, although it may spread to other organs- pulmonary TB is the infectious, lethal form of the disease. Massive efforts to combat this global pandemic have seen some success,[110,118] though they have failed to bring the spread of the disease under full control.

1.2.1. Anti-TB drugs

A large number of anti-TB drugs, with varying mechanisms of action, have been discovered, and many are effective in curing infections caused by *Mtb*. The first drug that was successfully used to treat TB was a natural product from *Streptomyces griseus*, the AG antibiotic STR.[119-121] While STR is still currently used in special cases, it is generally no longer used in the treatment of TB due to extremely high rates of resistance, likely the result of its long-term use as a mono-therapy.[122,123] Currently, the use of mono-therapies has been abandoned because *Mtb* rapidly develops resistance when treated with only a single drug. Instead, current therapeutic strategies incorporate several drugs into a single regimen that generally lasts up to or in excess of 6 months.[124,125] There are four first-line drugs for the treatment of TB, including isoniazid (INH), rifampicin (RMP), pyrazinamide (PZA), and ethambutol (EMB), all of which are applied in a typical anti-TB regimen (Fig. 1.9). There are also a number of second-line therapies including the AGs KAN and AMK, the polypeptides capreomycin (CAP) and viomycin (VIO), the

fluoroquinolones such as CIP and moxifloxacin (MXF), as well as ethionimide. The second-line therapeutics are generally used against *Mtb* that is resistant to the first-line therapies. While these two lines of anti-TB drugs generally show efficacy against TB, there are many problems- cost, patient compliance, toxicity and the development of further resistance- that require the further development of anti-TB drugs and treatment strategies.

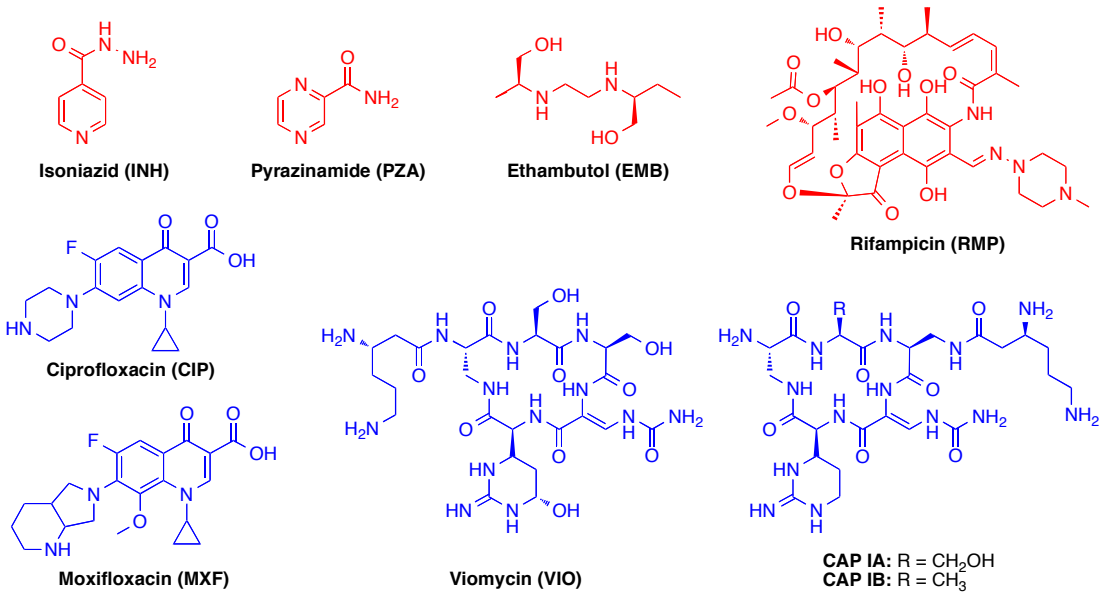

Fig. 1.9. Commonly used first-line (red) and second-line (blue) anti-TB drugs.

1.2.2. TB resistance and enhanced intracellular survival (Eis) protein

1.2.2.1. Resistance to anti-TB drugs

Bacterial communities naturally evolve resistance to the drugs commonly used against them through natural selection. The development of resistance to first- and second-line drugs is outpacing the discovery and development of novel, effective treatments against resistant strains of many bacteria, a process that may be accelerated when patients fail to complete the full course of treatment. This occurs most frequently in areas with sub-standard TB control programs, which often are also the places greatly affected by HIV, greatly complicating the issue. The development of resistance to anti-TB drugs by *Mtb* is especially problematic, considering that *Mtb* is naturally resistant to many common antibiotics due to their unique cell wall that prevents drugs from reaching their intracellular targets.[126,127]

Bacteria that display resistance to INH and RMP, the two most powerful first-line treatments for TB, are designated as multidrug-resistant (MDR). MDR-TB is fatal in more than one-third of the cases. It is likely that this type of resistance emerged due to therapy employing a single drug, allowing selective pressure to more rapidly cause the evolution of resistance.[128,129] Although multiple drug therapy is now used more commonly, the development of resistance is still rapidly progressing, and has led to extensively drug-resistant TB (XDR-TB). XDR-TB, a more severe form of MDR-TB identified in 2006, is characterized by resistance to RMP and INH, in addition to a fluoroquinolone, such as CIP, and at least one of the second-line anti-TB drugs including KAN, AMK, or CAP.[130-132] Recently, some of the most drug-resistant forms of TB ever encountered have been reported in India- extremely drug-resistant (XXDR-TB) and totally drug-resistant TB (TDR-TB)- though there is some controversy over the nomenclature, which has not yet been accepted by the World Health Organization (WHO).[133,134,135] The difficulty in treating drug-resistant strains of *Mtb* is a limiting factor in our ability to maintain effective treatments for TB infections. Thus, there is a great demand for anti-TB drugs with efficacy against MDR- and XDR-TB.[136-139]

1.2.2.2. Eis

The structural and functional characterization of the enhanced intracellular survival (Eis) protein from *Mtb* has been the goal of many research efforts recently.[75,140-148] The *eis* gene and its protein product, Eis, were discovered in *Mtb* H37Rv during an effort to identify *Mtb* genes necessary for survival within macrophages, leading it to be named as such.[147] Bioinformatic analysis predicted that Eis belonged to the GCN5-related *N*-acetyltransferase (GNAT) family of proteins,[145] and that it is capable of conferring resistance to KAN in the AG-susceptible *Mtb* strain H37Rv.[75] In one-third of cases, covering a large, diverse set of strains, clinical resistance of *Mtb* to KAN was shown to be the result of mutations in the promoter of the *eis* gene.[147,149] These studies led to the idea that Eis may confer resistance by acting as an AAC. Subsequently, through biochemical and structural studies (Fig. 1.10), our laboratory demonstrated that Eis acts as an unusually regio-versatile AAC in *Mtb*[140] and *Mycobacterium smegmatis* (*Msm*).[150]

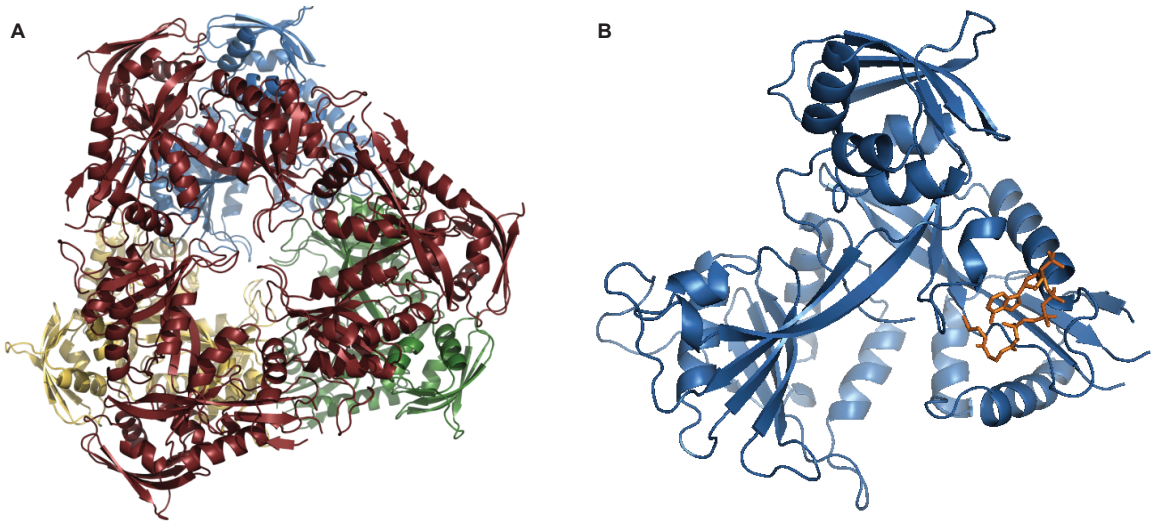

Fig. 1.10. Illustrations of the X-ray crystal structure of Eis from *Mtb* depicted in **A.** hexameric form and **B.** monomeric form with CoA bound in one monomer (PDB: 3R1K).[140]

It was recently reported that Eis from *Msm* (Eis_*Msm*) and Eis from *Mtb* (Eis_*Mtb*) are also capable of acetylating dual-protein phosphatase 16 (DUSP16)/mitogen-activated protein kinase phosphatase-7 (MKP-7) (DUSP16/MPK-7).[148] These modifications occur at Lys55, and this ability to modify primary amines on the amino acid residues of proteins suggests that Eis may have a much broader substrate profile than might be expected. Additionally, AACs are capable of acetylating classes of drugs other than AGs, including the second-line anti-TB drug CIP.[151] The identification of novel substrates of Eis, including both protein and small molecules, as well as the development of inhibitors[141,150] will likely continue to be the focus of many research efforts in the near future.

1.3. Chloramphenicol (CAM) and CAM acetyltransferase (CAT)

1.3.1. CAM as an antibacterial agent

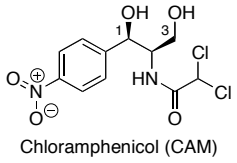

Chloramphenicol (CAM)

Fig. 1.11. Structure of CAM.

Chloramphenicol (CAM) (Fig. 1.11) is a potent broad-spectrum antibacterial agent that was isolated from *Streptomyces venezuelae* in 1948.[152] CAM was one of the most effective antibiotics in use for decades and was used to treat many different varieties of bacterial infections. Although toxicity issues are relatively rare, bone marrow toxicity may be a very serious

issue.[153-156] Despite the toxicity issues, CAM was often applied to the treatment of brain infections, such as those caused by *Neisseria meningitides*, due to its ability to cross the blood-brain barrier. CAM use has been almost completely halted in the United States and Europe due to the aforementioned bone marrow toxicity. However, owing to the rapid emergence of resistance to many common antibiotics, many believe that CAM should be seriously reconsidered as a wider-spectrum therapeutic.[157]

CAM antibacterial activity is achieved *via* inhibition of bacterial protein biosynthesis by binding to the 50S subunit of the bacterial ribosome. Crystal structures of the 50S subunit of the *Escherichia coli* and *Thermus thermophilus* ribosome in complex with CAM confirmed binding to A-site of the 50S subunit and showed that CAM occupies the binding site for the amino-acyl moiety of the A-site tRNA.[158,159] The 3-hydroxyl of CAM (Fig. 1.11), which interacts with the ribosome through direct hydrogen bonding, potassium ion-mediated electrostatic interactions, and van der Waals interactions with the RNA phosphosugar backbone, is critical for antibacterial activity.[158,159] Additionally, the 1-hydroxyl of CAM forms hydrogen bonds with RNA bases. Thus, any modification of the 1-hydroxyl or the 3-hydroxyl of CAM is likely to disrupt CAM-ribosome binding.[159]

1.3.2. Resistance to CAM

Similarly to AGs, there are multiple mechanisms of resistance to CAM. The least common mechanism of resistance to CAM is mutation of the 50S ribosomal target, specifically at the 23S rRNA, which decreases the affinity of CAM for its target.[160-162] A more common mechanism of resistance to CAM is the decreased permeability of the outer membrane of the bacteria.[163-165] This type of resistance manifests in lower concentrations of CAM reaching the interior of the cell. Because CAM is not transported into the cell in an energy-dependent manner, in contrast to AGs, the decrease in permeability generally only leads to low levels of resistance.

The covalent modification of CAM is catalyzed by a number of bacterial resistance enzymes, similar to the manner in which AGs are modified by AMEs (Fig. 1.12). In addition to the CAM acetyltransferases (CATs) discussed at length in the following

subsection, CAM *O*-phosphotransferases (CPTs) have been reported.[166-168] CAM nitroreductases have also been confirmed to confer resistance to CAM.[169] Additionally, in mammals, a number of modifications may take place that deactivate CAM, including dehalogenation, and glucuronidation, as well as reduction of the nitro group.[170]

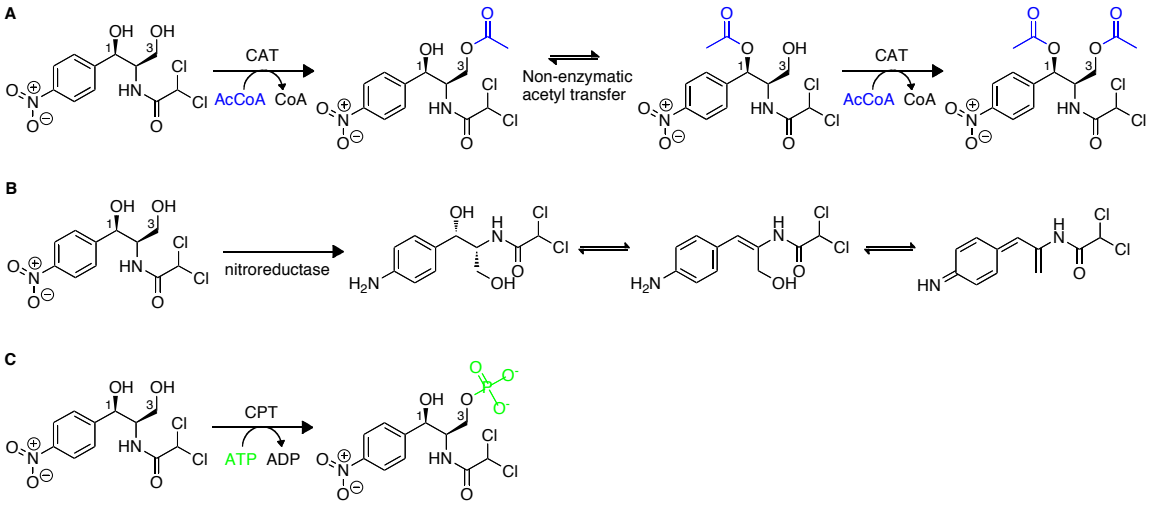

Fig. 1.12. Modifications causing resistance to CAM by **A.** CAT, **B.** a nitroreductase, and **C.** CPT.

1.3.2.1. Resistance conferred by CATs

The most common and most clinically relevant bacterial resistance to CAM is conferred by CAT enzymes, which catalyzes the transfer of an acetyl group from acetyl-coenzyme A (AcCoA) to the 3-hydroxyl group of CAM (Fig. 1.12).[171] Although two acetylations may be catalyzed by CAT, the second occurring after a intramolecular transfer of the first acetyl group, a single acetylation of CAM is sufficient to abolish its affinity for the ribosome[172] which is rationalized in the previously discussed structural observations.[158,159] CAT proteins are divided into three types- CAT_I, CAT_{II}, and CAT_{III}- but the differences between the three types are not particularly well-defined in terms of their amino acid sequences. Rather, certain functional properties of the proteins have been used to delineate the boundaries. For example, in addition to binding and acetylating CAM,[171] CAT_I, unlike CAT_{III}, binds a much bulkier antibiotic, fusidic acid (FA).[173] FA is a steroidal antibacterial agent that is generally applied against infections caused by Gram-positive pathogens. CAT_I does not covalently modify FA as with CAM, but instead it confers resistance by sequestering FA, which binds at the CAM binding site. Until

recently, the physical properties of CAT_I that confer this ability have not been well characterized.

This dissertation summarizes a significant amount of the research I performed under the supervision Professor Sylvie Garneau-Tsodikova. It is comprised of six chapters. Chapter one is the introduction providing relevant background on AG antibiotics, CAM, and acetyltransferases that confer resistance to antibiotics, as well as strategies used to overcome resistance. Chapter six suggests a number of future directions for these projects. Chapter two discusses the characterization of Eis from *Mtb* focusing on the development of NMR methodology to efficiently determine of the order and positions modified on various AGs. Chapter three reports the acetylation of CAP, a second-line drug for TB, by Eis and the activity of CAP against various mycobacteria. Chapter four focuses on the chemical synthesis of novel AGs aimed at overcoming antibacterial resistance. Chapter five describes the first crystal structure of CAT_I bound to CAM, focusing on the structural differences between CAT_I and CAT_{III} that lead to the increased substrate binding profile of CAT_I.

1.4. References

(1) Davies, J.; Wright, G. D. *Trends Microbiol* **1997**, *5*, 234.
(2) Lapidot, A.; Berchanski, A.; Borkow, G. *The FEBS journal* **2008**, *275*, 5236.
(3) Hegde, R.; Borkow, G.; Berchanski, A.; Lapidot, A. *The FEBS journal* **2007**, *274*, 6523.
(4) Blount, K. F.; Tor, Y. *Chembiochem* **2006**, *7*, 1612.
(5) Blount, K. F.; Zhao, F.; Hermann, T.; Tor, Y. *J Am Chem Soc* **2005**, *127*, 9818.
(6) Ennifar, E.; Paillart, J. C.; Bernacchi, S.; Walter, P.; Pale, P.; Decout, J. L.; Marquet, R.; Dumas, P. *Biochimie* **2007**, *89*, 1195.
(7) Tok, J. B.; Dunn, L. J.; Des Jean, R. C. *Bioorg Med Chem Lett* **2001**, *11*, 1127.
(8) Tok, J. B.; Fenker, J. *Bioorg Med Chem Lett* **2001**, *11*, 2987.
(9) Riguet, E.; Desire, J.; Boden, O.; Ludwig, V.; Gobel, M.; Bailly, C.; Decout, J. L. *Bioorg Med Chem Lett* **2005**, *15*, 4651.
(10) Belousoff, M. J.; Graham, B.; Spiccia, L.; Tor, Y. *Organic & biomolecular chemistry* **2009**, *7*, 30.
(11) Gorini, L.; Kataja, E. *Proc Natl Acad Sci U S A* **1964**, *51*, 487.
(12) Kellermayer, R. *Eur J Med Genet* **2006**, *49*, 445.
(13) Howard, M.; Frizzell, R. A.; Bedwell, D. M. *Nat Med* **1996**, *2*, 467.
(14) Bedwell, D. M.; Kaenjak, A.; Benos, D. J.; Bebok, Z.; Bubien, J. K.; Hong, J.; Tousson, A.; Clancy, J. P.; Sorscher, E. J. *Nat Med* **1997**, *3*, 1280.
(15) Rowe, S. M.; Clancy, J. P. *BioDrugs* **2009**, *23*, 165.
(16) Howard, M. T.; Anderson, C. B.; Fass, U.; Khatri, S.; Gesteland, R. F.; Atkins, J. F.; Flanigan, K. M. *Ann Neurol* **2004**, *55*, 422.

(17) Nudelman, I.; Rebibo-Sabbah, A.; Cherniavsky, M.; Belakhov, V.; Hainrichson, M.; Chen, F.; Schacht, J.; Pilch, D. S.; Ben-Yosef, T.; Baasov, T. *Journal of medicinal chemistry* **2009**, *52*, 2836.
(18) Welch, E. M.; Barton, E. R.; Zhuo, J.; Tomizawa, Y.; Friesen, W. J.; Trifillis, P.; Paushkin, S.; Patel, M.; Trotta, C. R.; Hwang, S.; Wilde, R. G.; Karp, G.; Takasugi, J.; Chen, G.; Jones, S.; Ren, H.; Moon, Y. C.; Corson, D.; Turpoff, A. A.; Campbell, J. A.; Conn, M. M.; Khan, A.; Almstead, N. G.; Hedrick, J.; Mollin, A.; Risher, N.; Weetall, M.; Yeh, S.; Branstrom, A. A.; Colacino, J. M.; Babiak, J.; Ju, W. D.; Hirawat, S.; Northcutt, V. J.; Miller, L. L.; Spatrick, P.; He, F.; Kawana, M.; Feng, H.; Jacobson, A.; Peltz, S. W.; Sweeney, H. L. *Nature* **2007**, *447*, 87.
(19) Moazed, D.; Noller, H. F. *Nature* **1987**, *327*, 389.
(20) Kondo, J.; Pachamuthu, K.; Francois, B.; Szychowski, J.; Hanessian, S.; Westhof, E. *ChemMedChem* **2007**, *2*, 1631.
(21) Ogle, J. M.; Ramakrishnan, V. *Annu Rev Biochem* **2005**, *74*, 129.
(22) Shandrick, S.; Zhao, Q.; Han, Q.; Ayida, B. K.; Takahashi, M.; Winters, G. C.; Simonsen, K. B.; Vourloumis, D.; Hermann, T. *Angew Chem Int Ed Engl* **2004**, *43*, 3177.
(23) Vicens, Q.; Westhof, E. *Biopolymers* **2003**, *70*, 42.
(24) Pfister, P.; Hobbie, S.; Vicens, Q.; Bottger, E. C.; Westhof, E. *Chembiochem* **2003**, *4*, 1078.
(25) Vicens, Q.; Westhof, E. *Chem Biol* **2002**, *9*, 747.
(26) Vicens, Q.; Westhof, E. *J Mol Biol* **2003**, *326*, 1175.
(27) Kondo, J.; Francois, B.; Russell, R. J.; Murray, J. B.; Westhof, E. *Biochimie* **2006**, *88*, 1027.
(28) Vicens, Q.; Westhof, E. *Structure* **2001**, *9*, 647.
(29) Dlugosz, M.; Trylska, J. *J Phys Chem B* **2009**, *113*, 7322.
(30) Wang, H.; Tor, Y. *J Am Chem Soc* **1997**, *119*, 8734.
(31) Jiang, L.; Patel, D. J. *Nat Struct Biol* **1998**, *5*, 769.
(32) Hobbie, S. N.; Pfister, P.; Bruell, C.; Sander, P.; Francois, B.; Westhof, E.; Bottger, E. C. *Antimicrob Agents Chemother* **2006**, *50*, 1489.
(33) Hobbie, S. N.; Pfister, P.; Brull, C.; Westhof, E.; Bottger, E. C. *Antimicrob Agents Chemother* **2005**, *49*, 5112.
(34) Francois, B.; Russell, R. J.; Murray, J. B.; Aboul-ela, F.; Masquida, B.; Vicens, Q.; Westhof, E. *Nucleic Acids Res* **2005**, *33*, 5677.
(35) Desai, T. K.; Tsang, T. K. *Am J Med* **1988**, *85*, 47.
(36) Corcoran, G. B.; Salazar, D. E.; Schentag, J. J. *Am J Med* **1988**, *85*, 279.
(37) Sander, P.; Prammananan, T.; Bottger, E. C. *Mol Microbiol* **1996**, *22*, 841.
(38) Springer, B.; Kidan, Y. G.; Prammananan, T.; Ellrott, K.; Bottger, E. C.; Sander, P. *Antimicrob Agents Chemother* **2001**, *45*, 2877.
(39) Pfister, P.; Risch, M.; Brodersen, D. E.; Bottger, E. C. *Antimicrob Agents Chemother* **2003**, *47*, 1496.
(40) Pfister, P.; Hobbie, S.; Brull, C.; Corti, N.; Vasella, A.; Westhof, E.; Bottger, E. C. *J Mol Biol* **2005**, *346*, 467.
(41) Prammananan, T.; Sander, P.; Brown, B. A.; Frischkorn, K.; Onyi, G. O.; Zhang, Y.; Bottger, E. C.; Wallace, R. J., Jr. *J Infect Dis* **1998**, *177*, 1573.
(42) Hainrichson, M.; Nudelman, I.; Baasov, T. *Organic & biomolecular chemistry* **2008**, *6*, 227.
(43) Chen, L.; Hainrichson, M.; Bourdetsky, D.; Mor, A.; Yaron, S.; Baasov, T. *Bioorganic & medicinal chemistry* **2008**, *16*, 8940.
(44) Guthrie, O. W. *Toxicology* **2008**, *249*, 91.
(45) Janknegt, R. *Pharm Weekbl Sci* **1990**, *12*, 81.
(46) Tange, R. A. *Ziekenhuisfarmacie* **1987**, *3*, 15.

(47) Huth, M. E.; Ricci, A. J.; Cheng, A. G. *International Journal of Otolaryngology* **2011**, *2011*.
(48) Guan, M. X. *Mitochondrion* **2011**, *11*, 237.
(49) Rybak, L. P.; Ramkumar, V. *Kidney international* **2007**, *72*, 931.
(50) Bindu, L. H.; Reddy, P. P. *Int J Audiol* **2008**, *47*, 702.
(51) Harvey, S. C.; Skolnick, P. *J Pharmacol Exp Ther* **1999**, *291*, 285.
(52) Hong, S. H.; Park, S. K.; Cho, Y. S.; Lee, H. S.; Kim, K. R.; Kim, M. G.; Chung, W. H. *Hear Res* **2006**, *211*, 46.
(53) Hobbie, S. N.; Akshay, S.; Kalapala, S. K.; Bruell, C. M.; Shcherbakov, D.; Bottger, E. C. *Proc Natl Acad Sci U S A* **2008**, *105*, 20888.
(54) Kondo, J.; Westhof, E. *Nucleic Acids Res* **2008**, *36*, 2654.
(55) Matt, T.; Ng, C. L.; Lang, K.; Sha, S. H.; Akbergenov, R.; Shcherbakov, D.; Meyer, M.; Duscha, S.; Xie, J.; Dubbaka, S. R.; Perez-Fernandez, D.; Vasella, A.; Ramakrishnan, V.; Schacht, J.; Bottger, E. C. *Proc Natl Acad Sci U S A* **2012**, *109*, 10984.
(56) Hancock, R. E.; Farmer, S. W.; Li, Z. S.; Poole, K. *Antimicrob Agents Chemother* **1991**, *35*, 1309.
(57) Taber, H. W.; Mueller, J. P.; Miller, P. F.; Arrow, A. S. *Microbiol Rev* **1987**, *51*, 439.
(58) Hancock, R. E. *Annu Rev Microbiol* **1984**, *38*, 237.
(59) Magnet, S.; Blanchard, J. S. *Chemical reviews* **2005**, *105*, 477.
(60) Putman, M.; van Veen, H. W.; Konings, W. N. *Microbiol Mol Biol Rev* **2000**, *64*, 672.
(61) Shakil, S.; Khan, R.; Zarrilli, R.; Khan, A. U. *Journal of biomedical science* **2008**, *15*, 5.
(62) Aires, J. R.; Kohler, T.; Nikaido, H.; Plesiat, P. *Antimicrob Agents Chemother* **1999**, *43*, 2624.
(63) Westbrock-Wadman, S.; Sherman, D. R.; Hickey, M. J.; Coulter, S. N.; Zhu, Y. Q.; Warrener, P.; Nguyen, L. Y.; Shawar, R. M.; Folger, K. R.; Stover, C. K. *Antimicrob Agents Chemother* **1999**, *43*, 2975.
(64) Masuda, N.; Sakagawa, E.; Ohya, S.; Gotoh, N.; Tsujimoto, H.; Nishino, T. *Antimicrob Agents Chemother* **2000**, *44*, 3322.
(65) Murakami, S.; Nakashima, R.; Yamashita, E.; Yamaguchi, A. *Nature* **2002**, *419*, 587.
(66) Yu, E. W.; Aires, J. R.; Nikaido, H. *J Bacteriol* **2003**, *185*, 5657.
(67) Bryan, L. E.; Kowand, S. K.; Van Den Elzen, H. M. *Antimicrob Agents Chemother* **1979**, *15*, 7.
(68) Miller, M. H.; Edberg, S. C.; Mandel, L. J.; Behar, C. F.; Steigbigel, N. H. *Antimicrob Agents Chemother* **1980**, *18*, 722.
(69) Doi, Y.; Yokoyama, K.; Yamane, K.; Wachino, J.; Shibata, N.; Yagi, T.; Shibayama, K.; Kato, H.; Arakawa, Y. *Antimicrob Agents Chemother* **2004**, *48*, 491.
(70) Chow, J. W. *Clin Infect Dis* **2000**, *31*, 586.
(71) Galimand, M.; Sabtcheva, S.; Courvalin, P.; Lambert, T. *Antimicrob Agents Chemother* **2005**, *49*, 2949.
(72) Yan, J. J.; Wu, J. J.; Ko, W. C.; Tsai, S. H.; Chuang, C. L.; Wu, H. M.; Lu, Y. J.; Li, J. D. *J Antimicrob Chemother* **2004**, *54*, 1007.
(73) Powers, T.; Noller, H. F. *EMBO J* **1991**, *10*, 2203.
(74) Kotra, L. P.; Haddad, J.; Mobashery, S. *Antimicrob Agents Chemother* **2000**, *44*, 3249.
(75) Zaunbrecher, M. A.; Sikes, R. D., Jr.; Metchock, B.; Shinnick, T. M.; Posey, J. E. *Proc Natl Acad Sci U S A* **2009**, *106*, 20004.
(76) Wright, G. D.; Berghuis, A. M.; Mobashery, S. *Advances in experimental medicine and biology* **1998**, *456*, 27.
(77) Mingeot-Leclercq, M. P.; Glupczynski, Y.; Tulkens, P. M. *Antimicrob Agents Chemother* **1999**, *43*, 727.
(78) Kim, C.; Hesek, D.; Zajicek, J.; Vakulenko, S. B.; Mobashery, S. *Biochemistry* **2006**, *45*, 8368.

(79) Dubois, V.; Poirel, L.; Marie, C.; Arpin, C.; Nordmann, P.; Quentin, C. *Antimicrob Agents Chemother* **2002**, *46*, 638.
(80) Mendes, R. E.; Toleman, M. A.; Ribeiro, J.; Sader, H. S.; Jones, R. N.; Walsh, T. R. *Antimicrob Agents Chemother* **2004**, *48*, 4693.
(81) Lovering, A. M.; White, L. O.; Reeves, D. S. *J Antimicrob Chemother* **1987**, *20*, 803.
(82) Sunada, A.; Nakajima, M.; Ikeda, Y.; Kondo, S.; Hotta, K. *J Antibiot (Tokyo)* **1999**, *52*, 809.
(83) Hegde, S. S.; Javid-Majd, F.; Blanchard, J. S. *The Journal of biological chemistry* **2001**, *276*, 45876.
(84) Wimberly, B. T.; Brodersen, D. E.; Clemons, W. M., Jr.; Morgan-Warren, R. J.; Carter, A. P.; Vonrhein, C.; Hartsch, T.; Ramakrishnan, V. *Nature* **2000**, *407*, 327.
(85) Carter, A. P.; Clemons, W. M.; Brodersen, D. E.; Morgan-Warren, R. J.; Wimberly, B. T.; Ramakrishnan, V. *Nature* **2000**, *407*, 340.
(86) Robicsek, A.; Strahilevitz, J.; Jacoby, G. A.; Macielag, M.; Abbanat, D.; Park, C. H.; Bush, K.; Hooper, D. C. *Nat Med* **2006**, *12*, 83.
(87) Neuhauser, M. M.; Weinstein, R. A.; Rydman, R.; Danziger, L. H.; Karam, G.; Quinn, J. P. *JAMA* **2003**, *289*, 885.
(88) Wolf, E.; Vassilev, A.; Makino, Y.; Sali, A.; Nakatani, Y.; Burley, S. K. *Cell* **1998**, *94*, 439.
(89) Javier Teran, F.; Alvarez, M.; Suarez, J. E.; Mendoza, M. C. *J Antimicrob Chemother* **1991**, *28*, 333.
(90) Hanessian, S.; Butterworth, R. F.; Nakagawa, T. *Carbohydr Res* **1973**, *26*, 261.
(91) Hanessian, S.; Masse, R.; Capmeau, M. L. *J Antibiot (Tokyo)* **1977**, *30*, 893.
(92) Hanessian, S.; Takamoto, T.; Masse, R. *J Antibiot (Tokyo)* **1975**, *28*, 835.
(93) Hanessian, S.; Vatele, J. M. *J Antibiot (Tokyo)* **1980**, *33*, 675.
(94) Greenberg, W. A.; Priestley, E. S.; Sears, P. S.; Alper, P. B.; Rosenbohm, C.; Hendrix, M.; Hung, S.-C.; Wong, C.-H. *J Am Chem Soc* **1999**, *121*, 6527.
(95) Ford, J. H.; Bergy, M. E.; Brooks, A. A.; Garrett, E. R.; Alberti, J.; Dyer, J. R.; Carter, H. E. *J Am Chem Soc* **1955**, *77*, 5311.
(96) da Silva, J. G.; Hyppolito, M. A.; de Oliveira, J. A.; Corrado, A. P.; Ito, I. Y.; Carvalho, I. *Bioorganic & medicinal chemistry* **2007**, *15*, 3624.
(97) Fridman, M.; Belakhov, V.; Yaron, S.; Baasov, T. *Org Lett* **2003**, *5*, 3575.
(98) Tatsuta, K. *Proc Jpn Acad Ser B Phys Biol Sci* **2008**, *84*, 87.
(99) Russell, R. J.; Murray, J. B.; Lentzen, G.; Haddad, J.; Mobashery, S. *J Am Chem Soc* **2003**, *125*, 3410.
(100) Cashman, D. J.; Rife, J. P.; Kellogg, G. E. *Bioorg Med Chem Lett* **2001**, *11*, 119.
(101) Zhanel, G. G.; Lawson, C. D.; Zelenitsky, S.; Findlay, B.; Schweizer, F.; Adam, H.; Walkty, A.; Rubinstein, E.; Gin, A. S.; Hoban, D. J.; Lynch, J. P.; Karlowsky, J. A. *Expert Rev Anti Infect Ther* **2012**, *10*, 459.
(102) Armstrong, E. S.; Miller, G. H. *Curr Opin Microbiol* **2010**, *13*, 565.
(103) Aggen, J. B.; Armstrong, E. S.; Goldblum, A. A.; Dozzo, P.; Linsell, M. S.; Gliedt, M. J.; Hildebrandt, D. J.; Feeney, L. A.; Kubo, A.; Matias, R. D.; Lopez, S.; Gomez, M.; Wlasichuk, K. B.; Diokno, R.; Miller, G. H.; Moser, H. E. *Antimicrob Agents Chemother* **2010**, *54*, 4636.
(104) Shaul, P.; Green, K. D.; Rutenberg, R.; Kramer, M.; Berkov-Zrihen, Y.; Breiner-Goldstein, E.; Garneau-Tsodikova, S.; Fridman, M. *Organic & biomolecular chemistry* **2011**, *9*, 4057.
(105) Kondo, S.; Hotta, K. *J Infect Chemother* **1999**, *5*, 1.
(106) Kawaguchi, H.; Naito, T.; Nakagawa, S.; Fujisawa, K. I. *J Antibiot (Tokyo)* **1972**, *25*, 695.
(107) Green, K. D.; Chen, W.; Houghton, J. L.; Fridman, M.; Garneau-Tsodikova, S. *Chembiochem* **2009**.

(108) Nudelman, I.; Chen, L.; Llewellyn, N. M.; Sahraoui, E.-H.; Cherniavsky, M.; Spencer, J. B.; Baasov, T. *Adv Synth Catal* **2008**, *350*, 1682.
(109) Llewellyn, N. M.; Spencer, J. B. *Chem Commun (Camb)* **2008**, 3786.
(110) WHO *Tuberculosis fact sheet 2011-2012* **2012**.
(111) Sepkowitz, K. A.; Raffalli, J.; Riley, L.; Kiehn, T. E.; Armstrong, D. *Clinical microbiology reviews* **1995**, *8*, 180.
(112) Sepkowitz, K. A. *Clin Infect Dis* **1995**, *20*, 232.
(113) WHO *Accelerating the implementation of collaborative TB HIV activities in the WHO european region, Vienna, Austri* **2010**.
(114) Sculier, D. *Priority research questions for TB HIV in HIV prevalent and resource limited settings, WHO* **2010**.
(115) Lawn, S. D.; Zumla, A. I. *Lancet* **2011**, *378*, 57.
(116) Jasmer, R. M.; Nahid, P.; Hopewell, P. C. *The New England journal of medicine* **2002**, *347*, 1860.
(117) WHO *Global tuberculosis control: epidemiology, strategy, financing* **2009**, 6.
(118) Yew, W. W.; Lange, C.; Leung, C. C. *The European respiratory journal : official journal of the European Society for Clinical Respiratory Physiology* **2011**, *37*, 441.
(119) *Tuberculosis* **2008**, *88*, 162.
(120) B, H.; ST., C. *International journal of antimicrobial agents* **1997**, *8*, 61.
(121) *British medical journal* **1948**, *2*, 769.
(122) Mitchison, D. A. *British medical bulletin* **1954**, *10*, 115.
(123) Canetti, G.; Rist, N.; Grosset, J. *The American review of respiratory disease* **1964**, *90*, 792.
(124) Mitchison, D. A. *American journal of respiratory and critical care medicine* **2005**, *171*, 699.
(125) Huebner, R. E.; Castro, K. G. *Annual review of medicine* **1995**, *46*, 47.
(126) Dutka-Malen, S.; Evers, S.; Courvalin, P. *Journal of clinical microbiology* **1995**, *33*, 1434.
(127) Doern, G. V.; Brueggemann, A.; Holley, H. P., Jr.; Rauch, A. M. *Antimicrob Agents Chemother* **1996**, *40*, 1208.
(128) Caminero, J. A. *The international journal of tuberculosis and lung disease : the official journal of the International Union against Tuberculosis and Lung Disease* **2006**, *10*, 829.
(129) Chan, E. D.; Laurel, V.; Strand, M. J.; Chan, J. F.; Huynh, M. L.; Goble, M.; Iseman, M. D. *American journal of respiratory and critical care medicine* **2004**, *169*, 1103.
(130) WHO *Tuberculosis MDR XDR 2011 progress report* **2011**.
(131) WHO *Report of the meeting of the WHO Global Task Force on XDR-TB, Geneva, Switzerland* **2006**.
(132) Banerjee, R.; Schecter, G. F.; Flood, J.; Porco, T. C. *Expert Rev Anti-Infe* **2008**, *6*, 713.
(133) Udwadia, Z. F.; Amale, R. A.; Ajbani, K. K.; Rodrigues, C. *Clin Infect Dis* **2012**, *54*, 579.
(134) Rowland, K. *Nature* **2012**.
(135) Velayati, A. A.; Masjedi, M. R.; Farnia, P.; Tabarsi, P.; Ghanavi, J.; Ziazarifi, A. H.; Hoffner, S. E. *Chest* **2009**, *136*, 420.
(136) Z, M.; C, L.; H, M.; AJ, N.; X., W. *Lancet* **2010**, *375*, 2100.
(137) E, L.; WN, R. *Expert Rev. Anti Infect. Ther.* **2010**, *8*, 801.
(138) Caminero, J. A.; Sotgiu, G.; Zumla, A.; Migliori, G. B. *Lancet Infect Dis* **2010**, *10*, 621.
(139) Ginsberg, A. M. *Tuberculosis (Edinb)* **2010**, *90*, 162.
(140) Chen, W.; Biswas, T.; Porter, V. R.; Tsodikov, O. V.; Garneau-Tsodikova, S. *Proc Natl Acad Sci U S A* **2011**, *108*, 9804.
(141) Green, K. D.; Chen, W.; Garneau-Tsodikova, S. *ChemMedChem* **2012**, *7*, 73.
(142) He, Z.; Li, S.; Zhou, X. *Curr Microbiol* **2011**.
(143) Lella, R. K.; Sharma, C. *The Journal of biological chemistry* **2007**, *282*, 18671.

(144) Roberts, E. A.; Clark, A.; McBeth, S.; Friedman, R. L. *J Bacteriol* **2004**, *186*, 5410.
(145) Samuel, L. P.; Song, C. H.; Wei, J.; Roberts, E. A.; Dahl, J. L.; Barry, C. E., 3rd; Jo, E. K.; Friedman, R. L. *Microbiology* **2007**, *153*, 529.
(146) Shin, D. M.; Jeon, B. Y.; Lee, H. M.; Jin, H. S.; Yuk, J. M.; Song, C. H.; Lee, S. H.; Lee, Z. W.; Cho, S. N.; Kim, J. M.; Friedman, R. L.; Jo, E. K. *PLoS Pathog* **2010**, *6*, e1001230.
(147) Wei, J.; Dahl, J. L.; Moulder, J. W.; Roberts, E. A.; O'Gaora, P.; Young, D. B.; Friedman, R. L. *J Bacteriol* **2000**, *182*, 377.
(148) Kim, K. H.; An, D. R.; Song, J.; Yoon, J. Y.; Kim, H. S.; Yoon, H. J.; Im, H. N.; Kim, J.; Kim do, J.; Lee, S. J.; Kim, K. H.; Lee, H. M.; Kim, H. J.; Jo, E. K.; Lee, J. Y.; Suh, S. W. *Proc Natl Acad Sci U S A* **2012**, *109*, 7729.
(149) Campbell, P. J.; Morlock, G. P.; Sikes, R. D.; Dalton, T. L.; Metchock, B.; Starks, A. M.; Hooks, D. P.; Cowan, L. S.; Plikaytis, B. B.; Posey, J. E. *Antimicrob Agents Chemother* **2011**, *55*, 2032.
(150) Chen, W.; Green, K. D.; Tsodikov, O. V.; Garneau-Tsodikova, S. *Biochemistry* **2012**.
(151) Vetting, M. W.; Park, C. H.; Hegde, S. S.; Jacoby, G. A.; Hooper, D. C.; Blanchard, J. S. *Biochemistry* **2008**, *47*, 9825.
(152) Carter, H. E.; Gottlieb, D.; Anderson, H. W. *Science* **1948**, *107*, 113.
(153) Shaw, W. V. *CRC Crit Rev Biochem* **1983**, *14*, 1.
(154) Martelo, O. J.; Manyan, D. R.; Smith, U. S.; Yunis, A. A. *J Lab Clin Med* **1969**, *74*, 927.
(155) Yunis, A. A.; Bloomberg, G. R. *Prog Hematol* **1964**, *4*, 138.
(156) Skolimowski, I. M.; Knight, R. C.; Edwards, D. I. *J Antimicrob Chemother* **1983**, *12*, 535.
(157) Nitzan, O.; Suponitzky, U.; Kennes, Y.; Chazan, B.; Raul, R.; Colodner, R. *Isr Med Assoc J* **2010**, *12*, 371.
(158) Dunkle, J. A.; Xiong, L.; Mankin, A. S.; Cate, J. H. *Proc Natl Acad Sci U S A* **2010**, *107*, 17152.
(159) Bulkley, D.; Innis, C. A.; Blaha, G.; Steitz, T. A. *Proc Natl Acad Sci U S A* **2010**, *107*, 17158.
(160) Ettayebi, M.; Prasad, S. M.; Morgan, E. A. *J Bacteriol* **1985**, *162*, 551.
(161) Anderson, L. M.; Henkin, T. M.; Chambliss, G. H.; Bott, K. F. *J Bacteriol* **1984**, *158*, 386.
(162) Baughman, G. A.; Fahnestock, S. R. *J Bacteriol* **1979**, *137*, 1315.
(163) Burns, J. L.; Hedin, L. A.; Lien, D. M. *Antimicrob Agents Chemother* **1989**, *33*, 136.
(164) Burns, J. L.; Rubens, C. E.; Mendelman, P. M.; Smith, A. L. *Antimicrob Agents Chemother* **1986**, *29*, 445.
(165) Burns, J. L.; Mendelman, P. M.; Levy, J.; Stull, T. L.; Smith, A. L. *Antimicrob Agents Chemother* **1985**, *27*, 46.
(166) Izard, T. *Protein Sci* **2001**, *10*, 1508.
(167) Izard, T.; Ellis, J. *EMBO J* **2000**, *19*, 2690.
(168) Mosher, R. H.; Camp, D. J.; Yang, K.; Brown, M. P.; Shaw, W. V.; Vining, L. C. *The Journal of biological chemistry* **1995**, *270*, 27000.
(169) Smith, A. L.; Erwin, A. L.; Kline, T.; Unrath, W. C.; Nelson, K.; Weber, A.; Howald, W. N. *Antimicrob Agents Chemother* **2007**, *51*, 2820.
(170) Schwarz, S.; Kehrenberg, C.; Doublet, B.; Cloeckaert, A. *FEMS Microbiol Rev* **2004**, *28*, 519.
(171) Shaw, W. V. *The Journal of biological chemistry* **1967**, *242*, 687.
(172) Shaw, W. V.; Unowsky, J. *J Bacteriol* **1968**, *95*, 1976.
(173) Bennett, A. D.; Shaw, W. V. *Biochem J* **1983**, *215*, 29.

Note:

This chapter is partially adapted from a published review article: **Houghton, J. L.**; Green, K. D.; Chen, W.; Garneau-Tsodikova, S. *ChemBioChem* **2010**, *11*, 880.

Chapter 2

Characterization of regio-promiscuity and regio-versatility of Eis *via* NMR spectroscopy

2.1. Abstract

The escalation of drug resistance, in many species of virulent bacteria, is a serious public health concern worldwide, and the emergence of drug-resistant tuberculosis (TB) is particularly troubling given the prevalence of the disease. One of the most recently characterized resistance mechanisms of TB is initiated by the expression of enhanced intracellular survival (Eis) protein. Eis has recently been shown to act as an unusually regio-versatile AAC, capable of multiply acetylating AGs, a characteristic unique among known AACs. It is known that Eis can sequentially modify the AG neamine (NEA) at 3 positions, but the reaction of additional AGs with Eis has not been characterized to date. Herein, we determined the number, position, and order of the acetylation of five additional AGs using NMR spectroscopy. These studies further our understanding of the capabilities of Eis as an AAC, and will guide future studies aimed at overcoming the resistance conferred by Eis.

2.2. Introduction

Antibacterial resistance is a growing health concern worldwide, and the emergence of resistance to many frontline and even second-line drugs is outpacing the discovery and development of novel, effective treatments against resistant infections. Bacterial communities naturally evolve such that resistance to the drugs employed against them arises through natural selection, and this process is often accelerated by improper treatment or poor patient compliance. Multidrug-resistant (MDR) and extensively drug-resistant (XDR) strains of the intracellular pathogen *Mycobacterium tuberculosis* (*Mtb*) are two prime examples of this paradigm that currently pose a serious, worldwide health

threat. It is estimated that there were 440,000 cases of MDR-TB that emerged in 2008 and over 1.6 million deaths related to *Mtb* infections in 2009. Our understanding of the resistance mechanisms adopted by MDR- and XDR-*Mtb* against second-line antibacterial therapies, such as the (AG) kanamycin A (KAN) and amikacin (AMK), is limited. Up-regulation of the enhanced intracellular survival (*eis*) gene bearing mutations in its promoter was the lone cause of KAN resistance in one-third of a large, diverse set *Mtb* clinical isolates,[1,2] and efforts to characterize the Eis protein are progressing rapidly.[1-11] The menace presented by drug-resistant strains of *Mtb* combined with our limited knowledge regarding the resistance mechanisms involved highlights a glaring gap in knowledge and serves as a limiting factor in our ability to keep pace with an aggressively evolving adversary.

The *eis* gene and its protein product, Eis, were discovered in *Mtb* H37Rv during an effort to identify *Mtb* genes necessary for survival within macrophages.[1] Bioinformatic analysis predicted that Eis belongs to the GCN5-related *N*-acetyltransferase (GNAT) family of proteins,[8] which was later supported by studies showing that overexpression of Eis leads to KAN resistance in *Mtb*.[10] GNAT proteins generally catalyze the transfer of an acetyl group from acetyl coenzyme A (AcCoA) to the primary amine of a substrate, liberating free coenzyme A (CoA) in the process. We have recently reported biochemical, spectroscopic, and crystallographic data confirming that Eis is an AAC that displays unusual regio-versatility against NEA and is capable of acetylating many other AGs, including those used as second-line MDR- and XDR-TB treatments such as KAN and AMK.[3]

To further understand the nature of Eis as an AAC, we characterized the reactions catalyzed by Eis with two sets of similar AG substrates. Tobramycin (TOB) (Fig. 2.5), KAN (Fig. 2.1), and AMK (Fig. 2.3) were chosen for their structural similarities, and the latter two compounds' relevance in the treatment of MDR- and XDR-TB. We also chose to investigate netilmicin (NET) and sisomicin (SIS) because they are both structurally distinct from TOB, KAN, and AMK, but nearly identical to one another, the *N*-1-ethyl group of NET being the only difference between the two structures. Using thin layer

chromatography (TLC) and nuclear magnetic resonance spectroscopy (NMR), we sought to determine the number, order, and regio-specificity of the multiple acetylations by Eis. We found that not only does Eis show a novel ability to catalyze multiple acetylations to each of the AGs studied, but also that these modifications occur at positions never before shown to be modified by other AACs.

2.3. Results: determination of positions of AGs modified by Eis *via* NMR and TLC

Eis exhibits unusual regio-versatility as an acetyltransferase, modifying some AGs as many as four times, which makes it unique among known AACs.[3] TLC may be used to qualitatively study the reaction progress of Eis with various AGs by following the appearance of compounds with increased retention factor (R_f) values, indicating acetylation has occurred. Side-by-side comparison of an Eis-modified AG to the analogous AG product formed by other AACs with known specificity allows for the prediction, and in some cases identification of the Eis-modified products (Table 2.1 and Figs. 2.1-2.5). AACs capable of acetylating the 6'-, 2'-, 3-, and 1-amines of various AGs have been reported, and examples of each, except AAC(1), were applied in this study. AAC(1) was reported in the past but is very rare and our significant efforts to obtain DNA or plasmids with the gene were not successful.

Table 2.1. R_f values[a] of mono- and di-, acetylated AGs by the AAC(2')-Ic, AAC(3)-IV, AAC(6'), and Eis proteins.

		Enzymes utilized												
		None	(2')[e]	(3)[f]	(6')[g]	(3)/(2')	(6')/(2')	(6')/(3)	Eis					
AG									1 min	5 min	10 min	30 min	2 h	O/N
AMK	Parent[b]	0.06							0.06	0.06	0.06	0.06		
	Mono[c]		×[h]	×[i]	0.10					0.10 / 0.36	0.10 / 0.36	0.10 / 0.36	0.36	
	Di[d]					×[h]	×[h]	×[i]					0.46	0.46
KAN	Parent	0.28							0.28					
	Mono		×[h]	0.33	0.43				0.33	0.33 / 0.43	0.33 / 0.43	0.33 / 0.43	0.33	
	Di					×[h]	×[h]	0.49					0.56	0.56
NET	Parent	0.06							×[j]	×[j]	×[j]		×[j]	
	Mono		×[j]	×[j]	0.26							0.26		
	Di					--[k]	0.37	0.41						0.37
SIS	Parent	0.05												
	Mono		0.08	0.16	0.24				0.24	0.24	0.24	0.24	0.24	
	Di					0.23	0.26	0.30						0.24 - 0.30
TOB	Parent	0.24							0.24	0.24				
	Mono		0.27	0.36	0.48				0.48	0.29[l] / 0.48	0.48	0.48		
	Di					--[k]	--[k]	0.71			0.62	0.62	0.62	0.62

[a]The eluent systems used for TLCs were 5:2/MeOH:NH_4OH, 5:2/MeOH:NH_4OH, 25:1/MeOH:NH_4OH, 12:1/MeOH:NH_4OH, and 5:2/MeOH:NH_4OH for AMK, KAN, NET, SIS, and TOB, respectively. [b]Parent indicates no acetylation. [c]Mono indicates mono-acetylation. [d]Di indicates di-acetylation. [e](2') indicates AAC(2')-Ic. [f](3) indicates AAC(3)-IV. [g](6') indicates AAC(6') of the AAC(6')/APH(2"). [h]× Because the 2'-NH_2 does not exist in AMK or KAN, these controls were not performed. [i]×AMK is not a substrate for AAC(3)-IV. [j]×These reactions were not performed. [k]-- Indicates that the di-acetylated product could not be visualized as it had an R_f value overlapping with that of the glycerol in the reaction mixture or as the sequential use of enzymes did not work in these cases. [l]Based on NMR analysis, this spot most likely corresponds to the 3"-acetyl-TOB.

To determine the position and order of the multiple acetylation reactions carried out by Eis, we first compared the R_f of Eis-modified AMK, KAN, SIS, NET, and TOB to the 3-, 2'-, and 6'-acetyl counterparts, and when applicable, to the 6',3-, 6',2'-, and 3,2'-*N*-di-acetyl compounds formed by sequential acylation, as previously described (Table 2.1 and Figs. 2.1-2.5).[3,12] No combination of AACs was found to be capable of generating tri-acetylated AGs.

Previous studies indicated that KAN and AMK were di-acetylated by Eis, and the *N*-1 AHB-containing AMK could be tri-acetylated to some extent, as determined by liquid chromatography-mass spectrometry (LCMS), but the positions modified and the order in which those acetylations occurred was not established.[3] The reaction progress followed by TLC indicated that KAN rapidly underwent two acetylations, but the modifications were not sequential in nature. The R_f value of the di-acylated KAN product of Eis did not match the product of any other AAC, or sequential combination thereof, capable of modifying KAN (Table 2.1 and Fig. 2.1). The R_f values of two of the intermediate mono-acetylated products did closely correlate to the 6'- and 3-*N*-acetyl-KAN (Table 2.1 and Fig. 2.1). The reaction was scaled up and the di-acetylated product was purified by flash chromatography for NMR analysis. A comparison of the 1D- and 2D-NMR spectra of KAN (Figs. 2.14-2.18) to the di-acetylated KAN product (Figs. 2.19-2.23) clearly indicated that the reactions occurred at the 6'-amine and the 3"-amine (Fig. 2.1 and Tables 2.4 and 2.5), showing Eis to be the first AAC reported to acetylate an AG at the 3"- position. TLC analysis of the Eis reaction with AMK suggested that as many as three total mono- or di-acetylated products may be formed over the course of the reaction, and that, similarly to KAN, their formation was not sequential in nature. AMK is only a good substrate for AAC(6') of all the enzymes used in this study, limiting the information that could be gathered from TLC experiments (Table 2.1 and Fig. 2.2).

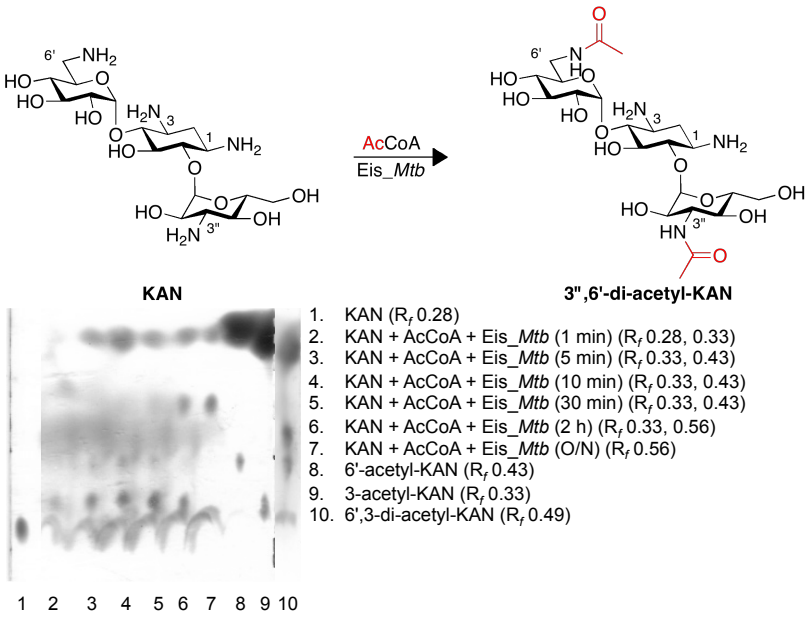

Fig. 2.1. The di-acetylation of KAN by Eis.

Of the three products formed by Eis that are visible over the course of the reaction, that with the lowest R_f value closely matched that of 6'-*N*-acetyl AMK (Table 2.1 and Fig. 2.2). The reaction was scaled up and purified by flash chromatography for NMR analysis. In order to reduce the amount of costly materials, namely AcCoA, and hasten the characterization process, our method was adapted to use solely ^{1}H-detected NMR studies. In doing so, we eliminated superfluous data that was ultimately unnecessary for the analysis of the products while at the same time greatly reducing the cost and amount of instrument time required. The results indicated that the ultimate product of the Eis reaction with AMK was di-acetylated (Fig. 2.2), similarly to KAN. However, in this case comparison of the AMK standard (Figs. 2.7-2.9) to those of the product (Figs. 2.10-2.13) showed that the reactions had taken place at the 3"-position and the γ-amine of the AHB moiety as determined by NMR (Fig. 2.2 and Table 2.3), making Eis the first AAC reported to modify the AHB of an AG.

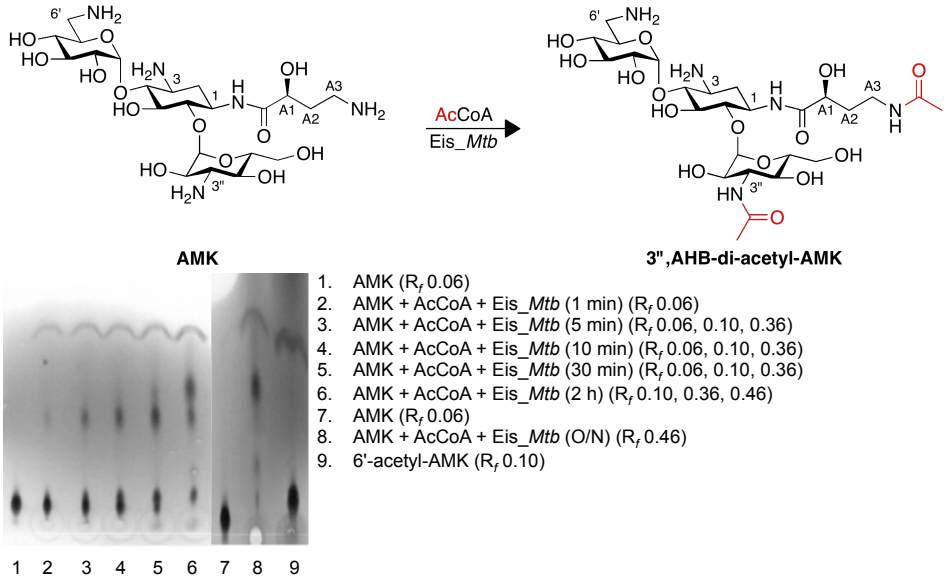

Fig. 2.2. The di-acetylation of AMK by Eis.

Time-course TLC analysis of the acetylation of SIS and NET by Eis showed that the reactions proceeded in a sequential manner and that the second sites of acetylation were converted significantly more slowly than with KAN, AMK, or TOB. For both SIS and NET, TLC indicated that Eis specifically and rapidly acetylated a single amine, and by comparing the R_f value of the Eis products to those of known AACs indicated the 6'-amine was likely the acetylated position in both cases (Table 2.1 and Fig. 2.3). This was then followed by a single, much slower reaction in the case of NET. SIS underwent two such slower reactions, but it was unclear whether the products observed were di-acetylated, tri-acetylated, or a mixture of both di- and tri-acetylated. In order to definitively determine the order of acetylation, we once again adapted our method. The experiments were designed so that the reaction progress was monitored in solution by NMR, negating the need for time-consuming purification of the products. The molar equivalents of AcCoA were regulated in order to control the reaction progress so that all NMR experiments on the mono-acetylated products could be performed before the subsequent acetylations had occurred.

Monitoring the reaction progress of NET with Eis by TLC indicated that the 6'-position was likely the first to be modified, based on the similarity of the R_f of the first Eis product

with that known to be 6'-*N*-acetyl-NET (Table 2.1 and Fig. 2.3). NMR analysis of a reaction mixture containing a 1:1 ratio of AcCoA and NET with Eis showed rapid, complete conversion (>95%) of NET (Table 2.6 and Figs. 2.24-2.26) to 6'-*N*-acetyl-NET (Table 2.6 and Figs. 2.27-2.29), as was predicted by TLC. Addition of a second equivalent of AcCoA yielded a single di-acetylated product. This second sequential acetylation occurred at the 2'-amine to give the 6',2'-*N*-di-acetyl NET product (Table 2.7 and Fig. 2.3), as determined by 1D- and 2D-NMR (Table 2.7 and Figs. 2.30-2.32).

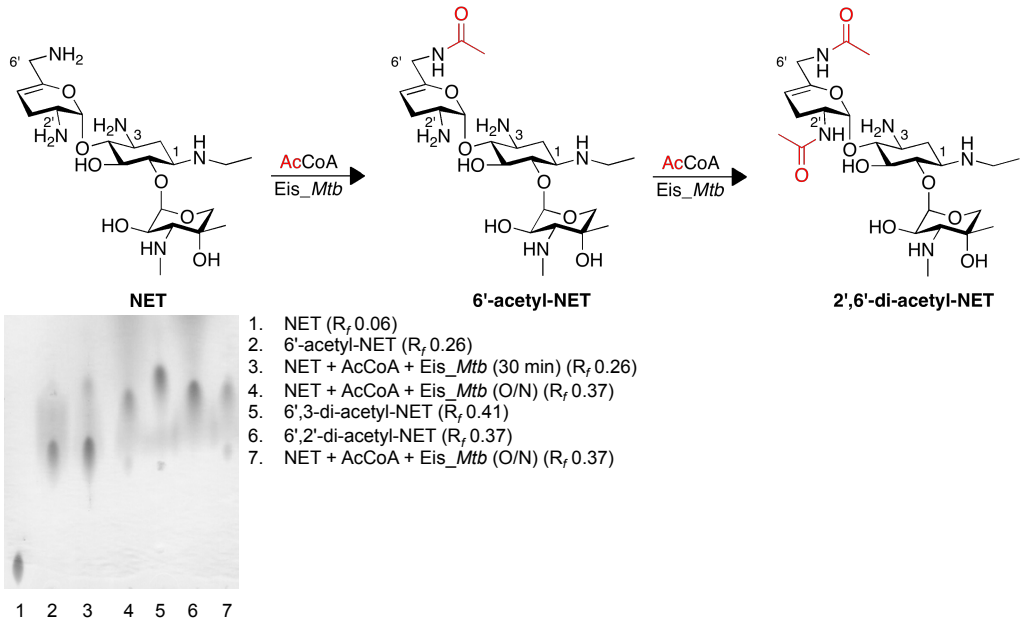

Fig. 2.3. The di-acetylation of NET by Eis.

Similarly to NET, the conversion of SIS by Eis, as monitored by TLC, indicated that the 6'-position was likely the first to be modified by Eis (Fig. 2.4 and Table 2.1). At first, the NMR analysis was carried out identically as with NET using a reaction mixture containing a 1:1 ratio of AcCoA and SIS. Complete conversion (>95%) of SIS (Figs. 2.33-2.38 and Table 2.8) into 6'-*N*-acetyl-SIS (Figs. 2.39-2.41 and Table 2.8) was observed as indicated by 1D- and 2D-^{1}H NMR. TLC experiments of the Eis reaction showed that like NET, SIS also underwent further reactions, but in this case two different products were formed. Comparison of the R_f values of the two additional SIS Eis products to those of known di-acetylated SIS products, indicated a close correlation to the 6',2'- and 6',3-*N*-di-acetyl-SIS (Fig. 2.4 and Table 2.1). The secondary Eis products

formed much more slowly than in the previous cases, and due to the slow hydrolysis of AcCoA under the conditions, an additional 4 molar equivalents of AcCoA were required to drive the reaction to completion (>95% conversion from the 6'-product). The CoA, formed upon reaction with Eis in addition to that formed by hydrolysis of the thioether of AcCoA, significantly hindered our ability to fully characterize the peaks of interest and consequently, a mixture of the two products was purified by flash chromatography for further NMR experiments. The relatively small difference in R_f values made complete separation of the two desired products extremely difficult, and as such, a mixture of the two compounds was used for NMR studies.

Analysis of the NMR data indicated that SIS was converted into two distinct di-acetylated products by Eis (Figs. 2.42-2.47 and Table 2.9), and that a tri-acetylated product was not formed in significant enough quantity to be detected by NMR. One of the products was unambiguously determined to be 6',2'-*N*-di-acetyl-SIS (Figs. 2.42-2.47 and Table 2.9). The second di-acetylated product was modified by Eis on the central 2-deoxystreptamine (2-DOS) ring, at either the 1- or 3-position (Figs. 2.42-2.47 and Table 2.9). The exact position could not be assigned with certainty, due to the symmetrical nature of the 2-DOS ring, but 1-*N*-acetylation is suspected because no 3-*N*-acetylation by Eis has been observed.

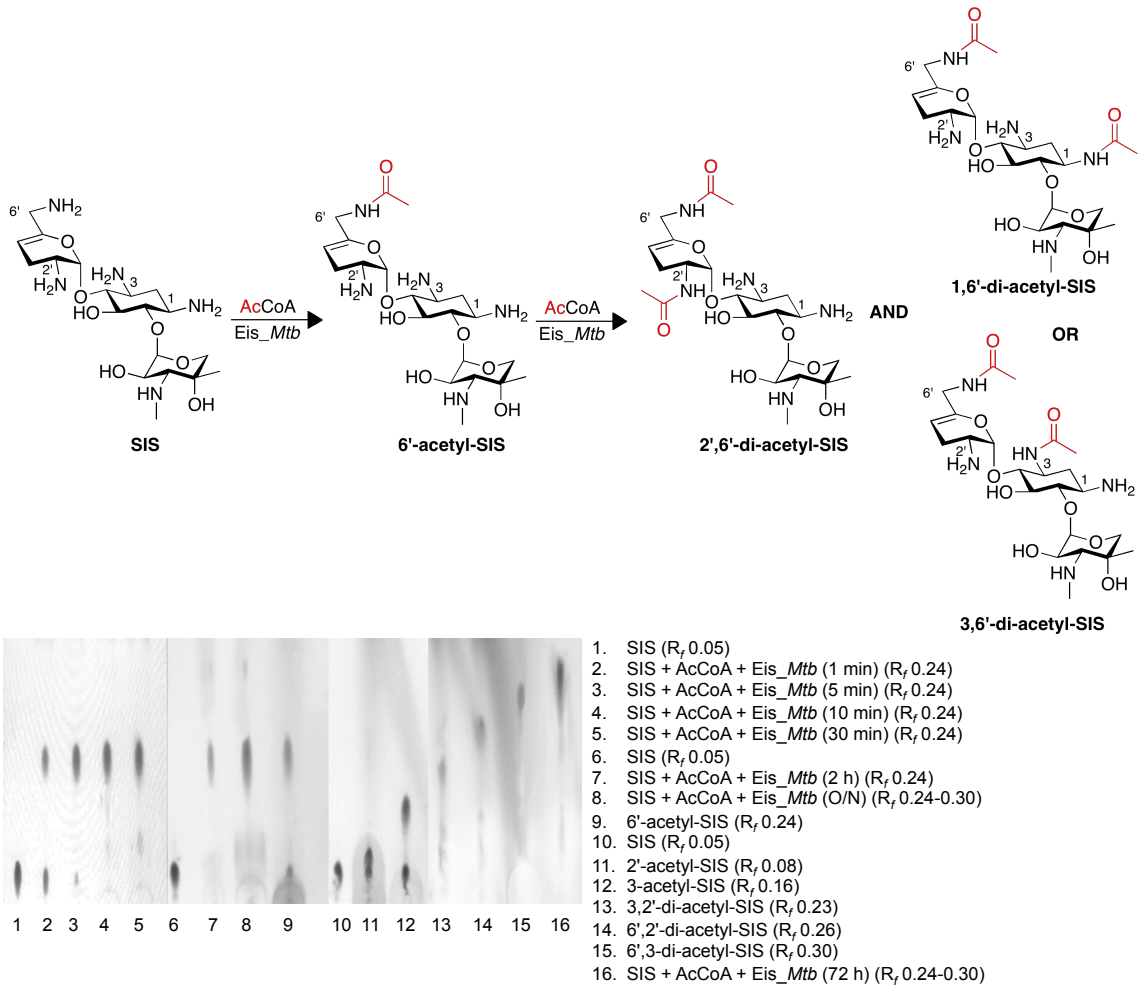

Fig. 2.4. The multiple di-acetylations of SIS by Eis.

Previous studies have shown qualitatively that TOB may be acetylated as many as four times by Eis, as determined by LCMS.[3] Reactions monitored by TLC indicated that TOB was di-acetylated (Fig. 2.5 and Table 2.1), but the modifications were not sequential, similar to KAN and AMK. Comparison of the R_f values of the Eis product to those with AACs of known specificity indicated that one of the mono-acetylated compounds formed en route to the di-acetylated products was likely modified at the 6'-amine (Fig. 2.5 and Table 2.1). NMR analysis of the reaction with Eis using a 1:1 ratio of TOB and AcCoA indicated that two products formed in an approximately 3:2 ratio (data not shown). Addition of a second molar equivalent of AcCoA resulted in the complete conversion of TOB to a single, di-acetylated product. 1D- and 2D-NMR analysis indicated that TOB

(Figs. 2.48-2.50 and Table 2.9) was converted to 6',3"-di-acetyl TOB (Figs. 2.51-2.53 and Table 2.9) similarly to KAN (Fig. 2.5).

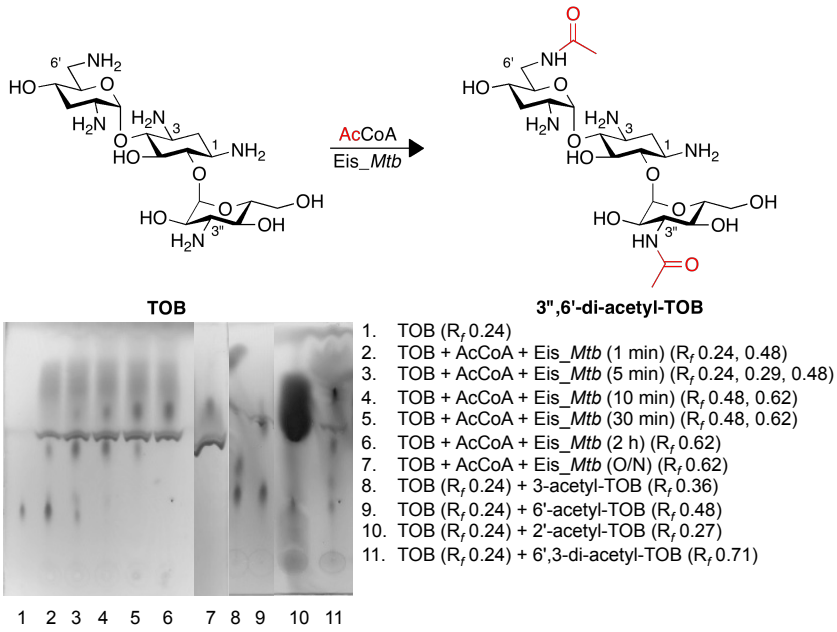

Fig. 2.5. The di-acetylation of TOB by Eis.

2.4. Discussion

Herein, we have reported that Eis is the first and only AAC reported that is capable of modifying either the 3"- or 1-*N*-AHB moiety of an AG in a manner dependent on the scaffold of the AG. Not only is it the first AAC that has shown regio-versatility as previously reported, but, since the acetylation pattern varies with the particular AG scaffold presented to Eis, it also the first and only AAC to demonstrate regio-promiscuity. Previous studies with Eis showed that it was capable of tri-acetylating NEA, a small AG that contains 4 primary amines (1, 3, 2', and 6') on two aminocyclitol rings, rather than the three or four ring system common to most AGs.[3] The novel regio-versatility was a surprising result because no other AACs had been proven to perform multiple acetylations on the same AG. However, the 1-, 3-, 2'-, and 6'-amines are all known to be modified on AGs by AACs belonging to one or another of the four classes previously reported in the literature. Furthermore, the number of acetylations performed by Eis on a particular AG was always observed to be less than or equal to the total number of 1-, 3-, 2', and 6'-amines present on the same AG. As such, the discovery that Eis not only shows unprecedented activity towards the amines at the 3"- and γ-amine of AHB, but also

acetylates various amine positions based on the chemical structure of a given AG makes it unique among AG-modifying enzymes (AMEs).

Three different patterns of acetylation were observed with the three distinct AG scaffolds investigated. The patterns of acetylation seen on the chemically distinct scaffold of NET and SIS are relatively unsurprising because, as seen with NEA, there were multiple acetylations but only in positions known to be modified by other AACs. The reasons for the sequential nature of the reactions of Eis with SIS and NET are unclear. A probable explanation for the trend seen with KAN, AMK, and TOB is that there exist (at least) two possible binding orientations in which the AGs may initially bind with similar affinities that will ultimately lead to acetylation. Since KAN, AMK, and TOB are di-acetylated by Eis in random order, it stands to reason that two of the possible binding orientations are in an equilibrium that does not significantly favor one over the other, allowing either of the respective positions to be acetylated. Conversely, NMR and TLC analysis suggests that there is one orientation that is initially preferred with SIS as well as one for NET that leads to complete conversion at the 6'-amine before a second acetylation may occur, suggesting the corresponding 6'-acetyl compound is the substrate for the second, slower reaction.

TOB, which has distinct molecular scaffold compared to NET and SIS and a similar scaffold to KAN and AMK, behaved more similarly to KAN and AMK, showing a random order of acetylation and identical pattern of acetylation to that of KAN with Eis. It would be reasonable to expect that one of the AGs that undergo a sequential acetylation might be a better candidate for crystallization, and further attempts to obtain unambiguous structures with the other 4 compounds are currently underway in our laboratory.

2.5. Conclusions

That fact that Eis modifies AGs in a way that varies from AG to AG is at the same time very interesting as well as very alarming in terms of the evolution of antibiotic resistance. The development of novel, synthetically modified AGs that avoid resistance enzymes,

reduce toxicity, and improve antimicrobial activity has been the goal of numerous research efforts. Together, the lack of effective treatments for TB and the increasing number and severity of outbreaks of MDR- and XDR-TB highlight a situation that requires prompt action within the scientific community. The combined versatility and promiscuity of Eis, particularly toward the AHB moiety which has been shown to improve many AGs when incorporated at the *N*-1 position, will make it particularly difficult to develop novel AGs as treatments, suggesting another course of action may be necessary. Developing inhibitors of bacterial resistance enzymes, such as the β-lactamase inhibitor clavulanic acid, has been a successful means of overcoming an analogous problem associated with β-lactam antibiotics such as ampicillin, and studies to this affect with Eis have been performed.[4,13]

We have shown that Eis is the most regio-versatile and regio-promiscuous AAC characterized to date. Its role in conferring resistance to AGs used in the treatment of TB is a serious concern, as few drugs are efficient treatments. The overall lack of effective treatments is exacerbated by the development and rapid spread of MDR- and XDR-TB. We are left to ask whether the expanded AG modifying capabilities of Eis as an AAC is the next advancement in bacteria's defensive arsenal or just an isolated evolutionary coincidence? If this type of capability starts expanding to other bacteria, it may mean that AGs begin to see an even smaller role as useful therapies against many types of bacteria. In any case, it highlights both the necessity to develop next generation antibacterial drugs, as well as the need to advance our understanding of these processes as thoroughly and rapidly as possible.

2.6. Materials and instrumentations

The Eis,[3] AAC(2')-Ic,[3] AAC(3)-IV,[12] and AAC(6')/APH(2")[12] enzymes were overexpressed and purified as previously described. For sake of simplicity, in the text that follows we will refer to the bifunctional AAC(6')/APH(2") enzyme as AAC(6') since none of the reactions performed in this study contain a nucleotide substrate for the APH(2") domain of this enzyme. Acetyl-CoA (AcCoA) and aminoglycosides (AGs) (AMK, KAN, and SIS) were bought from Sigma-Aldrich (Milwaukee, WI) (Fig. 2.1).

The AGs NET and TOB were purchased from AK Scientific (Mountain View, CA) (Fig. 2.1.). TLCs (Merck, Silica gel 60 F_{254}) were visualized using a cerium-molybdate stain ($(NH_4)_2Ce(NO_3)_6$ (5 g), $(NH_4)_6Mo_7O_{24}•4H_4O$ (120 g), H_2SO_4 (80 mL), H_2O (720 mL)). AMK, KAN, and SIS acetylated products were purified by SiO_2 flash chromatography (Dynamic Absorbents 32-63 m). ^1H, ^{13}C, gCOSY, gHMBC, gHSQC, and zTOCSY NMR spectra were recorded either on a Bruker Avance III^{TM} 600 MHz spectrometer equipped with a 3 mm cryo-probe, a Varian 400 MHz equipped with a 5 mm OneProbe, or a Varian 500 MHz equipped with a 3 mm OneProbe, as indicated in the figure legends of the NMR spectra. All NMR spectra were recorded either in D_2O or in 9:1/H_2O:D_2O at either pH 3.0 or 8.0, as indicated in the appropriate figure captions. LCMS was performed on a Shimadzu LCMS-2019EV equipped with a SPD-20AV UV-Vis detector and a LC-20AD liquid chromatograph.

2.7. Methods

2.7.1. Determination of amine positions acetylated by Eis on AMK, KAN, NET, SIS, and TOB

2.7.1.1. TLC assays

In order to establish the amine positions acetylated by Eis on AMK, KAN, NET, SIS, and TOB, we first performed TLC assays. Control experiments were done with three AG acetyltransferases of known specificity (AAC(2')-Ic, AAC(3)-IV, and AAC(6')) that were confirmed by us by UV-Vis assays and LCMS to acetylate only at the 2'-, 3-, and 6'-positions, respectively (whenever available) of all AG substrates used in this study. The eluent system utilized for all TLCs of reactions performed with AMK, KAN, NET, SIS, and TOB were 5:2/MeOH:NH_4OH, 5:2/MeOH:NH_4OH, 25:1/MeOH:NH_4OH, 12:1/MeOH:NH_4OH, and 5:2/MeOH:NH_4OH, respectively. The R_f values observed are reported in Table S1. The exact reaction conditions are reported below. The R_f values of the various mono- and di-acetylated AGs are reported in section 2.3 of the main text (Table 2.1).

2.7.1.1.1. Control TLCs of AGs mono-acetylated at the 2'-, 3-, and 6'-position by AAC(2')-Ic, AAC(3)-IV, and AAC(6'), respectively

Reactions (15 μL) were carried out at rt in MES buffer (50 mM, pH 6.6 adjusted at rt) for AAC(3)-IV and AAC(6') or in Na_2HPO_4 buffer (100 mM, pH 7.0 adjusted at rt) for AAC(2')-Ic in the presence of AcCoA (0.96 mM, 1.2 eq), AG (0.8 mM, 1 eq), and AAC enzyme (10 μM). After overnight incubation, aliquots (5 μL) of the reaction mixtures were loaded onto a TLC plate and eluted with the proper eluent system.

2.7.1.1.2. Control TLCs of AGs di-acetylated sequentially by pairwise treatment with AAC(2')-Ic, AAC(3)-IV, and AAC(6')

Di-acetylation reactions for use as reference standards were carried out by sequentially using the following pairs of enzymes: (i) AAC(6') followed by AAC(2')-Ic, (ii) AAC(3)-IV followed by AAC(2')-Ic, or (iii) AAC(6') followed by AAC(3)-IV. Reactions (10 μL) were carried out at rt in MES buffer (50 mM, pH 6.6 adjusted at rt) in the presence of AcCoA (1.92 mM, 2.4 eq), AG (0.8 mM, 1 eq), and the first AAC enzyme (10 μM). After overnight incubation, the second AAC enzyme (10 μM) was added to the reaction mixture, which was incubated for at least an additional 16 h. Aliquots (5 μL) of each di-acetylation reaction mixture were loaded onto a TLC plate and eluted with the proper eluent system.

2.7.1.1.3. TLCs of the time course of multi-acetylation of KAN, AMK, NET, SIS, and TOB by Eis

Reactions (30 μL) were carried out at rt in Tris-HCl buffer (50 mM, pH 8.0 adjusted at rt) in the presence of AcCoA (4 mM, 5 eq), AGs (0.8 mM, 1 eq), and Eis (5 μM). Aliquots (4 μL) were loaded onto a TLC plate after 0, 1, 5, 10, 30, and 120 min as well as after overnight incubation and eluted with the proper eluent system. R_f values are reported in section 2.3 of the main text (Table 2.1).

2.7.1.2. Mass spectrometry analysis of the multi-acetylated AMK, KAN, NET, SIS, and TOB Eis products

The masses of the AGs multi-acetylated by Eis were obtained by LCMS in positive ion mode using H_2O (0.1% formic acid) after dilution of the NMR samples described below (1 μL of 15 mM stock) with H_2O (1 mL) and injection of 20 μL (Table 2.2 and Fig. 2.6).

Table 2.2. Mass analysis of aminoglycosides (AGs) acetylated by Eis.

AG		Calculated $[M]^+$	Observed $[M+H]^+$
AMK	Di[a]	669.31	670.35
KAN	Di	568.26	569.30
NET	Mono[b]	517.31	518.35
	Di	559.32	560.30
SIS	Di	531.29	532.35 (554.20 +Na)
TOB	Di	551.28	552.25 (574.20 +Na)

[a]Di indicates di-acetylation. [b] Mono indicates mono-acetylation.

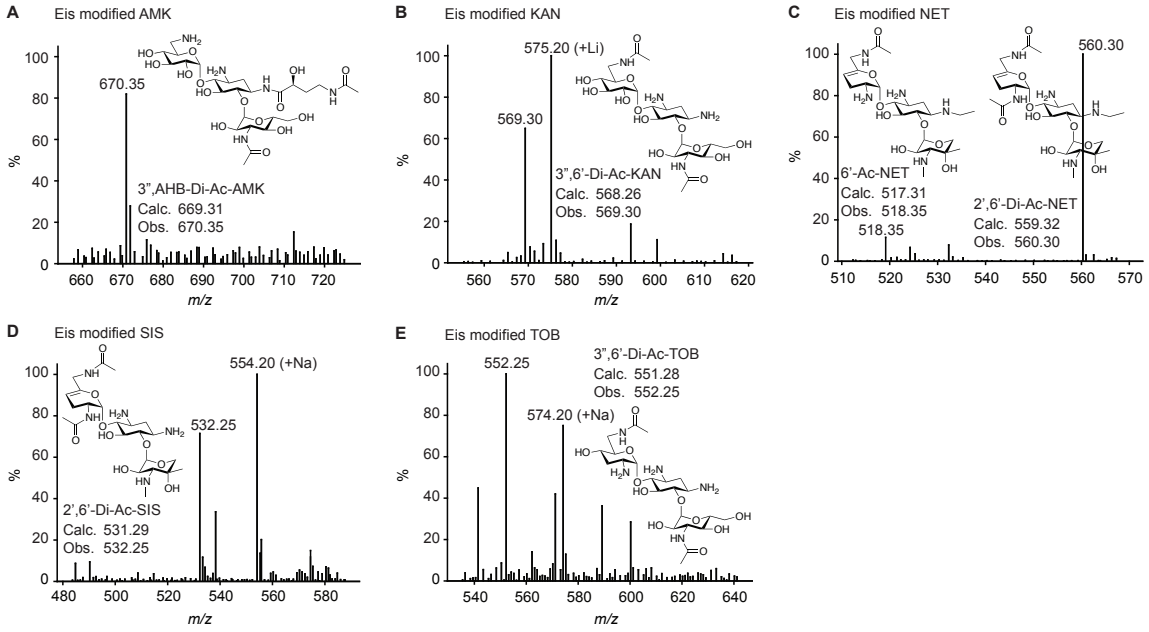

Fig. 2.6. Mass spectra of Eis-AG reaction products studied in this work.

2.7.1.3. NMR analysis of the multi-acetylated AMK, KAN, NET, SIS, and TOB Eis products

2.7.1.3.1. Di-acetylation of AMK by Eis and NMR analysis of the 3",AHB-di-acetyl-AMK product

To determine which two positions of AMK are acetylated by Eis, a reaction was performed to yield sufficient amount of product for NMR analysis. Briefly, a reaction mixture (4 mL) containing AMK (5 mM, 1 eq), AcCoA (20 mM, 4 eq), and Eis (0.5 mg/mL) in Na_2HPO_4 buffer (50 mM, pH 8.0 adjusted at rt; *Note*: Na_2HPO_4 replaced Tris-HCl to simplify purification) was incubated with gentle shaking at rt for 24 h prior to supplementing with additional portions of AcCoA (5 mM) and Eis (0.1 mg/mL) followed by further incubation for 48 h (*Note*: the reaction was pH adjusted using 1.0 M KOH solution prior to addition of enzyme as necessary to maintain pH 8.0). The progress of the Eis reaction was monitored by TLC. After >90% conversion of AMK into di-acetyl-AMK, the Eis enzyme was removed by addition of an equal volume of MeOH, cooling to 4 °C for 30 min, and centrifugation (15,000 rpm, 10 min, rt). The solution was separated from the precipitate and the solvents evaporated under reduced pressure. The residue was purified by flash chromatography (SiO_2) using a gradient of 0.0-2.0% Et_3N in MeOH. Fractions containing the product were pooled and the solvents removed under reduced pressure. The residue was dissolved in minimal volume of D_2O, adjusted to pH 3 with dilute sulfuric acid (0.5%), and lyophilized to give 3",AHB-di-acetyl-AMK as a white powder. For NMR analyses, 3",AHB-di-acetyl-AMK was dissolved in D_2O (400 mL), centrifuged (15,000 rpm, 10 min, rt) to remove any particulate, and the supernatant collected for analysis. The positions of acetylation, purity, and structure identification were confirmed by ^1H, zTOCSY, and gCOSY NMR as well as LCMS. Proton connectivity was assigned using zTOCSY and gCOSY spectra. Representative spectra for 3",AHB-di-acetyl-AMK are provided (Figs. 2.10-2.13).

To unambiguously establish the two acetylated positions on the AMK scaffold, the NMR spectra of the di-acetylated-AMK were compared to those of a standard of pure non-acetylated AMK (Tables 2.3). The sample of AMK for NMR was prepared as described for the 3",AHB-di-acetyl-AMK NMR sample. Additionally, the compound was prepared

in 9:1/H_2O:D_2O and both a ^1H and a zTOCSY spectra of the compound were obtained at 600 MHz resolution in order to resolve the amide bonds for further confirmation of the structure. Representative spectra for AMK are provided (Figs. 2.7-2.9)

Table 2.3. Proton chemical shifts determined for AMK and 3",AHB-di-acetyl-AMK.[a]

Ring	H position	AMK	3",AHB-di-acetyl-AMK	Δppm
II	1	4.10-3.95 (m)[b] [4.06][c]	4.14-4.00 (m) [4.07]	0.01
	2_{ax}	1.80 (m)	1.87-1.70 (m) [1.80]	0.00
	2_{eq}	2.22-2.09 (m) [2.19]	2.23-2.17 (m) [2.20]	0.01
	3	3.53 (m)	3.65-3.40 (m) [3.56]	0.03
	4	3.90-3.80 (m) [3.85]	3.95-3.65 (m) [3.90]	0.05
	5	3.90-3.80 (m) [3.88]	3.95-3.65 (m) [3.90]	0.02
	6	3.90-3.80 (m) [3.83]	3.95-3.65 (m) [3.84]	0.01
	C=OC<u>H</u>(OH)$CH_2CH_2NH_2$ (A1)	4.24 (dd, $J_{A1,A2a}$ = 2.8 Hz, $J_{A1,A2b}$ = 9.4 Hz)	[4.12] (dd, $J_{A1,A2a}$ = 2.8 Hz, $J_{A1,A2b}$ = 9.4 Hz)	-0.12
	C=OCH(OH)C<u>H_2</u>CH_2NH_2 ($A2_a$)	1.93 (m)	1.87-1.70 (m) [1.74]	-0.19
	C=OCH(OH)C<u>H_2</u>CH_2NH_2 ($A2_b$)	2.13 (m)	2.03-1.92 (m) [1.98]	-0.15
	C=OCH(OH)CH_2C<u>H_2</u>NH_2 (A3)	3.18-3.10 (m) [3.15]	3.31-2.26 (m) [3.29]	**0.14**
I	1'	5.54 (d, $J_{1',2'}$ = 3.6 Hz)	5.57 (d, $J_{1',2'}$ = 3.7 Hz)	0.03
	2'	368-3.62 (m) [3.63]	3.95-3.65 (m) [3.66]	0.03
	3'	3.80-3.70 (m) [3.74]	3.95-3.65 (m) [3.78]	0.04
	4'	3.37-3.32 (m) [3.35]	3.35 (dd (app. t), $J_{4',3'} = J_{4',5'}$ = 9.5 Hz)	0.00
	5'	4.10-3.95 (m) [3.98]	4.14-4.00 (m) [4.02]	0.04
	$6'_a$	3.43-3.31 (m) [3.41]	3.65-3.40 (m) [3.45]	0.04
	$6'_b$	3.18-3.10 (m) [3.14]	3.14 (dd, J = 13.3 Hz, J = 8.7 Hz)	0.00
III	1"	5.14 (d, $J_{1",2"}$ = 3.3 Hz)	5.13 (d, $J_{1",2"}$ = 3.7 Hz)	-0.01
	2"	3.80-3.70 (m) [3.75]	3.65-3.40 (m) [3.51]	-0.24
	3"	3.37-3.32 (m) [3.36]	4.14-4.00 (m) [4.05]	**0.69**
	4"	368-3.62 (m) [3.66]	3.65-3.40 (m) [3.46]	-0.20
	5"	4.10-3.95 (m) [4.05]	4.14-4.00 (m) [4.08]	0.03
	$6"_a$	3.87-3.72 (m) [3.78]	3.95-3.65 (m) [3.78]	0.00
	$6"_b$	3.87-3.72 (m) [3.76]	3.95-3.65 (m) [3.72]	-0.04
Amide	N<u>H</u>-1	7.62[‡]	8.52 (d, J = 9.8 Hz)*	
	C=OCH(OH)(C<u>H_2</u>)$_2$N<u>H</u>-C=OCH_3	×	8.00 (t, J = 6.2 Hz)*	
	N<u>H</u>-3"	×	8.08 (d, J = 10.4 Hz)*	
Acetyl	C<u>H_3</u>C=O on AHB	×	1.97 (s)	
	C<u>H_3</u>C=O on 3"	×	2.03 (s)	

[a]The chemical shift were established based on ^1H (400 MHz), zTOCSY, and gCOSY NMR. [b]Multiplicity and J are given in (). [c]The numbers in [] were determined from gCOSY and zTOCSY. *Indicates that the values were determined from spectra taken in 9:1/H_2O:D_2O at 600 MHz. ×Indicates that the acetyl moiety is not present in the molecule. [‡]Detected in the zTOCSY (400 MHz).

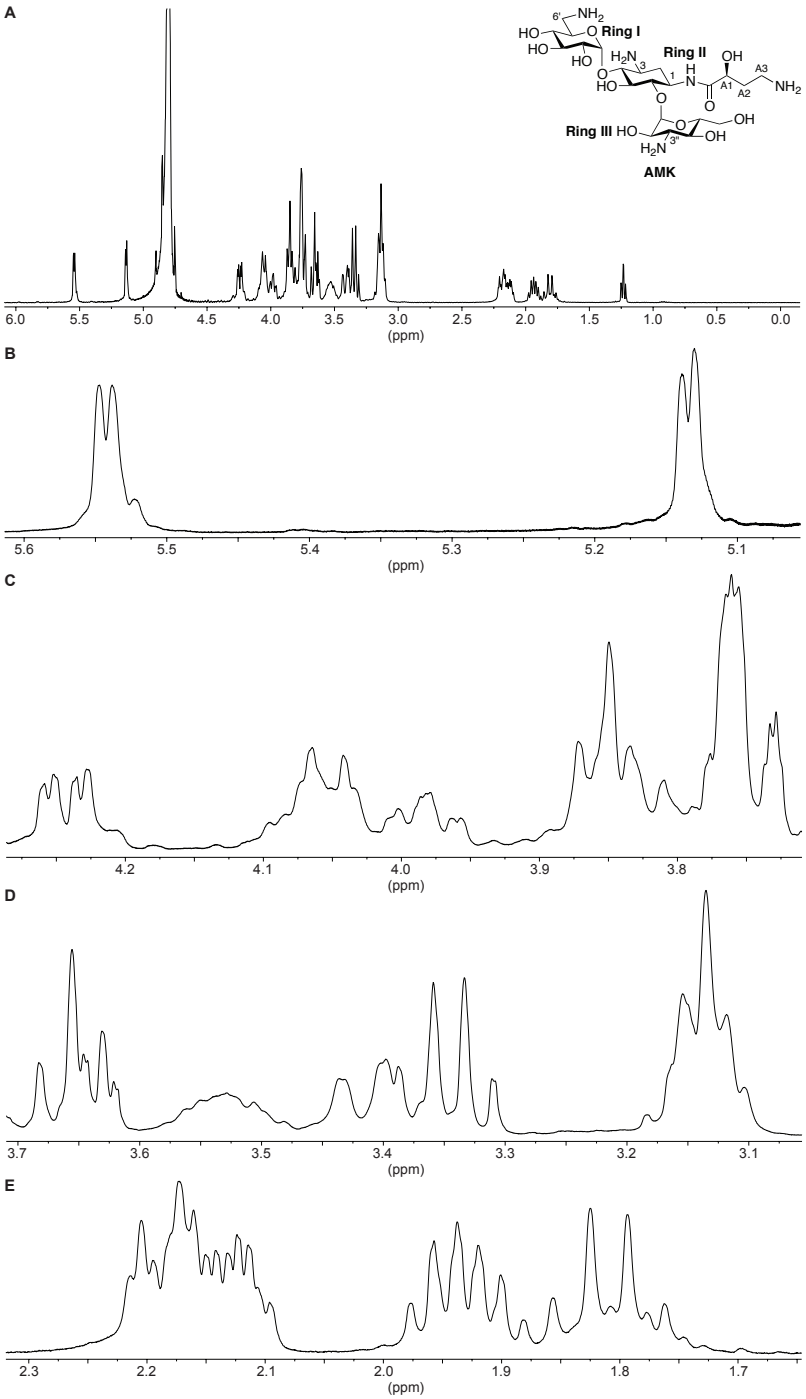

Fig. 2.7. ^{1}H NMR of AMK in D_2O at pH 3 (400 MHz). The full spectrum is shown in panel **A** and the expansions in panels **B-E**.

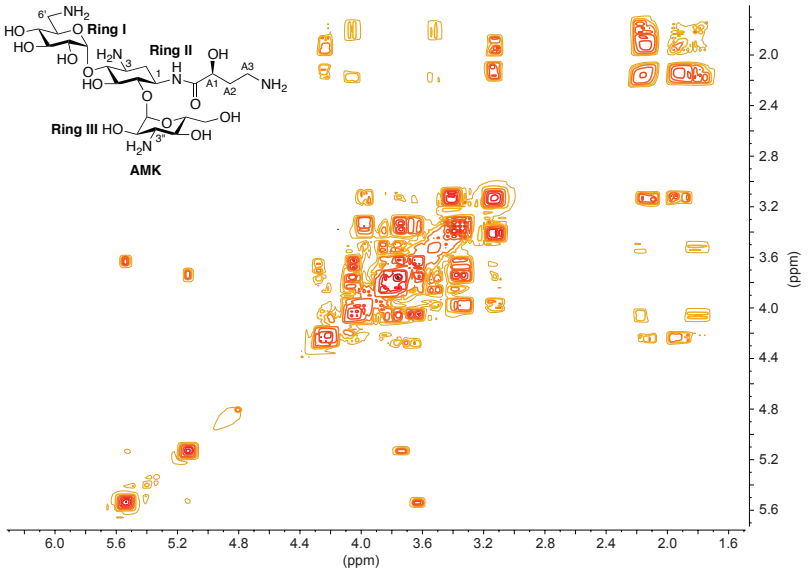

Fig. 2.8. gCOSY of AMK in D_2O at pH 3 (400 MHz).

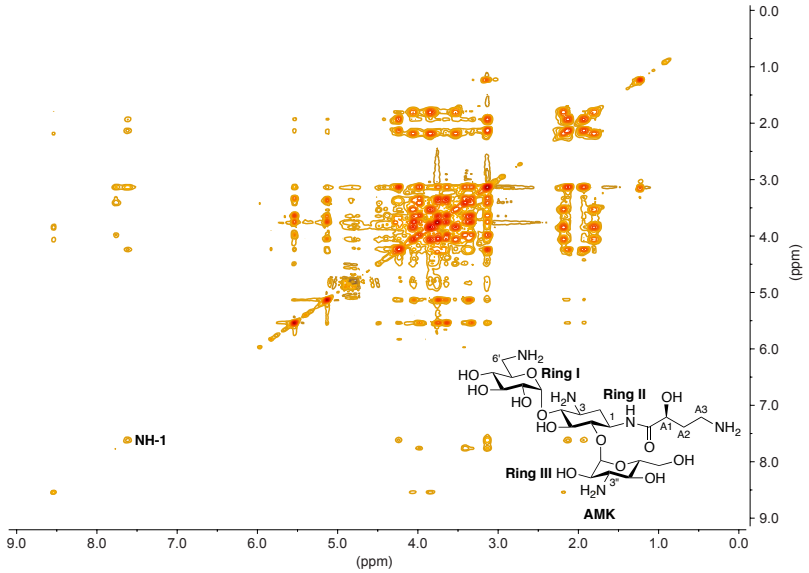

Fig. 2.9. zTOCSY of AMK in D_2O at pH 3 (400 MHz).

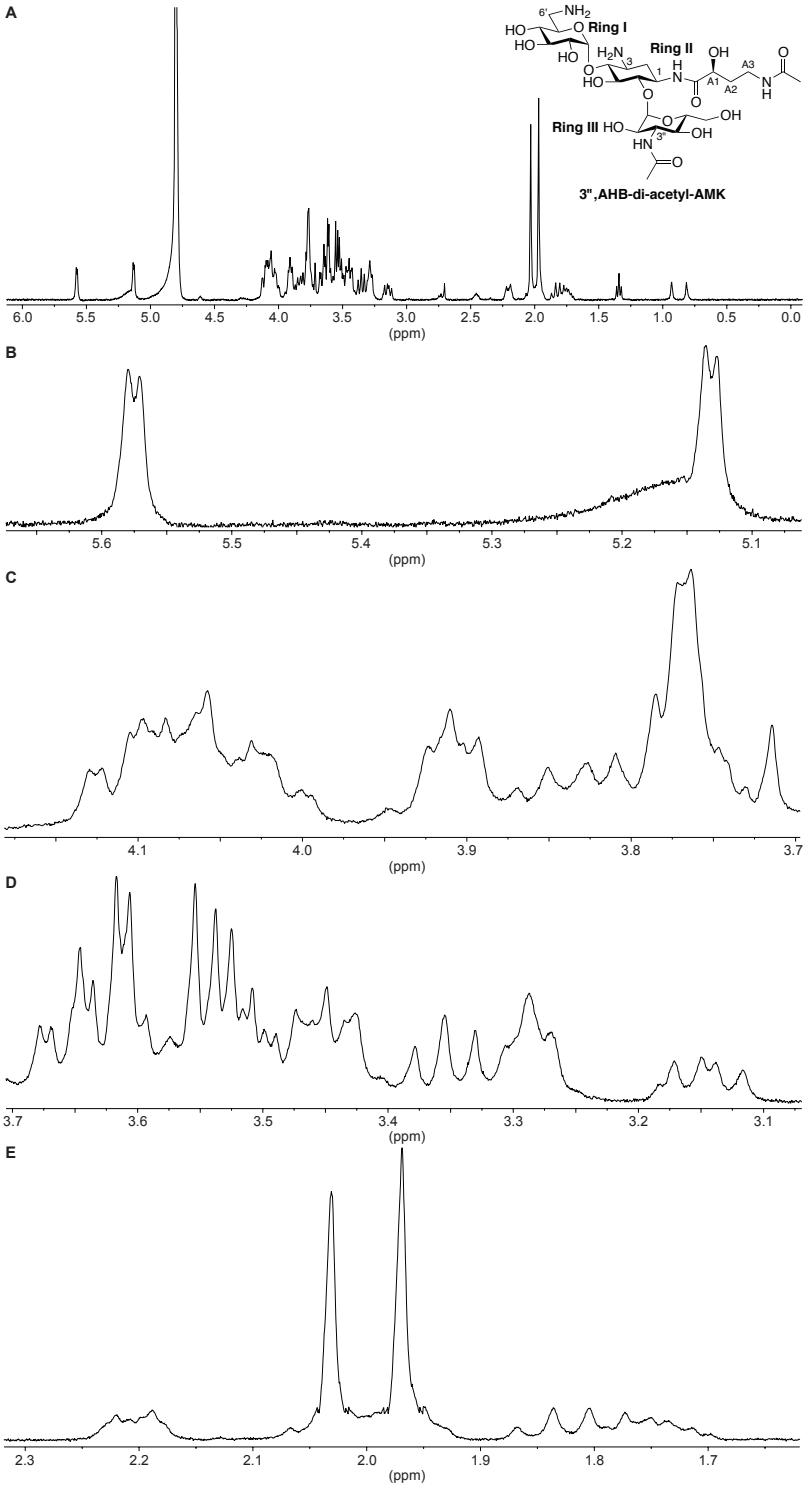

Fig. 2.10. ^{1}H NMR of 3",AHB-di-acetyl-AMK in D_2O at pH 3 (400 MHz). The full spectrum is shown in panel **A** and the expansions in panels **B-E**.

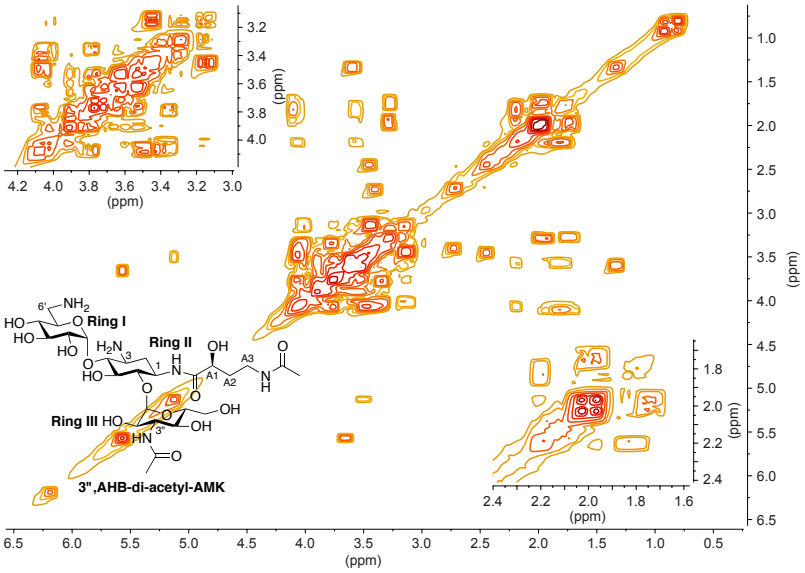

Fig. 2.11. gCOSY of 3",AHB-di-acetyl-AMK in D_2O at pH 3 (400 MHz). The inserts show portions of the spectrum more clearly.

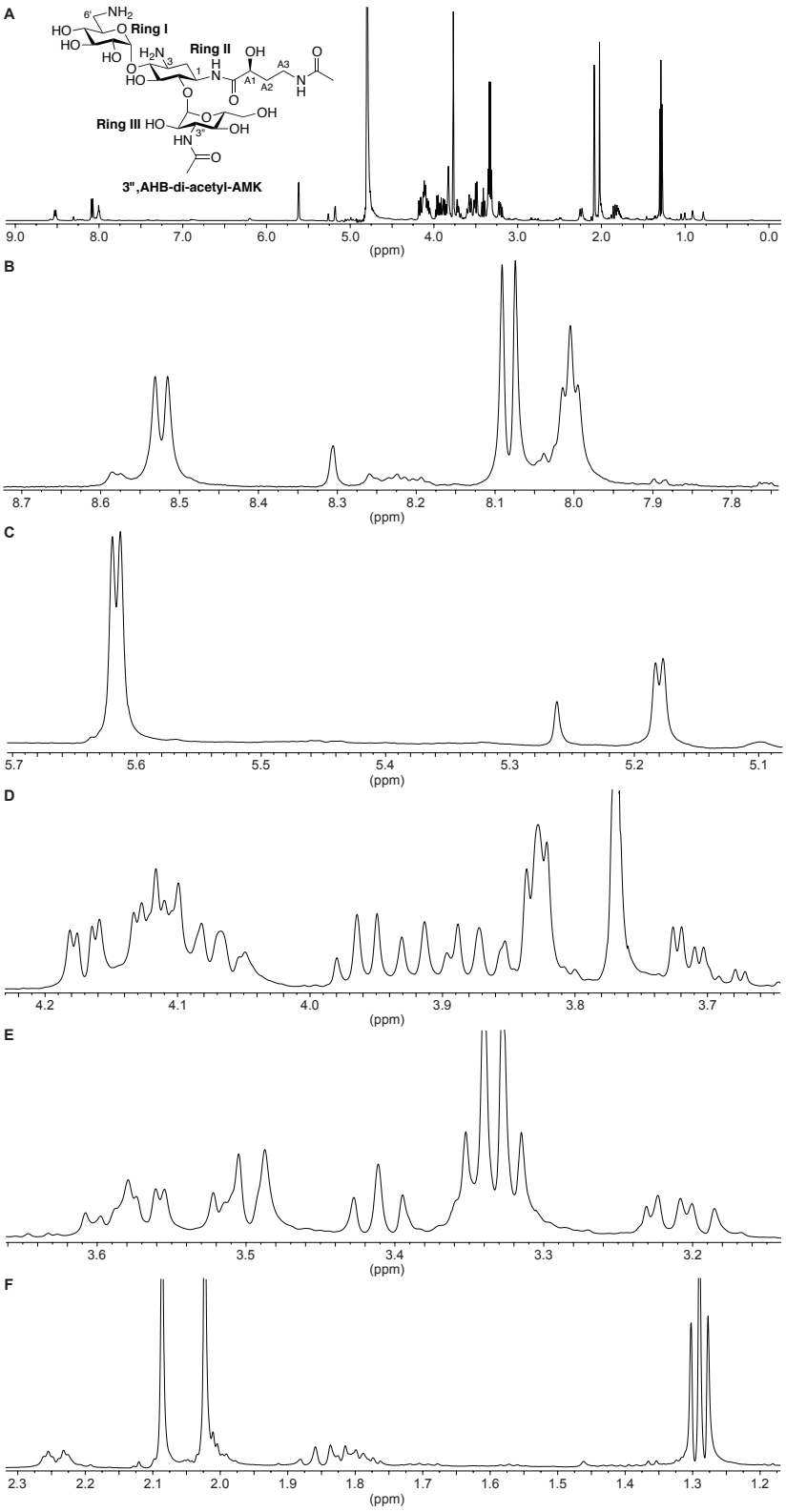

Fig. 2.12. ^{1}H NMR of 3",AHB-di-acetyl-AMK in 9:1/H_2O:D_2O (600 MHz). The full spectrum is shown in panel **A** and the expansions in panels **B-F**.

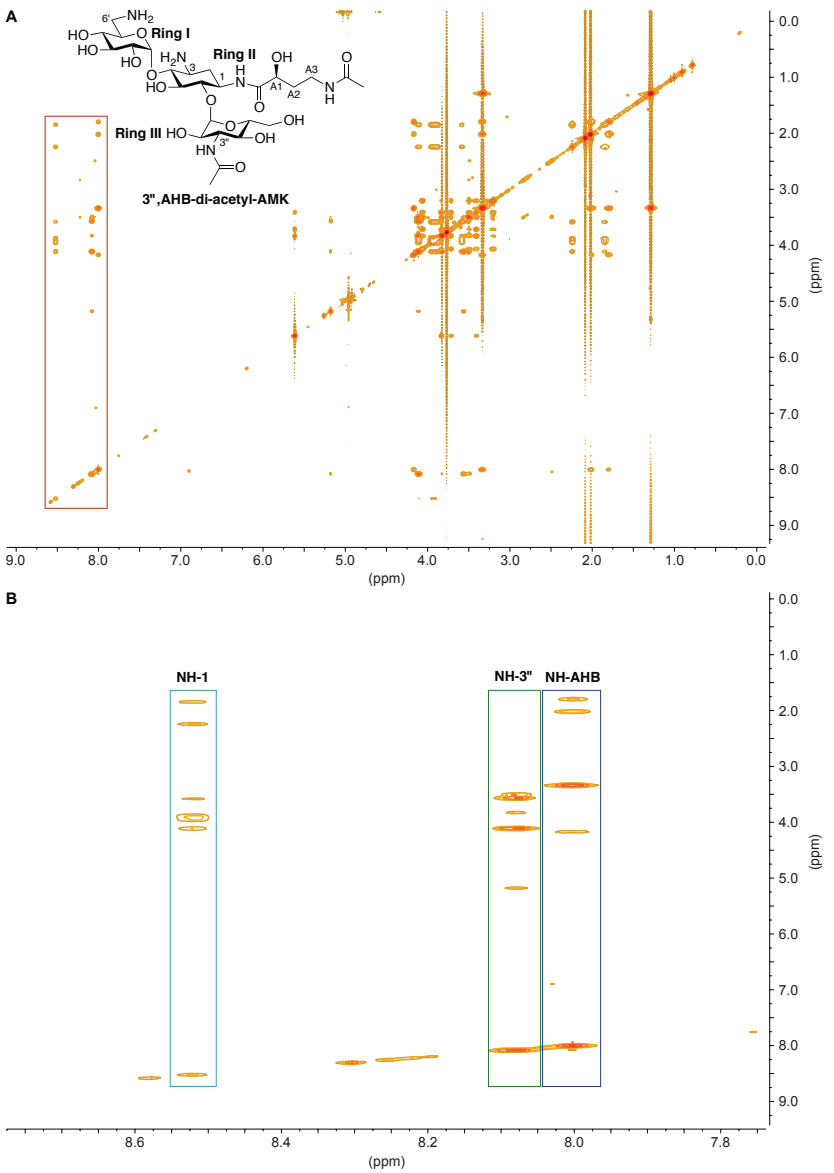

Fig. 2.13. zTOCSY of 3",AHB-di-acetyl-AMK in 9:1/H_2O:D_2O (600 MHz). The full spectrum is shown in panel **A** and the expansion showing the amide protons coupling to the protons at the 1-, 3"-, and AHB-positions in panel **B**. A red box in panel **A** indicates the portion of the spectrum expanded and shown in panel **B**. In panel **B**, the coupling of the amide protons at the 1-, 3"-, and A3 of the AHB-positions are indicated by turquoise, green, and blue boxes, respectively.

2.7.1.3.2. Di-acetylation of KAN by Eis and NMR analysis of the 3",6'-di-acetyl-KAN product

To determine which two positions of KAN are acetylated by Eis, a reaction was performed to yield sufficient amount of product for NMR analysis. Briefly, a reaction mixture (4 mL) containing KAN (5 mM, 1 eq), AcCoA (20 mM, 4 eq), and Eis (0.5 mg/mL) in Na_2HPO_4 buffer (50 mM, pH 8.0 adjusted at rt; *Note*: Na_2HPO_4 replaced Tris-HCl to simplify purification) was incubated with gentle shaking at rt for 24 h prior to addition of supplementing with additional portions of AcCoA (5 mM) and Eis (0.1 mg/mL) followed by further incubation for 48 h (*Note*: the reaction was pH adjusted prior to addition of enzyme as necessary to maintain pH 8.0). The progress of the Eis reaction was monitored by TLC. After >90% conversion of KAN into di-acetyl-KAN, the Eis enzyme was removed by addition of an equal volume of MeOH, cooling to 4 °C for 30 min, and centrifugation (15,000 rpm, 10 min, rt). The solution was separated from the precipitate and the solvents evaporated under reduced pressure. The residue was purified by flash chromatography (SiO_2) using a gradient of 0.0-2.0% Et_3N in MeOH. Fractions containing the product were pooled and the solvents removed under reduced pressure. The residue was dissolved in minimal volume of D_2O, adjusted to pH 3 with dilute sulfuric acid (0.5%), and lyophilized to give 3",6'-di-acetyl-KAN as a white powder. For NMR analyses, 3",6'-di-acetyl-KAN was dissolved in D_2O (400 μL), centrifuged (15,000 rpm, 10 min, rt) to remove any particulate, and the supernatant collected for analysis. The positions of acetylation, purity, and structure identification were confirmed by ^{1}H, ^{13}C, gCOSY, gHMBC, and gHSQC NMR as well as LCMS. Proton connectivities were assigned using ^{1}H, zTOCSY, and gCOSY spectra. Signals of all carbons were assigned using the ^{13}C, gHSQC, and gHMBC spectra. Representative spectra for 3",6'-di-acetyl-KAN are provided (Figs. 2.19-2.23).

To unambiguously establish the two acetylated positions on the KAN scaffold, the ^{1}H and ^{13}C NMR spectra of the di-acetylated-KAN were compared to those of a standard of pure non-acetylated KAN (Tables 2.4-2.5). The sample of KAN for NMR was prepared as described for the 3",6'-di-acetyl-KAN NMR sample. Representative spectra for KAN are provided (Figs. 2.14-2.18).

Table 2.4. Proton chemical shifts determined for KAN and 3",6'-di-acetyl-KAN.[a]

Ring	H position	KAN	3",6'-di-acetyl-KAN	Δppm
II	1	3.61-3.54[b] (m)[c] [3.59][d]	3.63-3.45 (m) [3.53]	-0.06
	2_{ax}	2.02 (ddd (app. q), $J_{2ax,2eq} = J_{2ax,1} = J_{2ax,3} = 12.5$ Hz)	1.93 (ddd (app. q), $J_{2ax,2eq} = J_{2ax,1} = J_{2ax,3} = 12.8$ Hz)	-0.09
	2_{eq}	2.54 (ddd (app. dt), $J_{2eq,2ax} = 12.5$ Hz, $J_{2eq,1} = J_{2eq,3} = 4.0$ Hz)	2.54 (ddd (app. dt), $J_{2eq,2ax} = 12.8$ Hz, $J_{2eq,1} = J_{2eq,3} = 4.2$ Hz)	0.00
	3	3.61-3.54[b] (m) [3.57]	3.63-3.45 (m) [3.59]	0.02
	4	4.01-3.89[c] (m) [3.90]	3.94-3.66 (m) [3.85]	-0.05
	5	3.84-3.74 (m) [3.81]	3.94-3.66 (m) [3.73]	-0.08
	6	4.01-3.89[c] (m) [3.95]	3.94-3.66 (m) [3.90]	-0.05
I	1'	5.62 (d, $J_{1',2'} = 3.9$ Hz)	5.45 (d, $J_{1',2'} = 3.9$ Hz)	-0.17
	2'	3.64 (dd, $J_{1',2'} = 3.9$ Hz, $J_{2',3'} = 10.1$ Hz)	3.60 (dd, $J_{2',1'} = 3.9$ Hz, $J_{2',3'} = 9.8$ Hz)	-0.04
	3'	3.84-3.74 (m) [3.78]	3.94-3.66 (m) [3.72]	-0.06
	4'	3.35 (dd (app. t), $J_{4',3'} = J_{4',5'} = 9.5$ Hz)	3.51-3.43 (m) [3.31]	-0.04
	5'	4.01-3.89 (m) [3.96]	3.94-3.66 (m) [3.81]	-0.15
	$6'_a$	3.45 (dd, $J_{6'a,6'b} = 13.3$ Hz, $J_{6'a,5'} = 2.9$ Hz)	3.65-3.45 (m) [3.60]	**0.15**
	$6'_b$	3.14 (dd, $J_{6'b,6'a} = 13.3$ Hz, $J_{6'b,5'} = 8.7$ Hz)	3.65-3.45 (m) [3.52]	**0.38**
III	1"	5.14 (d, $J_{1",2"} = 3.9$ Hz)	5.07 (d, $J_{1",2"} = 3.5$ Hz)	-0.07
	2"	4.01-3.89 (m) [3.93]	3.69 (dd, $J_{1",2"} = 3.5$ Hz)[†]	-0.24
	3"	3.50 (dd (app. t), $J_{3",2"} = J_{3",4"} = 10.5$ Hz)	4.11 (dd (app. t), $J_{3",2"} = J_{3",4"} = 10.3$ Hz)	**0.61**
	4"	3.69 (dd (app. t), $J_{4",3"} = J_{4",5"} = 10.5$ Hz)	3.49 (dd (app. t), $J_{4",3"} = J_{4",5"} = 10.3$ Hz)[†]	-0.20
	5"	4.01-3.89 (m) [3.93]	3.94-3.66 (m) [3.93]	-0.00
	$6"_a$	3.84-3.74 (m) [3.81]	3.94-3.66 (m) [3.80]	-0.01
	$6"_b$	3.84-3.74 (m) [3.78]	3.94-3.66 (m) [3.76]	-0.02
Acetyl	N<u>H</u>-3"	×	8.14 (d, $J_{NH,3"} = 9.7$ Hz)	
	N<u>H</u>-6'	×	8.06 (t, $J_{NH,6'} = 6.0$ Hz)	
	C<u>H</u>$_3$C=O on 3"	×	2.04 (s)	
	C<u>H</u>$_3$C=O on 6'	×	2.00 (s)	

[a]The chemical shift were established based on ^{1}H (400 MHz), zTOCSY, and gCOSY NMR. [b]Could be analogous position of the 2-deoxystreptamine (DOS) ring. [c]Multiplicity and *J* are given in (). [d]The numbers in [] were determined from gCOSY and/or zTOCSY. [e]Could be analogous position of the DOS ring. ×Indicates that the acetyl moiety is not present in the molecule. [†]Indicates partially obscured peak preventing determination of the second *J* value.

Table 2.5. Carbon chemical shifts determined for KAN and 3",6'-di-acetyl-KAN.[a]

Ring	C position	KAN[b]	3",6'-di-acetyl-KAN	Δppm
II	1	47.69	48.15	0.46
	2	27.36	27.50	0.14
	3	49.67	49.63	-0.04
	4	77.33	79.06	1.73
	5	83.70	83.45	-0.25
	6	72.72	72.95	0.23
I	1'	95.82	97.70	1.88
	2'	70.64	70.95	0.31
	3'	71.83	72.01	0.18
	4'	70.94	70.14	-0.95
	5'	68.56	71.08	2.52
	6'	40.34	39.44	**-0.90**
III	1"	100.40	100.84	0.44
	2"	68.06	69.99	1.93
	3"	54.77	53.85	**-0.92**
	4"	65.30	66.92	1.62
	5"	72.56	72.80	0.24
	6"	59.73	60.09	0.36
Acetyl	CH$_3$<u>C</u>=O on 3"	×	175.20	
	CH$_3$<u>C</u>=O on 6'	×	174.57	
	<u>C</u>H$_3$C=O	×	22.0	
	<u>C</u>H$_3$C=O	×	21.7	

[a]The chemical shift were established based on ^{13}C, gHSQC, and gHMBC NMR. ×Indicates that the acetyl moiety is not present in the molecule.

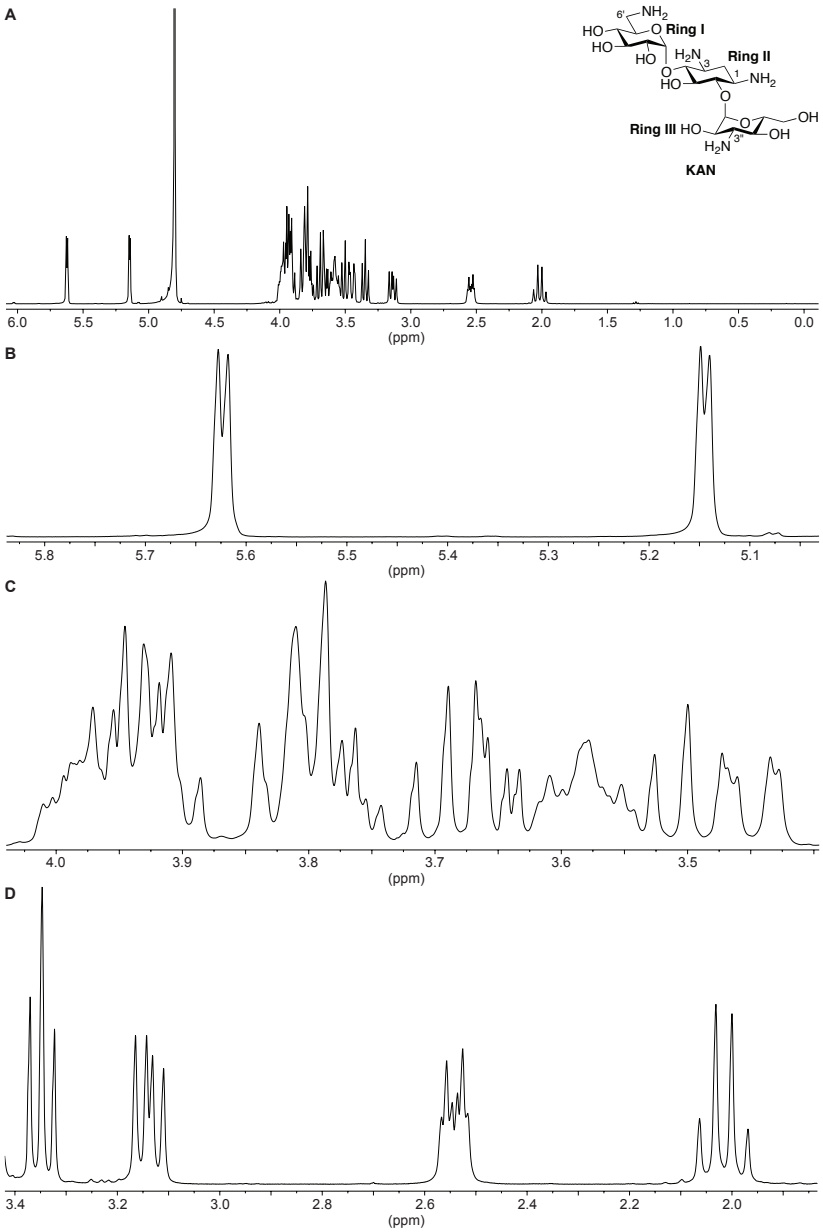

Fig. 2.14. ^{1}H NMR of KAN in D_2O at pH 3 (400 MHz). The full spectrum is shown in panel **A** and the expansions in panels **B-D**.

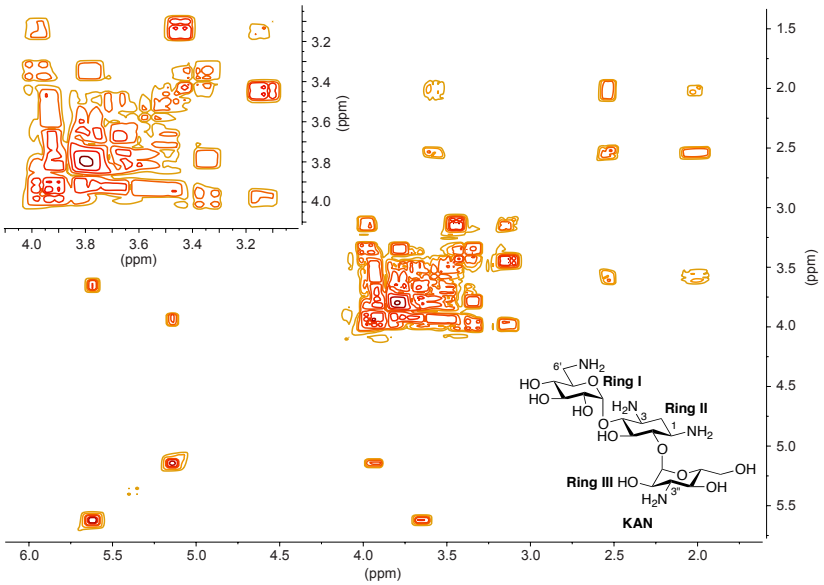

Fig. 2.15. gCOSY of KAN in D_2O at pH 3 (400 MHz). The insert shows a portion of the spectrum more clearly.

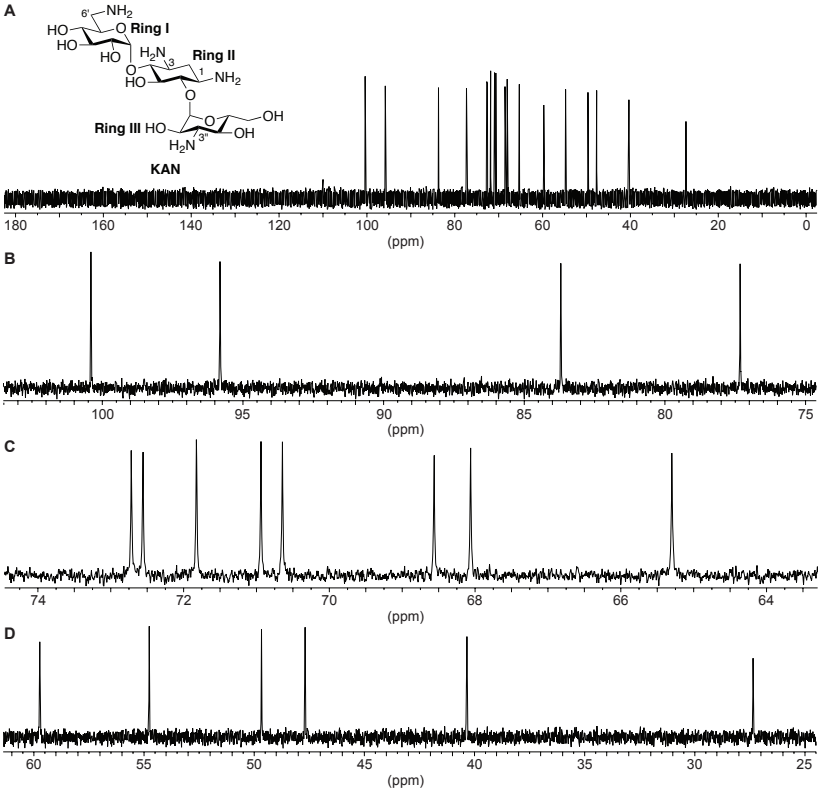

Fig. 2.16. ^{13}C NMR of KAN in D_2O at pH 3 (100 MHz). The full spectrum is shown in panel **A** and the expansions in panels **B-D**.

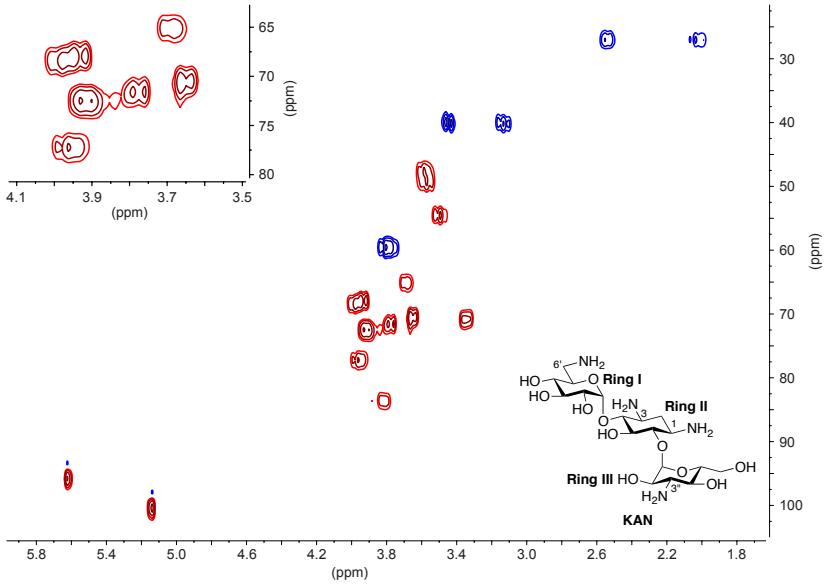

Fig. 2.17. gHSQC of KAN in D_2O at pH 3 (400 MHz). The insert shows a portion of the spectrum more clearly (*Note*: CH_2 shown in blue, CH and CH_3 shown in red).

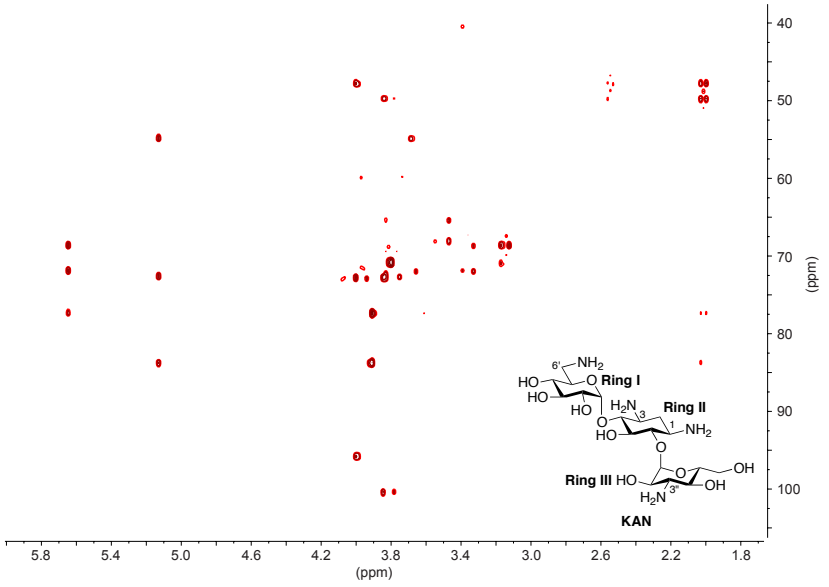

Fig. 2.18. gHMBC of KAN in D_2O at pH 3 (100 MHz).

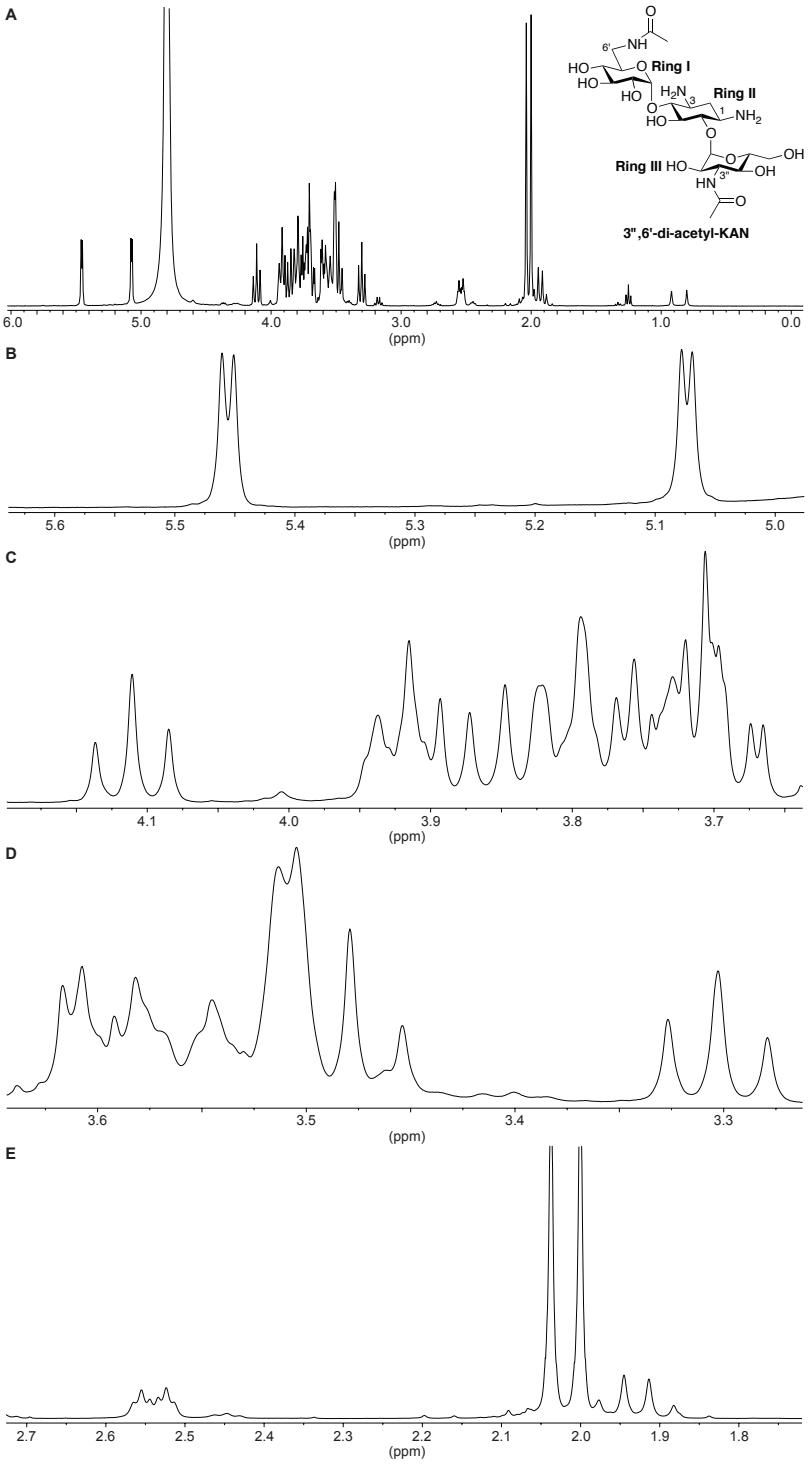

Fig. 2.19. ^{1}H NMR of 3",6'-di-acetyl-KAN in D_2O at pH 3 (400 MHz). The full spectrum is shown in panel **A** and the expansions in panels **B-E**.

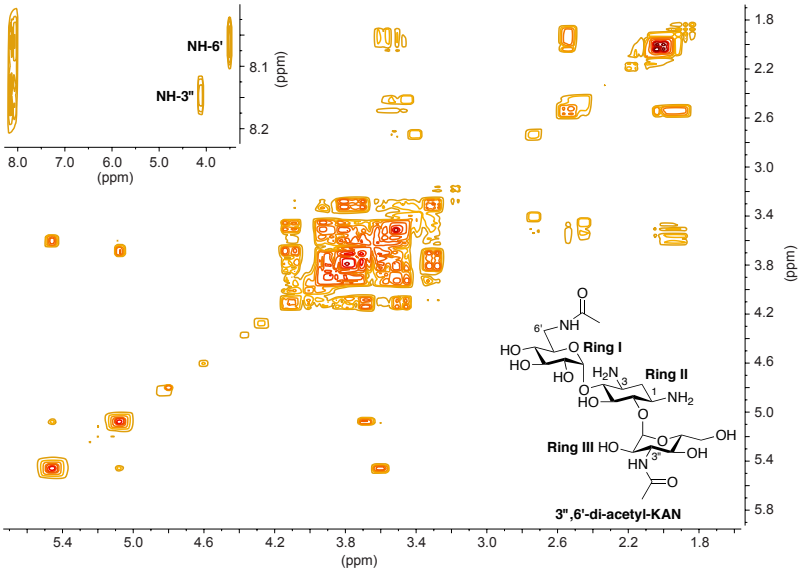

Fig. 2.20. gCOSY of 3",6'-di-acetyl-KAN in D_2O at pH 3 (400 MHz). The insert shows the amide protons coupling to the protons at the 3"- and 6'-positions.

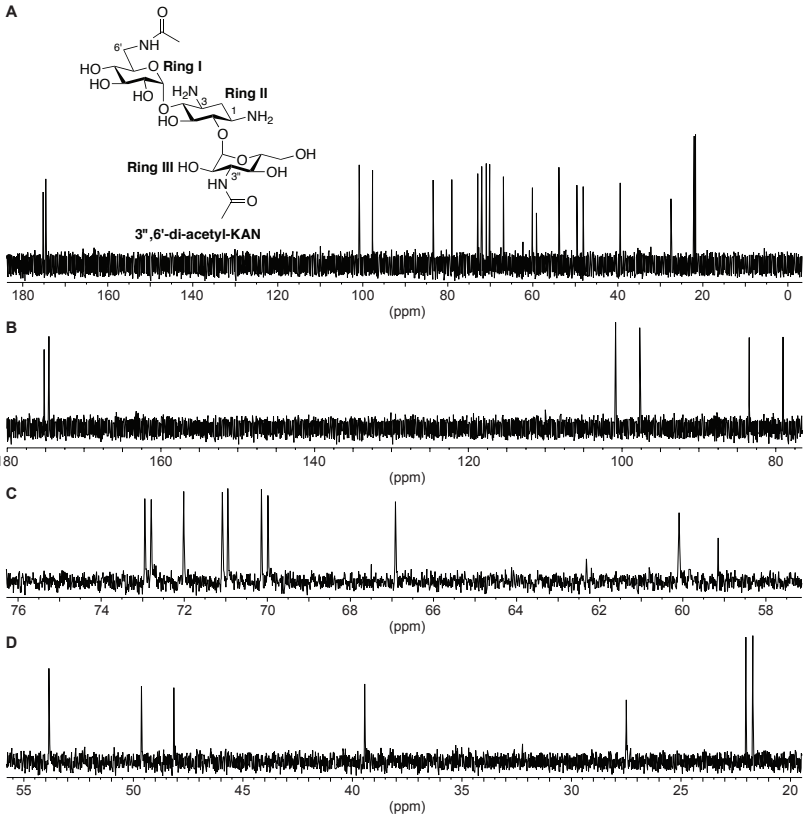

Fig. 2.21. ^{13}C NMR of 3",6'-di-acetyl-KAN in D_2O at pH 3 (100 MHz). The full spectrum is shown in panel **A** and the expansions in panels **B-D**.

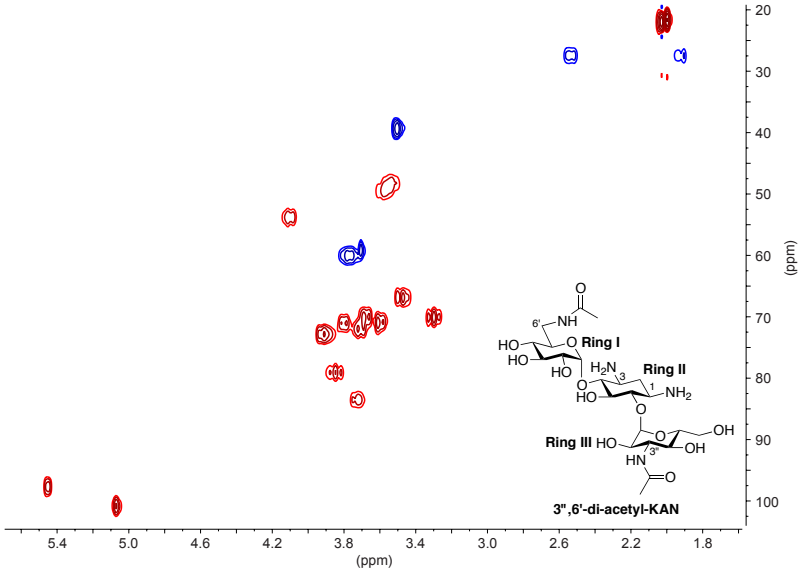

Fig. 2.22. gHSQC of 3",6'-di-acetyl-KAN in D_2O at pH 3 (400 MHz).

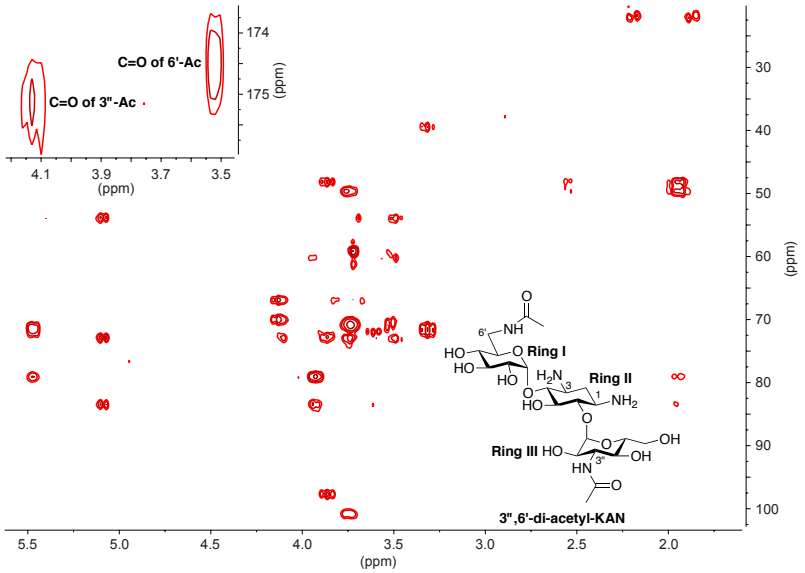

Fig. 2.23. gHMBC of 3",6'-di-acetyl-KAN in D_2O at pH 3 (100 MHz). The insert shows the carbonyl carbons coupling to the protons at the 3"- and 6'-positions.

2.7.1.3.3. Di-acetylation of NET by Eis and NMR analysis of the 2',6'-di-acetyl-NET product

To determine which two positions of NET are acetylated by Eis, the reaction was designed such that it could be monitored in solution by NMR without the need for purification. To determine which modification occurred first, a solution (400 mL) containing NET (15 mM, 1 eq), AcCoA (15 mM, 1 eq), and Eis (0.5 mg/mL) in Na_2HPO_4 buffer (25 mM, pH 8.0 adjusted at rt) containing 10% D_2O was prepared and allowed to proceed to >90% completion by TLC. ^1H, gCOSY, and zTOCSY NMR experiments were performed on the reaction solution, applying PURGE solvent suppression.[14] After the first acetylation was complete and all spectra obtained, an additional aliquot of AcCoA and Eis in 10% D_2O were added to yield a solution (600 mL) containing NET (10 mM, 1 eq), AcCoA (20 mM, 2 eq), and Eis (0.1 mg/mL) in Na_2HPO_4 buffer (25 mM, pH 8.0 adjusted at rt) containing 10% D_2O. Additional spectra were obtained after 48 h to determine the second site of acetylation. The positions of acetylation, purity, and structure identification were confirmed by ^1H, zTOCSY, and gCOSY NMR as well as LCMS. Proton connectivity was assigned using zTOCSY and gCOSY spectra. Representative spectra for 6'-acetyl-NET are provided (Figs. 2.27-2.29). Representative spectra for 2',6'-di-acetyl-NET are provided (Figs. 2.30-2.32).

To unambiguously establish the two acetylated positions on the NET scaffold, the NMR spectra were compared to those of a standard of pure NET [15 mM in Na_2HPO_4 buffer (25 mM, pH 8.0 adjusted at rt) containing 10% D_2O], which was prepared identically to the reaction mixture but omitted AcCoA and Eis (Tables 2.6-2.7). Representative spectra for the standard reaction solution of NET omitting AcCoA are provided (Figs. 2.24-2.26).

Table 2.6. Proton chemical shifts determined for NET and 6'-acetyl-NET.[a]

Ring	H position	NET	6'-acetyl-NET	Δppm
II	1	3.26-3.17 (m)[b] [3.22][c]	3.60-3.35 (m) [3.38]	0.16
	2_{ax}	1.75 (ddd (app. q), $J_{2ax,2eq} = J_{2ax,1} = J_{2ax,3} = 12.4$ Hz)	1.87 (ddd (app. q), $J_{2ax,2eq} = J_{2ax,1} = J_{2ax,3} = 12.0$ Hz)	0.12
	2_{eq}	2.47 (ddd (app. dt), $J_{2eq,2ax} = 12.4$, $J_{2eq,1} = J_{2eq,3} = 4.1$ Hz)	2.64-2.55 (m) [2.60]	0.13
	3	3.40-3.31 (m) [3.34]	3.60-3.35 (m) [3.42]	0.08
	4	3.80-3.70 (m) [3.75]	3.92-3.70 (m) [3.89]	0.14
	5	3.80-3.70 (m) [3.75]	3.92-3.70 (m) [3.75]	=
	6	3.86 (dd (app. t), $J_{6,1} = J_{6,5} = 9.4$ Hz)	3.92-3.70 (m) [3.89]	0.03
	7 ($NHC\underline{H}_2CH_3$)	3.10 (dq, $J_{7,7} = 12.1$ Hz, $J_{7,8} = 7.0$ Hz) /	3.05 (dq, $J_{7,7} = 12.3$ Hz, $J_{7,8} = 7.0$ Hz) /	-0.05
		3.26-3.17 (m) [3.21]	3.28 (dq, $J_{7,7} = 12.3$ Hz, $J_{7,8} = 7.0$ Hz)	0.07
	8 ($NHCH_2C\underline{H}_3$)	1.29 (t, $J = 7.0$ Hz)	1.30 (t, $J = 7.0$ Hz)	0.01
I	1'	5.61 (bs)	5.50 (s)	-0.11
	2'	3.80-3.70 (m) [3.75]	3.86-3.78 (m) [3.83]	0.08
	$3'_{ax}$	2.60 (ddd (app. dt), $J_{3'ax,3'eq} = 18.0$ Hz)	2.64-2.55 (m) [2.57]	-0.03
	$3'_{eq}$	2.32 (ddd (app. dt), $J_{3'eq,3'ax} = 18.0$ Hz)	2.30 (ddd (app. bd), $J_{3'eq,3'ax} = 18.4$ Hz)	-0.02
	4'	5.18 (m (app. bdd))[^]	[4.87][£]	-0.31
	$6'_a$	3.66 (s)	3.92-3.70 (m) [3.76]	**0.10**
	$6'_b$	3.66 (s)	3.92-3.70 (m) [3.76]	**0.10**
III	1"	5.12 (d, $J_{1",2"} = 3.7$ Hz)	5.14 (d, $J_{1",2"} = 3.5$ Hz)	0.02
	2"	4.23 (dd, $J_{2",1"} = 3.7$ Hz, $J_{2",3"} = 10.8$ Hz)	4.29-4.23 (m) [4.26]	0.03
	3"	3.38 (d, $J_{3",2"} = 10.8$ Hz)	3.60-3.35 (m) [3.42]	0.04
	$5"_{ax}$	3.49 (d, $J_{5"a,5"b} = 12.8$ Hz)	3.60-3.35 (m) [3.50]	0.01
	$5"_{eq}$	4.02 (d, $J_{5"b,5"a} = 12.8$ Hz)	[3.99]	-0.03
	$C\underline{H}_3$-4"	1.35 (s)	1.34 (s)	-0.01
	$NHC\underline{H}_3$	2.92 (s)	2.93 (s)	0.01
Acetyl	N<u>H</u>-6'	×	8.32 (t, $J_{NH,6'} = 6.0$ Hz)	
	$C\underline{H}_3C$=O on 6'	×	2.02 (s)	

[a]The chemical shift were established based on ^{1}H (400 MHz), zTOCSY, and gCOSY NMR. [b]Multiplicity and *J* are given in (). [c]The numbers in [] were determined from gCOSY and zTOCSY. ×Indicates that acetyl moiety is not present in the molecule. [£]Partially obscured by H_2O peak in the spectra.

Table 2.7. Proton chemical shifts determined for NET and 2',6'-di-acetyl-NET.[a]

Ring	H position	NET	2',6'-di-acetyl-NET	Δppm
II	1	3.26-3.17 (m)[b] [3.22][c]	[3.13]	-0.09
	2_{ax}	1.75 (ddd (app. q), $J_{2ax,2eq} = J_{2ax,1} = J_{2ax,3} = 12.4$ Hz)	[1.72]	-0.03
	2_{eq}	2.47 (ddd (app. dt), $J_{2eq,2ax} = 12.4$, $J_{2eq,1} = J_{2eq,3} = 4.1$ Hz)	[2.49]	0.02
	3	3.40-3.31 (m) [3.34]	[3.34]	=
	4	3.80-3.70 (m) [3.75]	[3.80-3.60][§]	X
	5	3.80-3.70 (m) [3.75]	[3.80-3.60][§]	X
	6	3.86 (dd (app. t), $J_{6,1} = J_{6,5} = 9.4$ Hz)	[3.80-3.60][§]	X
	7	3.10 (dq, $J_{7,7} = 12.1$ Hz, $J_{7,8} = 7.0$ Hz) /	[2.97] /	-0.13 /
	($NHC\underline{H}_2CH_3$)	3.26-3.17 (m) [3.21]	[3.21]	=
	8 ($NHCH_2C\underline{H}_3$)	1.29 (t, $J = 7.0$ Hz)	1.28 (t, $J = 6.8$ Hz)	-0.01
I	1'	5.61 (bs)	[5.32]	-0.29
	2'	3.80-3.70 (m) [3.75]	[4.20]	**0.45**
	$3'_{ax}$	2.60 (ddd (app. dt), $J_{3'ax,3'eq} = 18.0$ Hz)	[2.29]	-0.31
	$3'_{eq}$	2.32 (ddd (app. dt), $J_{3'eq,3'ax} = 18.0$ Hz)	[2.11]	-0.21
	4'	5.18 (m (app. bdd))[^]	[4.87]	-0.31
	$6'_a$	3.66 (s)	[3.73]	**0.07**
	$6'_b$	3.66 (s)	[3.73]	**0.07**
III	1"	5.12 (d, $J_{1",2"} = 3.7$ Hz)	5.14 (d, $J_{1",2"} = 3.5$ Hz)	0.02
	2"	4.23 (dd, $J_{2",1"} = 3.7$ Hz, $J_{2",3"} = 10.8$ Hz)	[4.25]	0.02
	3"	3.38 (d, $J_{3",2"} = 10.8$ Hz)	[3.37]	-0.01
	$5"_{ax}$	3.49 (d, $J_{5"a,5"b} = 12.8$ Hz)	[3.48]	-0.01
	$5"_{eq}$	4.02 (d, $J_{5"b,5"a} = 12.8$ Hz)	[4.00]	-0.02
	$C\underline{H}_3$-4"	1.35 (s)	1.33 (s)	-0.02
	$NHC\underline{H}_3$	2.92 (s)	2.92 (s)	=
Acetyl	N<u>H</u>-2'	×	[8.06]	
	N<u>H</u>-6'	×	[8.30]	
	$C\underline{H}_3C$=O on 2'	×	2.01 (s)	
	$C\underline{H}_3C$=O on 6'	×	2.01 (s)	

[a]The chemical shift were established based on ^{1}H (400 MHz), zTOCSY, and gCOSY NMR. [b]Multiplicity and *J* are given in (). [c]The numbers in [] were determined from gCOSY and zTOCSY. ×Indicates that the acetyl moiety is not present in the molecule. [§]Indicates that the peaks were not resolved due to interfering peaks from CoA.

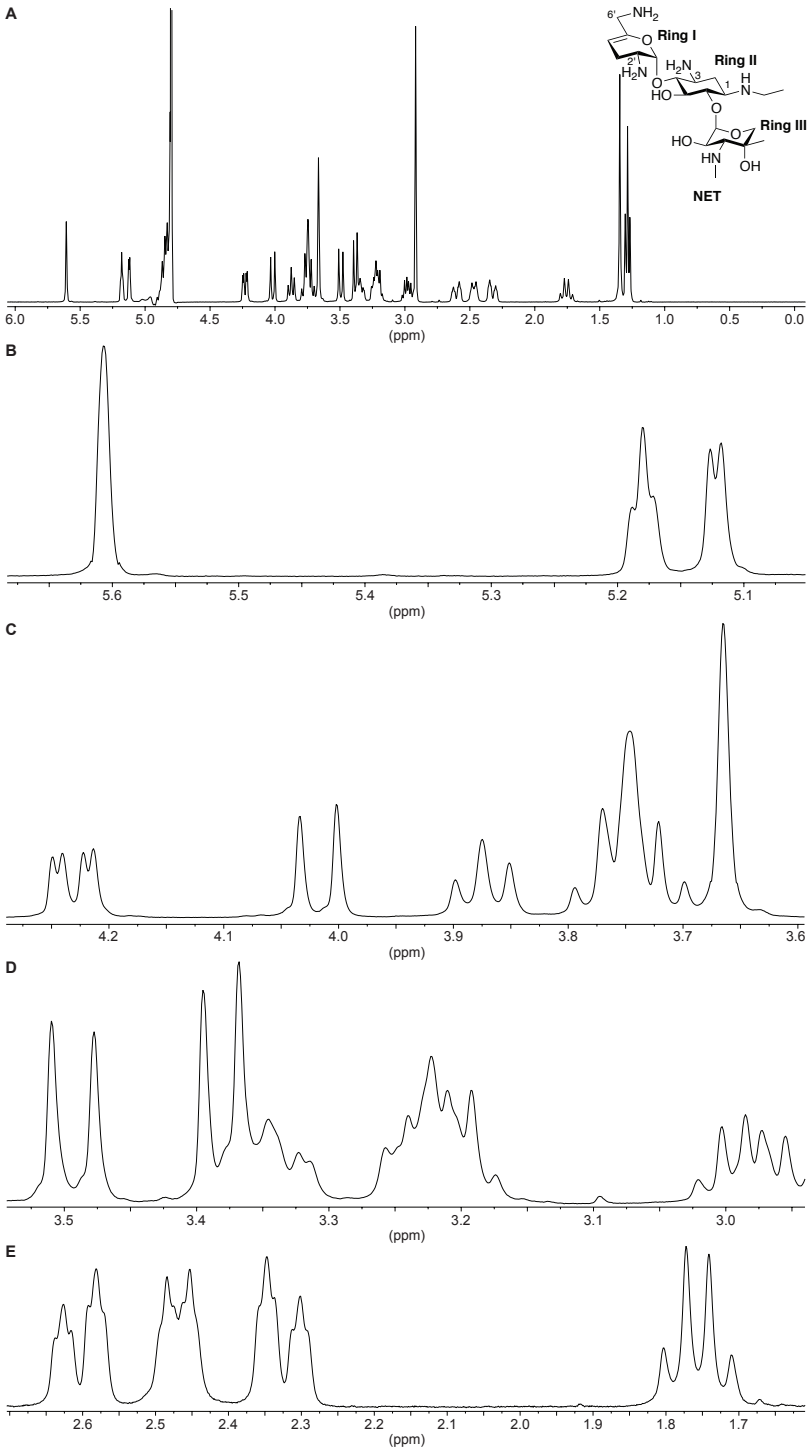

Fig. 2.24. ^{1}H NMR of NET (9:1/H_2O:D_2O, pH 8, 25 mM KH_2PO_4) (400 MHz). The full spectrum is shown in panel **A** and the expansions in panels **B-E**.

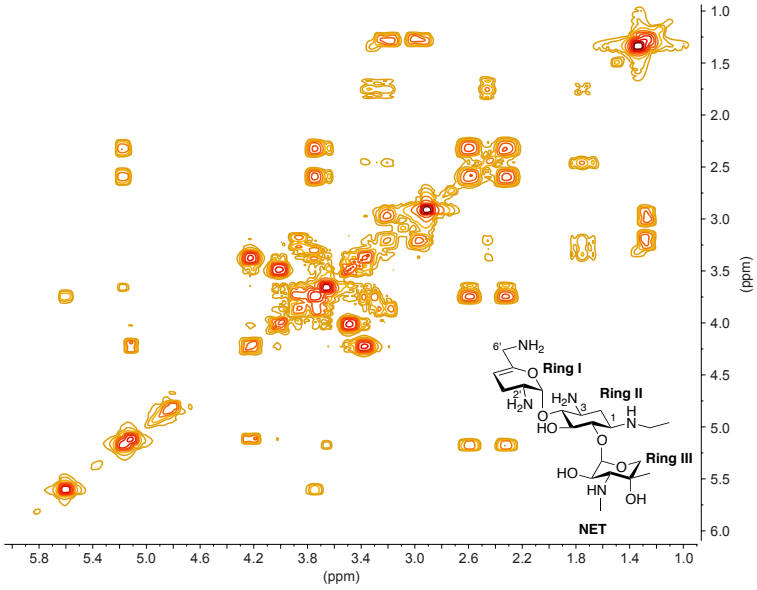

Fig. 2.25. gCOSY of NET (9:1/H_2O:D_2O, pH 8, 25 mM KH_2PO_4) (400 MHz).

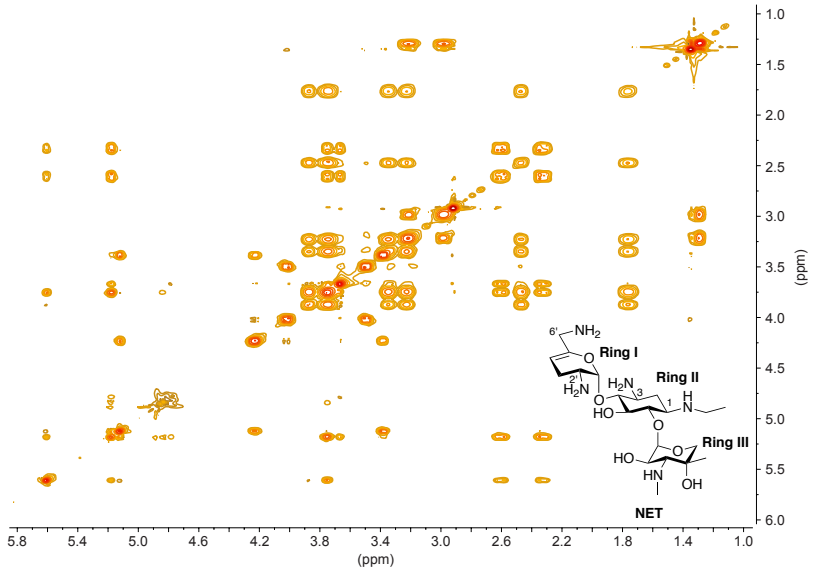

Fig. 2.26. zTOCSY of NET (9:1/H_2O:D_2O, pH 8, 25 mM KH_2PO_4) (400 MHz).

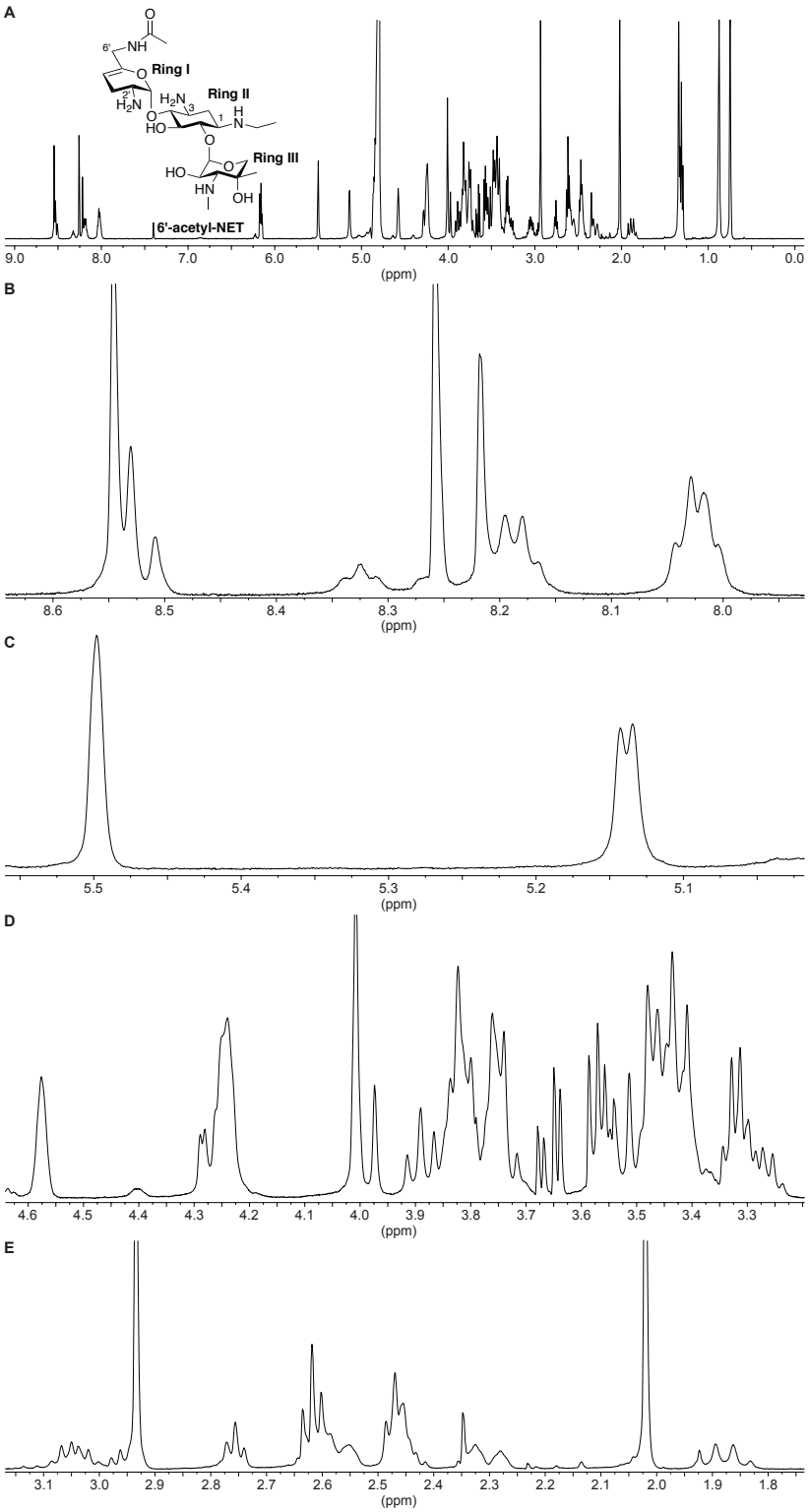

Fig. 2.27. ^{1}H NMR of 6'-acetyl-NET Eis reaction mixture (9:1/H_2O:D_2O, pH 8, 25 mM KH_2PO_4) (400 MHz). The full spectrum is shown in panel **A** and the expansions in panels **B-E**.

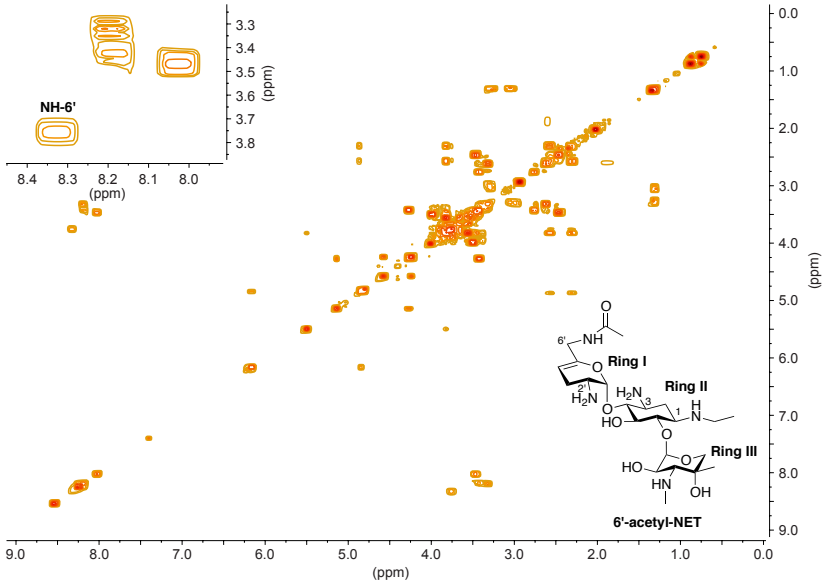

Fig. 2.28. gCOSY of 6'-acetyl-NET Eis reaction mixture (9:1/H_2O:D_2O, pH 8, 25 mM KH_2PO_4) (400 MHz). The insert shows the amide protons coupling to the protons at the 6'-position.

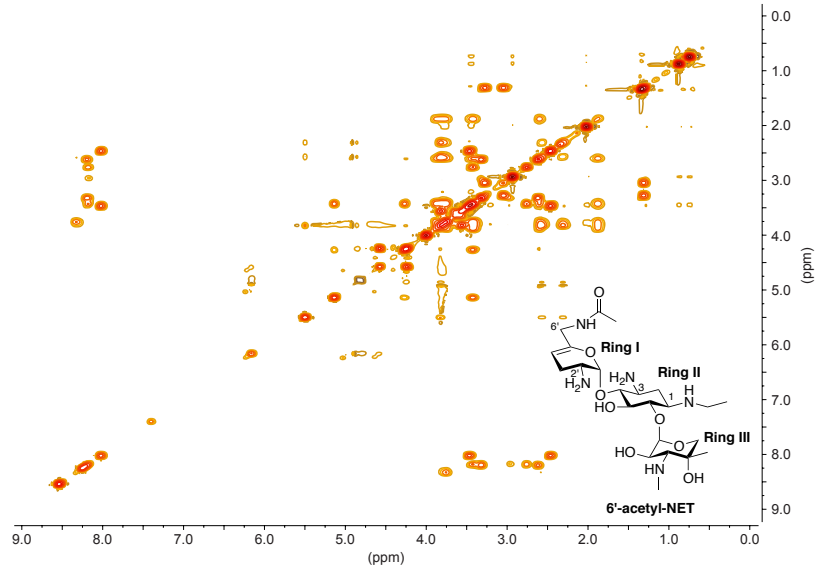

Fig. 2.29. zTOCSY of 6'-acetyl-NET Eis reaction mixture (9:1/H_2O:D_2O, pH 8, 25 mM KH_2PO_4) (400 MHz).

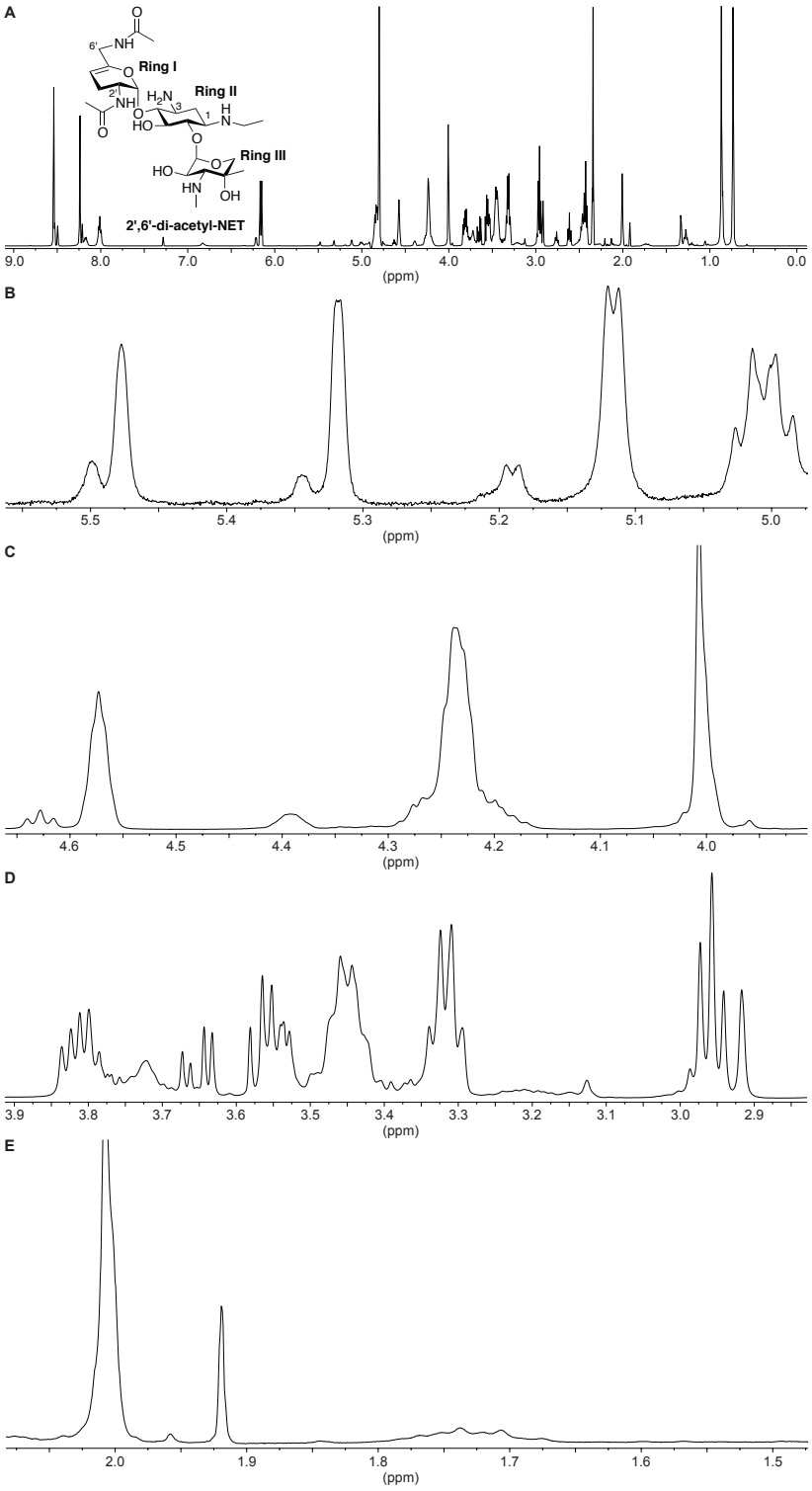

Fig. 2.30. ^{1}H NMR of 2',6'-di-acetyl-NET Eis reaction mixture (9:1/H_2O:D_2O, pH 8, 25 mM KH_2PO_4) (400 MHz). The full spectrum is shown in panel **A** and the expansions in panels **B-E**.

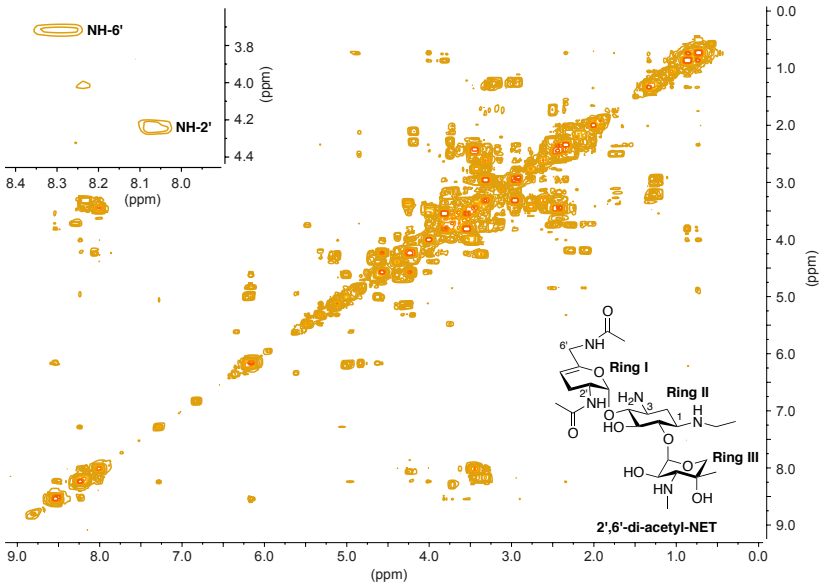

Fig. 2.31. gCOSY of 2',6'-di-acetyl-NET Eis reaction mixture (9:1/H_2O:D_2O, pH 8, 20 mM KH_2PO_4) (400 MHz). The insert shows the amide protons coupling to the protons at the 6'- and 2'-positions.

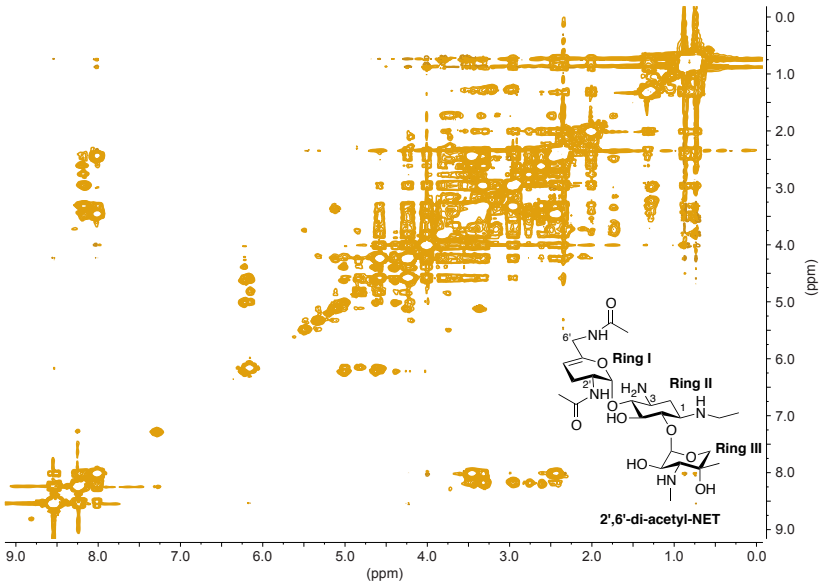

Fig. 2.32. zTOCSY of 2',6'-di-acetyl-NET Eis reaction mixture (9:1/H_2O:D_2O, pH 8, 25 mM KH_2PO_4) (400 MHz).

2.7.1.3.4. Dual di-acetylation of SIS by Eis and NMR analysis of the 2',6'- and 1/3,6'-di-acetyl-SIS products

To determine which positions of SIS are acetylated by Eis, the reaction was scaled-up and designed such that the initial acetylation reaction could be monitored in solution by NMR without the need for purification. To determine which modification occurred first, a solution (400 μL) containing SIS (15 mM, 1 eq), AcCoA (15 mM, 1 eq), and Eis (~0.05 mg/mL) in Na_2HPO_4 buffer (25 mM, pH 8.0 adjusted at rt) containing 10% D_2O was prepared and allowed to proceed to >90% completion by TLC. ^1H, gCOSY, and zTOCSY experiments were performed on the reaction solution, applying PURGE solvent suppression [14] and compared to a standard that was prepared identically without Eis and AcCoA. After the first acetylation was complete and all spectra obtained, additional aliquots of AcCoA (total of 4 eq) were added and additional spectra were obtained after incubating for 48 h to determine the subsequent sites of acetylation. Due to the complexity of the resulting spectra, the final mixture of di-acetlyated products was purified for further analysis. After >90% conversion of SIS into two distinct di-acetyl-SIS products, the Eis enzyme was removed by the addition of an equal volume of MeOH, cooling to 4 °C for 30 min, and centrifugation (15,000 rpm, 10 min, rt). The solution was separated from the precipitate and the solvents evaporated under reduced pressure. The residue was purified by flash chromatography (SiO_2) using a gradient of 0.0-2.0% Et_3N in MeOH. Fractions containing the product were pooled and the solvents removed under reduced pressure. The residue was dissolved in a minimal volume of D_2O and lyophilized to give a mixture of the two di-acetyl-SIS products as a white powder. For NMR analyses, the mixture of products was dissolved in 9:1/H_2O:D_2O (400 μL), yielding a solution of pH 8 which was centrifuged (15,000 rpm, 10 min, rt) to remove any particulate, and the supernatant collected. However, the spectra obtained under these conditions were insufficient to fully characterize the compounds. As such, the solution was adjusted to pH 3 with diluted sulfuric acid (0.5%) for further unambiguous analysis of the two di-acetylated products (*Note*: The values in Tables 2.8 and 2.9 are of the product at pH 3). The positions of acetylation, purity, and structure identifications were confirmed by ^1H, zTOCSY, and gCOSY NMR as well as LCMS. Proton connectivity was assigned using zTOCSY and gCOSY spectra. Representative spectra for 6'-acetyl-SIS are provided (Figs.

2.39-2.41). Representative spectra for the mixture of 2',6'-di-acetyl-SIS and 1/3,6'-di-acetyl-SIS are provided (Figs. 2.42-2.47).

To unambiguously establish the first position acetylated on the SIS scaffold, the NMR spectra were compared to those of a standard prepared identically to the reaction mixture from which Eis and AcCoA were omitted (Tables 2.8). The SIS standard and the solution containing the two di-acetyl-SIS products to which it was compared were prepared in an identical fashion. Representative spectra of these standards are provided (Figs. 2.36-2.38). Spectra of the standard at pH 8 in 9:1/H_2O:D_2O are provided (Figs. 2.33-2.35), but no values are reported in the tables. *Note*: The chemical shifts of the protons of Ring III of the di-acetylated-SIS compounds were omitted because they could not be distinguished from one another and, also, there are no possible sites of modification.

Table 2.8. Proton chemical shifts determined for SIS and 6'-acetyl-SIS.[a]

Ring	H position	SIS	6'-acetyl-SIS	Δppm
II	1	3.41-3.27[b] (m)[c] [3.31][d]	3.50-3.30 (m) [3.36]	0.05
	2_{ax}	1.82 (ddd (app. q), $J_{2ax,2eq} = J_{2ax,1} = J_{2ax,3} = 12.4$ Hz)	1.84 (ddd (app. q), $J_{2ax,2eq} = J_{2ax,1} = J_{2ax,3} = 12.5$ Hz)	0.02
	2_{eq}	2.40-2.30 (m) [2.38]	2.64-2.44 (m) [2.49]	0.11
	3	3.41-3.27[b] (m) [3.36]	3.50-3.30 (m) [3.45]	0.09
	4	3.75-3.65[e] (m) [3.68]	3.89-3.64 (m) [3.72]	0.04
	5	3.75-3.65 (m) [3.70]	3.89-3.64 (m) [3.76]	0.06
	6	3.91[c] (dd (app. t), $J_{6,1} = J_{6,5} = 9.4$ Hz)	3.89-3.64 (m) [3.85]	-0.06
I	1'	5.60 (s)	5.51[f]	-0.09
	2'	3.79 (bs)	3.89-3.64 (m) [3.81]	0.02
	$3'_{ax}$	2.40-2.30 (m) [2.34]	2.30 (dd (app. bd), $J_{3'ax,3'eq} = 17.8$ Hz)	-0.04
	$3'_{eq}$	2.63 (dd (app. bd), $J_{3'eq,3'ax} = 18.2$ Hz)	2.64-2.44 (m) [2.58]	-0.05
	4'	5.18 (bs)	4.89	-0.29
	$6'_a$	3.75-3.65 (m) [3.67]	3.89-3.64 (m) [3.81]	**0.14**
	$6'_b$	3.75-3.65 (m) [3.67]	3.89-3.64 (m) [3.81]	**0.14**
III	1"	5.15 (d, $J_{1",2"} = 3.6$ Hz)	5.15	=
	2"	4.20 (dd, $J_{2",1"} = 3.6$ Hz, dd, $J_{2",3"} = 10.8$ Hz)	4.26-4.19 (m) [4.22]	0.02
	3"	3.40 (d, $J_{3",2"} = 10.8$ Hz)	3.50-3.30 (m) [3.43]	0.03
	$5"_{ax}$	4.05 (dd, $J_{5"a,5"b} = 12.7$ Hz)	4.02 (dd, $J_{5"a,5"b} = 12.9$ Hz)	-0.03
	$5"_{eq}$	3.47 (dd, $J_{5"b,5"a} = 12.7$ Hz)	3.50-3.30 (m) [3.48]	0.01
	$C\underline{H}_3$-4"	1.35 (s)	1.35 (s)	=
	$NHC\underline{H}_3$	2.92 (s)	2.92 (s)	=
Acetyl	$N\underline{H}$-6'	×	8.20 (t)	
	$C\underline{H}_3C{=}O$ on 6'	×	2.03 (s)	

[a]The chemical shift were established based on ^{1}H (400 MHz), zTOCSY, and gCOSY NMR. [b]Could be analogous position of the DOS ring. [c]Multiplicity and *J* are given in (). [d]The numbers in [] were determined from gCOSY. [e]Could be analogous position of the DOS ring. ×Indicates that the acetyl moiety is not present in the molecule. [f]Obscured due to interference resulting from solvent suppression.

Table 2.9. Proton chemical shifts determined for SIS and 6',2''-di-acetyl-SIS as well as 6',3 or 1-di-acetyl-SIS.[a]

Ring	H position	SIS	6',3 or 1- (Δppm)	6',2''- (Δppm)
II	1	3.62-3.54[b] (m)[c] [3.57][d]	[3.53[b]] (-0.04)	[3.45] (-0.12)
	2_{ax}	2.12 (ddd (app. q), $J_{2ax,2eq} = J_{2ax,1} = J_{2ax,3} = 12.6$ Hz)	[1.78] (-0.34)	[1.99] (-0.13)
	2_{eq}	2.58 (ddd (app. dt), $J_{2eq,2ax} = 12.6$ Hz, $J_{2eq,1} = J_{2eq,3} =$ 4.3 Hz)	[2.25] (-0.33)	[2.59] (-0.01)
	3	3.62-3.54[b] (m) [3.57]	**[3.99[b]] (0.42)**	[3.58] (0.01)
	4	3.87[c] (dd (app. t), $J_{4,3} = J_{4,5} = 9.6$ Hz)	[3.83[c]] (-0.03)	[3.79] (-0.08)
	5	4.15 (dd (app. t), $J_{5,4} = J_{5,6} = 9.6$ Hz)	[4.12] (-0.03)	[4.04] (-0.11)
	6	3.80[c] (dd (app. t), $J_{6,1} = J_{6,5} = 9.6$ Hz)	[3.76[c]] (-0.04)	[3.80] (0.00)
I	1'	5.64 (s)	[5.54] (-0.10)	[5.39] (-0.25)
	2'	3.96 (d (app. bd), $J_{2',3'} = 4.3$ Hz)	[3.88] (-0.08)	**[4.26] (0.20)**
	$3'_{ax}$	2.75 (ddd (app. dt), $J_{3'ax,3'eq} = 18.9$ Hz)	[2.63] (-0.12)	[2.35] (-0.40)
	$3'_{eq}$	2.40 (ddd (app. bd), $J_{3'eq,3'ax} = 18.9$ Hz)	[2.33] (-0.07)	[2.15] (-0.25)
	4'	5.21 (t, $J_{4',3'} = 3.7$ Hz)	[4.90] (-0.31)	[4.92] (-0.29)
	$6'_a$	3.70 (d, $J_{6'a,6'b} = 14.0$ Hz)	**[3.83] (0.13)**	**[3.81] (0.11)**
	$6'_b$	3.75 (d, $J_{6'b,6'a} = 14.0$ Hz)	**[3.83] (0.08)**	**[3.81] (0.06)**
III	1''	5.16 (d, $J_{1'',2''} = 3.7$ Hz)		
	2''	4.24 (dd, $J_{2'',1''} = 3.7$ Hz, $J_{2'',3''} = 10.8$ Hz)		
	3''	3.62-3.48 (m) [3.51]		
	$5''_a$	4.03 (d, $J_{5''a,5''b} = 12.6$ Hz)		
	$5''_b$	3.51 (d, $J_{5''b,5''a} = 12.6$ Hz)		
	CH_3-4''	1.37 (s)		
	$NHCH_3$	2.95 (s)		
Acetyl	NH-6'	×	8.35	8.27
	NH-3/1 or NH-2'	×	8.21 (NH-3/1)	8.12 (NH-2')
	CH_3C=O on X	×		
	CH_3C=O on 6'	×		

[a]The chemical shift were established based on ^{1}H (400 MHz), 2D-TOCSY and 2D-COSY NMR. [b]Could be analogous position of the 2-deoxystreptamine (DOS) ring. [c]Multiplicity and *J* are given in (). [d]The numbers in [] were determined from gCOSY. [e]Could be analogous position of the DOS ring. ×Indicates that acetyl moiety is not present in the molecule.

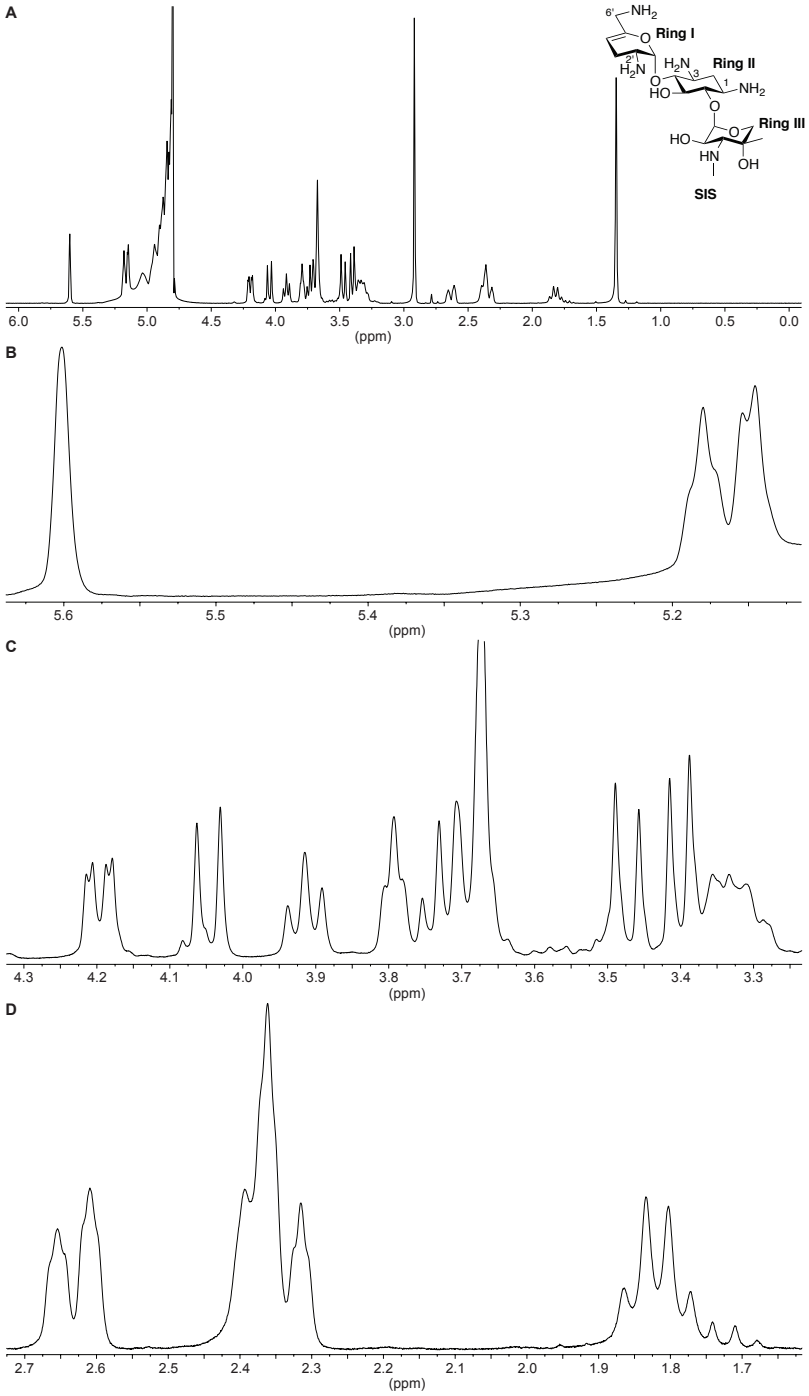

Fig. 2.33. ^{1}H NMR of SIS (9:1/H_2O:D_2O, pH 8, 25 mM KH_2PO_4) (400 MHz). The full spectrum is shown in panel **A** and the expansions in panels **B-D**.

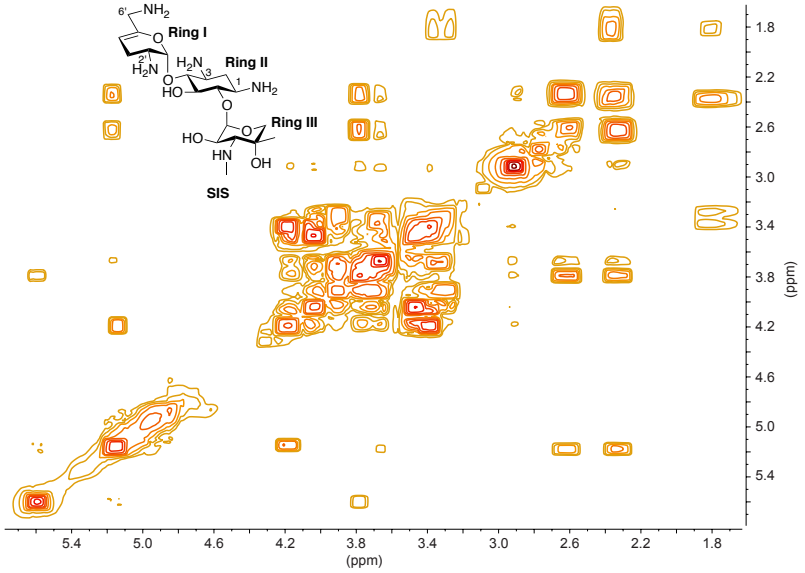

Fig. 2.34. gCOSY of SIS (9:1/H_2O:D_2O, pH 8, 25 mM KH_2PO_4) (400 MHz).

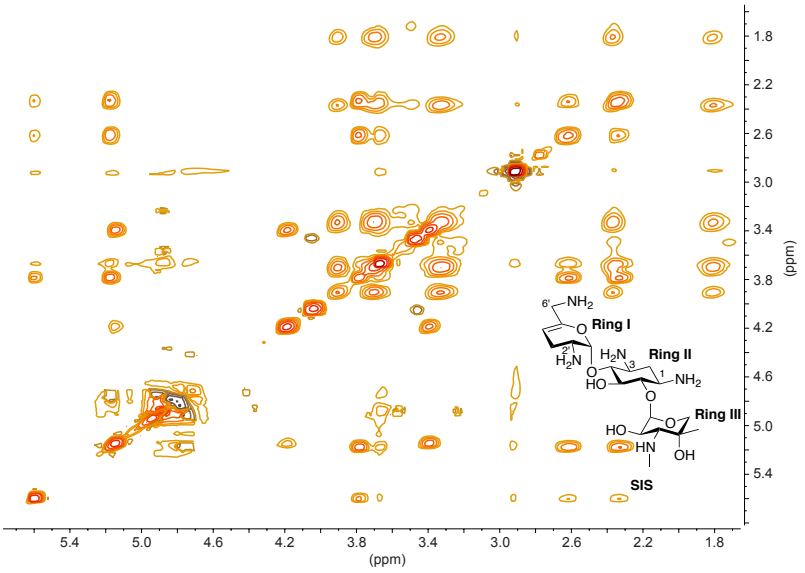

Fig. 2.35. zTOCSY of SIS (9:1/H_2O:D_2O, pH 8, 25 mM KH_2PO_4) (400 MHz).

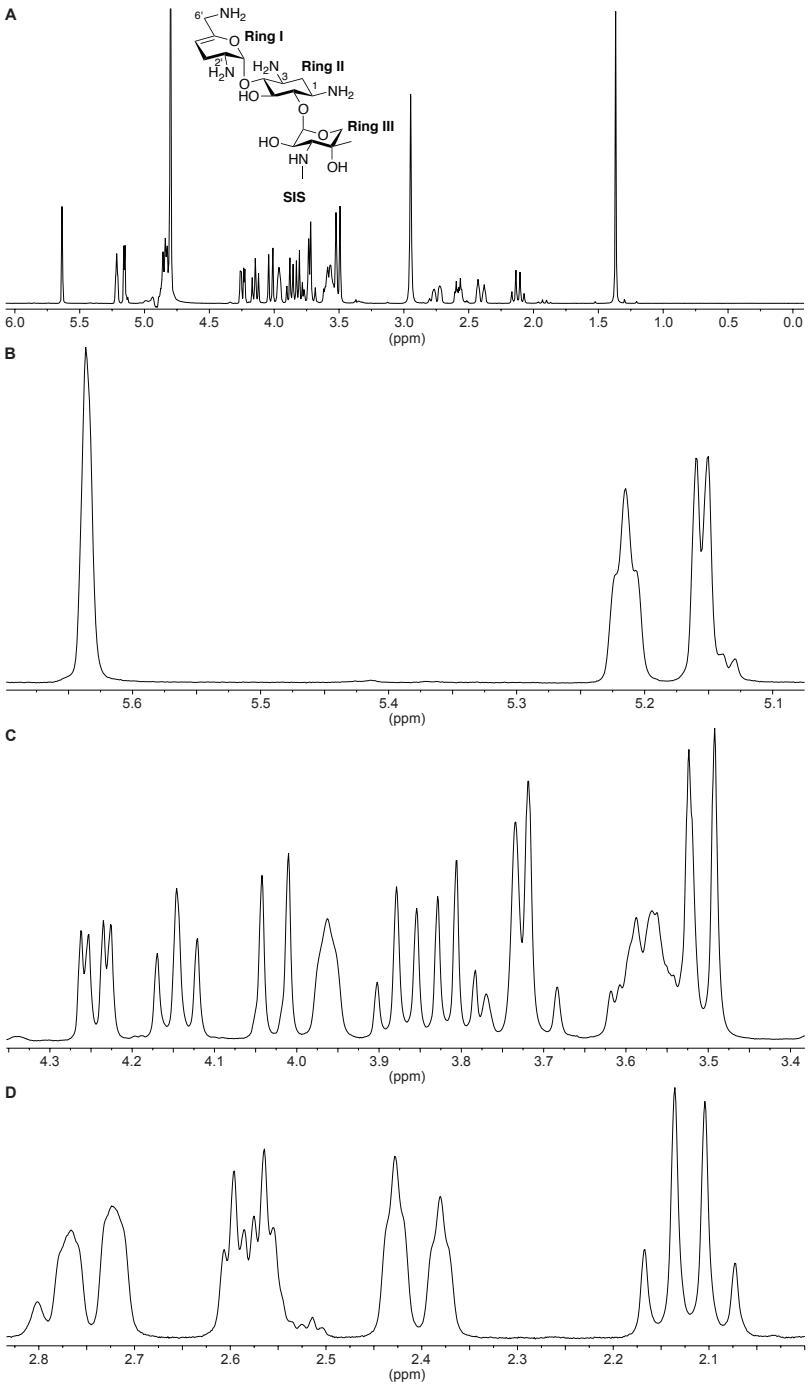

Fig. 2.36. ^{1}H NMR of SIS (9:1/H_2O:D_2O, pH 3) (400 MHz). The full spectrum is shown in panel **A** and the expansions in panels **B-D**.

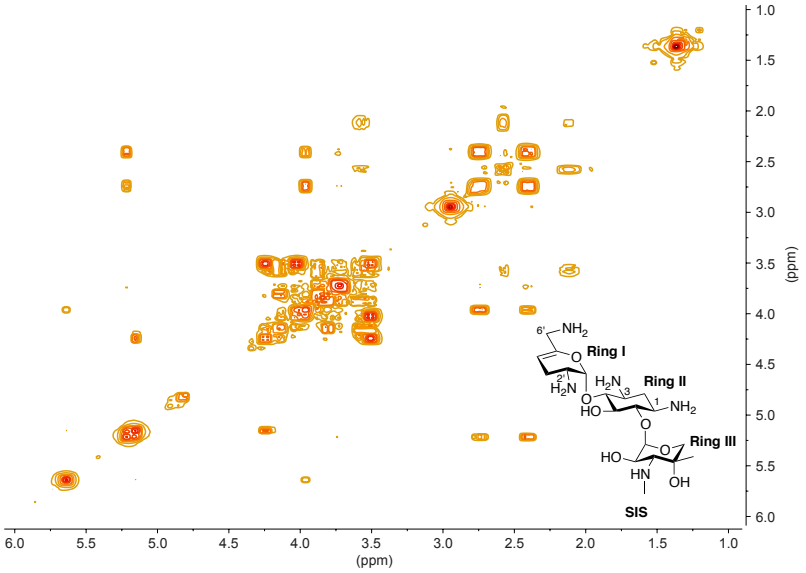

Fig. 2.37. gCOSY of SIS (9:1/H_2O:D_2O, pH 3) (400 MHz).

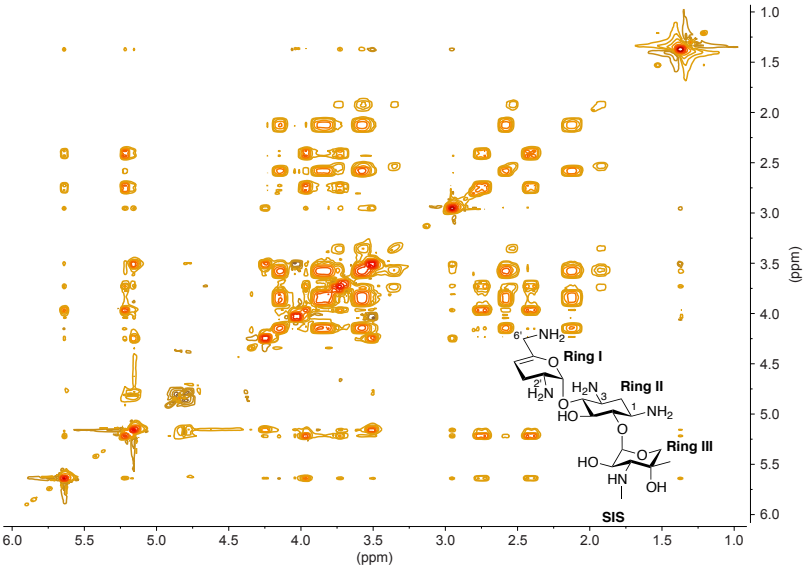

Fig. 2.38. zTOCSY of SIS (9:1/H_2O:D_2O, pH 3) (400 MHz).

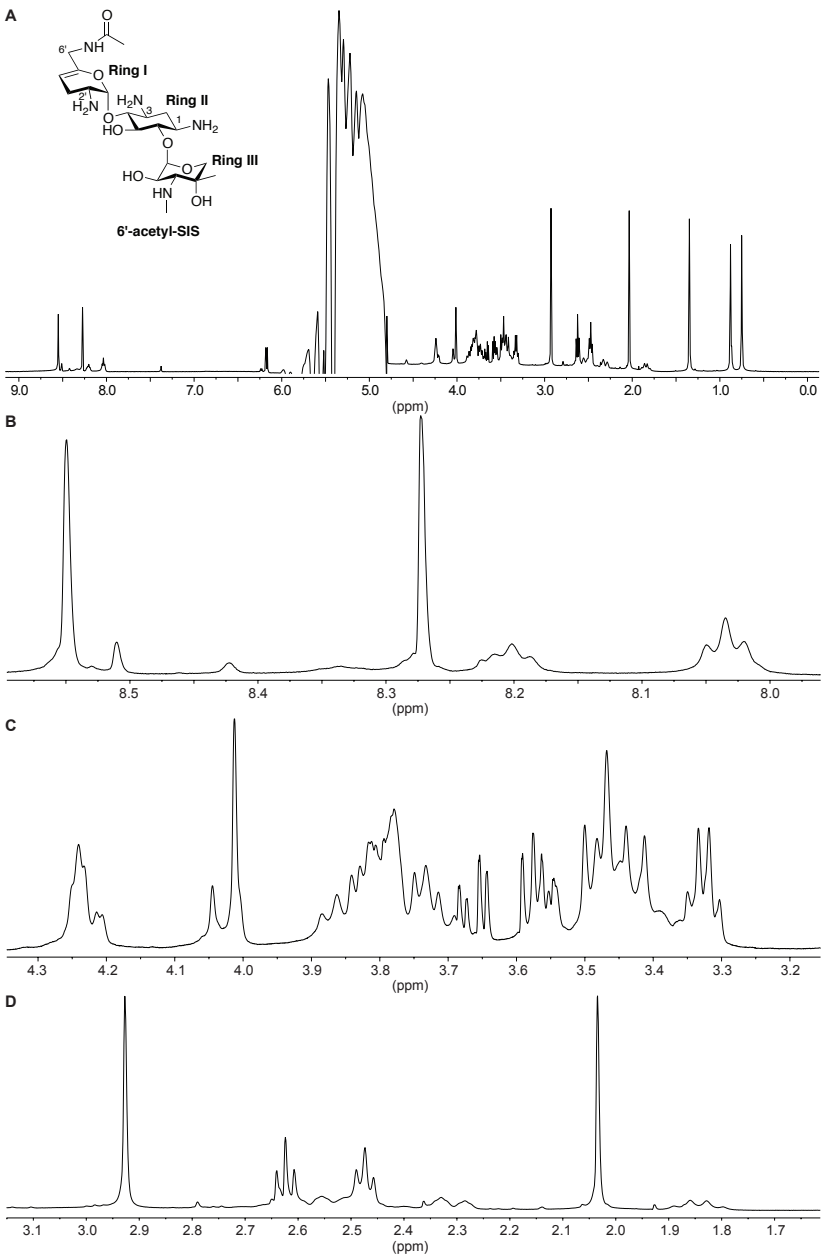

Fig. 2.39. ^{1}H NMR of 6'-acetyl-SIS Eis reaction mixture (9:1/H_2O:D_2O, pH 8, 25 mM KH_2PO_4) (400 MHz). The full spectrum is shown in panel **A** and the expansions in panels **B-D**.

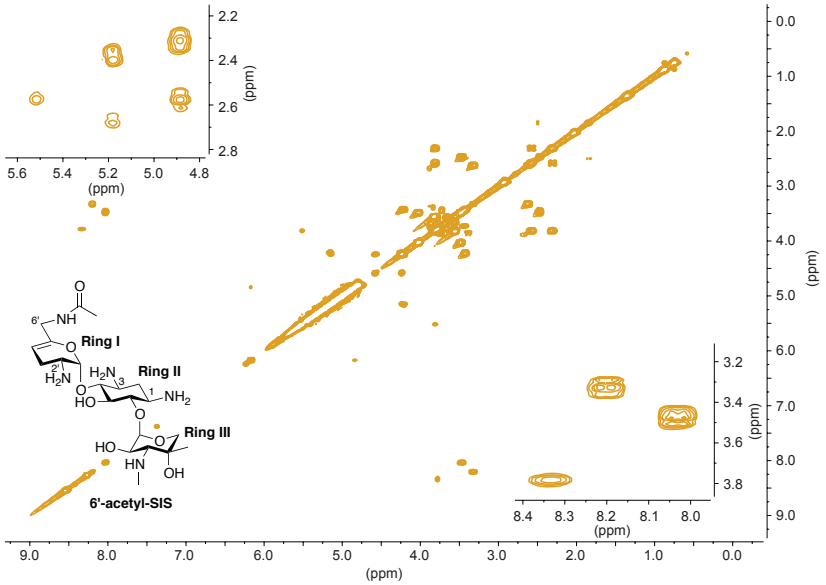

Fig. 2.40. gCOSY of 6'-acetyl-SIS Eis reaction mixture (9:1/H_2O:D_2O, pH 8, 25 mM KH_2PO_4) (400 MHz). The inserts show part of the spectra that is obscured in the ^1H (top left) and the amide protons coupling to the proton at the 6'-position (bottom right).

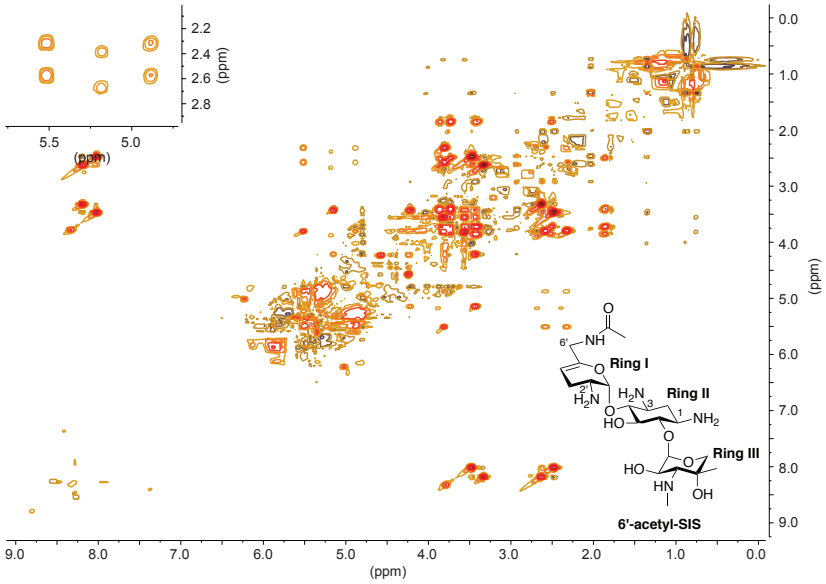

Fig. 2.41. zTOCSY of 6'-acetyl-SIS Eis reaction mixture (9:1/H_2O:D_2O, pH 8, 25 mM KH_2PO_4) (400 MHz). The inserts show part of the spectra that is obscured in the ^1H.

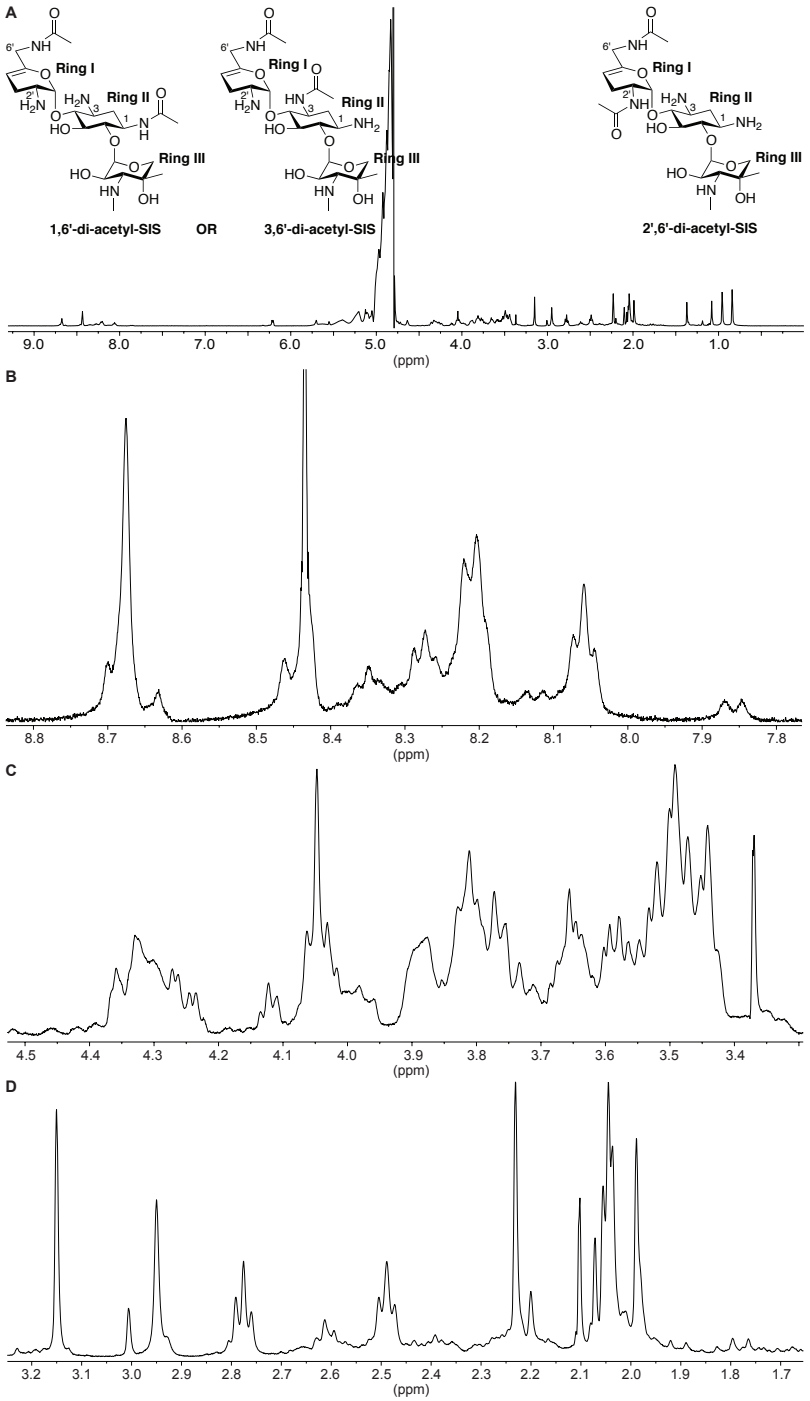

Fig. 2.42. ^{1}H NMR of a mixture of two di-acetylated SIS products (9:1/H_2O:D_2O, pH 3) (400 MHz). The full spectrum is shown in panel **A** and the expansions in panels **B-D**.

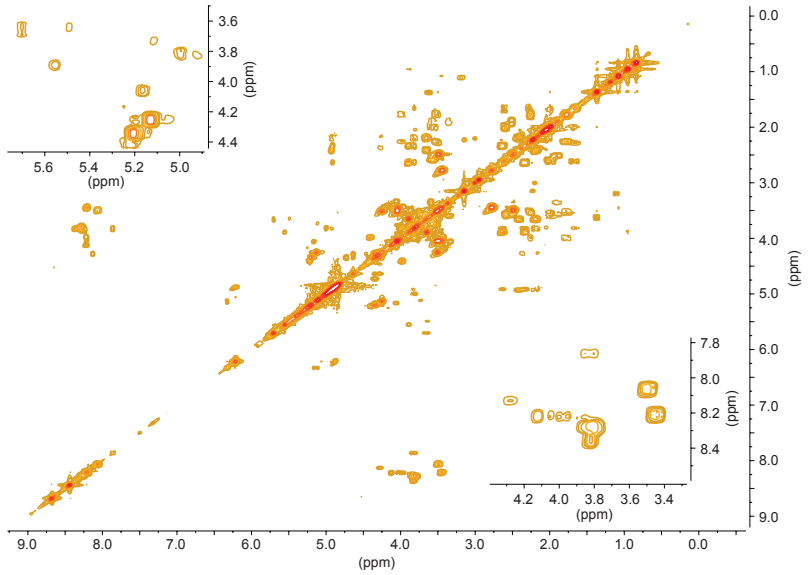

Fig. 2.43. gCOSY of a mixture of two di-acetylated SIS products (9:1/H_2O:D_2O, pH 3) (400 MHz). The inserts show part of the spectra that is obscured in the ^1H (top left) and the amide protons coupling to the protons of the AG (bottom right).

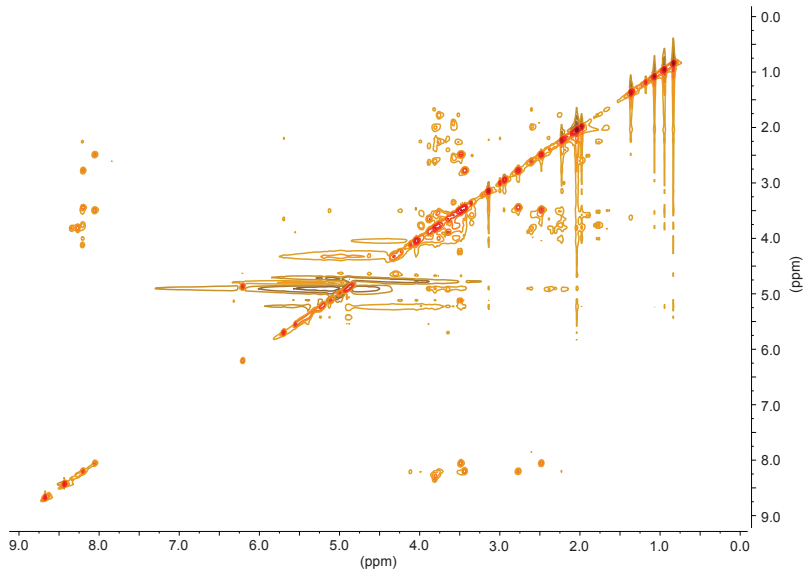

Fig. 2.44. zTOCSY of a mixture of two di-acetylated SIS products (9:1/H_2O:D_2O, pH 3) (400 MHz).

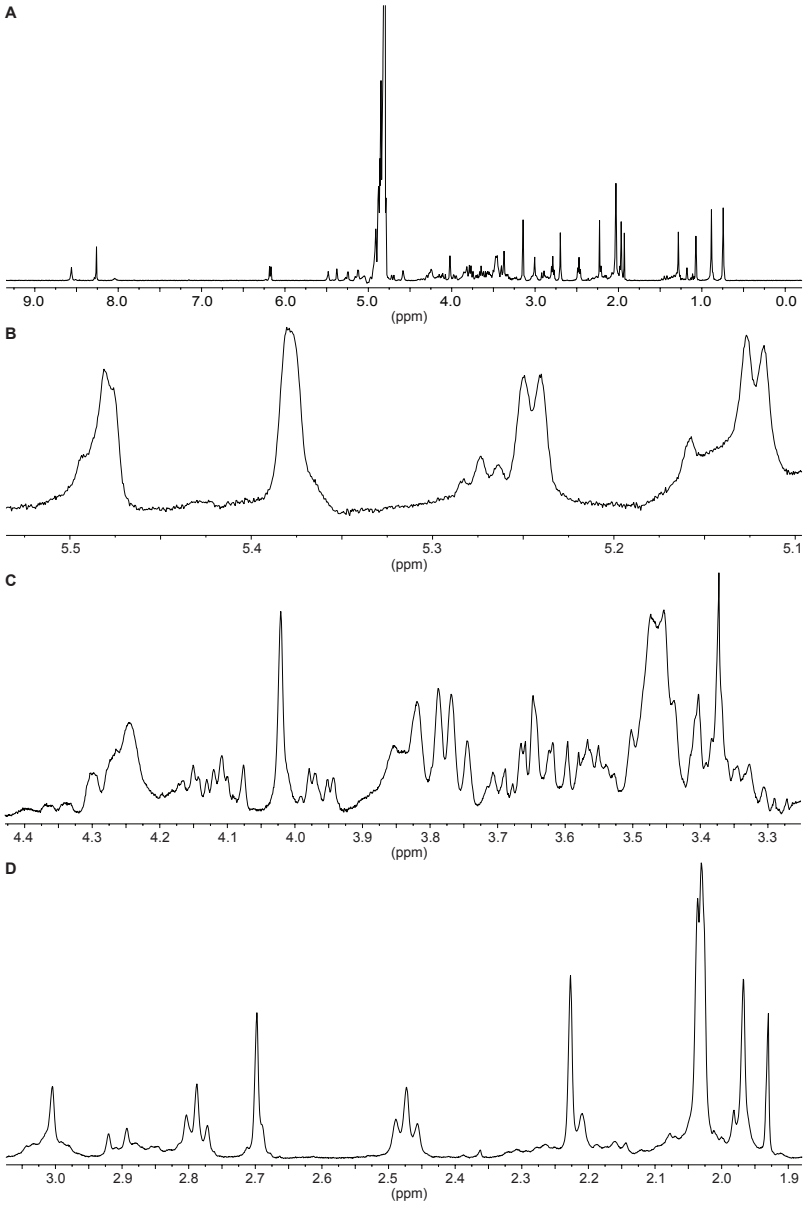

Fig. 2.45. ^{1}H NMR of a mixture of two di-acetylated SIS products (9:1/H_2O:D_2O, pH 8) (400 MHz). The full spectrum is shown in panel **A** and the expansions in panels **B-D**.

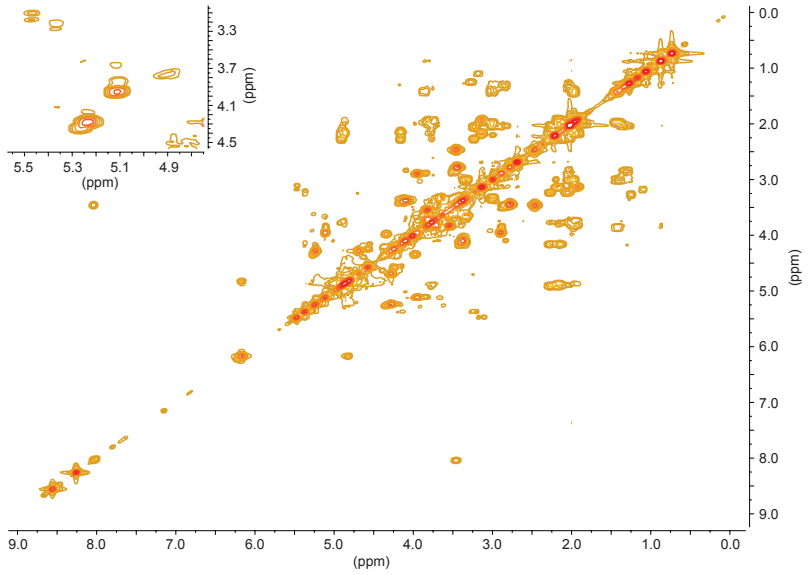

Fig. 2.46. gCOSY of a mixture of two di-acetylated SIS products (9:1/H_2O:D_2O, pH 8) (400 MHz). The insert shows part of the spectra that is obscured in the ^1H.

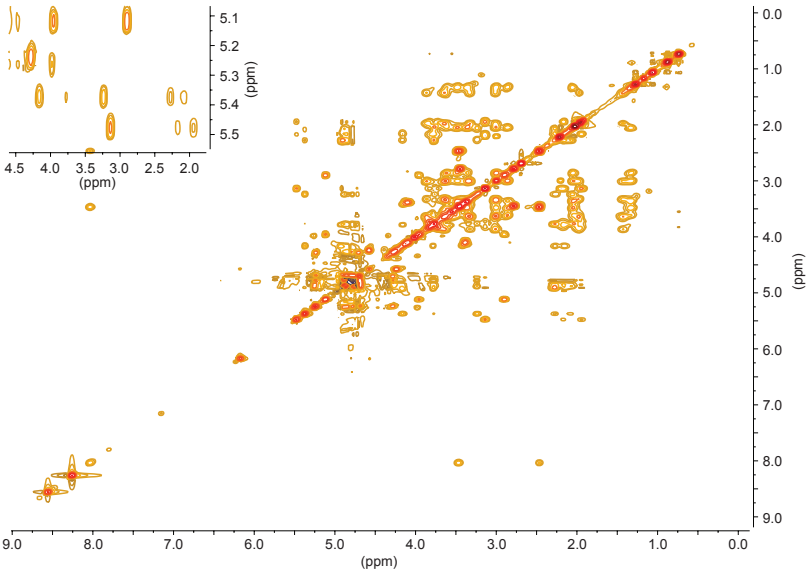

Fig. 2.47. zTOCSY of a mixture of two di-acetylated SIS products (9:1/H_2O:D_2O, pH 8) (400 MHz). The insert shows part of the spectra that is obscured in the ^1H.

2.7.1.3.5. Di-acetylation of TOB by Eis and NMR analysis of the 3",6'-di-acetyl-TOB product

To determine which two positions of TOB are acetylated by Eis, the reaction was scaled-up and designed such that it could be monitored in real time by NMR. To determine which modification occurred first, a solution (150 μL) containing TOB (15 mM, 1 eq), AcCoA (15 mM, 1 eq), and Eis (~0.02 mg) in Na_2HPO_4 buffer (25 mM, pH 8.0 adjusted at rt) containing 10% D_2O was prepared and allowed to proceed until the AcCoA was completely consumed as indicated by TLC. ^1H, gCOSY, and zTOCSY experiments were performed on the reaction solution, applying PURGE solvent suppression [14]. This reaction was not sequential in nature, yielding a mixture of mono-acetylated products: 3"- and 6'-acetyl-TOB (data not shown). After the first equivalent of AcCoA was consumed to give a mixture of products and all spectra obtained (not reported), an additional aliquot containing AcCoA (1 eq) was added and additional spectra were obtained after incubating for 12 h in order confirm that a single di-acetylated product, the 3",6'-di-acetyl-TOB, had been formed.

To unambiguously establish the two acetylated positions on the TOB scaffold, the NMR spectra were compared to those of a standard of pure TOB [15 mM in Na_2HPO_4 buffer (25 mM, pH 8.0 adjusted at rt) containing 10% D_2O], which was prepared identically to the reaction mixture but omitted AcCoA and Eis (Table 2.10). Proton connectivity of the final product was assigned using zTOCSY and gCOSY spectra. Representative spectra for 3",6'-di-acetyl-TOB are provided (Figs. 2.51-2.53).Representative spectra of the TOB standards are provided (Figs. 2.48-2.50).

Table 2.10. Proton chemical shifts determined for TOB and 3",6'-di-acetyl-TOB.[a]

Ring	H position	TOB	3",6'-di-acetyl-TOB	Δppm
II	1	3.21-3.11[b] (m)[c] [3.18][d]	[3.38]	0.20
	2_{ax}	1.68 (ddd (app. q), $J_{2ax,2eq} = J_{2ax,1} = J_{2ax,3} = 12.7$ Hz)	[1.85]	0.17
	2_{eq}	2.29-2.21 (m) [2.27]	[2.49]	0.22
	3	3.43-3.31[c] (m) [3.34]	[3.52]	0.18
	4	3.72-3.58[e] (m) [3.63]	[3.73]	0.10
	5	3.80-3.75 (m) [3.77]	[3.79]	0.02
	6	3.72-3.58[e] (m) [3.70]	[3.79]	0.19
I	1'	5.68 (bs)	5.47 (bs)	-0.21
	2'	3.51-3.46 (m) [3.48]	[3.59]	0.11
	3'a	1.68 (ddd (app. q), $J_{3'a,3'b} = J_{3'a,2'} = J_{3'a,4'} = 11.8$ Hz)	[1.95]	0.27
	3'b	2.29-2.21 (m) [2.23]	[2.26]	0.03
	4'	3.66-3.58 (m) [3.63]	[3.46]	-0.17
	5'	3.96-3.88 (m) [3.90]	[3.78]	-0.12
	$6'_a$	3.43-3.31 (m) [3.41]	[3.60]	**0.19**
	$6'_b$	3.43-3.31 (m) [3.41]	[3.60]	**0.19**
III	1"	5.11 (bs)	5.06 (bs)	-0.05
	2"	3.86-3.75 (m) [3.83]	(m) [3.69]	-0.14
	3"	3.43-3.31 (m) [3.36]	(m) [4.09]	**0.73**
	4"	3.66-3.58 (m) [3.60]	(m) [3.45]	-0.15
	5"	3.96-3.88 (m) [3.93]	(m) [3.91]	-0.02
	$6"_a$	(m) [3.79]	(m) [3.70]	-0.09
	$6"_b$	(m) [3.79]	(m) [3.70]	-0.09
Acetyl	NH-3"	×	(m) [8.14]	
	NH-6'	×	(m) [8.11]	
	CH_3C=O on 3"	×	2.03 (s)	
	CH_3C=O on 6'	×	1.98 (s)	

[a]The chemical shift were established based on ^{1}H (400 MHz), zTOCSY, and gCOSY NMR [b]Could be analogous position of the DOS ring. [c]Multiplicity and *J* are given in (). [d]The numbers in [] were determined from gCOSY and/or zTOCSY. [e]Could be analogous position of the DOS ring. ×Indicates that the acetyl moiety is not present in the molecule.

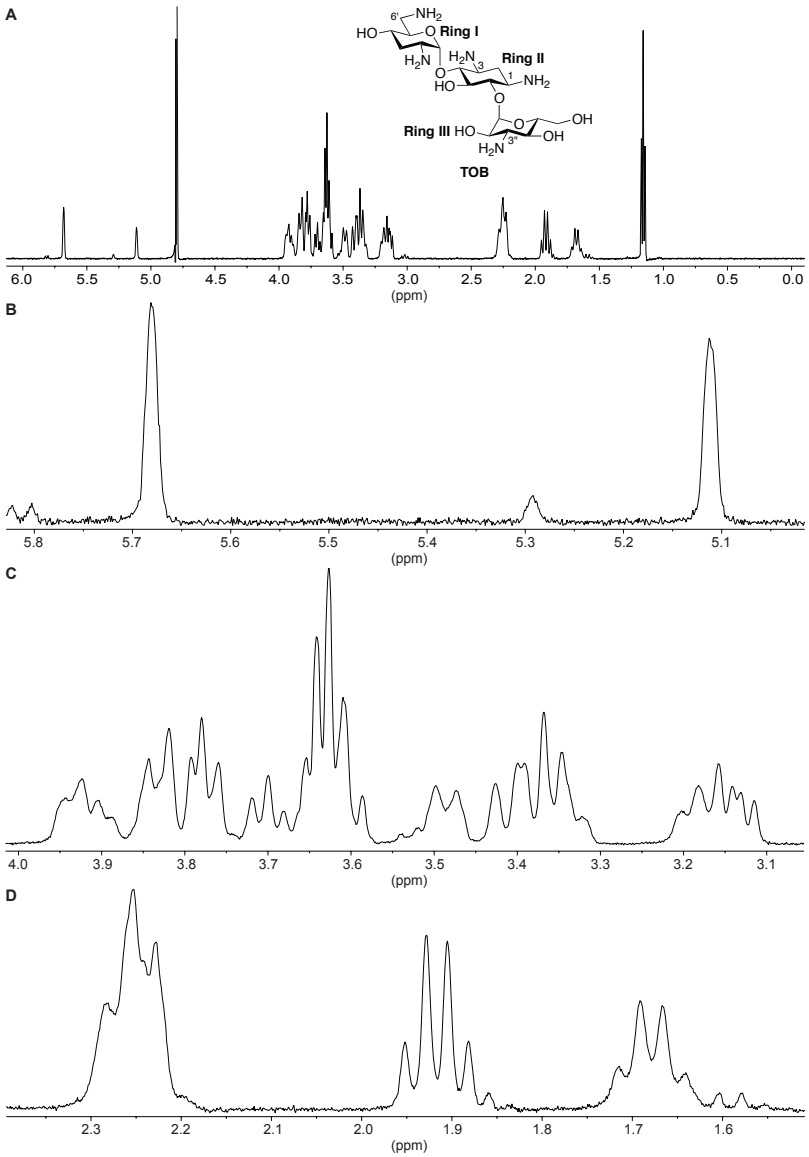

Fig. 2.48. ^{1}H NMR of TOB (9:1/H_2O:D_2O, pH 8, 25 mM KH_2PO_4) (500 MHz). The full spectrum is shown in panel **A** and the expansions in panels **B-D**.

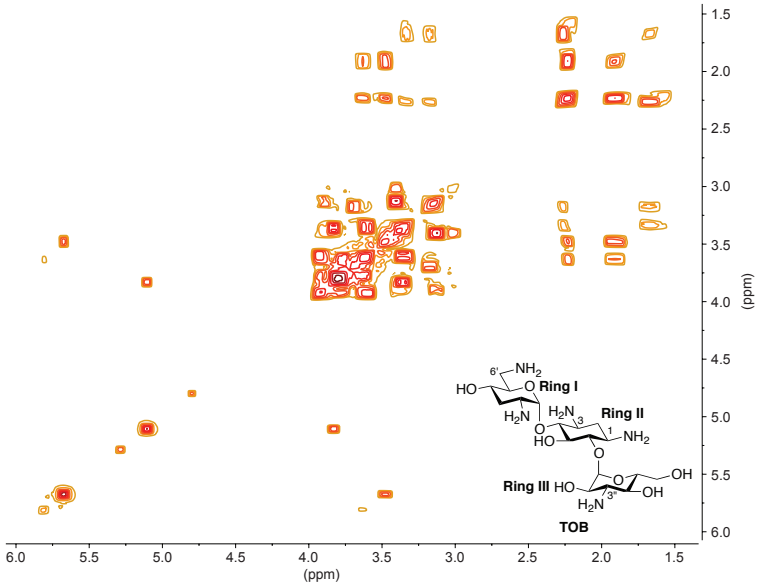

Fig. 2.49. gCOSY of TOB (9:1/H_2O:D_2O, pH 8, 25 mM KH_2PO_4) (500 MHz).

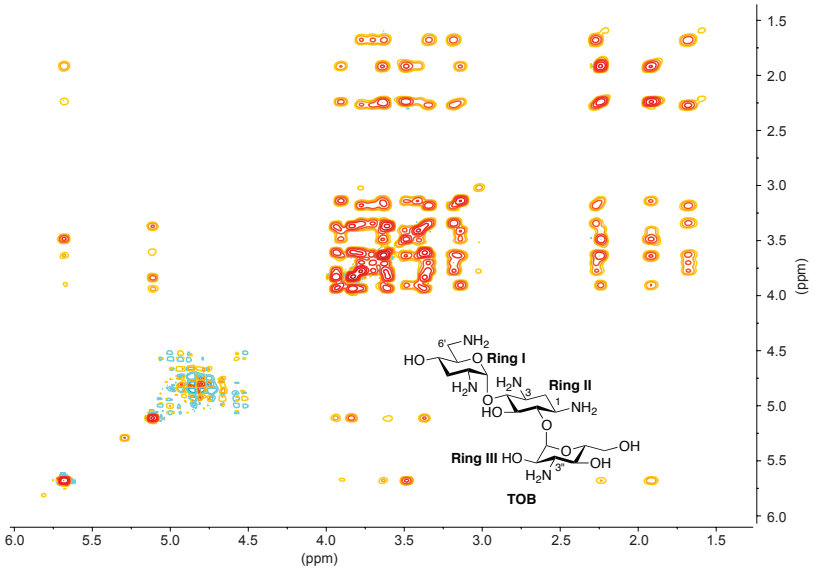

Fig. 2.50. zTOCSY of TOB (9:1/H_2O:D_2O, pH 8, 25 mM KH_2PO_4) (500 MHz).

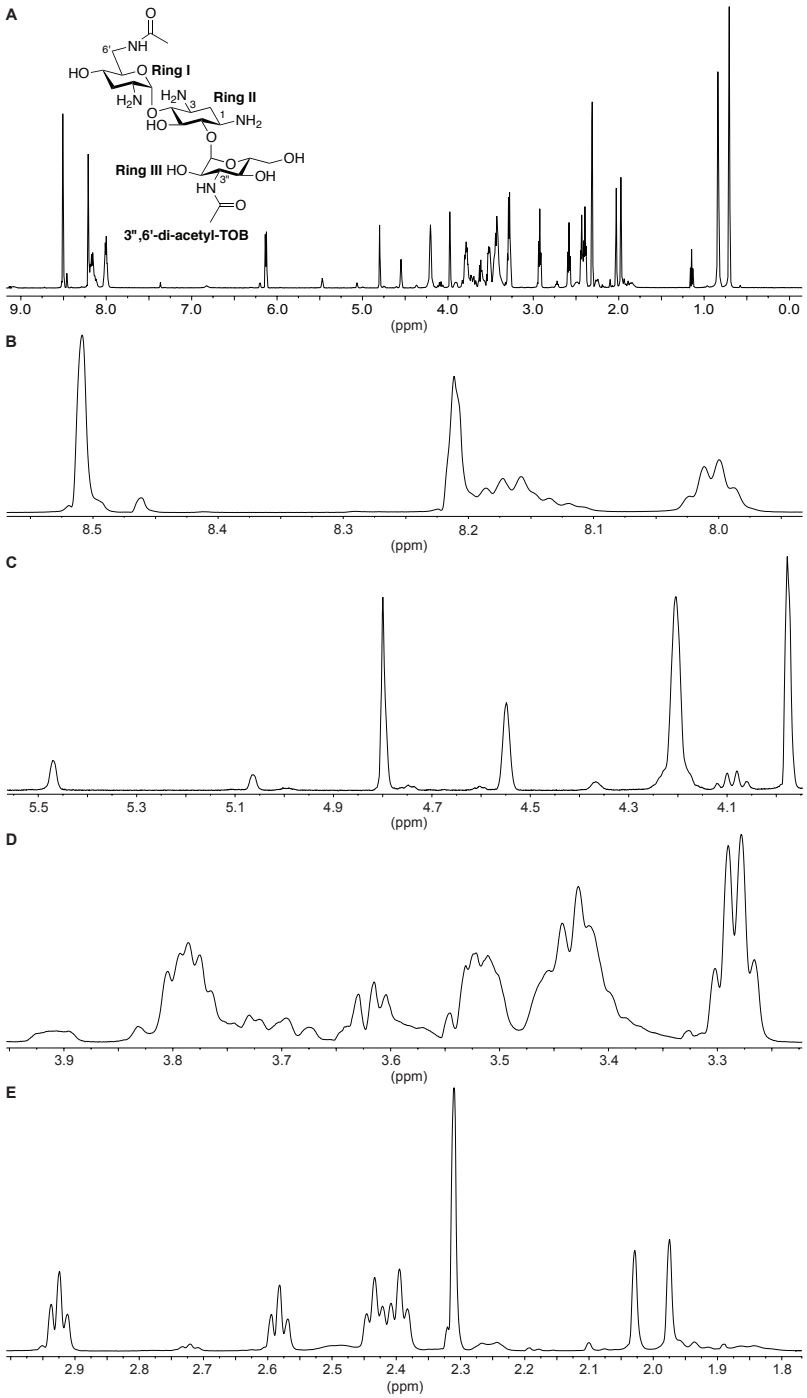

Fig. 2.51. ^{1}H NMR of 3",6'-di-acetyl-TOB Eis reaction mixture (9:1/H_2O:D_2O, pH 8, 25 mM KH_2PO_4) (500 MHz). The full spectrum is shown in panel **A** and the expansions in panels **B-E**.

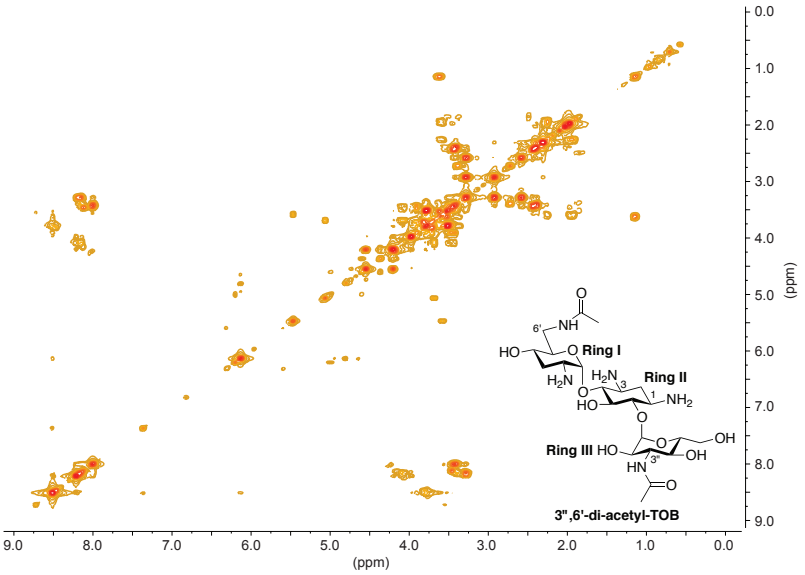

Fig. 2.52. gCOSY of 3",6'-di-acetyl-TOB Eis reaction mixture (9:1/H_2O:D_2O, pH 8, 25 mM KH_2PO_4) (500 MHz).

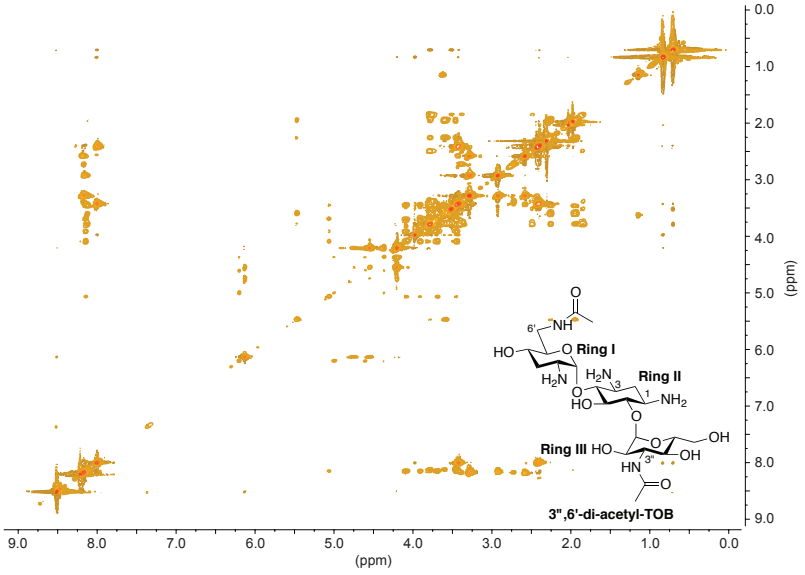

Fig. 2.53. zTOCSY of 3",6'-di-acetyl-TOB Eis reaction mixture (9:1/H_2O:D_2O, pH 8, 25 mM KH_2PO_4) (500 MHz).

2.8. References

(1) Wei, J.; Dahl, J. L.; Moulder, J. W.; Roberts, E. A.; O'Gaora, P.; Young, D. B.; Friedman, R. L. *J Bacteriol* **2000**, *182*, 377.
(2) Campbell, P. J.; Morlock, G. P.; Sikes, R. D.; Dalton, T. L.; Metchock, B.; Starks, A. M.; Hooks, D. P.; Cowan, L. S.; Plikaytis, B. B.; Posey, J. E. *Antimicrob Agents Chemother* **2011**, *55*, 2032.
(3) Chen, W.; Biswas, T.; Porter, V. R.; Tsodikov, O. V.; Garneau-Tsodikova, S. *Proc Natl Acad Sci U S A* **2011**, *108*, 9804.
(4) Green, K. D.; Chen, W.; Garneau-Tsodikova, S. *ChemMedChem* **2012**, *7*, 73.
(5) He, Z.; Li, S.; Zhou, X. *Curr Microbiol* **2011**.
(6) Lella, R. K.; Sharma, C. *J Biol Chem* **2007**, *282*, 18671.
(7) Roberts, E. A.; Clark, A.; McBeth, S.; Friedman, R. L. *J Bacteriol* **2004**, *186*, 5410.
(8) Samuel, L. P.; Song, C. H.; Wei, J.; Roberts, E. A.; Dahl, J. L.; Barry, C. E., 3rd; Jo, E. K.; Friedman, R. L. *Microbiology* **2007**, *153*, 529.
(9) Shin, D. M.; Jeon, B. Y.; Lee, H. M.; Jin, H. S.; Yuk, J. M.; Song, C. H.; Lee, S. H.; Lee, Z. W.; Cho, S. N.; Kim, J. M.; Friedman, R. L.; Jo, E. K. *PLoS Pathog* **2010**, *6*, e1001230.
(10) Zaunbrecher, M. A.; Sikes, R. D., Jr.; Metchock, B.; Shinnick, T. M.; Posey, J. E. *Proc Natl Acad Sci U S A* **2009**, *106*, 20004.
(11) Kim, K. H.; An, D. R.; Song, J.; Yoon, J. Y.; Kim, H. S.; Yoon, H. J.; Im, H. N.; Kim, J.; Kim do, J.; Lee, S. J.; Kim, K. H.; Lee, H. M.; Kim, H. J.; Jo, E. K.; Lee, J. Y.; Suh, S. W. *Proc Natl Acad Sci U S A* **2012**, *109*, 7729.
(12) Green, K. D.; Chen, W.; Houghton, J. L.; Fridman, M.; Garneau-Tsodikova, S. *Chembiochem* **2010**, *11*, 119.
(13) Chen, W.; Green, K. D.; Tsodikov, O. V.; Garneau-Tsodikova, S. *Biochemistry* **2012**.
(14) Simpson, A. J.; Brown, S. A. *J Magn Reson* **2005**, *175*, 340.

Authors' contribution:
WC performed TLC and LCMS experiments.
JLH performed TLC and NMR experiments.
JLH, WC, and SGT analyzed the data and wrote the manuscript.

Chapter 3

Unexpected modification of capreomycin by the *mycobacterial* enzyme Eis

3.1. Abstract

The enhanced intracellular survival (Eis) protein from *Mycobacterium tuberculosis* (Eis_*Mtb*), a regio-versatile *N*-acetyltransferase active towards many aminoglycosides (AGs), confers resistance to KAN in some cases of multidrug-resistant-tuberculosis (MDR-TB). We assessed the activity of Eis_*Mtb*, and the homologous Eis from *Mycobacterium smegmatis* (Eis_*Msm*), against a panel of anti-TB drugs. In addition to the AGs previously reported to be acetylated by Eis, both enzymes were capable of acetylating capreomycin (CAP) but not the other drugs tested. Modeling studies predicted the site of modification to be one of two primary amines located on the β-lysine side-chain. It was confirmed, with Eis_*Mtb*, that acetylation occurs on the terminal amine of the β-lysine side-chain *via* NMR spectroscopy. Additionally, MIC studies with CAP against several strains of *mycobacteria* were performed for comparison to reported values against susceptible and resistant strains of *Mtb*, indicating that CAP may be a useful anti-mycobacterial drug against strains other than *Mtb*.

3.2. Introduction

Causing 1.4 million deaths globally in 2010, TB is the second leading pathogen-related cause of death, surpassed only by HIV/AIDS. Although worldwide incidences of TB are beginning to modestly decline, occurrences of multidrug-resistant TB (MDR-TB) and extensively drug-resistant TB (XDR-TB) are increasing rapidly- the former proving fatal in more than one-third of the cases. Drug resistance to TB occurs when infected patients are treated with the wrong regimen of antibiotics or when the patients fail to complete the full course of treatment, which occurs most frequently in areas with sub-standard TB

control programs. Bacteria that are resistant to at least isoniazid (INH) and rifampicin, the two most powerful first-line treatments for TB, are designated as MDR-TB. Strains of *Mtb* are classified as XDR if they are shown to be resistant to rifampicin and INH, in addition to a fluoroquinolone, and at least one of the second-line anti-TB drugs such as kanamycin A (KAN), amikacin (AMK), or CAP.

Clinical resistance of *Mtb* to KAN was shown, in one-third of cases covering a large and diverse set of strains, to be the result of mutations in the promoter of the enhanced intracellular survival (*eis*) gene, named for its ability to enhance survival of *mycobacteria* in macrophages.[1,2] The mutation causes up-regulation of *eis*, a gene that encodes for the Eis protein. The structural and functional characterization of Eis from *Mtb* has been the goal of many research efforts recently.[2-10] Our laboratory has shown that Eis acts as an unusually regio-versatile AG acetyltransferase (AAC) in *Mtb*[3] and *Msm*,[11] and it has also been shown that Eis is capable of conferring resistance to KAN in the AG-susceptible *Mtb* strain H37Rv.[9] Additionally, it was recently reported that Eis from *Msm* (Eis_*Msm*) and Eis from *Mtb* (Eis_*Mtb*) are also capable of acetylating lysine residues of dual-protein phosphatase 16/mitogen-activated protein kinase phosphatase-7 (DUSP16/MPK-7).[10]

Due to the promiscuity of Eis towards a large number of AGs and precedents showing that some AACs are capable of acetylating classes of drugs other than AGs, including the second-line anti-TB drug ciprofloxacin (CIP) (Fig. 3.1),[12] it is plausible that Eis is capable of conferring resistance to other anti-TB drugs. CAP (Fig. 3.1), a cyclic peptide antibiotic with a β-lysine side-chain, is particularly effective against *Mtb*. Correlation between mutations in the *eis* promoter and resistance to CAP have been suggested,[13] though similar correlations are lacking with other non-AG anti-TB drugs.

In this study we sought to gain a greater understanding of the potential of Eis to acetylate other non-AG anti-TB drugs, with a focus on the second-line drug, CAP. We demonstrated that the Eis_*Mtb* and/or the Eis_*Msm* are both capable of acetylating CAP IA and CAP IB, but neither shows activity against other anti-TB drugs that were

investigated. The position of acetylation on CAP was confirmed as the terminal amine of the β-lysine using Eis_*Mtb*.

3.3. Results and discussion

3.3.1. Exploration of anti-TB drugs as potential substrates of Eis

It has been shown previously that Eis_*Mtb* and Eis_*Msm* are both capable of multi-acetylating AGs, and that a wide range of AGs are substrates for both enzymes, including KAN and AMK, two important second-line anti-TB drugs.[3,10,11] In addition to acting as an AAC against wide panels of AG antibiotics, Eis proteins from *Mtb* and *Msm* have demonstrated acetylation activity against lysine residues of DUSP16/MPK-7.[10] Given the substrate promiscuity of Eis, investigation of further possible acetylation targets was explored, focusing on anti-TB drugs. CAP was chosen for these experiments because aside from its use as a popular second-line anti-TB drug, its structure includes a β-lysine side-chain, which could potentially be acetylated. Previous studies have shown that INH (Fig. 3.1) becomes acetylated by arylamine *N*-acetyltransferase 2 on the hydrazide functional group, demonstrating its potential for deactivation *via* acetylation.[14,15] Pyrazinamide (PZA) (Fig. 3.1) was chosen for its structural similarity to INH, allowing for the comparison of INH to a similar drug that is not likely to be acetylated. CIP was selected since previous studies have identified AACs capable of conferring resistance to fluoroquinolones *via* acetylation.[12] Owing to the vast number of AG substrates previously identified as substrates for Eis enzymes, streptomycin (STR) (Fig. 3.1), the first AG used in anti-TB treatment, was chosen.

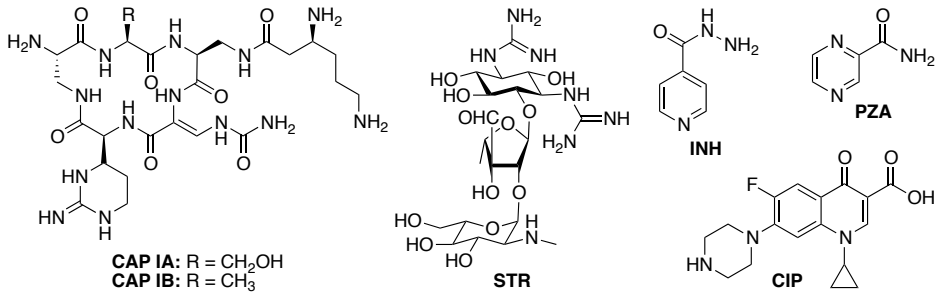

Fig. 3.1. Structures of anti-TB drugs tested against Eis proteins in this study. CAP = capreomycin; STR = streptomycin; INH = isoniazid; PZA = pyrazinamide; CIP = ciprofloxacin.

In order to determine whether Eis proteins from *Mtb* or *Msm* were capable of deactivating any of these anti-TB drugs, CAP, CIP, INH, PZA, and STR were screened using a UV-Vis spectrophotometric assay. We found that Eis proteins from *Mtb* and *Msm*, in the cases of CIP, INH, PZA, and STR, did not show any acetylation activity. In the cases of STR and PZA, these results are not particularly surprising, given the lack of nucleophilic primary amines likely to undergo acetylation.

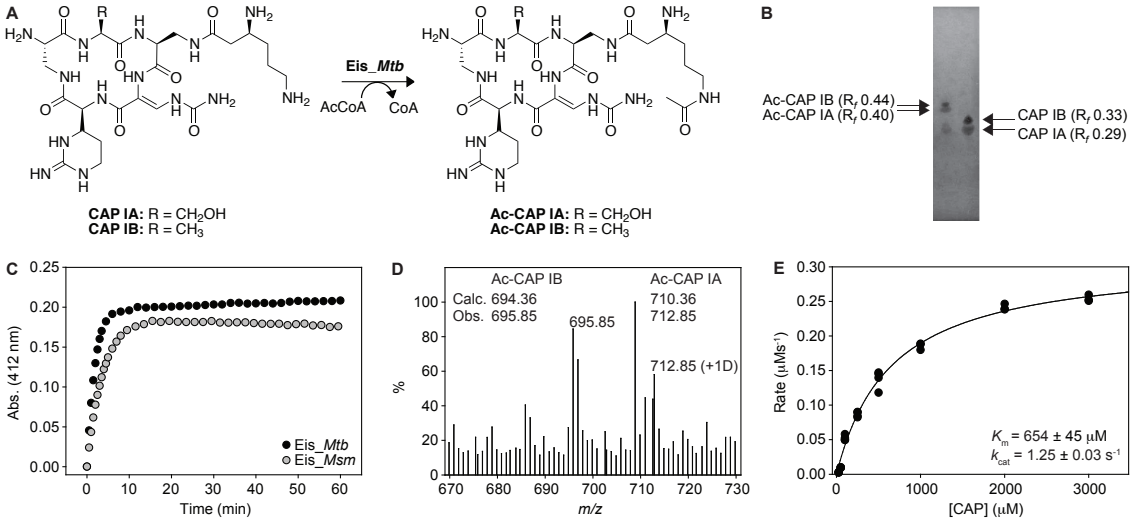

Fig. 3.2. Confirmation of mono-acetylation of CAP by Eis from *Mtb* and *Msm.* **A.** Scheme showing the acetylation of CAP by Eis from *Mtb,* **B.** TLC showing the mono-acetylation of CAP. **C.** UV-Vis assay confirming the mono-acetylation of CAP by Eis from *Mtb* and *Msm*. **D.** Confirmation of mono-acetylation by LCMS. **E.** Michaelis-Menten kinetics of the acetylation of CAP by Eis from *Mtb*.

We demonstrated using a UV-Vis spectrophotometric assay that Eis_*Mtb* and Eis_*Msm* are both capable of efficiently acetylating CAP (Figs. 3.2A and 3.2C). In contrast to the multiple acetylations carried out by both Eis enzymes on AGs, we confirmed, by TLC (Fig. 3.2B) and LCMS (Fig. 3.2D), that both CAP IA and CAP IB were converted to the respective mono-acetylated products. Given the ability of Eis to accommodate proteins in its substrate-binding site, it is not surprising that a relatively large biomolecule such as CAP is a substrate for Eis. CAP is a peptidic molecule, so given the ability of Eis to acetylate proteins, it is not surprising it is modified, despite its structure being very different from that of AGs. In fact, determination of the kinetic parameters for CAP with Eis_*Mtb* (Fig. 3.2E) indicated that the K_m and k_{cat} values were 654 ± 45 μM and 1.25 ± 0.03 s^{-1}, respectively. While these values were within an order of magnitude of those for

the AGs studied to date with both Eis_*Mtb* and Eis_*Msm*, the k_{cat} and K_m were both slightly higher than with most AGs.[3,10,11] As a result, the catalytic efficiency (k_{cat}/K_m) of 1911 ± 139 $s^{-1}M^{-1}$ is equivalent to or greater than many of the AGs previously tested.[3,11] This suggests that while CAP does not have as strong an affinity to the substrate binding pocket of Eis, it is still capable of undergoing a particularly facile and efficient acetylation, possibly due to Eis' affinity for the lysine moiety.

3.3.2. Regio-specificity of CAP acetylation by Eis_*Mtb*

In order to predict which amine of CAP Eis_*Mtb* acetylates, molecular modeling studies were performed. These studies were performed using Sybyl-X for energy minimization of the CAP IB structure and GOLD for docking the energy-minimized molecule into the structure of Eis_*Mtb* (PDB code: 3R1K).[3] The resultant binding prediction was used to identify the most likely site(s) of modification of CAP IB by Eis_*Mtb*. The energy-minimized complex of CAP IB with Eis_*Mtb* indicated that the large binding pocket of Eis_*Mtb* could accommodate the scaffold of CAP (Fig. 3.3A). CAP is predicted to bind in a manner that places both amines of the β-lysine side-chain in proximity of the acetyl thioester of AcCoA (Fig. 3.3B). This suggests the potential for multiple acetylations, yet, in contrast to the activity of Eis towards most AGs, CAP is only mono-acetylated. (Figs. 3.2A and 3.2B). The acetylation of the lysine 55 residue in DUSP16/MPK-7 occurs at the α-amine or the terminal/ε-amine, with Eis_*Msm* and Eis_*Mtb*, respectively.[10] Given these observations, it was predicted that the terminal amine is favored for acetylation. This probability was further enhanced by the supposition that the terminal amine position would have increased flexibility and superior nucleophilic behavior, due to lower steric hindrance and increased electron density, respectively.

In order to unambiguously establish the specificity of Eis_*Mtb* towards CAP, 1D- and 2D-NMR experiments were performed on the Eis_*Mtb* reaction product for comparison to a CAP standard. Tables were constructed to allow for simple side-by-side analysis of the chemical shifts of the protons of interest (Table 3.2). Analysis of the Eis_*Mtb* reaction with CAP indicated that the terminal primary amine of the β-lysine side-chain was

acetylated, as indicated by a change in the chemical shift of the protons directly adjacent to the terminal amine of the β-lysine side-chain.

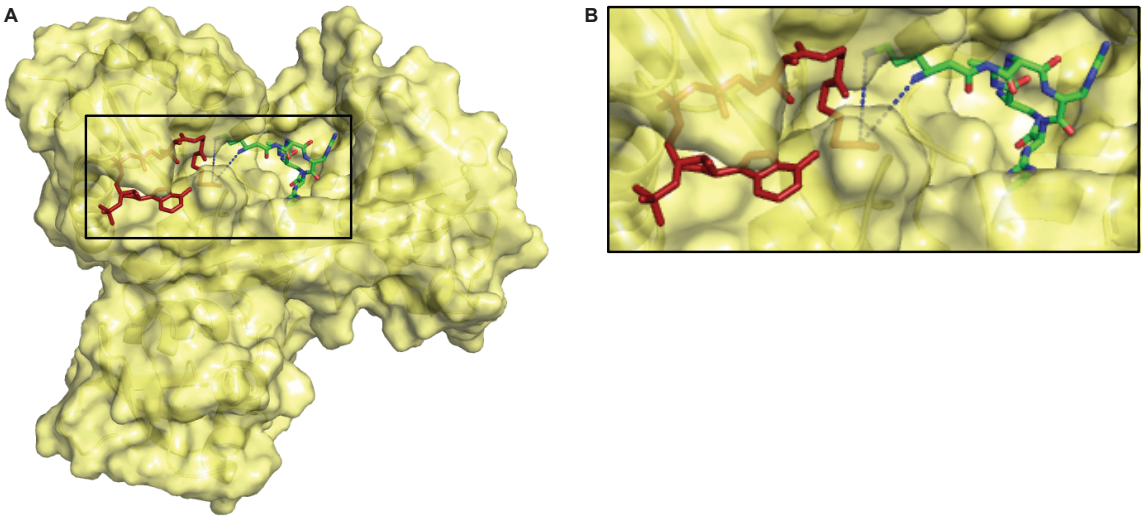

Fig. 3.3. Docking of CAP in the binding pocket of Eis from *Mtb* showing **A.** CAP and AcCoA bound to Eis from *Mtb* and **B.** the potential for acetylation at either amine of the β-lysine side-chain.

A recent systematic review of *Mtb* mutations that are associated with resistance to CAP, as well as KAN and AMK, found that Eis promoter mutations have been reported in as many as 9% of CAP-resistant strains.[13] The same study suggested that CAP-resistance of *Mtb* may be predicted by concurrent mutations in the *rrs* gene and *eis* promoter region, suggesting that Eis may have some role in inactivating CAP, although evidence suggests that mutations in the *eis* promoter region alone are insufficient to cause significant levels of resistance to CAP in *Mtb*. Additionally, X-ray crystal structures of CAP with the 70S ribosome have indicated that the β-lysine side-chain of CAP does not appear to be crucial to its ability to bind to the ribosome,[16] implying that acetylation of the β-lysine side-chain may not be sufficient to rescue bacteria harboring Eis from the effects of CAP.

3.3.3. MIC values for CAP against various *mycobacteria*

To assess the relative susceptibility of *mycobacteria* to CAP, MIC values were determined against *Msm* str. MC2155 and four additional strains of *mycobacteria*, including *M. avium* subsp. *avium* ATCC 25291, *M. abscessus* ATCC 19977, *M. intracellulare* ATCC 13950, and *M. parascrofulaceum* ATCC BAA-614 (Table 3.1). In

general, CAP showed anti-mycobacterial activity in the strains tested, though the MIC for *M. abscessus* was notably higher. This is not surprising based on recent reports of the difficulties in treatment of infections caused by *M. abscessus*.[17] MIC values for the other four strains, compared to previously reported MIC values[18] against *wtMtb* strains as well as those with a combination of mutations in *rrs* or *tlyA* and the *eis* promoter region or only the *eis* promoter region, suggest that CAP could be an equally viable anti-mycobacterial treatment for those strains, with the exception of *M. abscessus*.

Table 3.1. MIC (μg/mL) values for CAP against *mycobacteria*.

Species	MIC
M. abscessus ATCC 19977	75
M. avium subsp. *avium* ATCC 25291	18.8
M. intracellulare ATCC 13950	9.4
M. parascrofulaceum ATCC BAA-614	18.8
M. smegmatis str. MC2155	4.7
M. tuberculosis (wt)	< 4.0[18]
M. tuberculosis + *eis* mutation	1-4[18]
M. tuberculosis + *rrs* mutation	0.5-32[18]
M. tuberculosis + *eis* + *rrs* mutations	1-16[18]
M. tuberculosis + *tylA* mutation	0.5-16.0[18]

3.4. Conclusions

We have assessed the potential of Eis proteins from *Mtb* and *Msm* to acetylate various first- and second-line anti-TB drugs, finding that CAP is the only non-AG drug tested to date that is modified by either protein. This finding expands upon our understanding of Eis proteins as acetyltransferases, specifically in terms of their ability to modify a broad range of small molecules as well as proteins- to date, all known acetylations occur at a primary amine. We conclusively confirmed *via* NMR spectroscopy that CAP is modified at the terminal amine of the β-lysine residue, which studies have suggested, may not be crucial for binding to the ribosome. *In silico* assessment of the binding mode of a novel peptide scaffold such as CAP with Eis will aid the discovery of novel inhibitors of Eis, an emerging strategy for overcoming the resistance conferred by Eis.[4,11] Additionally, we assessed the MIC values for CAP against several strains of *mycobacteria*, our results suggest that CAP could be used in the treatment of *mycobacteria* other than *Mtb*. MIC studies of *Mtb* that have shown A1401G *rrs* mutations combined with mutations in the *eis* promoter may confer some low level resistance to CAP. These previous studies coupled with our current studies suggest the possibility that CAP resistance may in fact be mediated or enhanced *via* acetylation.

3.5. Materials and methods

3.5.1. Materials and instrumentation

The Eis enzymes from *Mycobacterium tuberculosis* (Eis_*Mtb*)[19] and *Mycobacterium smegmatis* (Eis_*Msm*)[11] were overexpressed and purified as previously described. Acetyl-CoA (AcCoA), capreomycin (CAP; as a mixture of CAP IA and IB) (*Note*: If IA or IB are not indicated, CAP represents the mixture of both CAP IA and IB), isoniazid (INH), pyrazinamide (PZA), streptomycin (STR), ciprofloxacin (CIP), and DTNB were bought from Sigma-Aldrich (Milwaukee, WI) (Fig. 3.1). TLCs (Merck, Silica gel 60 F_{254}) were visualized using iodine. ^{1}H, gCOSY, gHSQC, and zTOCSY NMR spectra were recorded on a Varian 500 MHz equipped with a 3 mm OneProbe. All NMR spectra were recorded either in D_2O or 9:1/H_2O:D_2O at pH 8.0. Liquid chromatography-mass spectrometry (LCMS) was performed on a Shimadzu LCMS-2019EV equipped with a SPD-20AV UV-Vis detector and a LC-20AD liquid chromatograph. UV-Vis assays were performed using a multimode SpectraMax M5 plate reader and 96-well plates (Fisher Scientific). *M. avium* subsp. *avium* ATCC 25291, *M. abscessus* ATCC 19977, *M. intracellulare* ATCC 13950, and *M. parascrofulaceum* ATCC BAA-614 were purchased from the American Type Culture Collection (ATCC; Manassas, VA). *M. smegmatis* str. MC2 155 was a generous gift from Dr. Sabine Ehrt (Weill Cornell Medical College).

3.5.2. Determination of Eis_*Mtb* and Eis_*Msm* acetylation activity with anti-TB drugs by UV-Vis assays

The acetylation of the anti-TB drugs INH, PZA, STR, CIP, and CAP was explored using the previously described Ellman method[4,11] monitoring the reaction of CoASH released by the Eis enzymes with the Ellman's reagent (DTNB). Briefly, Eis (from *Mtb* or *Msm*, 0.5 mM) was added to a mixture containing Tris (50 mM, pH 8.0, adjusted at rt), AcCoA (500 μM), anti-TB drug (100 μM), and DTNB (2 mM) to initiate reactions (200 μL total volume). The reaction progress at 25 °C was monitored at 412 nm (ε_{412} = 14,150 $M^{-1}cm^{-1}$) by taking measurements every 30 s for 1 h (Fig. 3.2C).

The kinetic parameters (K_m and k_{cat}) for CAP were determined as above using varying concentrations of CAP (0, 20, 50, 100, 250, 500, 1000, 2000 μM) and AcCoA (500 μM).

The first 2-5 min of reactions were used to calculate the initial rates and the data were fit to a Michaelis-Menten curve using SigmaPlot 11.0 to determine the K_m and k_{cat} values (Fig. 3.2E).

3.5.3. TLC and LCMS assays showing the conversion of CAP into mono-acetyl-CAP (Ac-CAP) products

An aliquot (5 μL) of the CAP acetylation reaction used for NMR analysis (10 mM in Na_2HPO_4 buffer (25 mM, pH 8.0 adjusted at rt)) and an aliquot of the CAP standard used for NMR analysis (10 mM in D_2O) were loaded onto a silica gel TLC plate and eluted in a mixture of phenol:H_2O:NH_4OH/30:10:1. After drying for 2 h, the TLC plate was stained for visualization in a sealed chamber containing I_2/SiO_2 for 8 h (Fig. 3.2B).

To confirm the single *N*-acetylation of both CAP IA and IB, the masses of the novel acetylated CAP were determined using the NMR sample (20 μL) by LCMS in positive mode using H_2O (0.1% formic acid). The mass spectrum obtained is provided in Fig. 3.2D.

3.5.4. Molecular modeling of CAP IB with Eis_*Mtb*

The CAP IB structure was built with Sybyl-X software and minimized to 0.01 kcal/mol by the Powell method, using Gasteiger-Hückel charges and the Tripos force field. The protein coordinates (PDB code: 3R1K)[19] were downloaded from the Protein Data Bank website. With the exception of CoA, the H_2O molecules, acetamide, and all other substructures were removed from the structure. An acetyl group was added to CoA by modifying the natural ligand using Sybyl-X. The surrounding protein residues were then kept frozen while the AcCoA was subjected to energy minimization using the Steepest Descent method to get rid of steric clashes. Hydrogen atoms were added to the Eis_*Mtb*-AcCoA complex and its energy was minimized using the Amber force field with Amber charges. The energy-optimized CAP IB was docked into the AG binding site in the Eis_*Mtb* protein using GOLD.[20] The parameters were set as the default values for GOLD. The maximum distance between hydrogen bond donors and acceptors for hydrogen bonding was set to 3.5 Å. After docking, the top three CAP IB conformations were

individually merged into the minimized Eis_*Mtb*-AcCoA complex. To relax the protein side chains, the three new Eis_*Mtb*-AcCoA-CAP IB complexes were subsequently subjected to energy minimization using the Amber force field with Amber charges. During the energy minimization, the structure of CAP IB and residues within an 8-Å radius were allowed to move. The remaining residues were kept frozen in order to reduce calculation time. The energy minimization, in all three cases, was performed using the Powell method with a 0.05 kcal/mol energy gradient convergence criterion and a distance dependent dielectric function. The model of the Eis_*Mtb*-AcCoA CAP IB complex is depicted in Figs. 3.3A and 3.3B.

3.5.5. Acetylation of CAP by Eis_*Mtb* analyzed by NMR: analysis of the 6'-*N*-acetyl-CAP (Ac-CAP) products and comparison to the parent compounds

To determine which position of CAP becomes acetylated by Eis_*Mtb*, the reaction was performed by monitoring the solution *via* NMR in a manner that did not require the need for purification of the acetylated products. A solution (200 μL) containing CAP (10 mM, 1 eq), AcCoA (25 mM, 2.5 eq), and Eis_*Mtb* (5 μM) in Na_2HPO_4 buffer (25 mM, pH 8.0 adjusted at rt) containing 10% D_2O was prepared and allowed to proceed to completion (O/N) at rt. ^1H, gCOSY, zTOCSY, and gHSQC NMR experiments were performed on the reaction solution, applying PURGE solvent suppression.[21] Proton connectivity was assigned using zTOCSY and gCOSY spectra. Representative spectra for 6'-*N*-acetyl-CAP products are provided in Figs. 3.8-3.11. (*Note*: According to standard nomenclature, the terminal amine of the β-lysine is notated as the 6'-position, which is indicated on the spectra of the appropriate figures.)

To unambiguously establish the position acetylated on CAP, the NMR spectra of the product were compared to those of a standard of pure CAP (as a mixture of CAP IA and IB) [10 mM in 10% D_2O] (Tables 3.2 and 3.3). Representative spectra for the CAP standard are provided in Figs. 3.4-3.7.

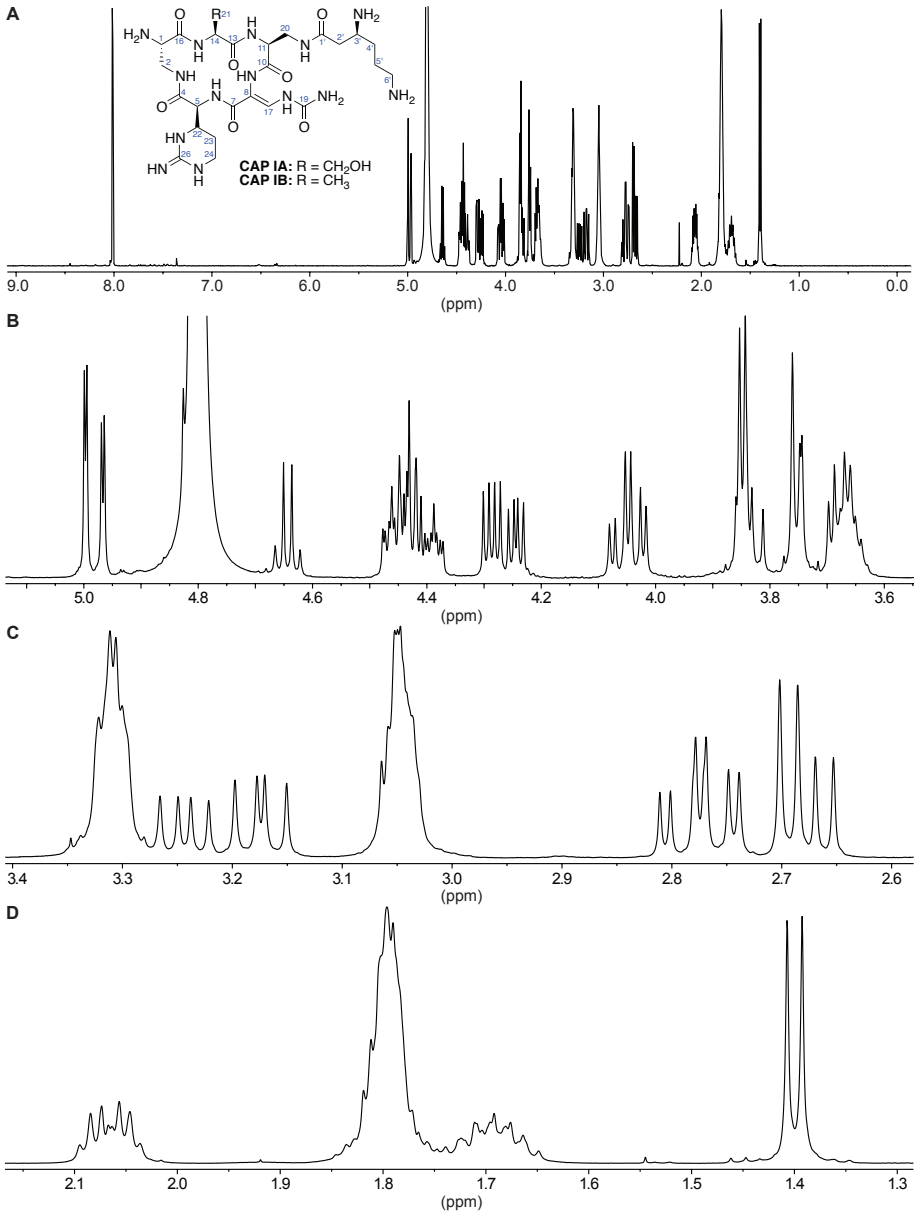

Fig. 3.4. ^{1}H of CAP (9:1/H_2O:D_2O, 25 mM Na_2HPO_4, pH 8.0) (500 MHz). The full spectrum is shown in panel **A** and the expansions in panels **B-D**.

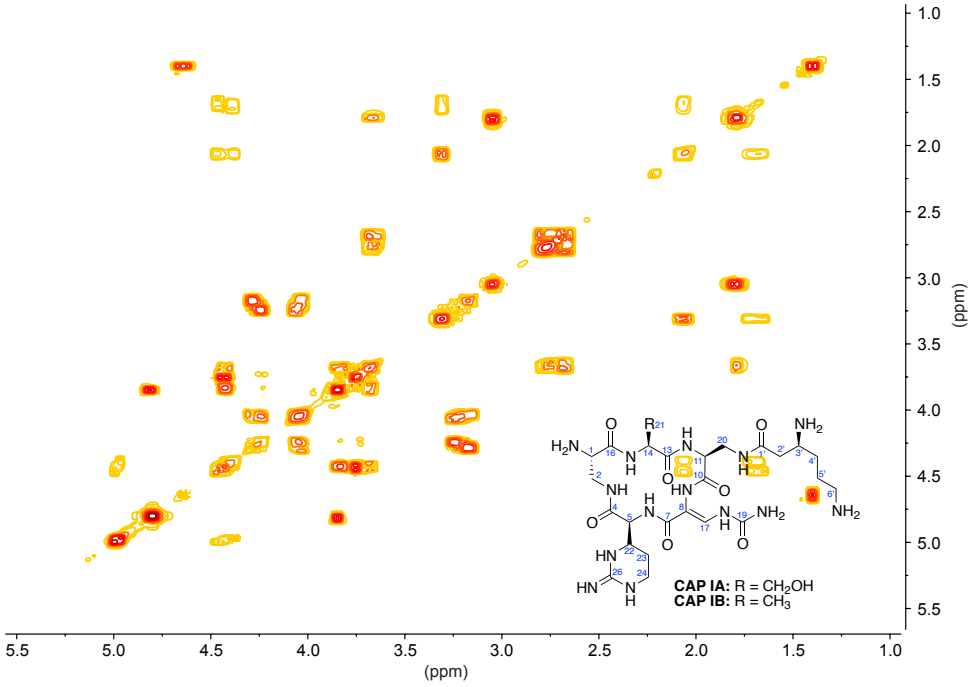

Fig. 3.5. gCOSY of CAP (9:1/H_2O:D_2O, 25 mM Na_2HPO_4, pH 8.0) (500 MHz).

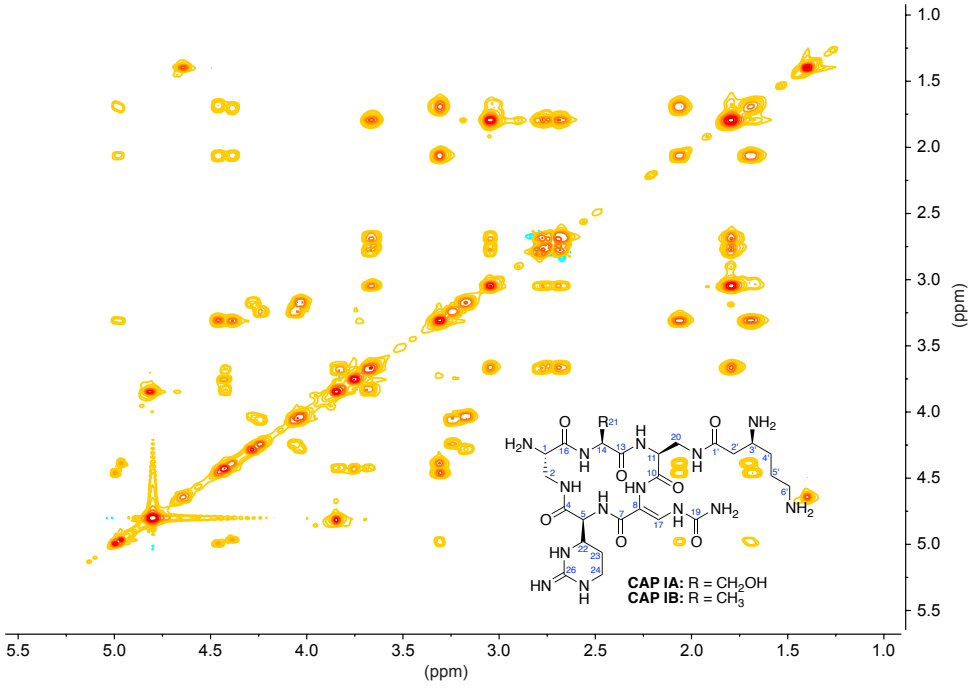

Fig. 3.6. zTOCSY of CAP (9:1/H_2O:D_2O, 25 mM Na_2HPO_4, pH 8.0) (500 MHz).

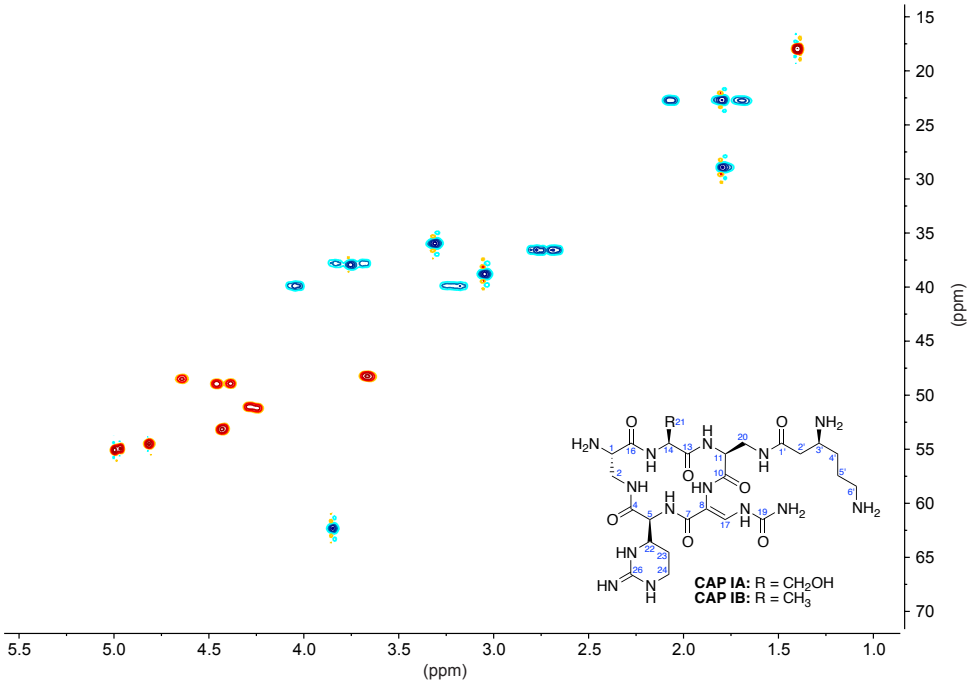

Fig. 3.7. gHSQC of CAP (9:1/H_2O:D_2O, 25 mM Na_2HPO_4, pH 8.0) (500 MHz).

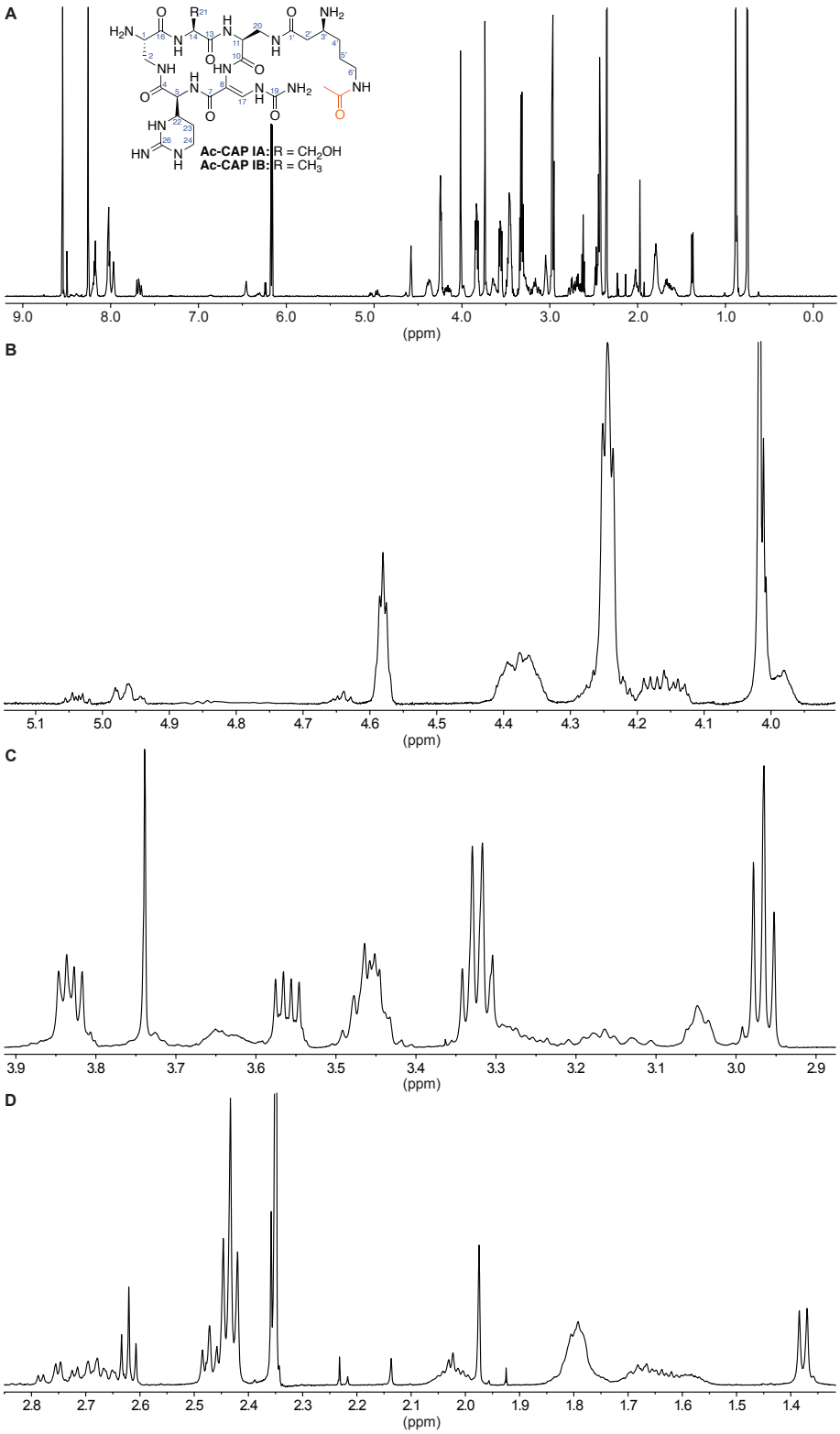

Fig. 3.8. ^{1}H of 6'-*N*-acetyl CAP in 9:1/H_2O:D_2O (500 MHz). The full spectrum is shown in panel **A** and the expansions in panels **B-D**.

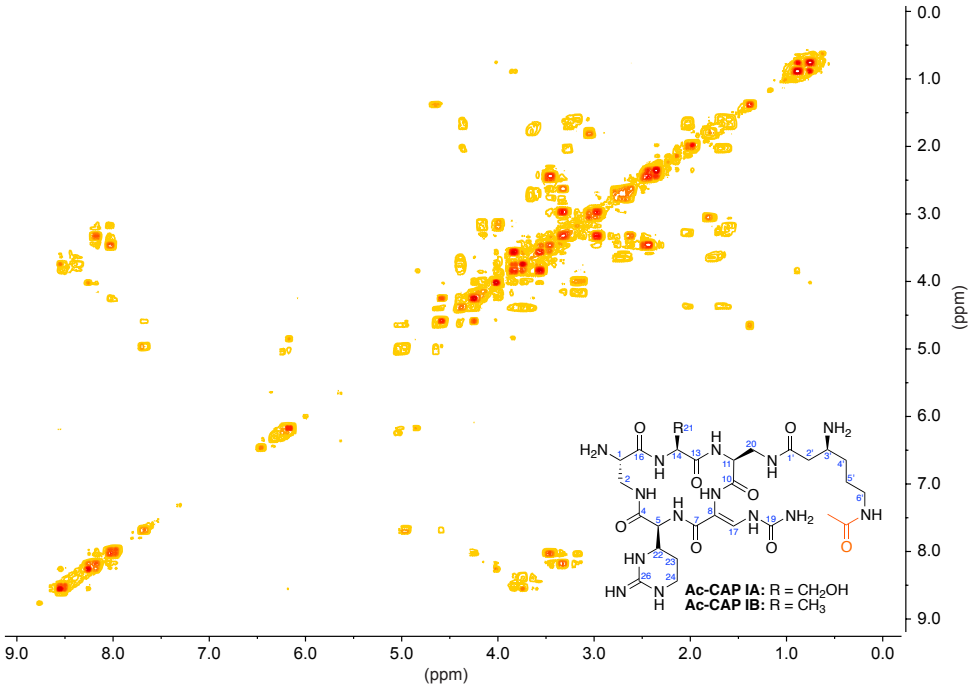

Fig. 3.9. gCOSY 6'-*N*-acetyl CAP in 9:1/H_2O:D_2O (500 MHz).

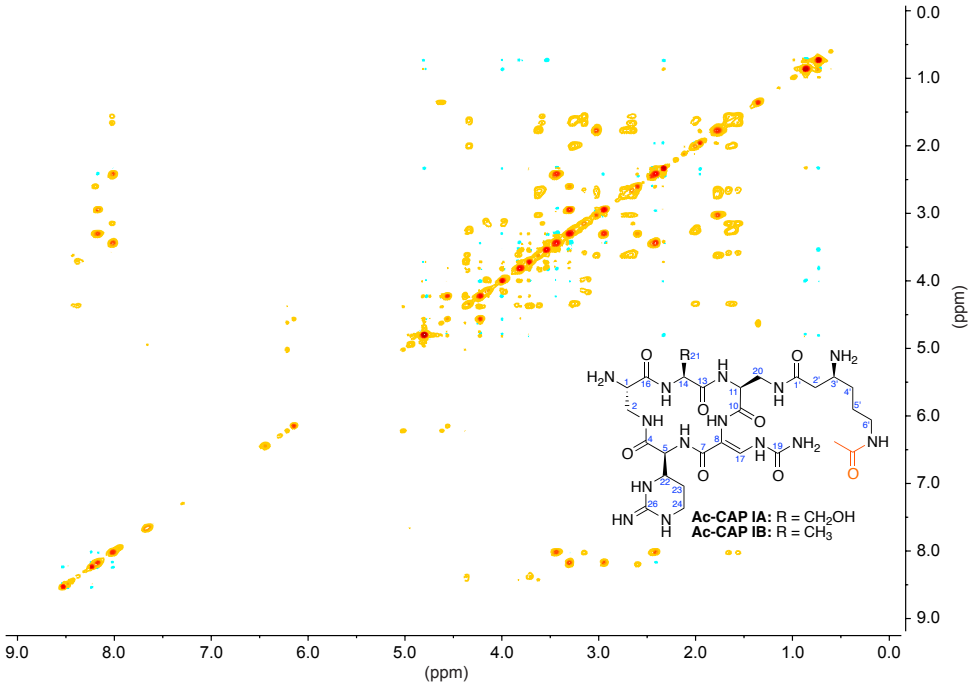

Fig. 3.10. zTOCSY of 6'-*N*-acetyl CAP in 9:1/H_2O:D_2O (500 MHz).

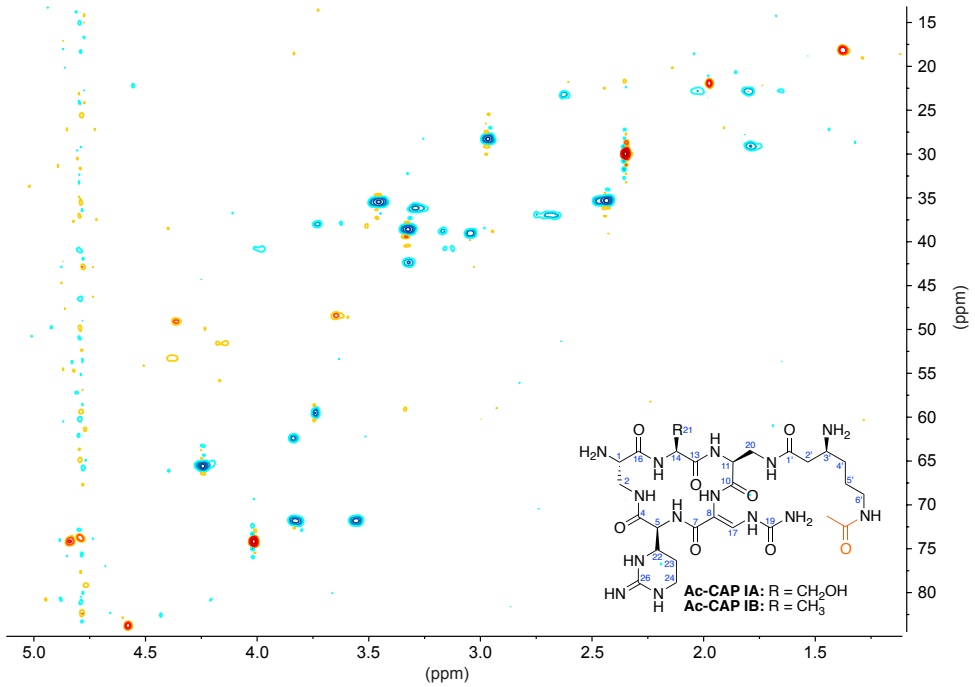

Fig. 3.11. gHSQC of 6'-*N*-acetyl CAP in 9:1/H_2O:D_2O (500 MHz).

Table 3.2. Proton chemical shifts determined for CAP IA and 6'-*N*-acetyl-CAP IA (Ac-CAP IA).[a]

H position	CAP IA	6'-*N*-acetyl-CAP IA	Δppm
1	4.48-4.41 (m)[b] [4.44][c]	4.41-4.33 (m) [4.38]	-0.06
2a/b	3.75 (m)	3.77-3.70 (m) [3.72]	-0.03
5	5.00 (d, $J_{5,22}$ = 2.2 Hz)	5.06-4.93 (m) [5.02]	0.02
11	4.29 (dd, $J_{11,20a}$ = 5.0 Hz, $J_{11,20b}$ = 10.0 Hz)	4.20-4.12 (m) [4.16]	-0.13
14	[4.81][£]	[4.83][£]	0.02
17	8.02 (s)	8.05-7.99 (m)[†]	[†]
20a	4.03 (dd, $J_{20a,11}$ = 5.0 Hz, $J_{20a,20b}$ = 13.7 Hz)	4.03-3.95 (m) [3.97]	-0.06
20b	3.17 (dd, $J_{20b,11}$ = 10.0 Hz, $J_{20b,20a}$ = 13.7 Hz)	3.22-3.09 (m) [3.13]	-0.04
21	3.86-3.81 (m) [3.85]	3.85-3.81 (m) [3.84]	-0.01
22	4.48-4.41 (m) [4.46]	4.42-4.33 (m) [4.38]	-0.08
23a	2.07 (ddd (app. dq), $J_{23a,22}$ = 5.3 Hz, $J_{22,23b}$ = $J_{22,24}$ = 13.7 Hz)	2.07-1.98 (m) [2.06]	-0.01
23b	1.75-1.65 (m) [1.69]	1.73-1.54 (m) [1.69]	=
24	3.34-3.28 (m) [3.31]	3.36-3.22 (m) [3.31]	=
2'a	2.78 (dd (app. t), $J_{2'a,2'b}$ = 16.2 Hz, $J_{2'a,3'}$ = 15.0 Hz)	2.79-2.60 (m) [2.73]	-0.05
2'b	2.68 (dd, $J_{2'b,2'a}$ = 16.2 Hz, $J_{2'b,3'}$ = 8.2 Hz)	2.79-2.60 (m) [2.65]	-0.03
3'	3.70-3.63 (m) [3.66]	3.68-3.60 (m) [3.64]	-0.02
4'	1.84-1.75 (m) [1.80]	1.73-1.55 (m) [1.70]	-0.10
5'	1.84-1.75 (m) [1.80]	1.73-1.55 (m) [1.60]	-0.20
6'	3.07-3.02 (m) [3.05]	3.36-3.10 (m) [3.19]	**0.14**
NH-6'	×	8.06-7.99 (m) [8.03]	
CH$_3$C=O on 6'	×	1.97 (s)	

[a]The chemical shift values were established based on ^{1}H (500 MHz), zTOCSY, and gCOSY NMR. [b]Multiplicity and *J* are given in (). [c]The numbers in [] were determined from gCOSY and zTOCSY. ×Indicates that acetyl moiety is not present in the molecule. [£]Obscured by H_2O peak in the ^{1}H spectrum. [†]No correlation in spectra so specific chemical shift undetermined.

Table 3.3. Proton chemical shifts determined for CAP IB and 6'-*N*-acetyl-CAP IB (Ac-CAP IB).[a]

H position	CAP IA	6'-*N*-acetyl-CAP IA	Δppm
1	4.48-4.41 (m)[b] [4.42][c]	4.41-4.33 (m) [4.36]	-0.06
2a	3.86-3.81 (m) [3.83]	3.88-3.79 (m) [3.84]	0.01
2b	3.70-3.63 (m) [3.68]	3.68-3.60 (m) [3.61]	-0.07
5	4.97 (d, $J_{5,22}$ = 2.5 Hz)	5.06-4.93 (m) [4.94]	-0.03
11	4.24 (dd, $J_{11,20a}$ = 8.1 Hz, $J_{11,20b}$ = 5.0 Hz)	4.20-4.12 (m) [4.14]	-0.10
14	4.64 (q, $J_{14,21}$ = 7.3 Hz)	4.67-4.62 (m) [4.64]	=
17	8.01 (s)	8.05-7.99 (m)[†]	[†]
20a	4.06 (dd, $J_{20a,11}$ = 5.0 Hz, $J_{20a,20b}$ = 13.7 Hz)	4.03-3.95 (m) [3.97]	-0.09
20b	3.24 (dd, $J_{20b,11}$ = 8.1 Hz, $J_{20b,20a}$ = 13.7 Hz)	3.22-3.09 (m) [3.17]	-0.07
21	1.40 (d, $J_{21,14}$ = 7.3 Hz)	1.39 (d, $J_{21,14}$ = 7.2 Hz)	-0.01
22	4.39 (dd, $J_{22,5}$ = 2.5 Hz, $J_{22,23a}$ = 5.3 Hz, $J_{22,23b}$ = 8.1 Hz)	4.42-4.33 (m) [4.34]	-0.05
23a	2.07 (ddd (app. dq), $J_{23a,22}$ = 5.3 Hz, $J_{22,23b}$ = $J_{22,24}$ = 13.7 Hz)	2.07-1.98 (m) [2.06]	-0.01
23b	1.75-1.65 (m) [1.69]	1.73-1.54 (m) [1.69]	=
24	3.34-3.28 (m) [3.31]	3.36-3.22 (m) [3.31]	=
2'a	2.77 (dd (app. t), $J_{2'a,2'b}$ = 16.2 Hz, $J_{2'a,3'}$ = 15.0 Hz)	2.79-2.60 (m) [2.73]	-0.04
2'b	2.68 (dd, $J_{2'b,2'a}$ = 16.2 Hz, $J_{2'b,3'}$ = 8.2 Hz)	2.79-2.60 (m) [2.65]	-0.03
3'	3.70-3.63 (m) [3.66]	3.68-3.60 (m) [3.64]	-0.02
4'	1.84-1.75 (m) [1.80]	1.73-1.55 (m) [1.70]	-0.10
5'	1.84-1.75 (m) [1.80]	1.73-1.55 (m) [1.60]	-0.20
6'	3.07-3.02 (m) [3.05]	3.36-3.10 (m) [3.19]	**0.14**
N<u>H</u>-6'	×	8.06-7.99 (m) [8.03]	
C<u>H</u>$_3$C=O on 6'	×	1.97 (s)	

[a]The chemical shift values were established based on ^{1}H (500 MHz), zTOCSY, and gCOSY NMR. [b]Multiplicity and *J* are given in (). [c]The numbers in [] were determined from gCOSY and zTOCSY. ×Indicates that acetyl moiety is not present in the molecule. [†]No correlation in spectra so specific chemical shift undetermined.

3.5.6. Determination of the MIC values for CAP against various *mycobacteria*

MIC experiments were performed against a variety of *mycobacteria*, using the double dilution method. Compounds were added to 7H9 media containing ADC supplement. *M. avium* subsp. *avium* ATCC 25291, *M. abscessus* ATCC 19977, *M. intracellulare* ATCC 13950, and *M. parascrofulaceum* ATCC BAA-614 were grown for 6 days before MIC readings were taken, while *M. smegmatis* readings were taken 1-3 days after dilution. Concentrations of CAP tested ranged from 150 mg/mL to 0.3 mg/mL. All experiments were completed in sets of duplicate or triplicate experiments. MIC values are reported in Table 3.1.

3.6. References

(1) Campbell, P. J.; Morlock, G. P.; Sikes, R. D.; Dalton, T. L.; Metchock, B.; Starks, A. M.; Hooks, D. P.; Cowan, L. S.; Plikaytis, B. B.; Posey, J. E. *Antimicrob Agents Chemother* **2011**, *55*, 2032.

(2) Wei, J.; Dahl, J. L.; Moulder, J. W.; Roberts, E. A.; O'Gaora, P.; Young, D. B.; Friedman, R. L. *J Bacteriol* **2000**, *182*, 377.

(3) Chen, W.; Biswas, T.; Porter, V. R.; Tsodikov, O. V.; Garneau-Tsodikova, S. *Proc Natl Acad Sci U S A* **2011**, *108*, 9804.

(4) Green, K. D.; Chen, W.; Garneau-Tsodikova, S. *ChemMedChem* **2012**, *7*, 73.

(5) Lella, R. K.; Sharma, C. *J Biol Chem* **2007**, *282*, 18671.

(6) Roberts, E. A.; Clark, A.; McBeth, S.; Friedman, R. L. *J Bacteriol* **2004**, *186*, 5410.

(7) Samuel, L. P.; Song, C. H.; Wei, J.; Roberts, E. A.; Dahl, J. L.; Barry, C. E., 3rd; Jo, E. K.; Friedman, R. L. *Microbiology* **2007**, *153*, 529.

(8) Shin, D. M.; Jeon, B. Y.; Lee, H. M.; Jin, H. S.; Yuk, J. M.; Song, C. H.; Lee, S. H.; Lee, Z. W.; Cho, S. N.; Kim, J. M.; Friedman, R. L.; Jo, E. K. *PLoS Pathog* **2010**, *6*, e1001230.
(9) Zaunbrecher, M. A.; Sikes, R. D., Jr.; Metchock, B.; Shinnick, T. M.; Posey, J. E. *Proc Natl Acad Sci U S A* **2009**, *106*, 20004.
(10) Kim, K. H.; An, D. R.; Song, J.; Yoon, J. Y.; Kim, H. S.; Yoon, H. J.; Im, H. N.; Kim, J.; Kim do, J.; Lee, S. J.; Kim, K. H.; Lee, H. M.; Kim, H. J.; Jo, E. K.; Lee, J. Y.; Suh, S. W. *Proc Natl Acad Sci U S A* **2012**, *109*, 7729.
(11) Chen, W.; Green, K. D.; Tsodikov, O. V.; Garneau-Tsodikova, S. *Biochemistry* **2012**.
(12) Vetting, M. W.; Park, C. H.; Hegde, S. S.; Jacoby, G. A.; Hooper, D. C.; Blanchard, J. S. *Biochemistry* **2008**, *47*, 9825.
(13) Georghiou, S. B.; Magana, M.; Garfein, R. S.; Catanzaro, D. G.; Catanzaro, A.; Rodwell, T. C. *PLoS One* **2012**, *7*, e33275.
(14) Sim, E.; Sandy, J.; Evangelopoulos, D.; Fullam, E.; Bhakta, S.; Westwood, I.; Krylova, A.; Lack, N.; Noble, M. *Curr Drug Metab* **2008**, *9*, 510.
(15) Sim, E.; Walters, K.; Boukouvala, S. *Drug Metab Rev* **2008**, *40*, 479.
(16) Stanley, R. E.; Blaha, G.; Grodzicki, R. L.; Strickler, M. D.; Steitz, T. A. *Nat Struct Mol Biol* **2010**, *17*, 289.
(17) Nessar, R.; Cambau, E.; Reyrat, J. M.; Murray, A.; Gicquel, B. *J Antimicrob Chemother* **2012**, *67*, 810.
(18) Engstrom, A.; Perskvist, N.; Werngren, J.; Hoffner, S. E.; Jureen, P. *J Antimicrob Chemother* **2011**, *66*, 1247.
(19) Chen, W.; Biswas, T.; Porter, V. R.; Tsodikov, O. V.; Garneau-Tsodikova, S. *Proc Natl Acad Sci U S A* **2011**, *108*, 9804.
(20) Verdonk, M. L.; Cole, J. C.; Hartshorn, M. J.; Murray, C. W.; Taylor, R. D. *Proteins* **2003**, *52*, 609.
(21) Simpson, A. J.; Brown, S. A. *J Magn Reson* **2005**, *175*, 340.

Note:
This chapter is adapted from article an to be submitted: **Jacob L. Houghton**, Keith D. Green, Rachel E. Pricer, Abdelrahman S. Mayhoub, and Sylvie Garneau-Tsodikova.

Authors' contribution:
JLH performed NMR, TLC, and LCMS experiments and analysis.
KDG performed UV-Vis, LCMS, and MIC assays.
REP performed UV-Vis assays.
ASM performed modelling experiments.
JLH, KDG, ASM, REP, and SGT analyzed the data and wrote the manuscript.

Chapter 4

Towards the development of novel aminoglycosides *via* chemical modification of known aminoglycosides

4.1. Abstract

Despite issues with toxicity and resistance, aminoglycosides (AGs) have remained an effective and widely used class of antibacterials since their discovery. Efforts to synthesize novel AGs that overcome some of the problems with this class of compounds, including their toxicity and bacterial resistance, have been a major focus research efforts for decades. 1-*N*-acylation has proved to be one of the most successful strategies for improving the overall properties of AGs, including their ability to avoid certain resistance mechanisms. More recently, 6'-*N*-acylation arose as another possible strategy, leading us to question what other positions could be modified and what types of acyl groups will lead to increased activity of AGs. In this study we report on the progress of strategies to generate novel AGs with improved activity and the ability to avoid resistance. Also we report progress towards the synthesis of AGs with the most reactive amines protected, for future use in the synthesis of AGs acylated at positions previously difficult to selective access in a short number of steps.

4.2. Introduction

AGs are a potent class of natural product antibacterial agents that are effective in the treatment of many Gram-positive and Gram-negative antibacterial infections, including those that accompany other diseases such as cancer and HIV.[1,2] The synthesis of complex carbohydrates like AGs, which are comprised of as few as two or as many as five aminosugars, and in some cases, ribose, is often a daunting task, and their total synthesis from basic chemical building blocks is rarely an efficient means of developing novel, effective compounds. Additionally, the numerous protecting group manipulations

required to selectively modify known AGs in a predictable manner is also quite difficult owing to the large number of amine and hydroxyl groups with similar reactivity.[3-10] In most cases, the overall yields of syntheses are rather low, requiring large quantities of starting material and many steps to achieve a single product.

The manifestation of a number of resistance mechanisms that reduce the efficacy of AGs is another obstacle in the development of novel AGs. Some mechanisms, such as the increased efflux or decreased uptake of AGs by bacterial cells[1,11-19] and modifications of the ribosome,[20-23] are generally effective against most AGs, because they reduce the intracellular concentration of AGs or modify the binding site common to most AGs, respectively. In these cases, modifying the AG scaffold may not provide any benefit. However, AG-modifying enzymes (AMEs), which covalently modify AGs leading to decreased affinity for the ribosome, are the most common mechanism of resistance and tend to be more specific towards particular AGs.[24-29] The activity of AMEs may, in fact, be circumvented by small manipulations of the scaffolds of known AGs to yield products that retain their activity against bacteria but are no longer modified by AMEs. The development of semi-synthetic AGs has proven a successful strategy in overcoming, to some extent, the AG resistance problem.[30-37] In particular, the incorporation of a γ-amino-β-hydroxybutyric acid (AHB), exemplified by plazomicin (PZN),[36,37] or glycinyl group to the scaffold of known AGs has been one successful strategy used to circumvent AMEs while retaining or improving upon their antibacterial properties.[30] Herein, we report progress towards the development of strategies to further expand our ability to access novel AGs through facile synthetic methods.[3-5,10,38]

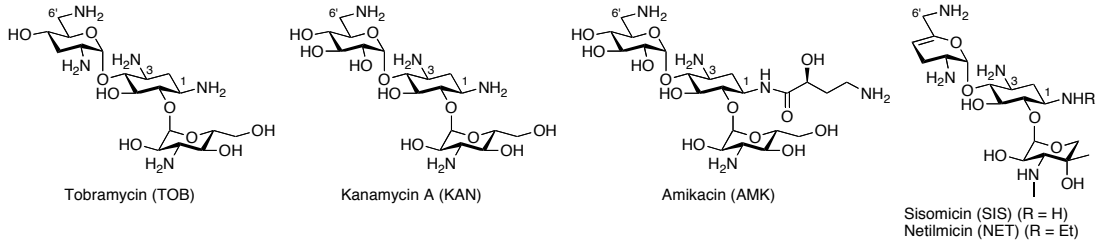

Fig. 4.1. The structures of AGs that were synthetically modified to generate novel AGs in this study.

4.3. Results and discussion

A series of 6'-*N*-glycinyl compounds (**9-13**) (Fig. 4.3) were prepared using an activated ester in the form of *O*-azidoacetyl-*N*-hydroxysuccinimide (**1**) to selectively append an α-zidoacetyl group. Compound **1** was prepared *via* the DCC mediated coupling of α-azidoacetic acid and *N*-hydroxysuccinimide in THF (Fig. 4.2).

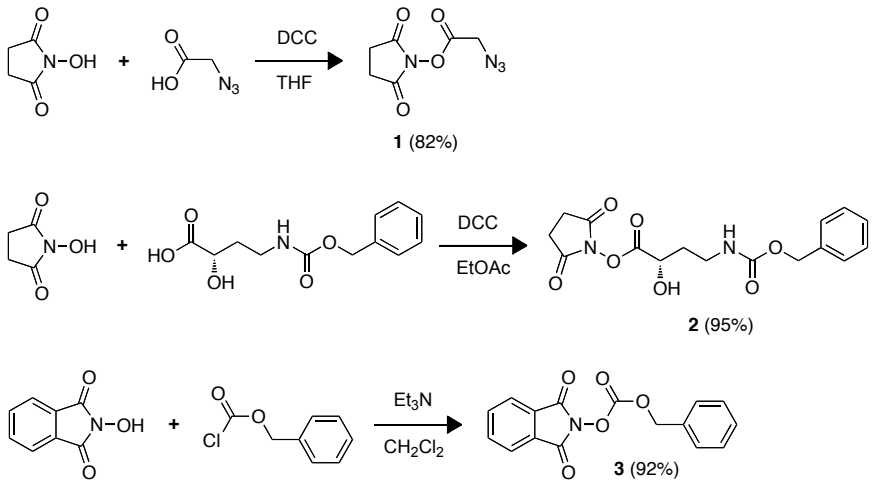

Fig. 4.2. Synthesis of coupling reagents (**1-3**) used in this study.

The reaction of tobramycin (TOB), kanamycin A (KAN), amikacin (AMK), sisomicin (SIS), or netilmicin (NET) with **1** using potassium carbonate as base in a 1:1 mixture of H_2O and MeOH afforded the 6'-*N*-azidoacetyl compounds (**4-8**) in yields ranging from 26-60% after purification by SiO_2 flash chromatography. The 6'-*N*-azidoacetyl compound was the primary product in each of the reactions (Fig. 4.3A) and was in each case isolable as pure compound for use in the following steps. Some side-products were present, such as di-*N*-azidoacetyl as well as a mixture of other mono-*N*-azidoacetyl (*i.e*. 6'-, 3-, or 1-*N*-azidoacetyl), but isolation of these compounds revealed that the other compounds were purified as mixtures of various side products. The 6'-*N*-azidoacetyl compounds were all isolated as single spots on TLC and used directly in the following step. In the case of AMK, the acylation reaction occurred at a relatively equal rate at the 6'-amine and terminal amine of the AHB. For this reason, **6** was prepared in the same fashion as all other 6'-*N*-azidoacetyl compounds but with an additional molar equivalent of the acylating reagent **1**.

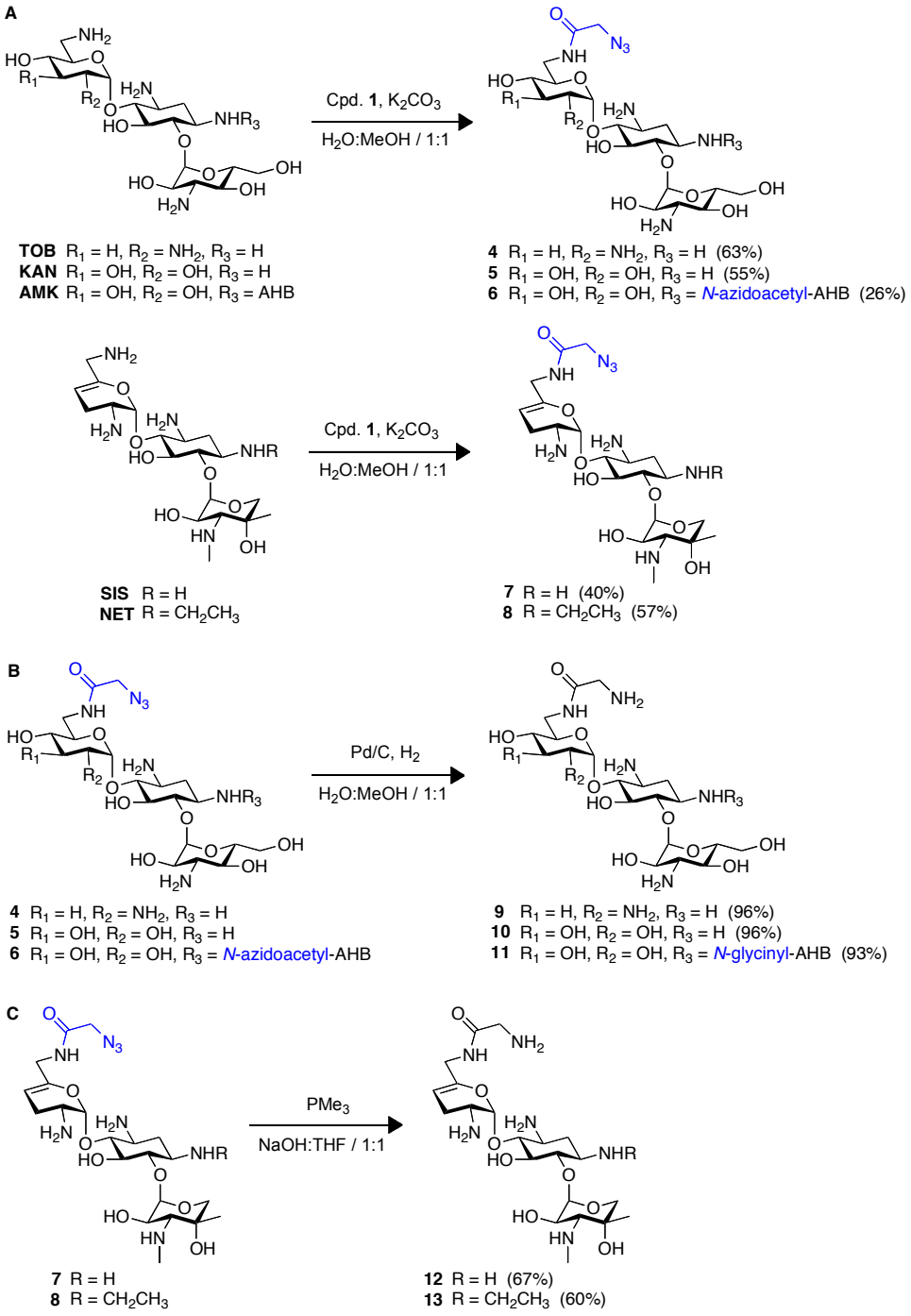

Fig. 4.3. A. Representative synthetic scheme illustrating the preparation of the 6'-*N*-azidoacetyl compounds (**4**-**8**). **B.** Representative synthetic scheme illustrating the conversion of 6'-*N*-azidoacetyl compounds **4**-**6** to the respective 6'-*N*-glycinyl compounds **9**-**11** by catalytic hydrogenation. **C.** Representative synthetic scheme illustrating the conversion of 6'-*N*-azidoacetyl compounds **7** and **8** to the respective 6'-*N*-glycinyl compounds **12** and **13** by Staudinger reaction.

For compounds **4-6**, the azide functionalities were then converted to the free amines to yield afford compounds **9-11** *via* catalytic hydrogenation (Fig. 4.3B), and, after removal of the catalyst by filtration through Celite, no further purification was necessary. The synthetic strategy and purification were adapted from a previously reported method that takes advantage of the increased nucleophilicity of the 6'-amine to selectively acylate that position, without additional acylation at the other primary amines.[30]

6'-*N*-azidoacetyl compounds **7** and **8** both contain an alkene that is not compatible with catalytic hydrogenation, and for that reason they were converted to the repective 6'-*N*-glycinyl compounds using a Staudinger reaction. Treatment of compound **7** and **8** with trimethyl phospine in a 1:1 mixture of aqueous NaOH (1 mM) and THF yielded compounds **12** and **13**, respectively (Fig. 4.3C).

The synthesis and antibacterial testing of 6'-*N*-glycinyl-TOB (**9**) was previously reported,[30] but we report a slightly modified method that improved yield, achieved by slower addition of the acylating reagent and use of an adjusted solvent gradient during the purification process. Previous reports have indicated that **9** demonstrates potent antibacterial activity against a number of bacterial strains,[30] including those that express AMEs that are capable of conferring resistance to the parent compound. It was shown that the ability of AAC(3) and AAC(6') to modify and deactivate TOB was reduced significantly by the incorporation of a 6'-*N*-glycinyl moiety. Interestingly, this same trend was not observed with the compound in this study- TOB was more effective or equally as ineffective against all strains tested compared to **9** (Tables 4.1-4.3). One possible explanation for this is the formulation of the compound used in MIC testing- previous studies used a sulfate salt generated at pH 3, whereas the compound was used in MIC testing in its free-base form (~pH 8). Contamination of the sample was unlikely to be a factor as they were otherwise prepared in an identical fashion. In this study, compound **9** did show some antibacterial activity, but in each case, the parent compound, TOB, was already very effective.

MIC values for **10** against all strains were all poor and no improvement compared to KAN was observed (Tables 4.1-4.3). The same was true of compound **11**, which showed poor activity against all strains (Tables 4.1-4.3). These results suggest that in the case of KAN, the 6'-amine is likely crucial to antibacterial activity, and therefore, its affinity for the ribosome target. The same is true of the combination of the 6'-amine and terminal amine of AHB from AMK. The syntheses of mono-glycinyl-AMK derivatives were attempted using chelation control with zinc acetate and by selectively protecting the AHB amine with a Cbz group followed by selective acylation of the 6'-amine. These strategies did not lead to the desired products, possibly because protection of the 6'-amine interferes with the chelation. Further efforts to identify other possible methods of chelation and or variations on the protecting groups will be pursued.

The best compounds, in terms of MIC values, were compounds **12** and **13**, 6'-*N*-glycinyl-SIS and -NET derivatives, respectively (Tables 4.1-4.3). SIS and NET both showed the overall best antibacterial activity in these studies, so it is not necessarily surprising that this was the case. However, compounds **12** and **13** were, in all cases, inferior to the parent AG (Tables 4.1-4.3)- a trend that held true of all compounds tested in this study.

Table 4.1. Antibacterial activity of AGs against Gram-negative bacteria: MIC values (μg/mL) determined by double dilution.

CPD	A	B	C	D	E	F	G	H	I	J	K
KAN	>150	>150	9.4	4.7	4.7	150	>150	2.3	>150	>150	>150
10	>150	>150	150	75	150	>150	>150	150	>150	>150	>150
AMK	37.5	75	9.4	4.7	9.4	>150	75	2.3	150	75	75
11	>150	>150	>150	>150	>150	>150	>150	>150	>150	>150	>150
17	>150	>150	>150	>150	>150	>150	>150	>150	>150	>150	>150
18	>150	>150	>150	37.5	>150	>150	>150	75	>150	>150	>150
TOB	9.4	9.4	9.4	4.7	2.3	75	>150	1.2	>150	>150	>150
9	75	150	18.8	18.8	18.8	>150	>150	37.5	>150	>150	>150
19	>150	>150	150	37.5	150	>150	>150	75	>150	>150	>150
NET	4.7	9.5	4.7	1.2	2.3	37.5	>150	0.6	4.7	>150	>150
13	37.5	159	75	9.4	18.8	>150	>150	4.7	37.5	>150	>150
SIS	4.7	9.4	9.4	2.3	2.3	37.5	>150	0.6	4.7	>150	>150
12	37.5	150	75	9.4	18.8	>150	>150	9.4	37.5	>150	>150

A. *B. subtilis* 168, **B.** *B. subtilis* 168 with pBF16 harboring AAC(6')/APH(2"), **C.** *B. cereus* ATCC 17788, **D.** *B. anthtacis* str. Sterne, **E.** *L. monocytogenes* ATCC 19115, **F.** *E. faecalis* ATCC 29212, **G.** *E. faecium* BM4105-RF, **H.** *S. aureus* ATCC 29213, **I.** MRSA, **J.** VRE, **K.** *S. aureus* Nor A.

Table 4.2. Antibacterial activity of AGs against Gram-positive bacteria: MIC values (μg/mL) determined by double dilution.

CPD	L	M	N	O	P	Q	R	S	T	U	V	W
KAN	>150	>150	>150	>150	37.5	9.4	37.5	150	>150	37.5	>150	>150
10	>150	>150	>150	>150	>150	150	>150	>150	>150	150	>150	>150
AMK	150	75	75	75	37.5	37.5	2.3	4.7	37.5	9.4	18.8	4.7
11	>150	>150	>150	>150	>150	>150	>150	150	>150	>150	>150	>150
17	>150	>150	>150	>150	>150	>150	>150	>150	>150	>150	>150	>150
18	>150	>150	>150	>150	>150	>150	150	150	>150	>150	>150	>150
TOB	150	150	9.4	9.4	9.4	4.7	0.6	X	4.7	4.7	9.4	4.7
9	>150	>150	150	150	75	75	18.8	X	>150	75	150	37.5
19	>150	>150	>150	>150	>150	>150	75	X	>150	>150	>150	>150
NET	37.5	150	9.4	4.7	9.4	2.3	2.3	2.3	9.4	4.7	2.3	2.3
13	150	>150	150	75	75	37.5	37.5	75	150	75	>150	37.5
SIS	75	75	9.4	9.4	9.4	4.7	1.2	2.3	9.4	4.7	9.4	4.7
12	>150	>150	150	75	75	37.5	18.8	37.5	150	75	>150	37.5

L. *E. coli* BL21 (DE3) with pET22b harboring AAC(6')/APH(2"), **M.** *E. coli* BL21 (DE3) with pET19b-pps harboring AAC(3)-IV, **N.** *E. coli* BL21 (DE3) with pET28a harboring Eis, **O.** *E. coli* BL21 (DE3) with pET22b, **P.** *E. coli* MC1061, **Q.** *H. influenzae* ATCC 51907, **R.** *P. aeruginosa* PA01, **S.** *P. aeruginosa* PA14, **T.** *S. enterica* ATCC 14028, **U.** *K. pneumoniae* ATCC 27736, **V.** *A. baumannii* ATCC 19606, **W.** *E. coli* Tol C. X = not determined.

Table 4.3. Antibacterial activity of AGs against various *mycobacteria*: MIC values (μg/mL) determined by double dilution.

CPD	X	Y	Z	AA	AB
KAN	0.3	>150	>150	>150	9.4
10	4.7	>150	>150	>150	>150
AMK	<0.3	150	9.4	2.3	4.7
11	37.5	>150	>150	>150	>150
17	18.8	>150	>150	>150	>150
18	4.7	>150	>150	75	>150
TOB	0.3	>150	150	2.3	9.4
9	2.3	>150	>150	9.4	>150
19	9.4	>150	>150	>150	>150
NET	0.3	37.5	2.3	>150	18.8
13	2.3	>150	18.8	>150	>150
SIS	2.3	18.8	4.7	>150	9.4
12	4.7	>150	18.8	>150	>150

X. *M. smegmatis str.* MC2 155, **Y.** *M. abscessus* ATCC 19977, **Z.** *M. parascrofulaceum* ATCC BAA-614, **AA.** *M. intracellulare* ATCC 13950, **AB.** *M. avium* subsp. *avium* ATCC 25291.

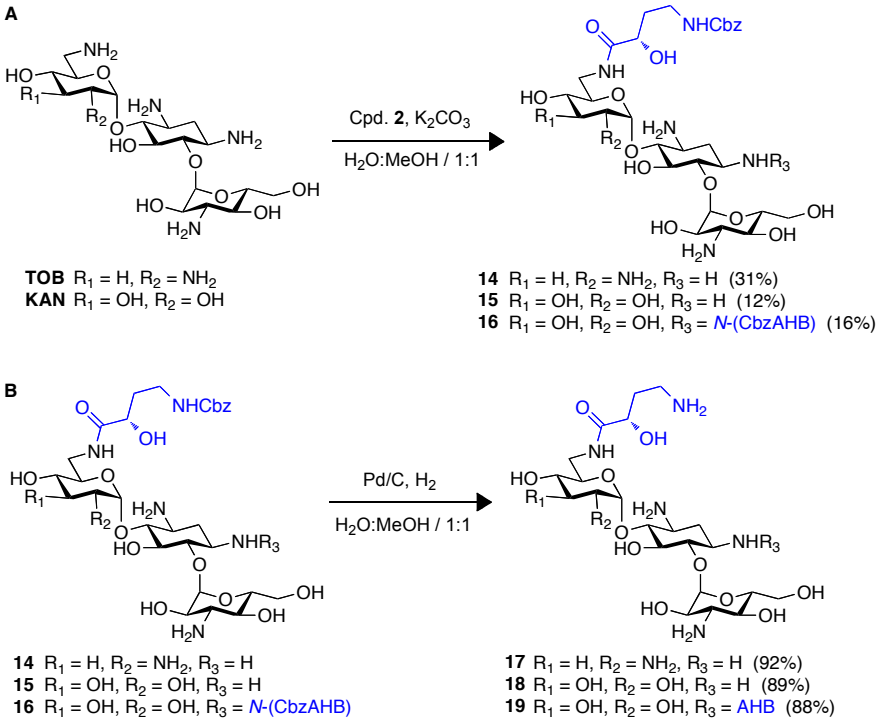

Fig. 4.4. A. Representative synthetic scheme illustrating the preparation of the 6'- and di-*N*-(CbzAHB) compounds (**14-16**) from TOB or KAN. **B.** Representative synthetic scheme illustrating the conversion of 6'- and di-*N*-(CbzAHB) compounds **14-16** to the respective 6'- and di-*N*-(CbzAHB) compounds **17-19** by catalytic hydrogenation.

Since the incorporation of an AHB group has proven a successful strategy in the development of novel AGs, attempts to expand the current methodology to selectively incorporate the AHB group at the *N*-1 position of TOB were attempted. Similar reaction conditions, in which **1** was replaced by *O*-γ-benzyloxycarbonylamino-α-hydroxybutyrate-*N*-hydroxysuccinimide (**2**), were used in our attempts to prepare compounds with an AHB group at the *N*-1 position. The use of chelation with zinc di-acetate has been shown to work well to incorporate protecting groups with KAN. However, attempts to use the same strategy starting from TOB under several conditions proved unsuccessful, as our attempts led only to a mixture of products. However, the reaction of TOB with **2**, using potassium carbonate as base in a 1:1 mixture of H_2O and MeOH, afforded compound **14** (Fig. 4.4A). Two additional *N*-(CbzAHB) derivatives, compounds **15** and **16** (Fig. 4.4A), were synthesized. Catalytic hydrogenation of compounds **14-16** (Fig. 4.4B) provided the respective *N*-AHB products, **17-19**, which were tested for antibacterial activity. Unfortunately, none of the compounds with an AHB

moiety showed improved activity against any of the bacterial strains tested compared to their respective parent compounds.

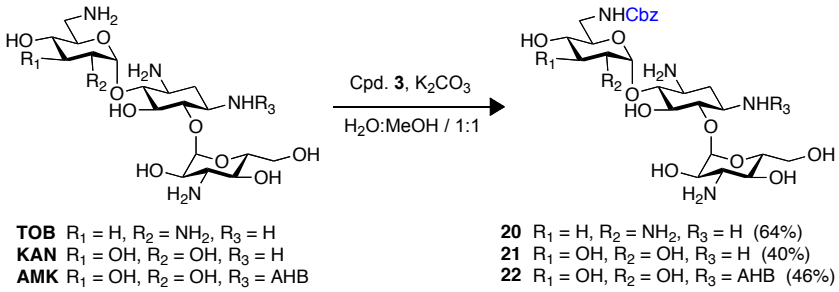

Fig. 4.5. Representative synthetic scheme illustrating the preparation of the *N*-Cbz compounds (**20**-**22**).

We have shown that it is possible to acylate, for example, the 3-*N* and retain activity against some bacteria[39] while in other cases it deleterious to antibacterial activity.[40] Therefore, the selective protection of the most nucleophilic groups (*i.e*. 6'- and AHB-amine) of AGs to generate compounds for use in the synthesis of novel AGs that are modified at positions that are typically more difficult to selectively modify is a strategy that could potentially yield compounds with antibacterial activity. Towards this end, a method for the selective Cbz-protection of AGs at the 6'- and AHB-amine was developed (Fig 4.5). *O*-Cbz-*N*-hydroxyphthalimide (**3**) was synthesized from *N*-hydroxyphthalimide and benzylchloroformate using Et_3N as a base in dichloromethane for use as the acylating reagent (Fig. 4.2). Compounds **20**-**22** were prepared from the reaction of the respective parent AG and **3**, using potassium carbonate as base in a 1:1 mixture of H_2O and MeOH (Fig. 4.5). These compounds were synthesized in order to provide a starting material for reactions that had the most reactive amine protected. We attempted syntheses using chelation control and without chelation, in an attempt to eventually generate compounds with mono- and di-acylations (glycinyl or AHB) at positions not generally accessible through concise synthetic routes. Unfortunately, the use of these compounds as starting materials did not yield novel AGs with the desired selectivity, giving, in all cases after purification, complex mixtures of compounds. Further experiments are necessary to determine any further usefulness of the Cbz-protected AGs in the development of novel *N*-acylated AGs.

4.4. Conclusions

Two series of novel *N*-acylated AGs were synthesized and tested against a large panel of Gram-positive and Gram-negative bacterial strains as well as several strains of *mycobacteria*. The determination of the MIC values of the compounds indicated that most of the synthetically modified AGs were inferior to their parent AG compounds. Interestingly, these results were not in agreement with previous reports of the activity of **9**. One possible reason for this is the formulation of the compounds for testing, which varied between studies. The compounds tested in this studied were utilized in their free base form, whereas previous studies employed compounds as sulfate salts that had been adjusted to pH 3 or lower prior to determination of the MIC values. The compounds reported herein will be reformulated for further investigation of this possibility. Additionally, a series of AGs that were Cbz-protected at the most reactive amine of each respective compound were synthesized, for use in the generation of further series of compounds modified at positions other than the 6'- or AHB-amines. However, results with this strategy were poor and further work will be necessary to accomplish a short, efficient method for generation of further *N*-glycinyl and *N*-AHB AGs.

4.5. Materials and instrumentation

The AGs AMK, KAN, and SIS were purchased from Sigma-Aldrich (Milwaukee, WI) (Fig. 4.1). The AGs NET and TOB were purchased from AK Scientific (Mountain View, CA) (Fig. 4.1). TLCs (Merck, Silica gel 60 F_{254}) were visualized using a cerium-molybdate stain ($(NH_4)_2Ce(NO_3)_6$ (5 g), $(NH_4)_6Mo_7O_{24}•4H_4O$ (120 g), H_2SO_4 (80 mL), H_2O (720 mL)). Synthetic products were purified by SiO_2 flash chromatography (Dynamic Absorbents 32-63 m). ^1H, ^{13}C, gCOSY, gHMBC, gHSQC, and zTOCSY NMR spectra were recorded either on a Varian 400 MHz equipped with a 5 mm OneProbe or a Varian 500 MHz equipped with a 3 mm OneProbe. Liquid chromatography-mass spectrometry (LCMS) was performed on a Shimadzu LCMS-2019EV equipped with a SPD-20AV UV-Vis detector and a LC-20AD liquid chromatograph. *O*-azidoacetyl-*N*-hydroxysuccinimide (**1**)[37] and *N*-hydroxysuccinimide ester of γ-benzyloxycarbonylamino-α-hydroxybutyric acid (**2**) were prepared in the manner previously described.[41]

4.6. Methods

4.6.1. Chemistry

4.6.1.1. Preparation of coupling reagents

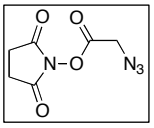

***O*-azidoacetyl-*N*-hydroxysuccinimide (1)**. Azidoacetic acid (2.53 g, 25 mmol) was dissolved in THF (20 mL) and cooled to 0 °C. *N*-hydroxysuccinimide (2.88 g, 25 mmol) was added to the solution and stirred for 10 min. DCC (5.16 g, 25 mmol) was dissolved in THF (15 mL) and added dropwise over 10 min, and the reaction was allowed to stir at 0 °C for 4 h. The mixture was vacuum filtered and the filtrate was added Et_2O and stored at 4 °C overnight to form white crystals, which were then filtered, rinsed with Et_2O (30 mL), and dried under vacuum to yield **1** as a white crystalline solid (4.08 g, 82%). Characterization of the compound was in agreement with previous reports.[37]

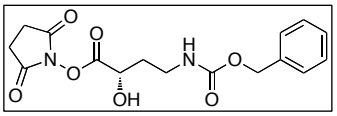

***O*-γ-benzyloxycarbonylamino- α-hydroxybutyryl-*N*-hydroxysuccinimide (2).** γ-benzyloxycarbonylamino-α-hydroxybutyric acid (2.53 g, 10 mmol, 1 eq) was dissolved in EtOAc (80 mL) and cooled to 0 °C. *N*-hydroxysuccinimide (1.15 g, 10 mmol, 1 eq) was added to the solution and stirred for 10 min. DCC (2.07 g, 10 mmol, 1 eq) was dissolved in EtOAc (20 mL) and added dropwise over 10 min, and the reaction was allowed to warm to rt while stirring for 8 h. The mixture was vacuum filtered to remove the urea and the solvent removed under reduced pressure to give **2** (3.33 g, 95%). The resulting white solid was used without further purification. ^{1}H NMR (400 MHz, $CDCl_3$) δ 7.40-7.30 (m, 5H), 5.15 (d, *J* = 12.1 Hz, 1H), 5.06 (d, *J* = 12.1 Hz, 1H), 3.65-3.53 (m, 1H), 3.44 (ddd (app. dq), *J* = 14.6, 5.7 Hz, 1H), 2.89-2.60 (m, 4H), 2.33-2.10 (m, 2H).

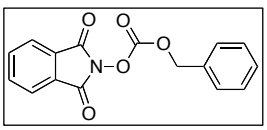

***O*-Cbz-*N*-hydroxyphthalimide (3).** *N*-hydroxyphthalimide (4.90 g, 30 mmol, 1eq) was dissolved in CH_2Cl_2 (45 mL) and Et_3N (4.18 mL, 30 mmol, 1 eq) was added at rt before cooling the solution to 0 ºC. Benzylchloroformate (4.45 mL, 30 mmol, 1 eq) was added dropwise to the stirring solution over 5 min. The reaction was allowed to warm to rt while stirring O/N (16 h). After concentration under reduced pressure, the residue was purified by SiO_2 flash

chromatography (CH_2Cl_2:MeOH/98:2, R_f = 0.29) to yield the product as a white solid (8.2 g, 92%). ^{1}H NMR (400 MHz, $CDCl_3$) δ 7.82 (dd, J_1 = 5.4, J_2 = 3.1 Hz, 2H), 7.74 (dd, J_1 = 5.5, J_2 = 3.1 Hz, 2H), 7.57-7.53 (m, 2H), 7.41-7.37 (m, 3H), 5.23 (s, 2H).

4.6.1.2. General procedure for preparation of *N*-azidoacetyl compounds

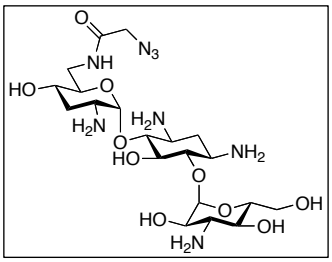

6'-*N*-azidoacetyl-TOB (4). TOB (468 mg, 1.0 mmol, 1 eq) and K_2CO_3 (276 mg, 2.0 mmol, 2 eq) were dissolved in MeOH:H_2O/1:1 (5 mL) and *O*-azidoacetyl-*N*-hydroxysuccinimide (**1**) (297 mg, 1.5 mmol, 1.5 eq) was added in three equal portions at least 2 h apart. The progress of the reaction was monitored by TLC (MeOH:NH_4OH/4:1), while stirring at rt. After 20 h, the reaction was complete. The mixture was concentrated under reduced pressure and purified by SiO_2 flash chromatography, eluting with MeOH and a gradient of Et_3N (0-2%) (R_f = 0.78 in MeOH:NH_4OH/3:2). TLC was used to determine the fractions containing the product, which were then concentrated under reduced pressure. The residue was dissolved in a minimal volume of H_2O and lyophilized to provide the pure product, **4**, as white powder (348 mg, 63%). The product was a single spot by TLC and was used as directly in the following step without further characterization. NMR of the corresponding final product (**9**) is reported in Section 4.6.1.4.

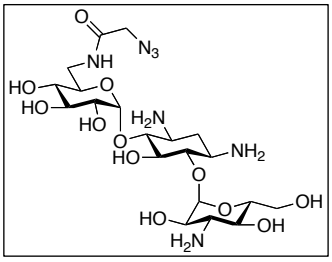

6'-*N*-azidoacetyl-KAN (5). 5 was prepared as described for **4**. The reaction of KAN (1.75 g, 3.0 mmol, 1 eq), K_2CO_3 (830 mg, 6.0 mmol, 2 eq), and *O*-azidoacetyl-*N*-hydroxysuccinimide (**1**) (890 mg, 4.5 mmol, 1.5 eq) in MeOH:H_2O/1:1 (16 mL) yielded, after SiO_2 flash chromatography eluting with MeOH and a gradient of Et_3N (0-2%), **5** (937 mg, 55%), as a white powder (R_f = 0.67 in MeOH:NH_4OH/3:2). The product was a single spot by TLC and was used as directly in the following step without further characterization. NMR of the corresponding final product (**10**) is reported in Section 4.6.1.4.

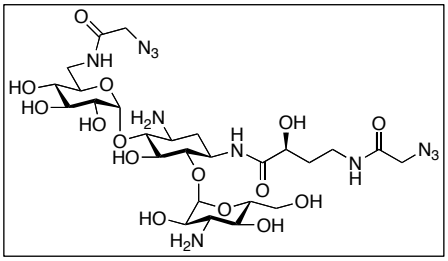

6',AHB-di-*N*-azidoacetyl-AMK (6). 6 was prepared as described for **4**. The reaction of AMK (469 mg, 0.6 mmol, 1 eq), K_2CO_3 (166 mg, 1.2 mmol, 2 eq), and *O*-azidoacetyl-*N*-hydroxysuccinimide (**1**) (297 mg, 1.5 mmol, 2.5 eq) in MeOH:H_2O/1:1 (8 mL) yielded the product **6** (110 mg, 26%) as a white powder (R_f = 0.53 in MeOH:NH_4OH/3:2), after SiO_2 flash chromatography eluting with MeOH and a gradient of Et_3N (0-2%). The product was a single spot by TLC and was used as directly in the following step without further characterization. NMR of the corresponding final product (**11**) is reported in Section 4.6.1.4.

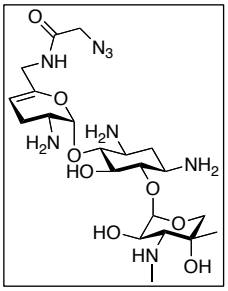

6'-*N*-azidoacetyl-SIS (7). 7 was prepared as described for **4**. The reaction of SIS (140 mg, 0.20 mmol, 1 eq), K_2CO_3 (55 mg, 0.4 mmol, 2 eq), and *O*-azidoacetyl-*N*-hydroxysuccinimide (**1**) (59 mg, 0.3 mmol, 1.5 eq) in MeOH:H_2O/1:1 (2 mL) yielded, after SiO_2 flash chromatography eluting with MeOH and a gradient of Et_3N (0-2%), **7** (42 mg, 40%) as a white powder (R_f = 0.42 in MeOH:NH_4OH/4:1). The product was a single spot by TLC and was used as directly in the following step without further characterization. NMR of the corresponding final product (**12**) is reported in Section 4.6.1.4.

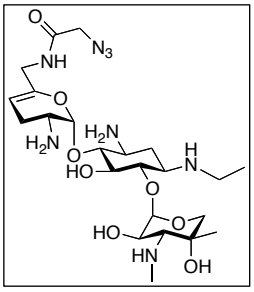

6'-*N*-azidoacetyl-NET (8). 8 was prepared as described for **4**. The reaction of NET (100 mg, 0.14 mmol, 1 eq), K_2CO_3 (39 mg, 0.28 mmol, 2 eq), and *O*-azidoacetyl-*N*-hydroxysuccinimide (**1**) (42 mg, 0.21 mmol, 1.5 eq) in MeOH:H_2O/1:1 (2 mL) yielded, after SiO_2 flash chromatography eluting with MeOH and a gradient of Et_3N (0-2%), **8** (45 mg, 57%) as a white powder (R_f = 0.50 in MeOH:NH_4OH/4:1). The product was a single spot by TLC and was used as directly in the following step without further characterization. NMR of the corresponding final product (**10**) is reported in Section 4.6.1.4.

4.6.1.3. General procedure for preparation of *N*-γ-benzyloxycarbonylamino-α-hydroxybutyric acid (*N*-(CbzAHB)) compounds

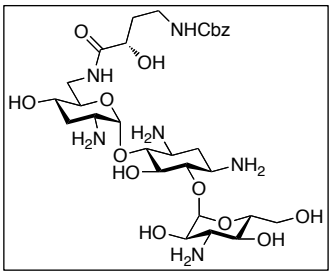

6'-*N*-(CbzAHB)-TOB (14). TOB (234 mg, 0.5 mmol, 1 eq) and $Zn(OAc)_2$ (110 mg, 0.6 mmol, 1.2 eq) were dissolved in DMF:H_2O/5:1 (3 mL) and the mixture was stirred at rt for 16 h. **3** (175 mg, 0.5 mmol, 1 eq) was added to the reaction mixture which was stirred for an additional 24 h. The reaction mixture was concentrated under reduced pressure and the residue was purified by SiO_2 flash chromatography, eluting with MeOH and a gradient of Et_3N (0-2%). Fractions with the product were pooled and concentrated under reduced pressure. The residue was dissolved in minimal volume of H_2O, flash frozen, and lyophilized to give the product (108 mg, 31%, R_f = 0.61 in MeOH:NH_4OH/3:2) as a white powder. The product was a single spot by TLC and was used as directly in the following step without further characterization. NMR of the corresponding final product (**17**) is reported in Section 4.6.1.4.

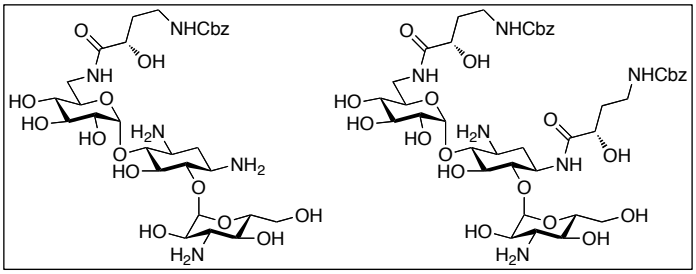

6'-*N*-(CbzAHB)-KAN (15) and 6',1-*N*-di-(AHB)-KAN (16). Both compounds were prepared in the same manner as **14**. The reaction of KAN (291 mg, 0.5 mmol, 1 eq), $Zn(OAc)_2$ (110 mg, 0.6 mmol, 1.2 eq) and **3** (350 mg, 1.0 mmol, 2 eq) in DMF:H_2O/5:1 (4 mL). (*Note*: *The equivalents of acylating reagent were increased to generate both the mono- and di-N-(CbzAHB) KAN products.*) Purification by SiO_2 flash chromatography, eluting with MeOH and a gradient of Et_3N (0-2%), yielded **15** (42 mg, 12%, R_f = 0.32 in MeOH:NH_4OH/3:2) and **16** (75 mg, 16%, R_f = 0.55 in MeOH:NH_4OH/3:2). The product was a single spot by TLC and was used as directly in the following step without further characterization. NMR of the corresponding final products (**18** and **19**) are reported in Section 4.6.1.4.

4.6.1.4. General procedure for hydrogenation reactions

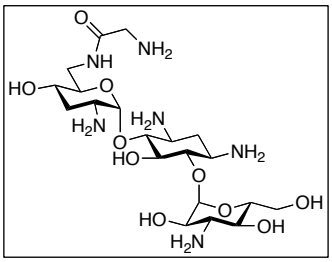

6'-*N*-glycinyl-TOB (9). 4 (730 mg, 1.33 mmol) was thoroughly dissolved in MeOH:H_2O/1:1 (4 mL) and hydrogenated using H_2 and 10% Pd/C (100 mg) at rt for 4 h. The resulting mixture was monitored for completion by TLC and upon completion was filtered through Celite and concentrated under reduced pressure with gentle heating. The residue was dissolved in minimal volume of H_2O and lyophilized to generate the pure product **9** (665 mg, 96%, R_f = 0.62 in MeOH:NH_4OH/3:2) as a white powder. (Note: This procedure described above was used in each case to convert the N_3 and/or the NHCbz into NH_2.) ^{1}H NMR (H_2O:D_2O/9:1, 400 MHz) δ 3.90-3.74 (m, 2H, CH_2 of Gly), **Ring I:** 5.58 (d, J = 3.2 Hz, 1H, H1), 4.05-3.90 (m, 1H, H5), 3.73-3.47 (m, 4H, $H6_a$, $H6_a$, H2, and H4), 2.57 (ddd (app. dt), J_1 = 12.2, J_2 = 4.1 Hz, 1H, $H3_a$), 2.03 (m, 1H, $H3_b$), **Ring II:** 3.73-3.47 (m, 1H, H5), 3.73-3.47 (m, 4H, H1, H3, H4 and H6), 2.34-2.20 (m, 1H. $H2_a$), 2.03 (m, 1H, $H2_b$), **Ring III:** 5.15 (d, J = 3.6 Hz, 1H, H1), 4.05-3.90 (m, 1H, H5), 3.90-3.74 (m, 3H, $H6_a$, $H6_b$, and H2), 3.73-3.47 (m, 1H, H4), 3.73-3.47 (m, 1H, H3). *m/z* calcd for $C_{20}H_{40}N_6O_{10}$: 524.28; found 525.35 $[M+H]^+$ and 547.25 $[M+Na]^+$.

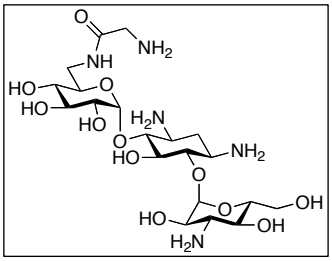

6'-*N*-glycinyl-KAN (10). Compound **10** was prepared and purified as described for compound **9**. The reaction of **5** (114 mg, 0.2 mmol) with 10% Pd/C (114 mg) in MeOH:H_2O/1:1 (4 mL) under H_2 atmosphere yielded **10** (104 mg, 96%, R_f = 0.54 in MeOH:NH_4OH/3:2). ^{1}H NMR (H_2O:D_2O/9:1, 500 MHz) δ 3.43-3.24 (m, 2H, CH_2 of Gly), **Ring I:** 5.27 (d, J = 4.0 Hz, 1H, H1), 3.90-3.85 (m, 1H, H3), 3.76-3.58 (m, 3H, H2, H5, and $H6_a$), 3.50 (dd, J_1 = 14.4, J_2 = 6.9 Hz, 1H, $H6_b$), 3.43-3.24 (m, 1H, H4), **Ring II:** 3.76-3.58 (m, 1H, H5), 3.43-3.24 (m, 2H, H4 and H6), 2.96 (ddd, J = 12.5, 9.6, 4.2 Hz, 1H, H3), 2.88 (ddd, J_1 = 12.5, J_2 = 9.6, J_3 = 4.2 Hz, 1H, H1), 2.01 (ddd (app. dt), J_1 = 12.5, J_2 = 4.2 Hz, 1H, $H2_a$), 1.26 (ddd (app. q), J = 12.9 Hz, 1H, $H2_b$), **Ring III:** 5.07 (d, J = 3.8 Hz, 1H, H1), 3.94 (ddd (app. dt), J_1 = 10.1, J_2 = 3.5 Hz, 1H, H5), 3.83-3.76 (m, 2H, $H6_a$ and $H6_b$), 3.55 (dd, J_1 = 10.2, J_2 = 3.8 Hz, 1H,

H2), 3.43-3.24 (m, 1H, H4), 3.05 (dd (app. t), J = 10.2 Hz, 1H, H3). *m/z* calcd for $C_{20}H_{39}N_5O_{12}$: 541.26; found 542.45 $[M+H]^+$ and 564.35 $[M+Na]^+$.

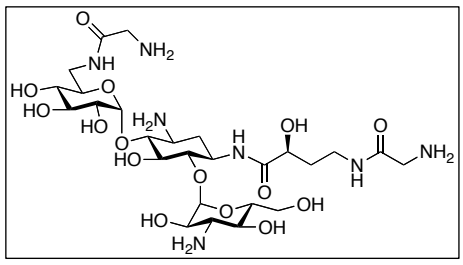

6',AHB-di-*N*-glycinyl-AMK (11). Compound **11** was prepared and purified as described for compound **9**. The reaction of **6** (75 mg, 0.1 mmol) with 10% Pd/C (75 mg) in MeOH:H_2O/1:1 (3 mL) under H_2 atmosphere yielded **11** (65 mg, 93%, R_f = 0.44 in MeOH:NH_4OH/3:2). ^{1}H NMR (H_2O:D_2O/9:1, 500 MHz) δ 4.16 (dd, J_1 = 9.5, J_2 = 3.5 Hz, 1H), 4.07-3.96 (m, 4H, CH_2 of Gly), 3.47-3.29 (m, 1H, AHB), 2.08-1.95 (m, 1H, AHB), 1.85-1.77 (m, 1H, AHB), **Ring I:** 5.26 (d, J = 3.9 Hz, 1H, H1), 3.89 (ddd, J_1 = 10.0, J_2 = 7.3, J_3 = 2.8 Hz, 1H, H5), 3.82-3.65 (m, 2H, H3 and $H6_a$), 3.63 (dd, J_1 = 9.9, J_2 = 3.9 Hz, 1H, H2), 3.50 (dd, J_1 = 14.4, J_2 = 7.4 Hz, 1H, $H6_b$), 3.47-3.29 (m, 1H, H4), **Ring II:** 4.07-3.96 (m, 1H, H1), 3.82-3.65 (m, 2H, H5 and H6), 3.47-3.29 (m, 1H, H4), 2.93 (m, 1H, H3), 2.08-1.95 (m, 1H, $H2_a$), 1.44 (ddd, (app. q), J = 12.6 Hz, 1H, $H2_b$), **Ring III:** 5.09 (d, J = 3.8 Hz, 1H, H1), 4.07-3.96 (m, 1H, H5), 3.82-3.65 (m, 2H, $H6_a$ and $H6_b$), 3.47-3.29 (m, 2H, H2 and H4), 3.07 (dd (app.t), J = 10.0 Hz, 1H, H3). *m/z* calcd for $C_{26}H_{29}N_7O_{15}$: 699.33; found 722.60 $[M+Na]^+$.

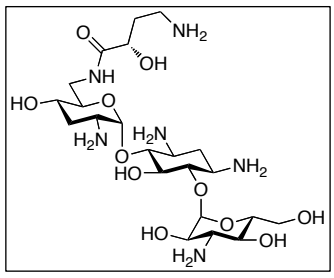

6'-*N*-AHB-TOB (17). Compound **17** was prepared and purified as described for compound **9**. The reaction of **14** (50 mg, 0.071 mml) with 10% Pd/C (50 mg) in MeOH:H_2O/1:1 (2 mL) under H_2 atmosphere yielded **17** (37 mg, 92%, R_f = 0.38 in MeOH:NH_4OH/3:2). ^{1}H NMR (H_2O:D_2O/9:1, 500 MHz) δ 4.31 (dd, J_1 = 8.6, J_2 = 3.8 Hz, 1H, AHB), 3.22-2.99 (m, 2H, AHB), 2.19-1.89 (m, 2H, AHB), **Ring I:** 5.19 (d, J = 3.8 Hz, 1H, H1), 3.84-3.73 (m, 1H, H5), 3.70-3.46 (m, 3H, H4, $H6_a$, and $H6_b$), 3.22-2.99 (m, 1H, H2), 2.19-1.89 (m, 1H, $H2_a$), 1.72 (ddd (app. q), J = 11.9 Hz, 1H, $H2_b$), **Ring II:** 5.06 (d, J = 3.8 Hz, 1H, H1), 3.70-3.46 (m, 1H, H5), 3.44-3.32 (m, 2H, H4 and H6), 3.22-2.99 (m, 1H, H3), 2.96-2.89 (m, 1H, H1), 2.19-1.89 (m, 1H, $H2_a$), 1.33 (ddd (app. q), J = 12.4 Hz, 1H, $H2_b$), **Ring III:** 3.95-3.90 (m, 1H, H5), 3.84-3.73 (m, 1H, $H6_a$ and $H6_b$), 3.70-3.46 (m, 1H, H2), 3.44-3.32 (m, 1H, H4),

3.22-2.99 (m, 1H, H3). *m/z* calcd for $C_{22}H_{44}N_6O_{11}$: 568.31; found 569.25 $[M+H]^+$ and 591.40 $[M+Na]^+$.

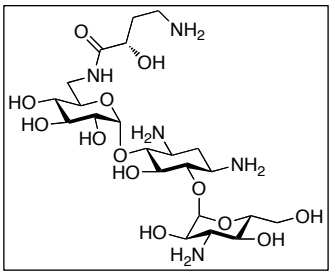

6'-*N*-AHB-KAN (18). Compound **18** was prepared and purified as described for compound **9**. The reaction of **15** (40 mg, 0.56 mmol) with 10% Pd/C (50 mg) in MeOH:H_2O/1:1 (2 mL) under H_2 atmosphere yielded **18** (29 mg, 89%, R_f = 0.12 in MeOH:NH_4OH/3:2). ^1H NMR (H_2O:D_2O/9:1, 500 MHz) δ 4.30 (dd, J_1 = 8.2, J_2 = 3.7 Hz, 1H, AHB), 3.09-2.99 (m, 2H, AHB), 2.09 (dtd, J_1 = 14.6, J_2 = 8.2, J_3 = 3.7 Hz, 1H), 1.96-1.82 (m, 1H, AHB), **Ring I:** 5.28 (d, J = 3.9 Hz, 1H, H1), 3.96-3.85 (m, 1H, H3), 3.83-3.50 (m, 4H, H2, H5, $H6_a$, and $H6_b$), 3.39-3.26 (m, 1H, H4), **Ring II:** 3.83-3.50 (m, 1H, H5), 3.39-3.26 (m, 2H, H4 and H6), 2.98-2.91 (m, 1H, H1), 2.90-2.84 (m, 1H, H3), 2.04-1.96 (m, 1H, $H2_a$), 1.25 (ddd (app. q), J = 12.4 Hz, 1H, $H2_b$), **Ring III:** 5.07 (d, J = 3.8 Hz, 1H, H1), 3.96-3.85 (m, 1H, H5), 3.83-3.50 (m, 3H, H2, $H6_a$, and $H6_b$), 3.39-3.26 (m, 1H, H4), 3.09-2.99 (m, 1H, H3). *m/z* calcd for $C_{22}H_{43}N_5O_{13}$: 585.29; found 586.30 $[M+H]^+$ and 608.40 $[M+Na]^+$.

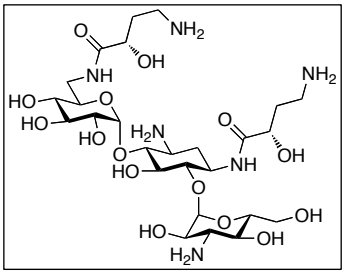

6',1-di-*N*-AHB-KAN (19). Compound **19** was prepared and purified as described for compound **9**. The reaction of **16** (60 mg, 0.063 mmol) with 10% Pd/C (60 mg) in MeOH:H_2O/1:1 (2 mL) under H_2 atmosphere yielded **19** (38 mg, 88%, R_f = 0.28 in MeOH:NH_4OH/3:2). ^1H NMR (H_2O:D_2O/9:1, 500 MHz) δ 4.38-4.12 (m, 2H, AHB), 3.21-2.95 (m, 4H, AHB), 2.14-2.03 (m, 2H, AHB), 2.02-1.84 (m, 2H, AHB), **Ring I:** 5.27 (d, J = 4.2 Hz, 1H, H1), 4.06-3.86 (m, 1H, H3), 3.83-3.46 (m, 4H, H2, H5, $H6_a$ and $H6_b$), 3.43-3.24 (m, 1H, H4), **Ring II:** 3.83-3.46 (m, 2H, H1 and H5), 3.43-3.24 (m, 2H, H4, and H6), 2.94-2.84 (m, 1H, H3), 2.02-1.84 (m, 1H, $H2_a$), 1.54-1.38 (m, 1H, $H2_b$), **Ring III:** 5.08 (d, J = 3.7 Hz, 1H, H1), 4.06-3.86 (m, 1H, H5), 3.83-3.46 (m, 3H, H2, $H6_a$, and $H6_b$), 3.43-3.24 (m, 1H, H4), 3.21-2.95 (m, 1H, H3). *m/z* calcd for $C_{26}H_{50}N_6O_{15}$: 686.33; found 687.75 $[M+H]^+$ and 709.55 $[M+Na]^+$.

4.6.1.5. General procedure for Staudinger reactions

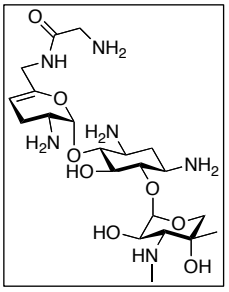

6'-*N*-glycinyl-SIS (12). Compound **12** was prepared from **7** using a Staudinger reaction. **7** (18 mg, 0.034 mmol) was dissolved in a mixture of aqueous NaOH (1 mM, 1.0 mL) and THF (1.0 mL) and stirred at rt for 15 min. PMe_3 (1 M solution in THF, 0.51 mL, 0.51 mmol, 15 eq) was added to the stirring solution, which was monitored for completion *via* TLC ($MeOH:NH_4OH$/4:1). After 1 h, the solution was concentrated under reduced pressure and loaded onto a short SiO_2 column. The column was washed thoroughly (THF (50 mL), EtOH (50 mL), and MeOH (50 mL)) and then eluted with 1% Et_3N in MeOH. Fractions containing the product were pooled and concentrated under reduced pressure. The residue was then dissolved in minimal H_2O, flash frozen, and lyophilized to give the pure product, **12**, as a white powder (12 mg, 67%, R_f = 0.76 in $MeOH:NH_4OH$/3:2). ^1H NMR ($H_2O:D_2O$/9:1, 400 MHz) δ 3.78-3.15 (m, 2H, CH_2 of Gly), **Ring I:** 5.41 (d, J = 3.6 Hz, 1H, H1), 4.83* (m, 1H, H5), 3.88-3.77 (m, 2H, $H6_a$, and $H6_b$), 3.78-3.15 (m, 2H, H2 and H4), 2.38-2.26 (m, 1H, $H3_a$), 2.18-2.06 (m, 1H, $H3_b$), **Ring II:** 3.78-3.15 (m, 3H, H4, H5, and H6), 3.13-2.85 (m, 2H, H1 and H3), 2.18-2.06 (m, 1H, $H2_a$), 1.45-1.09 (m, 1H, $H2_b$), **Ring III:** 5.04 (d, J = 3.4 Hz, 1H, H1), 4.18-3.98 (m, 1H, H2 and and $H5_a$), 3.78-3.15 (m, 1H, $H5_b$), 3.13-2.85 (m, 1H, H3), 2.77 (s, 3H, $NHC\underline{H}_3$), 1.45-1.09 (m, 3H, CH_3). *m/z* calcd for $C_{21}H_{40}N_6O_8$: 504.29; found 527.35 $[M+Na]^+$.

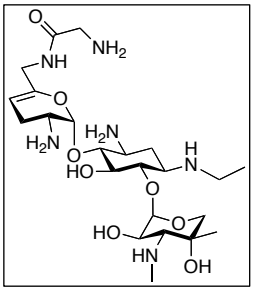

6'-*N*-glycinyl-NET (13). Compound **13** was prepared and purified as described for compound **12**. The reaction of **8** (15 mg, 0.027 mmol, 1 eq) and PMe_3 (1 M solution in THF, 0.345 mL, 0.405 mmol, 15 eq) in a mixture of aqueous NaOH (1 mM, 1.0 mL) and THF (1.0 mL) yielded **13** as a white powder (9 mg, 60% R_f = 0.82 in $MeOH:NH_4OH$/3:2). ^1H NMR ($H_2O:D_2O$/9:1, 400 MHz) δ 3.59-3.16 (m, 2H, CH_2 of Gly), **Ring I:** 5.42 (d, J = 2.1 Hz, 1H), 4.91* (m, 1H, H5), 3.89-3.78 (m, 3H, H4, $H6_a$, and $H6_b$), 3.59-3.16 (m, 1H, H2), 2.42-2.27 (m, 1H, $H3_a$), 2.17-2.06 (m, 1H, $H3_b$)**, Ring II:** 3.68-3.60 (m, 1H, H5), 3.59-3.16 (m, 2H, H4 and H6), 3.09-2.85 (m, 3H, H1, H3, and $C\underline{H}_{2a}CH_3$), 2.80-2.67 (m, 1H, $C\underline{H}_{2b}CH_3$), 2.42-2.27 (m, 1H, $H2_a$), 1.44-

1.09 (m, 4H, $H2_a$ and $CH_2C\underline{H}_3$), **Ring III:** 5.04 (d, J = 3.8 Hz, 1H), 4.04 (m, 2H, H2 and $H5_a$), 3.59-3.16 (m, 1H, 5_b), 3.09-2.85 (m, 1H, H3), 2.80-2.67 (m, 3H, CH_3 of $NHC\underline{H}_3$), 1.44-1.09 (m, H, CH_3). *m/z* calcd for $C_{23}H_{44}N_6O_8$: 532.32; found 533.45 $[M+H]^+$ and 555.35 $[M+Na]^+$. *Note*: An asterix denotes peak obscured by solvent suppression that is detected in 2D spectra.

4.6.1.6. General procedure for Cbz coupling reactions

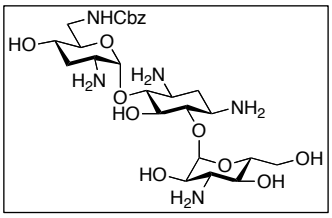

6'-*N*-Cbz-TOB (20). TOB (234 mg, 0.5 mmol, 1 eq) and K_2CO_3 (138 mg, 1.0 mmol, 2 eq) were dissolved in MeOH:H_2O/1:1 (5 mL) and Cbz-*N*-hydroxyphthalimide (**2**) (223 mg, 0.75 mmol, 1.5 eq) was added. The progress of the reaction was monitored by TLC (MeOH:NH_4OH/4:1), while stirring at rt. After 18 h, the reaction was complete. The mixture was concentrated under reduced pressure and purified by SiO_2 flash chromatography, eluting with MeOH and a gradient of Et_3N (0-2%). TLC was used to determine the fractions containing the product, which were then concentrated under reduced pressure. The residue was dissolved in a minimal volume of H_2O and lyophilized to provide the pure product, **20**, as white powder (195 mg, 64%, R_f = 0.82 in MeOH:NH_4OH/3:2). ^1H NMR (H_2O:D_2O/9:1, 400 MHz) δ 7.65 (d, J = 7.5 Hz, 1H aromatic), 7.59-7.46 (m, 4H, aromatic), 4.83* (m, 2H, CH_2 of Cbz), **Ring I:** 5.51 (d, J = 3.3 Hz, 1H, H1), 3.97-3.90 (m, 1H, H5), 3.86-3.64 (m, 3H, $H6_a$, $H6_b$, and H4), 3.61-3.48 (m, 1H, H2), 2.30-2.21 (m, 1H, $H3_a$), 1.97 (ddd (app. q), J = 11.2 Hz, 1H, $H3_b$), **Ring II:** 3.86-3.64 (m, 1H, H5), 3.61-3.48 (m, 2H, H4 and H6), 3.27-3.19 (m, 2H, H1 and H3), 2.30-2.21 (m, 1H, $H2_a$), 1.66 (ddd (app. q), J = 12.6 Hz, 1H, $H2_b$), **Ring III:** 5.09 (d, J = 3.7 Hz, 1H, H1), 3.97-3.90 (m, 1H, H5), 3.86-3.64 (m, 3H, $H6_a$, $H6_b$, and H2), 3.61-3.48 (m, 1H, H4), 3.31 (dd (app. t), J = 10.4 Hz, 1H, H3). *Note*: An asterix denotes peak obscured by solvent suppression that is detected in 2D spectra.

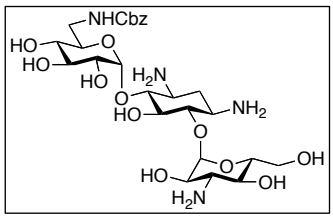

6'-*N*-Cbz-KAN (21). Compound **21** was prepared as described for compound **20**. The reaction of KAN (291 mg, 0.5 mmol, 1 eq), K_2CO_3 (138 mg, 1.0 mmol, 2 eq), and **2** (223 mg, 1.5 mmol, 1.5 eq) yielded, after SiO_2 flash

chromatography (MeOH and a gradient of Et_3N (0-2%)), compound **21** (124 mg, 40%, R_f = 0.73 in MeOH:NH_4OH/3:2). ^1H NMR (H_2O:D_2O/9:1, 400 MHz) δ 7.64 (dd, *J* = 7.4, 1.6 Hz, 1H aromatic), 7.59-7.46 (m, 4H, aromatic), 4.80* (m, 2H, CH_2 of Cbz), **Ring I:** 5.49 (d, *J* = 3.9 Hz, 1H, H1), 3.96-3.90 (m, 1H, H5), 3.88-3.71 (m, 2H, $H6_a$ and H3), 3.71-3.54 (m, 2H, $H6_b$ and H2), 3.53-3.39 (m, 1H, H4), **Ring II:** 3.88-3.71 (m, 1H, H5), 3.71-3.54 (m, 1H, H6), 3.53-3.39 (m, 1H, H4), 3.36-3.08 (m, H, H1 and H3), 2.22 (ddd (app. dt), J_1 = 12.7, J_2 = 4.2 Hz, 1H, $H2_a$), 1.61 (ddd (app. q), *J* = 12.7 Hz, 1H, $H2_b$), **Ring III:** 5.08 (d, *J* = 3.6 Hz, 1H, H1), 3.96-3.90 (m, 1H, H5), 3.88-3.71 (m, 3H, $H6_a$, $H6_b$, and H2), 3.71-3.54 (m, 1H, H4), 3.36-3.08 (m, 1H, H3). *Note*: An asterix denotes peak obscured by solvent suppression that is detected in 2D spectra.

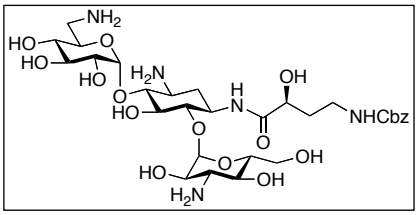

AHB-*N*-Cbz-AMK (22). Compound **22** was prepared as described for compound **20**. The reaction of AMK (291 mg, 0.5 mmol, 1 eq), K_2CO_3 (138 mg, 1.0 mmol, 2 eq), and **2** (223 mg, 1.5 mmol, 1.5 eq) yielded, after SiO_2 flash chromatography (MeOH and a gradient of Et_3N (0-2%)), compound **22** (29 mg, 8% R_f = 0.56 in MeOH:NH_4OH/3:2). (*Note*: Di-N-Cbz-AMK was the major product, 46%) ^1H NMR (H_2O:D_2O/9:1, 400 MHz) δ 7.63 (d, *J*= 7.3 Hz, 1H, aromatic), 7.59-7.46 (m, 4H, aromatic), 4.29 (dd, J_1 = 3.9, J_2 = 9.1 Hz, 1H, AHB), 3.68-3.47 (m, 2H, AHB), 2.15-2.03 (m, 1H, AHB), 1.96-1.85 (m, 1H, AHB), **Ring I:** 5.54 (d, *J*= 3.8 Hz, 1H, H1), 4.09-4.00 (m, 1H, H5), 3.85-3.70 (m, 1H, H3), 3.68-3.47 (m, 1H, H2), 3.45-3.34 (m, 2H, H4 and $H6_a$), 3.22-3.12 (m, H, $H6_b$), **Ring II:** 4.09-4.00 (m, 1H, H1), 3.85-3.70 (m, 2H, H5 and H6), 3.68-3.47 (m, 1H, H4), 2.15-2.03 (m, 1H, $H2_b$), 1.57 (ddd (app. q), *J* = 12.5 Hz, 1H, $H2_b$), 3.22-3.12 (m, 1H, H3), **Ring III:** 5.20 (d, *J* = 3.8 Hz, 1H, H1), 4.09-4.00 (m, 1H, H5), 3.85-3.70 (m, 3H, H2, $H6_a$, and $H6_b$), 3.68-3.47 (m, 1H, H4), 3.28 (dd (app. t), *J* = 10.4 Hz, 1H, H3).

4.6.2. Mass spectrometry analysis of the acylated AMK, KAN, NET, SIS, and TOB synthetic products

The masses of the synthetic AGs were obtained by LCMS in positive ion mode using H_2O (0.1% formic acid). 20 μL of a 1 μg/mL solution of the compound dissolved in H_2O was injected for analysis.

4.6.3. Determination of the MIC values against various bacteria

MIC experiments were performed using the double dilution method against a variety of bacteria- values are reported in Tables 4.1-4.3 in the main text. *A) B. subtilis* 168, B) *B. subtilis* 168 with pBF16 harboring AAC(6')/APH(2''), C) *B. cereus* ATCC 17788, D) *B. anthtacis* str. Sterne, E) *L. monocytogenes* ATCC 19115, F) *E. faecalis* ATCC 29212, G) *E. faecium* BM4105-RF, H) *S. aureus* ATCC 29213, I) MRSA, J) VRE, K) *S. aureus* Nor A, L) *E. coli* BL21 (DE3) with pET22b harboring AAC(6')/APH(2''), M) *E. coli* BL21 (DE3) with pET19b-pps harboring AAC(3)-IV, N) *E. coli* BL21 (DE3) with pET28a harboring Eis, O) *E. coli* BL21 (DE3) with pET22b, P) *E. coli* MC1061, Q) *H. influenzae* ATCC 51907, R) *P. aeruginosa* PA01, S) *P. aeruginosa* PA14, T) *S. enterica* ATCC 14028, U) *K. pneumoniae* ATCC 27736, V) *A. baumannii* ATCC 19606, W) *E. coli* Tol C, X) *M. smegmatis* str. MC2 155, Y) *M. abscessus* ATCC 19977, Z) *M. parascrofulaceum* ATCC BAA-614, AA) *M. intracellulare* ATCC 13950, AB) *M. avium* subsp. *avium* ATCC 25291.

M. avium subsp. *avium* ATCC 25291, *M. abscessus* ATCC 19977, *M. intracellulare* ATCC 13950, and *M. parascrofulaceum* ATCC BAA-614 were grown for 6 days before determining the MIC values, while the values for *M. smegmatis* str. MC2 155 were determined after 1-3 days. The rest of the MIC values were determined after 16 h. The concentrations of the compounds evaluated were in the range of 150 μg/mL to 0.3 μg/mL. All experiments were performed in duplicate or triplicate sets.

4.7. References

(1) Shakil, S.; Khan, R.; Zarrilli, R.; Khan, A. U. *Journal of biomedical science* **2008**, *15*, 5.
(2) Houghton, J. L.; Green, K. D.; Chen, W.; Garneau-Tsodikova, S. *Chembiochem* **2010**, *11*, 880.
(3) Greenberg, W. A.; Priestley, E. S.; Sears, P. S.; Alper, P. B.; Rosenbohm, C.; Hendrix, M.; Hung, S.-C.; Wong, C.-H. *J Am Chem Soc* **1999**, *121*, 6527.
(4) Ford, J. H.; Bergy, M. E.; Brooks, A. A.; Garrett, E. R.; Alberti, J.; Dyer, J. R.; Carter, H. E. *J Am Chem Soc* **1955**, *77*, 5311.
(5) da Silva, J. G.; Hyppolito, M. A.; de Oliveira, J. A.; Corrado, A. P.; Ito, I. Y.; Carvalho, I. *Bioorg Med Chem* **2007**, *15*, 3624.
(6) Hanessian, S.; Butterworth, R. F.; Nakagawa, T. *Carbohydr Res* **1973**, *26*, 261.
(7) Hanessian, S.; Masse, R.; Capmeau, M. L. *J Antibiot (Tokyo)* **1977**, *30*, 893.
(8) Hanessian, S.; Takamoto, T.; Masse, R. *J Antibiot (Tokyo)* **1975**, *28*, 835.
(9) Hanessian, S.; Vatele, J. M. *J Antibiot (Tokyo)* **1980**, *33*, 675.
(10) Fridman, M.; Belakhov, V.; Yaron, S.; Baasov, T. *Org Lett* **2003**, *5*, 3575.
(11) Magnet, S.; Blanchard, J. S. *Chemical reviews* **2005**, *105*, 477.
(12) Putman, M.; van Veen, H. W.; Konings, W. N. *Microbiol Mol Biol Rev* **2000**, *64*, 672.
(13) Aires, J. R.; Kohler, T.; Nikaido, H.; Plesiat, P. *Antimicrob Agents Chemother* **1999**, *43*, 2624.
(14) Westbrock-Wadman, S.; Sherman, D. R.; Hickey, M. J.; Coulter, S. N.; Zhu, Y. Q.; Warrener, P.; Nguyen, L. Y.; Shawar, R. M.; Folger, K. R.; Stover, C. K. *Antimicrob Agents Chemother* **1999**, *43*, 2975.
(15) Taber, H. W.; Mueller, J. P.; Miller, P. F.; Arrow, A. S. *Microbiol Rev* **1987**, *51*, 439.
(16) Hancock, R. E. *Annu Rev Microbiol* **1984**, *38*, 237.
(17) Masuda, N.; Sakagawa, E.; Ohya, S.; Gotoh, N.; Tsujimoto, H.; Nishino, T. *Antimicrob Agents Chemother* **2000**, *44*, 3322.
(18) Murakami, S.; Nakashima, R.; Yamashita, E.; Yamaguchi, A. *Nature* **2002**, *419*, 587.
(19) Yu, E. W.; Aires, J. R.; Nikaido, H. *J Bacteriol* **2003**, *185*, 5657.
(20) Doi, Y.; Yokoyama, K.; Yamane, K.; Wachino, J.; Shibata, N.; Yagi, T.; Shibayama, K.; Kato, H.; Arakawa, Y. *Antimicrob Agents Chemother* **2004**, *48*, 491.
(21) Chow, J. W. *Clin Infect Dis* **2000**, *31*, 586.
(22) Galimand, M.; Sabtcheva, S.; Courvalin, P.; Lambert, T. *Antimicrob Agents Chemother* **2005**, *49*, 2949.
(23) Yan, J. J.; Wu, J. J.; Ko, W. C.; Tsai, S. H.; Chuang, C. L.; Wu, H. M.; Lu, Y. J.; Li, J. D. *J Antimicrob Chemother* **2004**, *54*, 1007.
(24) Kotra, L. P.; Haddad, J.; Mobashery, S. *Antimicrob Agents Chemother* **2000**, *44*, 3249.
(25) Wright, G. D.; Berghuis, A. M.; Mobashery, S. *Advances in experimental medicine and biology* **1998**, *456*, 27.
(26) Mingeot-Leclercq, M. P.; Glupczynski, Y.; Tulkens, P. M. *Antimicrob Agents Chemother* **1999**, *43*, 727.
(27) Kim, C.; Hesek, D.; Zajicek, J.; Vakulenko, S. B.; Mobashery, S. *Biochemistry* **2006**, *45*, 8368.
(28) Dubois, V.; Poirel, L.; Marie, C.; Arpin, C.; Nordmann, P.; Quentin, C. *Antimicrob Agents Chemother* **2002**, *46*, 638.
(29) Mendes, R. E.; Toleman, M. A.; Ribeiro, J.; Sader, H. S.; Jones, R. N.; Walsh, T. R. *Antimicrob Agents Chemother* **2004**, *48*, 4693.
(30) Shaul, P.; Green, K. D.; Rutenberg, R.; Kramer, M.; Berkov-Zrihen, Y.; Breiner-Goldstein, E.; Garneau-Tsodikova, S.; Fridman, M. *Org Biomol Chem* **2011**, *9*, 4057.

(31) Nudelman, I.; Rebibo-Sabbah, A.; Cherniavsky, M.; Belakhov, V.; Hainrichson, M.; Chen, F.; Schacht, J.; Pilch, D. S.; Ben-Yosef, T.; Baasov, T. *Journal of medicinal chemistry* **2009**, *52*, 2836.
(32) Kondo, J.; Francois, B.; Russell, R. J.; Murray, J. B.; Westhof, E. *Biochimie* **2006**, *88*, 1027.
(33) Russell, R. J.; Murray, J. B.; Lentzen, G.; Haddad, J.; Mobashery, S. *J Am Chem Soc* **2003**, *125*, 3410.
(34) Cashman, D. J.; Rife, J. P.; Kellogg, G. E. *Bioorg Med Chem Lett* **2001**, *11*, 119.
(35) Zhanel, G. G.; Lawson, C. D.; Zelenitsky, S.; Findlay, B.; Schweizer, F.; Adam, H.; Walkty, A.; Rubinstein, E.; Gin, A. S.; Hoban, D. J.; Lynch, J. P.; Karlowsky, J. A. *Expert Rev Anti Infect Ther* **2012**, *10*, 459.
(36) Armstrong, E. S.; Miller, G. H. *Curr Opin Microbiol* **2010**, *13*, 565.
(37) Aggen, J. B.; Armstrong, E. S.; Goldblum, A. A.; Dozzo, P.; Linsell, M. S.; Gliedt, M. J.; Hildebrandt, D. J.; Feeney, L. A.; Kubo, A.; Matias, R. D.; Lopez, S.; Gomez, M.; Wlasichuk, K. B.; Diokno, R.; Miller, G. H.; Moser, H. E. *Antimicrob Agents Chemother* **2010**, *54*, 4636.
(38) Tatsuta, K. *Proc Jpn Acad Ser B Phys Biol Sci* **2008**, *84*, 87.
(39) Green, K. D.; Chen, W.; Garneau-Tsodikova, S. *Antimicrob Agents Chemother* **2011**, *55*, 3207.
(40) Green, K. D.; Chen, W.; Houghton, J. L.; Fridman, M.; Garneau-Tsodikova, S. *Chembiochem* **2010**, *11*, 119.
(41) Naito, T.; Susumu, N.; Oka, M. Patent #3,860,574, U.S.A.

Authors' contribution:
JLH and KDG performed the MIC assays.
JLH synthesized and analyzed all the compounds and wrote the chapter.

4.8. Appendix

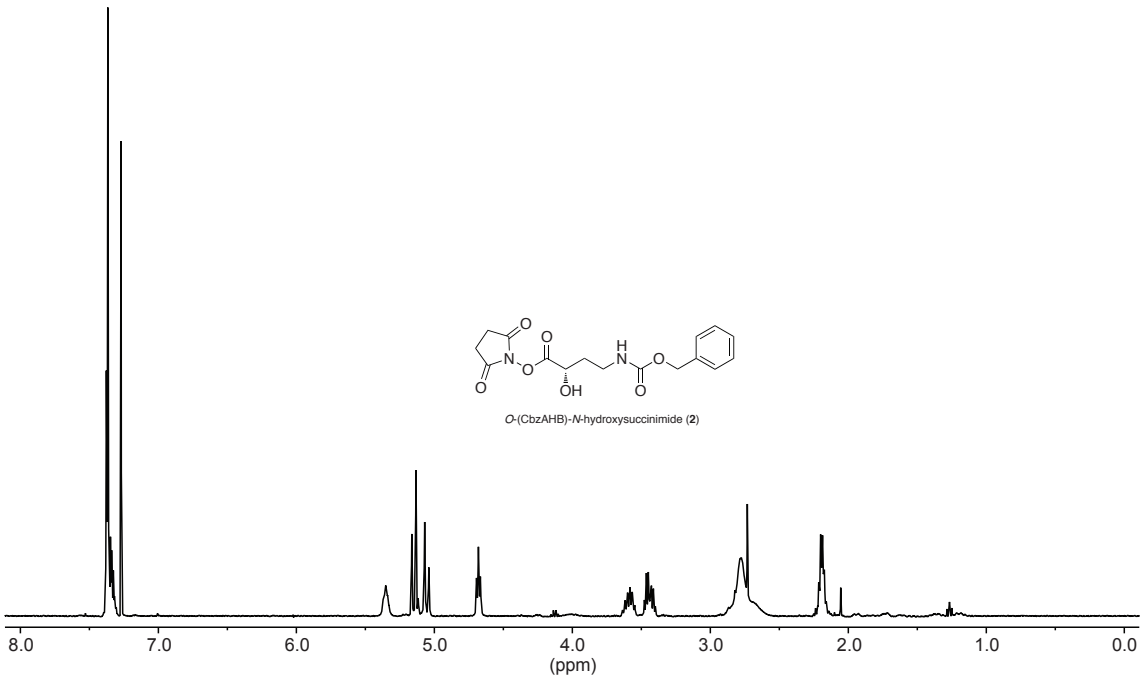

Fig. 4.6. ^{1}H of *O*-(CbzAHB)-*N*-hydroxysuccinimide (**2**) in $CDCl_3$ (400 MHz).

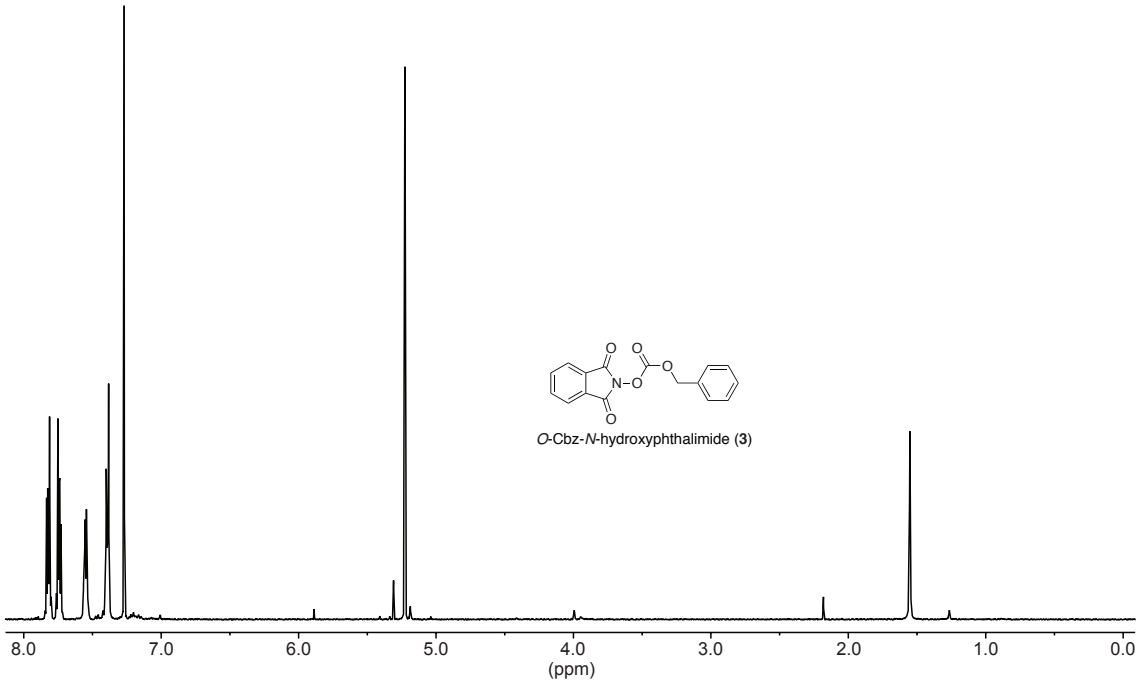

Fig. 4.7. ^{1}H of *O*-Cbz-*N*-hydroxyphthalimide (**3**) in $CDCl_3$ (400 MHz).

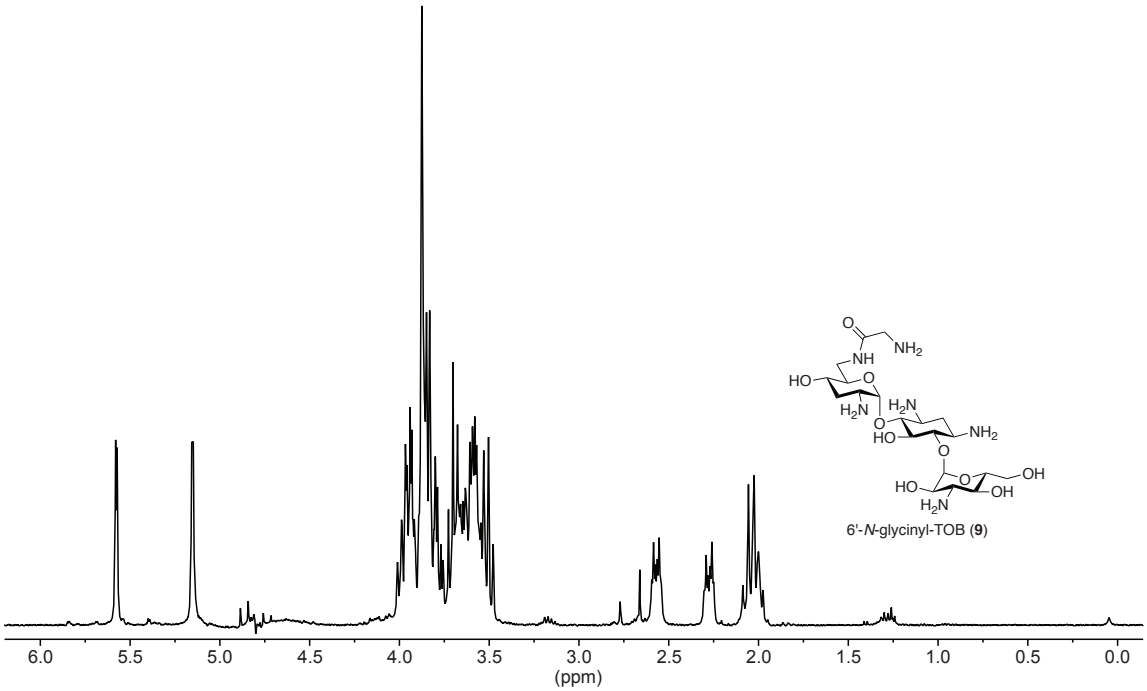

Fig. 4.8. ^{1}H of 6'-*N*-glycinyl-TOB (**9**) in 9:1/H_2O:D_2O (400 MHz).

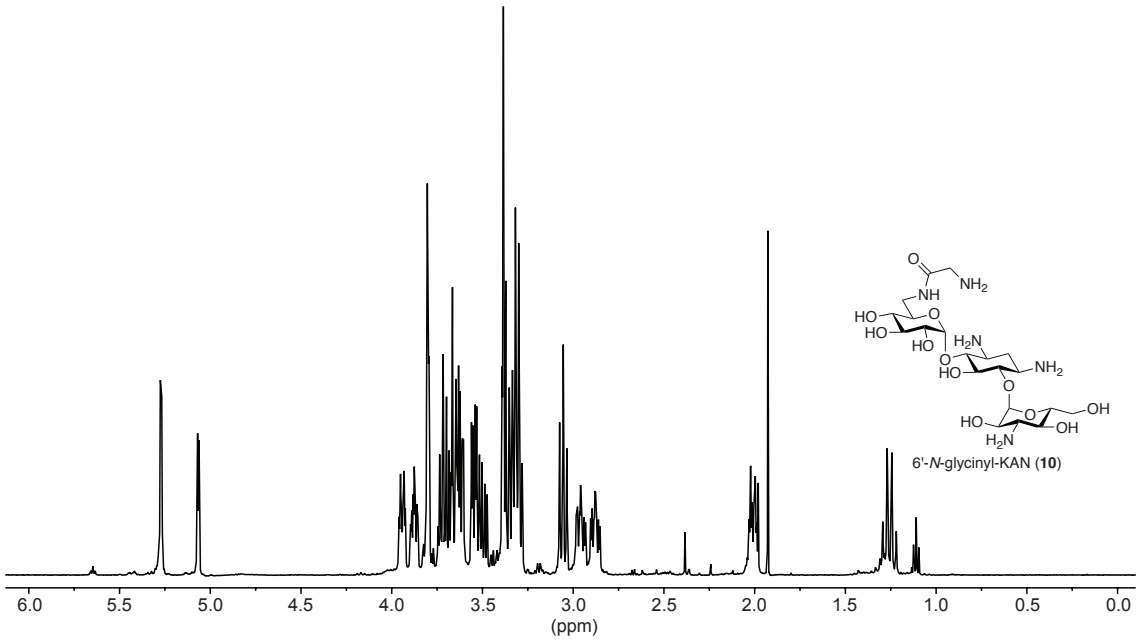

Fig. 4.9. ^{1}H of 6'-*N*-glycinyl-KAN (**10**) in 9:1/H_2O:D_2O (500 MHz).

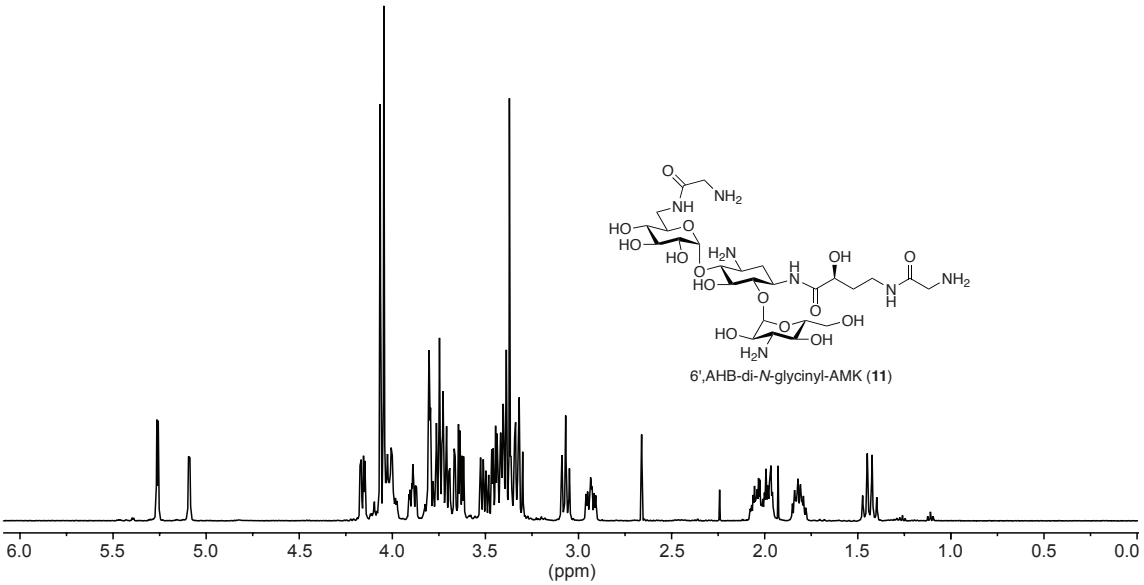

Fig. 4.10. ^{1}H of 6',AHB-di-*N*-glycinyl-AMK (**11**) in 9:1/H_2O:D_2O (500 MHz).

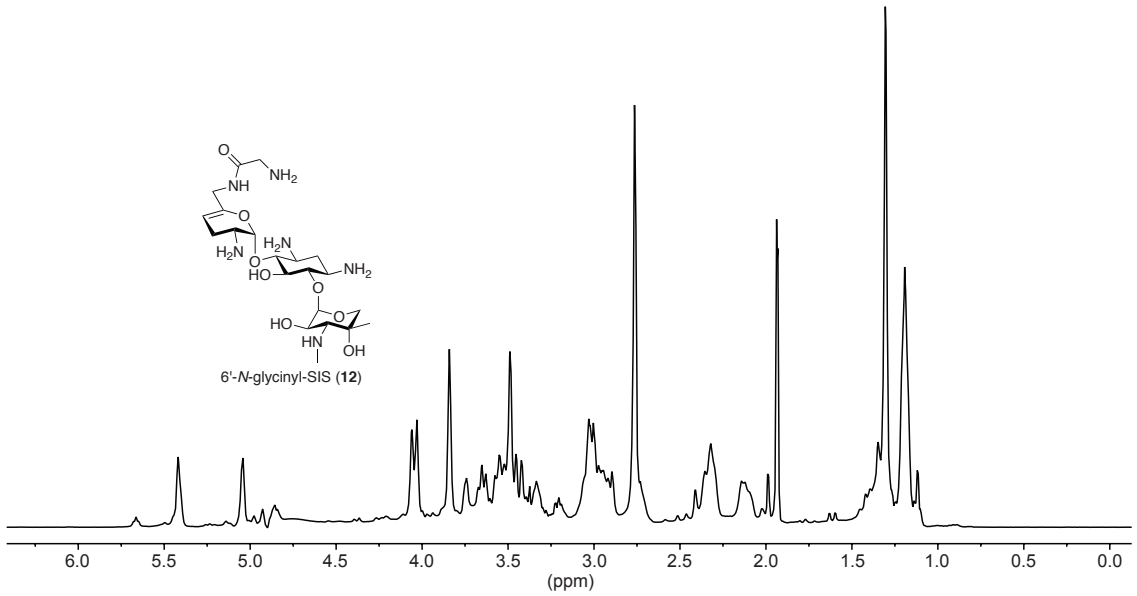

Fig. 4.11. ^{1}H of 6'-*N*-glycinyl-SIS (**12**) in 9:1/H_2O:D_2O (400 MHz).

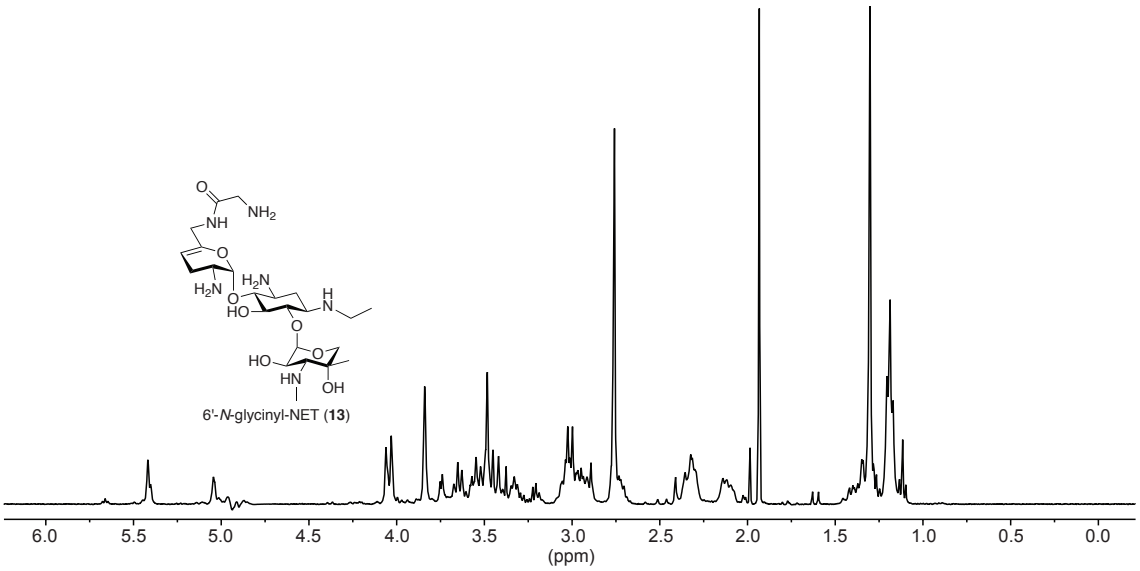

Fig. 4.12. ^{1}H of 6'-*N*-glycinyl-NET (**13**) in 9:1/H_2O:D_2O (400 MHz).

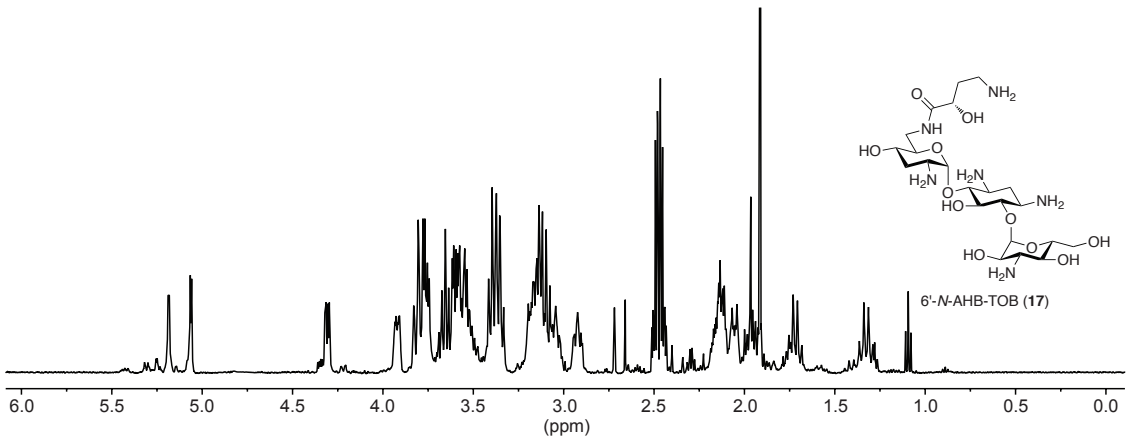

Fig. 4.13. ^{1}H of 6'-*N*-AHB-TOB (**17**) in 9:1/H_2O:D_2O (500 MHz).

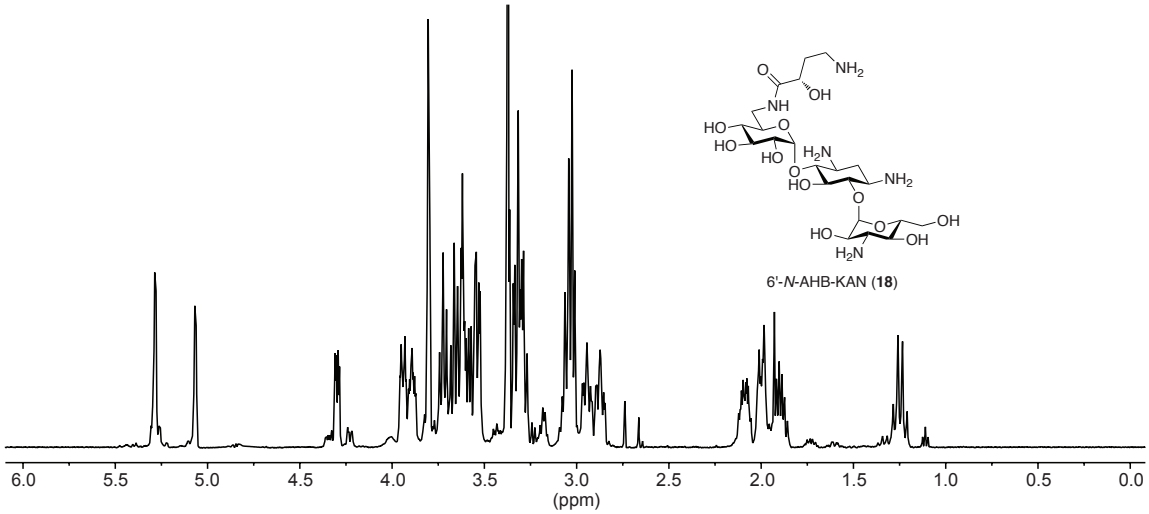

Fig. 4.14. ^{1}H of 6'-*N*-AHB-KAN (**18**) in 9:1/H_2O:D_2O (500 MHz).

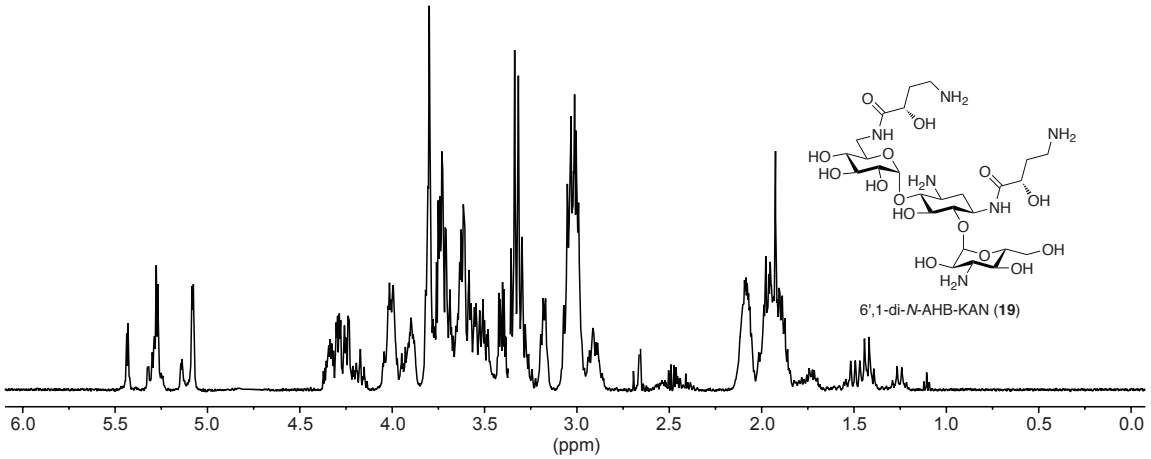

Fig. 4.15. ^{1}H of 6',1-di-*N*-AHB-KAN (**19**) in 9:1/H_2O:D_2O (500 MHz).

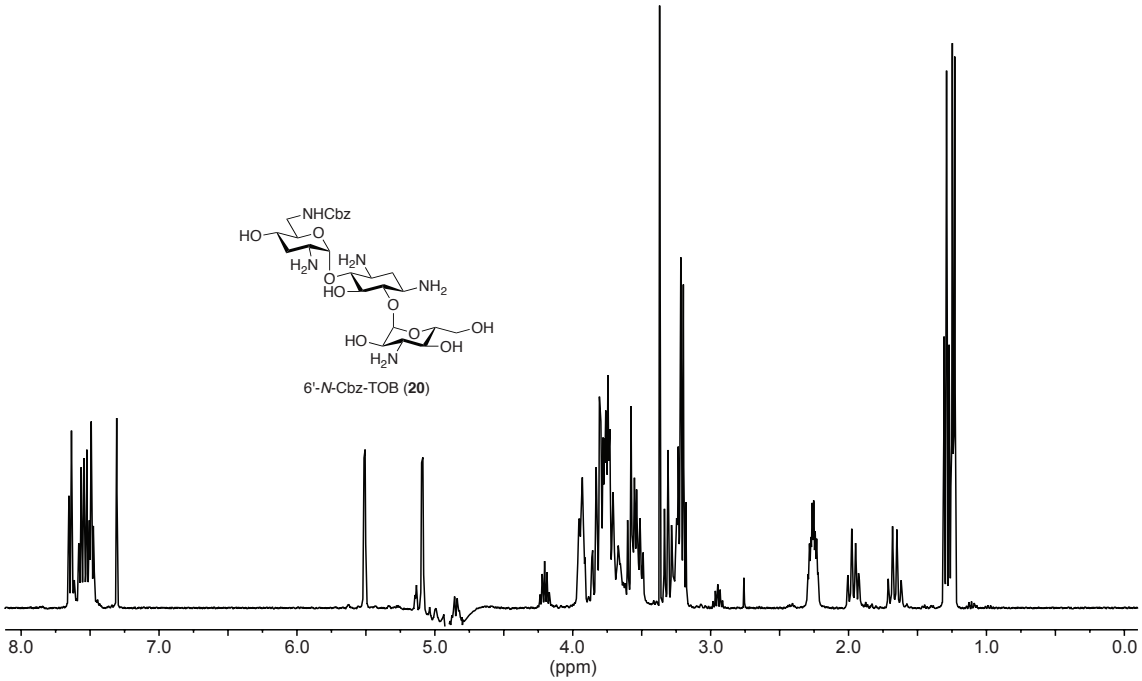

Fig. 4.16. ^{1}H of 6'-*N*-Cbz-TOB (**20**) in 9:1/H_2O:D_2O (500 MHz).

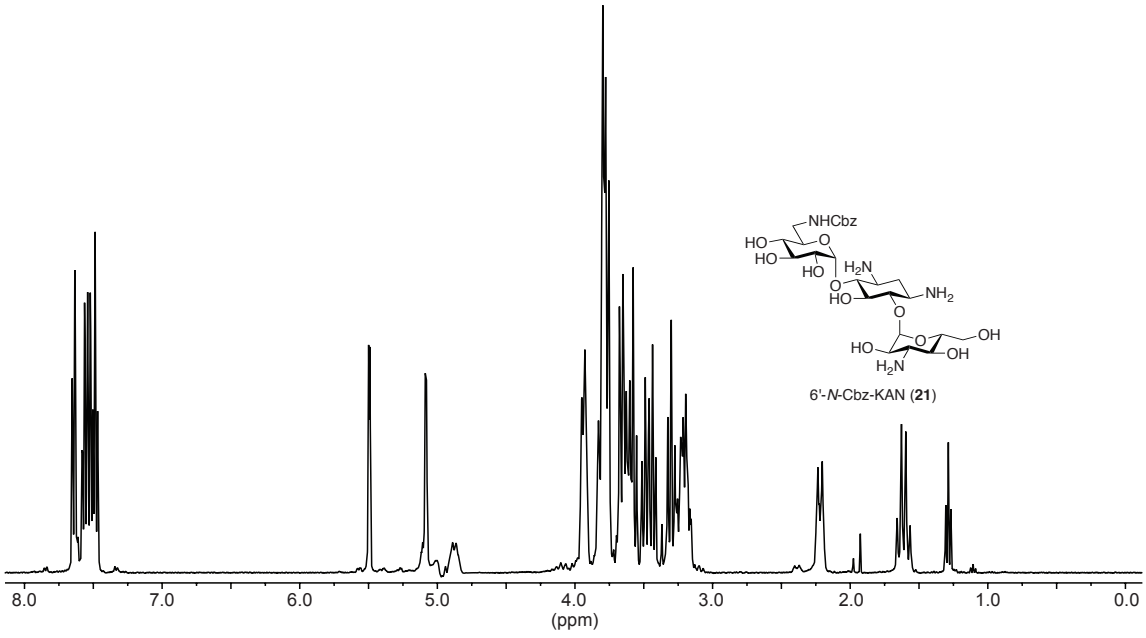

Fig. 4.17. ^{1}H of 6'-*N*-Cbz-KAN (**21**) in 9:1/H_2O:D_2O (500 MHz).

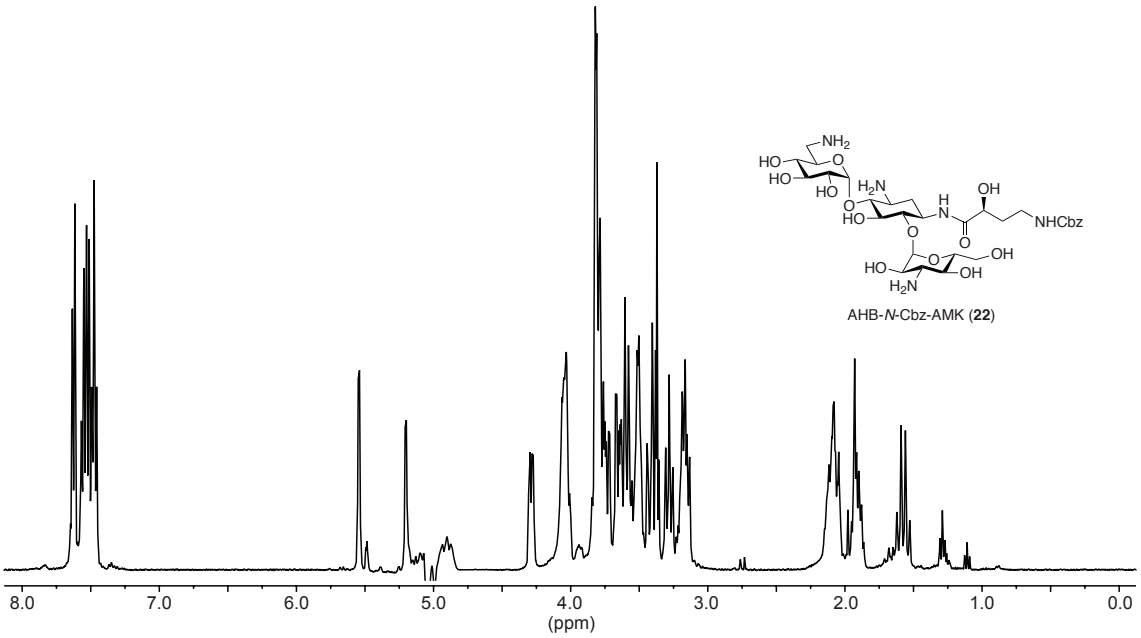

Fig. 4.18. ^{1}H of 6'-*N*-Cbz-AMK (**22**) in 9:1/H_2O:D_2O (500 MHz).

Chapter 5

The structural basis for substrate versatility of chloramphenicol acetyltransferase CAT_I

5.1. Abstract

Novel antibiotics are needed to overcome the challenge of continually evolving bacterial resistance. This has led to a renewed interest in mechanistic studies of once popular antibiotics like chloramphenicol (CAM). Chloramphenicol acetyltransferases (CATs) are enzymes that covalently modify CAM, rendering it inactive against its target, the ribosome, and thereby causing resistance to CAM. Out of the three major types of CAT (CAT_{I-III}), the CAM-specific CAT_{III} has been studied extensively. Much less is known about another clinically important type, CAT_I. In addition to inactivating CAM and unlike CAT_{III}, CAT_I confers resistance to a structurally distinct antibiotic, fusidic acid (FA). The origin of the broader substrate specificity of CAT_I has not been fully elucidated. To understand the substrate binding features of CAT_I, its crystal structures in the unbound (apo) and CAM-bound forms were determined. The analysis of these and previously determined CAT_I-FA and CAT_{III}-CAM structures revealed interactions responsible for CAT_I binding to its substrates and clarified the broader substrate preference of CAT_I compared to that of CAT_{III}.

5.2. Introduction

Chloramphenicol (CAM) (Fig. 5.1A) is a potent broad-spectrum antibacterial agent. Since its isolation from *Streptomyces venezuelae* in 1948,[1] CAM was one of the primary agents used to treat many infections in the decades that followed. To date, despite its relatively high toxicity,[2] CAM is used in many countries due to its affordability and its broad spectrum of activity. In the Western world, CAM is used in treatment of ophthalmic infections and as a last resort in cases of life-threatening brain infections,

such as those caused by *Neisseria meningitides*, which do not respond to other agents. CAM's ability to cross the blood-brain barrier makes it a potent therapeutic against brain infections. Due to the emergence of pathogens resistant to multiple drugs, CAM is now being reconsidered as a wider-spectrum therapeutic.[3]

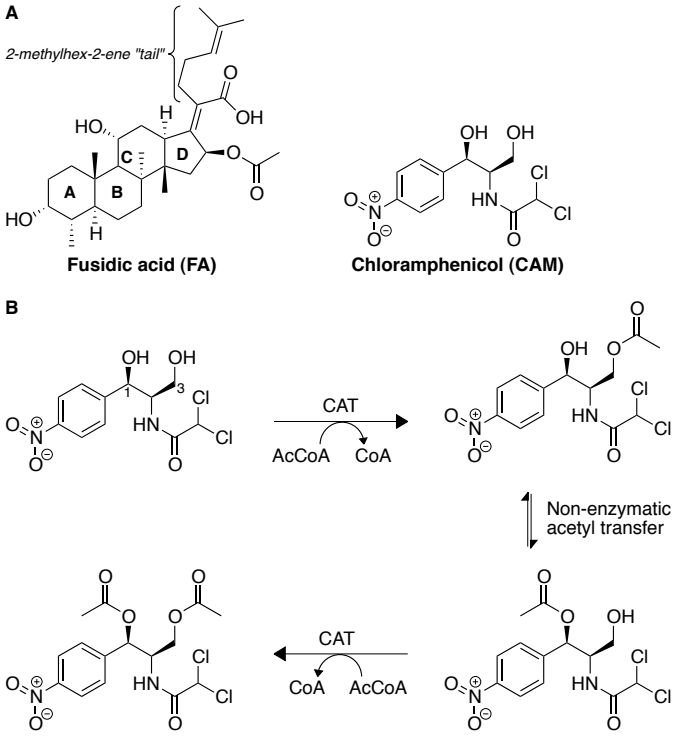

Fig. 5.1. A. Chemical structures of CAM and FA. **B.** Acetylation of CAM by CATs.

CAM inhibits protein biosynthesis by binding to the 50S subunit of the bacterial ribosome. Recent crystal structures of the 50S subunit of the *Escherichia coli* and *Thermus thermophilus* ribosome in complex with CAM revealed that CAM binds to the A-site of the 50S subunit and occupies the binding site for the amino-acyl moiety of the A-site tRNA.[4,5] The 3-hydroxyl of CAM is buried in the interface with the ribosome through direct hydrogen bonding, potassium ion-mediated electrostatic interactions, as well as through van der Waals interactions with the RNA phosphosugar backbone.[4,5] The 1-hydroxyl of CAM forms hydrogen bonds with RNA bases. Therefore, any modification of the 1-hydroxyl or the 3-hydroxyl of CAM is predicted to be disruptive of CAM-ribosome binding.[5] Bacterial resistance to CAM is caused by the chromosomally or plasmid-encoded enzyme chloramphenicol acetyltransferase (CAT) that catalyzes the

transfer of an acetyl group from acetyl-coenzyme A (AcCoA) to the 3-hydroxyl group of CAM (Fig. 5.1B).[6] A subsequent slow, non-enzymatic transfer of this acetyl group to the neighboring 1-hydroxyl group allows for a second CAT-catalyzed acetyl transfer from AcCoA onto the 3-hydroxyl group of the same CAM molecule, resulting in a di-acetylated CAM.[7,8] However, a single acetylation of CAM is sufficient to abolish its affinity for the ribosome[9] as explained by the above structural observations.[4,5]

CAT proteins are historically divided into three types: CAT_I, CAT_{II}, and CAT_{III}, with all three types capable of catalyzing the acetyl transfer to CAM to generate 3-*O*-acetyl-CAM. Genomic analysis of different CAT sequences indicates that the boundaries between these CAT types are not sharp. Members of the CAT_I family are present in many important pathogens such as *E. coli*, *Shigella flexneri*, *Serratia marcescens*, and *Salmonella enterica*. CAT_I family enzymes display high sequence conservation among themselves (*e.g. S. flexneri* and *S. marcescens* CAT_I proteins are 98% and 99% identical to *E. coli* CAT_I, respectively); however, they display only a modest sequence identity to CAT_{II} (~46%) and CAT_{III} (32% to 47%) (Fig. 5.2). The CAT_{II} family is not easily distinguishable from CAT_{III} and has been defined historically only through its extreme susceptibility to thiol-modifying agents compared with that of CAT_I and CAT_{III}.[10] There are no obvious additional Cys residues or other sequence features in CAT_{II} distinguishing it from the type-III variants. A slight variation in the pK_a of the Cys31 (in CAT_{III} nomenclature), the only Cys in vicinity of the substrate or the cosubstrate binding sites, was suggested to be responsible for the difference in reactivity with thiol-modifying agents,[11] although there is no evidence confirming this idea.

The sequence differences between CAT_I and CAT_{III} include several substitutions in the binding site (Fig. 5.2), potentially resulting in positional differences of CAM bound to these two proteins. A major consequence of this divergence is reflected in different substrate selectivities of CAT_I and CAT_{III}. In addition to binding and modifying CAM,[6] CAT_I, unlike CAT_{III}, binds a much bulkier antibiotic, fusidic acid (FA).[12] FA (Fig. 5.1A) is a steroidal antibacterial agent that is used topically or systemically, usually against infections caused by Gram-positive pathogens. CAT_I does not modify FA; rather, it

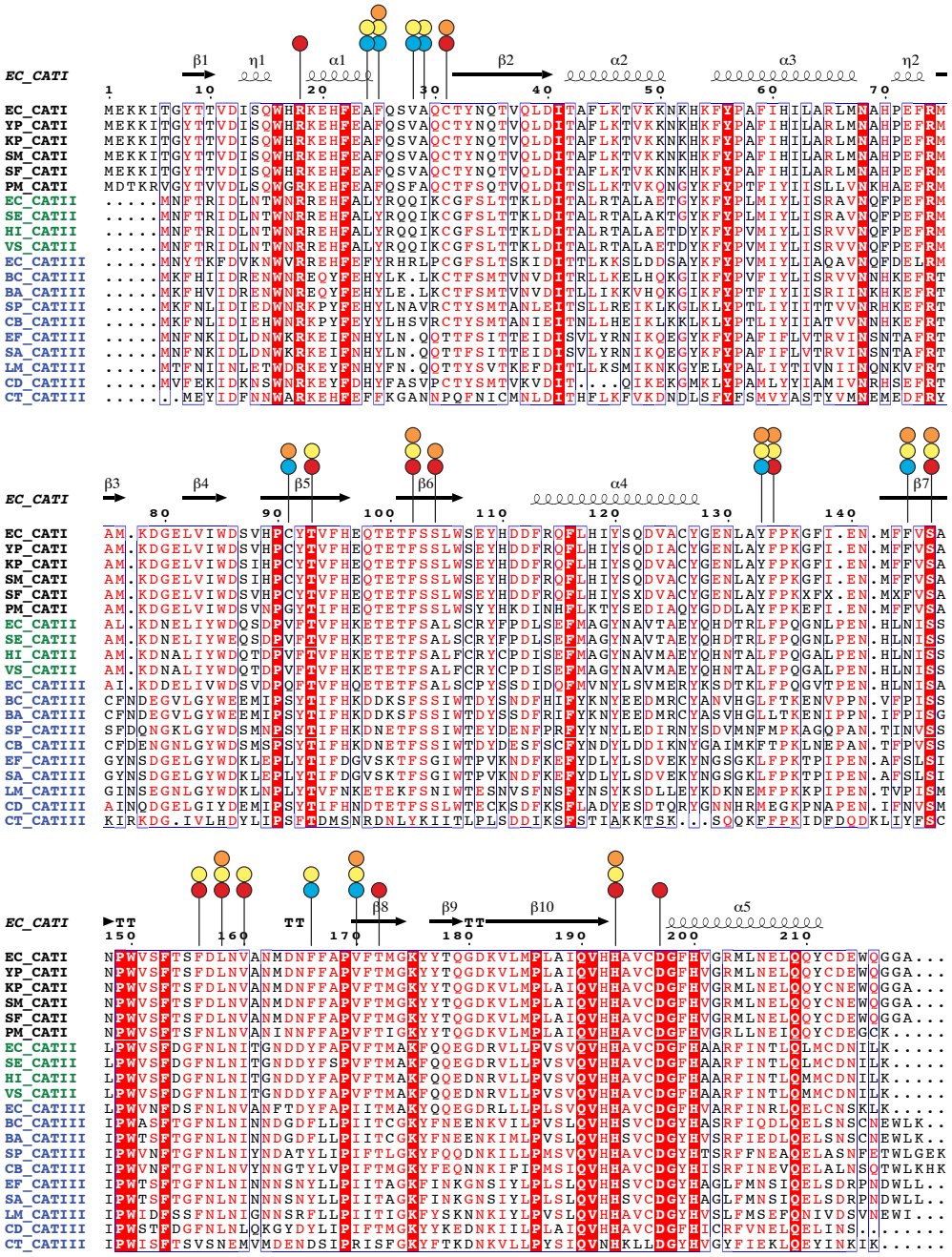

Fig. 5.2. Sequence alignment[13] of CAT_I, CAT_{II}, and CAT_{III} enzymes from various bacteria (EC = *Escherichia coli*, YP = *Yersinia pestis*, KP = *Klebsiella pneumoniae*, SM = *Serratia marcescens*, SF = *Shigella flexneri*, PM = *Proteus mirabilis*, HI = *Haemophilus influenzae*, SE = *Salmonella enterica*, VS = *Vibrio sp.*, BC = *Bacillus cereus*, BA = *Bacillus anthracis*, SP = *Streptococcus pneumoniae*, EF = *Enterococcus faecium*, LM = *Listeria monocytogenes*, SA = *Staphylococcus aureus*, CD = *Clostridium difficile*, CB = *Clostridium botulinum*, and CT = *Clostridium tetani*). Important residues in the active site that are either conserved or non-conserved (vary) between CAT_I and CAT_{III} are indicated by red and blue circles, respectively. Residues involved in CAM and FA binding are marked by orange and yellow circles, respectively.

sequesters it through binding by its CAM binding site. This type of mechanism of resistance through sequestration is not uncommon and has been observed for other antibiotics such as bleomycin and thiocoraline.[14-18] Kinetic studies have shown that FA competes with CAM for binding to CAT_I, but not the other CAT types.[12] Various bile salts and some triphenylmethane dyes also exhibit similar competitive binding to CAT_I, but not to $CAT_{II/III}$.[12,19-21]

CAT_I plays an important role in antibiotic resistance of many pathogenic bacteria. In addition, CAT_I has been used as a biochemical and proteomic tool in a number of systems[22-26] and as a common CAM resistance marker encoded in laboratory plasmids. Despite its importance in drug resistance and biotechnology, CAT_I[27] has been much less investigated than CAT_{III}. Structural and biochemical studies of CAT_{III}[28-34] have been mostly used to understand general features of CAT_I proteins. Despite this progress, differences in the substrate selectivity between CAT_I and CAT_{III} remain unclear in absence of analysis of CAT_I-CAM and CAT_I-FA structures.

Herein we report crystal structures of CAT_I alone and in complex with CAM, which explain how CAT_I binds CAM despite differences in its binding site residues from those in CAT_{III}. Analysis of these structures along with that of the structure of CAT_I in complex with FA (deposited in the Protein Data Bank (PDB) by Roidis and Kokkinidis; accession code: 1Q23[35]) provides an explanation of the differences in substrate preference among CAT types.

5.3. Results

5.3.1. Overall structure of CAT_I

E. coli CAT_I protein was initially co-crystallized with CAM in the P1 space group (Table 5.1). Molecular replacement using either a monomer or trimer of apo-CAT_I (from the structure of a serendipitous complex of the nitric oxide synthase oxygenase domain with CAT_I; PDB code: 1NOC[36]) as a search model did not yield a solution. This complication likely arose due to the presence of several copies of the protein molecules within a very large unit cell. Further crystallization trials yielded crystals of CAT_I alone (the apo form)

in the $P2_1$ space group with a smaller asymmetric unit. These crystals grew under conditions similar to those of CAT_I-CAM crystals. Molecular replacement with a CAT_I trimer from the 1NOC entry as a search model, yielded an apo-CAT_I structure with three CAT_I trimers in the asymmetric unit (Table 5.1). This three-trimer structure was then successfully used as a molecular replacement search model to determine the structure of the CAT_I-CAM complex in the P1 crystal form. The asymmetric unit of the P1 crystal form contained six CAT_I-CAM trimers. The crystal structure of the apo-CAT_I and that of the CAT_I-CAM complex were refined to 3.2 Å and 2.9 Å resolution, respectively (Table 5.1).

Table 5.1. X-ray diffraction data collection and refinement statistics for apo-CAT_I and CAT_I-CAM structures.

	Apo-CAT_I	CAT_I-CAM
Data collection		
Space group	$P2_1$	P1
Number of trimers per asymmetric unit	3	6
Unit cell dimensions		
a, b, c (Å)	115.2, 102.7, 114.1	107.5, 114.5, 114.5
α, β, γ (°)	90, 119.9, 90	119.9, 97.8, 98.7
Resolution (Å)	50.0-3.2 (3.3-3.2)[a]	50.0-2.9 (3.0-2.9)[a]
I/s	9.3 (2.1)	14.3 (2.3)
Completeness (%)	98.4 (86.1)	87.3 (85.0)
Redundancy	4.3 (3.5)	1.7 (1.7)
R_{merge}	0.15 (0.476)	0.06 (0.38)
Number of unique reflections	35,818	82,522
Structure refinement statistics		
Resolution (Å)	40.0-3.2	35.0-2.9
R (%)	23.8	24.0
R_{free} (%)	30.1	30.9
Bond length deviation (rmsd) from ideal (Å)	0.009	0.006
Bond angle deviation (rmsd) from ideal (°)	1.08	0.907
Ramachadran plot statistics[b]		
% of residues in most allowed regions	84.9	88.7
% of residues in additional allowed regions	12.9	10.5
% of residues in generously allowed regions	2.3	0.8
% of residues in disallowed regions	0 (0 residue)	0 (0 residue)

[a] Numbers in parentheses indicate the values in the highest-resolution shell. [b] Indicates Procheck statistics.[37]

The structure of CAT_I in the apo form reported here is very similar to the structure of apo-CAT_I (PDB code: 1NOC) used for the molecular replacement (Ca RMSD = 0.7 Å) and to another previously deposited structure of apo-CAT_I (PDB code: 1PD5; Cα RMSD

= 0.7 Å). Furthermore, the structures of apo-CAT_I are highly similar to the structure of CAT_I in complex with CAM (Cα RMSD ~ 0.4 Å), suggesting that no major protein conformational changes occur upon CAM binding. Analogously, no major conformational differences were observed for CAT_{III} in the apo and the CAM-bound forms.[28] The overall fold and the oligomeric organization of CAT_I (Fig. 5.3A) resemble those of the previously characterized CAT_{III}[28] variant. Three identical monomers of CAT_I form a trimer with a 3-fold rotational symmetry. The overall trimeric scaffold is formed by three 7-stranded β-sheets, each of which is formed by six strands (β6, β5, β7, β9, β10, and β2) from one monomer and one strand (β8) from another monomer (Fig. 5.3B). In each monomer, this β-sheet is flanked on the outside by 5 α-helices and a small 3-stranded β-sheet. In the trimeric core, the aliphatic parts of buried Asp157 side-chains (in strand β8) of the three monomers come together to form intimate hydrophobic contacts with each other while their carboxyl groups are engaged in intricate, asymmetric network of hydrogen bonding interactions with the side-chains of Ser155 and Asn159. The hydrophobic interactions between the Asp157 residues are likely critical for complex stability as this residue is either an Asp or an Asn in most CAT_I/CAT_{III} proteins. Ser155 could however be substituted for a Gly (Fig. 5.2). The side-chains of Asp157 residues are distorted so that the carboxyl groups form hydrogen bonds with their own backbone amide NH moieties justifying a weaker conservation of the Ser155. As the side-chains in these β-strands are generally buried away from the solvent, their identities are well conserved among CAT homologs.

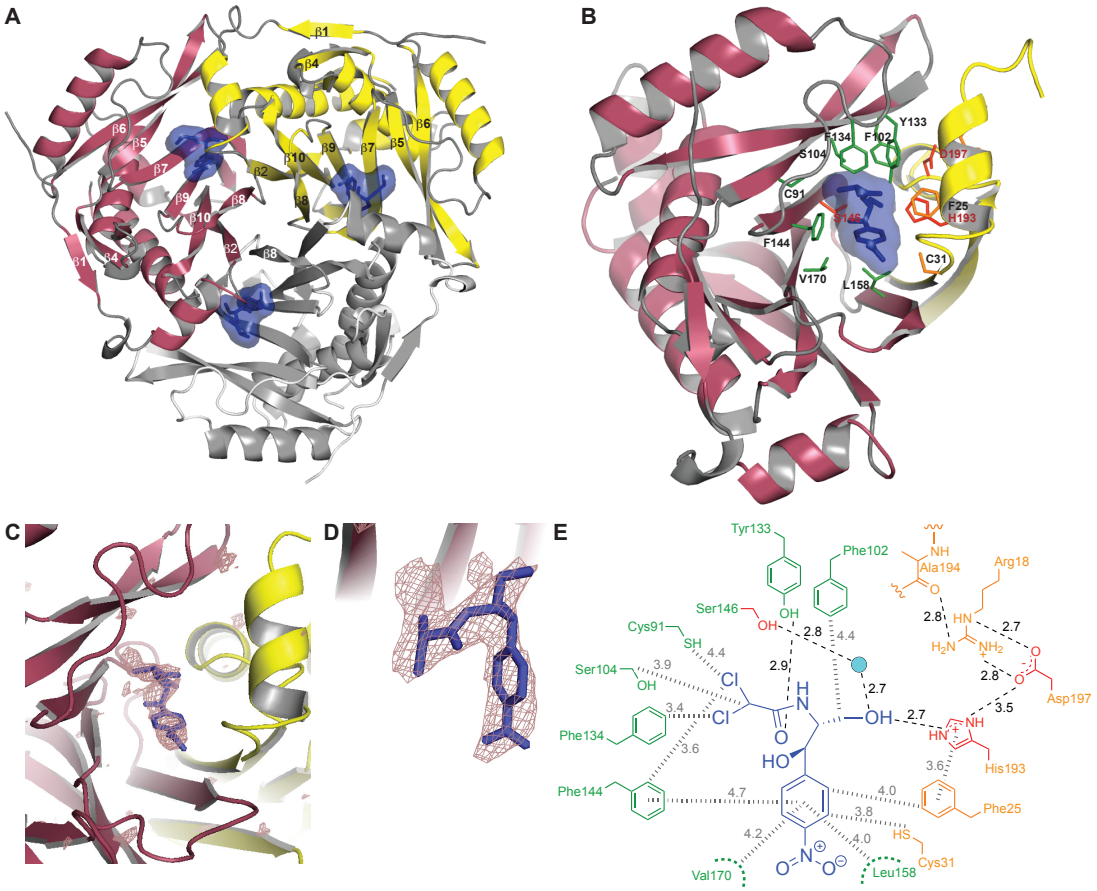

Fig. 5.3. A. Overall fold and trimeric organization of CAM-bound form. The strands of the β-sheets comprising the central scaffold are marked. The CAM molecule and its molecular surface are shown in blue. **B.** A close-up view of the active site at the interface of two monomers in CAT_I-CAM structure. Substrate binding residues of the binding monomer and catalytic monomer are colored in green and orange, respectively. A few highly conserved residues involved in catalysis are marked in red. **C.** A representative view of one of the CAT_I active sites. The violet mesh clearly defining the CAM molecule (blue sticks) is Fo-Fc omit electron density generated without the CAM in the model and contoured at 3σ. **D.** A zoomed in view of the active site shown in panel C, depicted in a slightly different orientation. **E.** A schematic view of residues of the CAT_I active site and their interactions with CAM. Hydrogen bonds and hydrophobic contacts are marked by black dashed lines and the grey hashed lines, respectively. The color coding is consistent with that of panel B.

5.3.2. Chloramphenicol (CAM) interactions in the active site

Upon trimerization, the active site is formed at the interface of two β-sheets predominantly with residues from strands β6, β5, β7, β9, and β8 of one monomer (termed as the binding monomer) and strands β2, and β10 of the other (the catalytic monomer). Each trimer contains three identical substrate binding sites (Fig. 5.3A). The nature of this conserved trimeric assembly strongly suggests that CAT_I monomers either require trimeric assembly for proper folding or, if folded, CAT_I would be catalytically

active only in the context of a trimer. Indeed, monomeric mutants of the CAT_{III}, whose overall fold is highly similar to that of CAT_I, were shown to be catalytically inactive.[38] Below, we discuss features of the active site of CAT_I and highlight its differences from that of CAT_{III} that specify the distinct substrate recognition properties of these two proteins.

In the structure of CAT_I-CAM complex, all three active site pockets of the CAT_I trimer are occupied with CAM molecules (Fig. 5.3A), whose positions are clearly defined in the electron density map (Figs. 3C and 3D). One of the two monomers forming a binding site (called here the binding monomer) provides the majority of the residues (Cys91, Phe102, Ser104, Phe134, Phe144, Ser146, Leu158, and Val170) involved in binding of the CAM while the other one (called here the catalytic monomer) provides His193, which has been demonstrated to be one of the primary conserved catalytic residues[7,39,40] (Fig. 5.3B). A few other residues from the catalytic monomer (Phe25 and Cys31) also provide an important CAM-binding surface in the binding pocket. The disposition of the conserved catalytic residues (*e.g.* His193, Ser146, and Asp197; highlighted in red in Fig. 5.3B) in the CAT_I-CAM structure is highly similar to that observed previously in CAT_{III}-CAM complex.[41] The position of His193, the likely general base, relative to the bound CAM is identical to its counterpart in CAT_{III} (His195). The Nε2 atom of His193 is located 2.7 Å away from the 3-hydroxyl of CAM (Fig. 5.3E). The side-chain of His193 is in a distorted conformation (His193 χ_1 = -150.2° and χ_2 = -41.0° with CAM bound and χ_1 = -142.0° and χ_2 = -32.6° with FA bound). This conformation likely ensures that the imidazole ring is aligned appropriately for abstracting the 3-hydroxyl proton of CAM, promoting a nucleophilic attack by the oxygen on the acetyl group carbonyl of AcCoA,[29,30,34] similarly to the proposed mechanism of the CAT_{III} variant.[40] The imidazole ring of His193 is positioned at a proper distance (approximately 3.6 Å) for a face-to-face π-π stacking contact with Phe25. This overall structural arrangement of the catalytic monomer for proper positioning of His193 at the subunit interface is stabilized by several interactions that include a chain of hydrogen bonds between His193, Asp197, Arg18, and the backbone carbonyl oxygen of Ala194 (Fig. 5.3E). The conserved Ser146 (another catalytically important residue) of CAT_I is positioned similarly in the active site of all

three CAT_I structures, and likely stabilizes the transition state oxyanion by donating a hydrogen bond (possibly water-mediated in CAT_I), as proposed for Ser148 of CAT_{III}.[42]

The sequence alignment of CAT_I and CAT_{III} from *E. coli* demonstrates that out of the 20 amino acid residues lining the CAM binding site, 9 are different between the two types (Fig. 5.2, blue circles). These differences [Ala24 (CAT_{III}, Phe24), Phe25 (CAT_{III}, Tyr25), Ala29 (CAT_{III}, Leu29), Cys91 (CAT_{III}, Gln92), Tyr133 (CAT_{III}, Leu134), Phe144 (CAT_{III}, Asn146), Phe166 (CAT_{III}, Tyr168), and Val170 (CAT_{III}, Ile172)] are significant as they include changes in the size and hydrophobicity of the residues. Remarkably, despite these differences, CAM binding affinities for CAT_I and CAT_{III} appear to be very similar.[43] Furthermore, the superposition of CAT_I-CAM and CAT_{III}-CAM structures demonstrates that the orientations of the CAM molecule in the active sites of the two proteins are nearly identical. The *p*-NO_2 group of CAM is solvent exposed when bound in the CAT_I active site and the aromatic ring rests on the hydrophobic surface provided primarily by Leu158 and Val170, as observed in the CAT_{III}-CAM structure. The side-chains of Leu158, Val160, and Phe166 that line the very bottom of the substrate binding pocket (Fig. 5.4C) are positioned through interactions of the trimeric assembly and show only minor alterations between CAT_I and CAT_{III}. The dichloroacetyl moiety of CAM closely interacts with Phe134 (Phe135 in CAT_{III}), likely indicating a strong hydrophobic interaction. A major difference between the CAT_I-CAM and CAT_{III}-CAM structures is that the residue analogous to Tyr133 of CAT_I is non-polar (Leu134) in CAT_{III}. Tyr133 forms a strong hydrogen bond (2.9 Å) with the carbonyl group of CAM. Interestingly, this interaction occurs in place of the interaction of that between the hydroxyl of Tyr25 in CAT_{III} (Phe25 in CAT_I) and the carbonyl group of CAM, located at an O-O distance of 2.8 Å from each other.

5.3.3. Fusidic acid (FA) interactions in the active site

In the CAT_I-FA complex (Fig. 5.4A), FA occupies the same binding site as CAM, which explains its observed behavior as a competitive inhibitor of CAM acetylation.[12] The differences between the active site residues of CAT_I (as described above) and those of CAT_{III} while having little effect on CAM binding,[41,44] create a unique surface suitable for

binding to FA in CAT_I. In particular, the placement of Ala24 and Ala29 of CAT_I shapes the substrate binding cavity such that the ring D and the 2-methylhex-2-ene "tail" of FA can be accommodated. The hydrophobic steroid ring system of FA makes numerous hydrophobic contacts with active site residues, including Thr93, Phe102, Phe134, Phe144, Ser146, Phe156, Leu158, Val160, Phe166, and Val170 of the binding subunit, as well as Ala24, Phe25, Val28, and Ala29 of the catalytic subunit (Figs. 4A and 4C). The hydroxyl moiety of ring A of FA closely aligns with the 3-hydroxyl of CAM and forms a very strong hydrogen bond the Nε2 atom of His193 at a distance of 2.9 Å (Fig. 5.4C). The hydroxyl group of Tyr133 points inward towards the binding pocket forming a hydrogen bond with the hydroxyl moiety of ring C, the atoms being separated by a distance of about 2.6 Å (Fig. 5.4C), similarly to the interaction between the 3-hydroxyl and Tyr133 in the CAT_I-CAM structure (Fig. 5.3E). Residues from both the binding monomer (Phe134) and the catalytic monomer (Ala24 and Val28) form a hydrophobic zone near the entrance of the binding pocket in CAT_I that cradle the "tail" section of FA and dictate its conformation (Figs. 4A and 4C).

Valuable insight can be gained by comparing this structure with the previously reported structures of a CAT_{III} in complex with CAM[29] and a quadruple mutant of CAT_{III} in complex with FA.[43] In the quadruple mutant of CAT_{III}, four catalytic pocket residues were mutated (Gln92Cys/Asn146Phe/Tyr168Phe/Ile172Val) to mimic those of CAT_I. This comparison (Fig. 5.4B) indicates a disruption of the FA tail-interacting hydrophobic zone in the quadruple mutant of CAT_{III}, in particular due to the Ala24Phe and Val28Arg substitutions. The carboxylic acid and acetoxy moieties of ring D are highly solvent exposed when bound to both CAT_I and the CAT_{III} mutant. The acetoxy group of FA makes a hydrophobic contact with Phe166 in CAT_I (Phe168 in CAT_{III}) (Figs. 4C and 4D). Despite the same general protein backbone scaffold of CAT_I and the mutant CAT_{III} structures, there are several differences in the FA-protein contacts for the two enzymes. Most strikingly, several bulkier residues of CAT_{III}: Phe24 (Ala24 in CAT_I), Tyr25 (Phe25 in CAT_I), Arg28 (Val28 in CAT_I), and Leu29 (Ala29 in CAT_I) prevent the FA molecule from binding in a position similar to that in CAT_I. A required shift of the FA molecule must not be accommodated due to structural rigidity of wild-type CAT_{III} resulting in the

lack of binding to FA. The mutations of the CAT_{III} quadruple mutant apparently relax this rigidity, and surprisingly accommodate the FA molecule in a very different position from that seen in the CAT_I-FA structure and in an altered conformation. The hydrophobic "tail" of FA now adopts a very different conformation and gets buried in the disordered loop region (residues 138-141) of the CAT_{III} mutant. This disorder is very likely due to both the Asn146Phe and the Gln92Cys substitutions in the CAT_{III} mutant, which cause displacement of the His144 and Thr140 side-chains, respectively, thereby distorting of the local backbone. This displacement allows the FA-tail to occupy its altered position in CAT_{III} mutant.[43] Notably, Tyr25 in the CAT_{III} quadruple mutant structure (positionally analogous to Phe25 of CAT_I) forms hydrogen bond with FA, at a distance of 2.8 Å to the hydroxyl on the A-ring (Fig. 5.4D), and stabilize the altered FA orientation. Phe168 and Val172 residues in the CAT_{III} quadruple mutant make direct hydrophobic contacts with the FA molecule, which explains the contribution of these substitutions to the change in binding affinity to FA.[43]

We observe no major differences in the backbone conformations near the active site of CAT_I in the structures of apo-CAT_I (PDB code: 3U9B), CAT_I bound to CAM (PDB code: 3U9F), and CAT_I bound to FA (PDB code: 1Q23[35]). This strongly suggests that CAT_I has evolved to bind multiple ligands, even as large as an FA molecule, without any major protein conformational changes in its backbone.

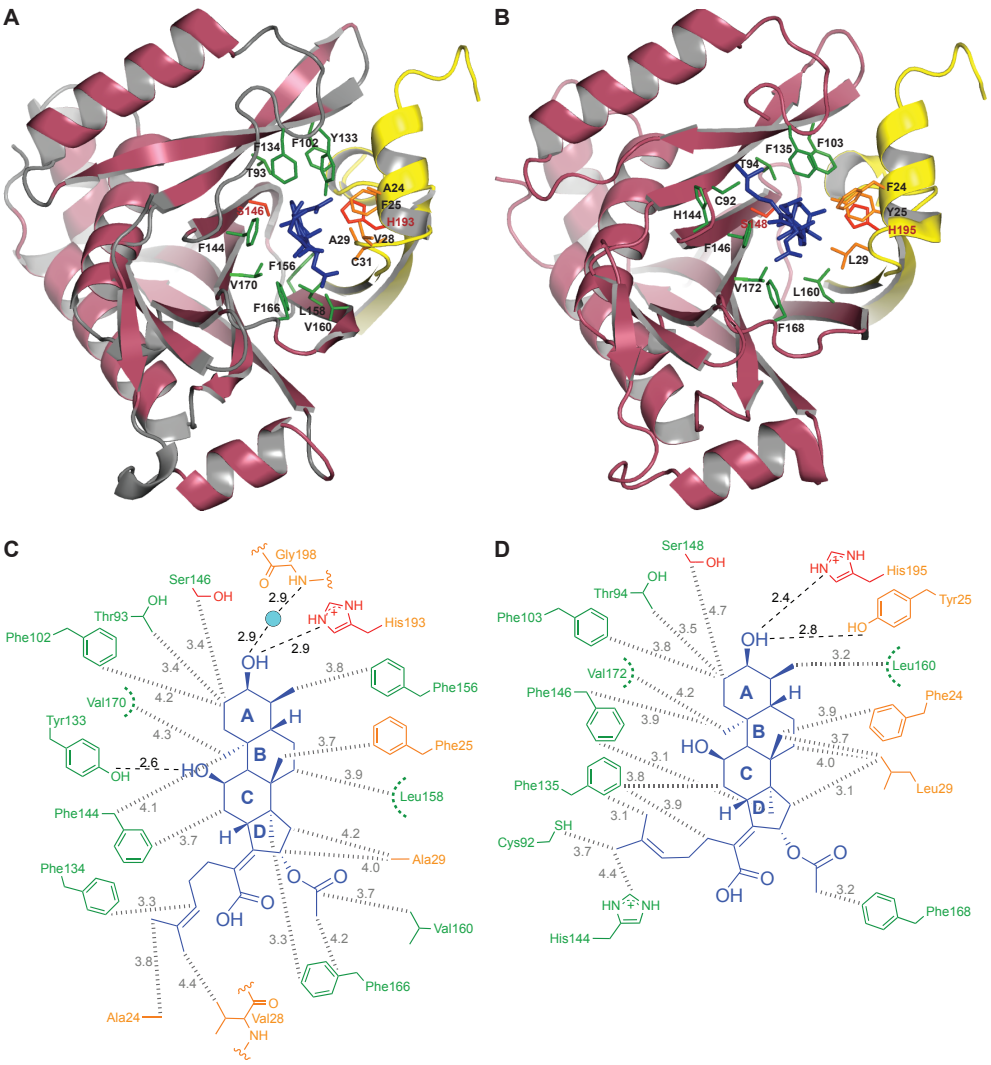

Fig.5.4. A. Close-up views of interactions of FA with active-site residues of CAT_I and **B.** Close-up views of interactions of FA with active-site residues of CAT_{III} (quadruple mutant). **C.** Schematic views of interactions of FA with CAT_I. **D.** Schematic views of interactions of FA with CAT_{III} (quadruple mutant). The color coding is consistent with that of Fig.5.3. (FA is shown in blue).

5.4. Discussion

Chloramphenicol acetyltransferase (CAT) is found in many pathogenic bacteria and is often the cause of resistance against chloramphenicol (CAM), once a widely used antibiotic. Of many known CATs, the type-I appears to be the most prevalent. Recent studies have found CAT_I in many pathogenic bacteria. CAT_I has a preference for binding to a variety of substrates; not only does it inactivate chloramphenicol but it also binds and sequesters other antibiotics such as FA. A clear understanding of the mechanism of

substrate binding by CAT_I is important to address the intriguing question of how CAT proteins from different classes with similar overall structures display different substrate selectivity profiles. In comparison to CAT_{III} that has been studied almost exclusively, there are only few mechanistic studies that have been performed on CAT_I.

The general fold and the trimeric organization of CAT proteins have been observed in enzymes of primary metabolic pathways in bacteria and eukaryotes, such as pyruvate dehydrogenases[45,46] and a-keto acid dehydrogenases.[47,48] Therefore, CAT appears to be a product of an ancient gene duplication event, which underwent subsequent specialization through evolution to serve a protective role against toxic compounds such as CAM. The general catalytic mechanism proposed for CAT proteins is based on studies of many such proteins. The residue primarily responsible for catalysis of CAT_I appears to be His193 (His195 in CAT_{III}).[28] This role was proposed based on a previous study in which a mutant (His195Tyr) CAT_{III} was shown to be devoid of catalytic activity.[49] Another conserved residue, Ser146, likely stabilizes the oxyanion formed upon an attack on the AcCoA carbonyl carbon by the 3-hydroxyl of CAM. Mutagenesis studies with CAT_{III} confirmed that Ser148 (Ser146 in CAT_I) is crucial for efficient catalysis.[42]

The CAT_I protein structure is similar in the apo form and in CAM- and FA-bound states, indicating that no major changes in the backbone conformations or in positions of the side-chains occur upon ligand binding. It is quite remarkable that such a nearly rigid scaffold is evolutionary conserved and yet CAT_I can bind chemically diverse substrates. Analysis of the aligned sequences shows that several residues of CAT_I are different than corresponding residues in CAT_{III}. Our investigation of the CAT_I structures indicates that many of these differences are in residues lining the substrate binding pocket (Fig. 5.2, blue circles). The most striking differences are concentrated around a small patch of residues (Ala24-Cys31, contributed by the catalytic monomer) that enable the FA molecule to be accommodated only in the pocket of CAT_I. The bulkier residues of CAT_{III} at this patch would push the FA towards the opposite side of the pocket and consequently disrupt the structure. Interestingly, the flexibility (apparently resulting in the reduced rigidity and increased disorder of the backbone) of the quadruple mutant of CAT_{III} helps

it accommodate the pushed out FA in a different conformation. The "tail" of FA now finds a different hydrophobic pocket to rest in and in turn provides stability to the FA in this altered binding pocket. The mutant CAT_{III} shows a 200-fold higher affinity to FA than the wild-type CAT_{III}. However, the quadruple mutant of CAT_{III} binds FA with a much (4-fold) weaker affinity[43] than CAT_I. In addition, the K_m for CAM acetylation by the CAT_{III} quadruple mutant was somewhat compromised (with respect to either CAT_I or CAT_{III}) and the value of k_{cat} was between those for CAT_{III} and CAT_I. With the direct structural evidence, it is now clear how the tail of FA nests in a hydrophobic pocket and renders CAT_I more energetically favorable to bind to FA. In CAT_{III}, a similarly positioned FA "tail" would get sterically blocked by Phe24 and Arg28, and it is not surprising that CAT_{III} does not show affinity towards FA.

Our understanding of CAM's mechanism of action as well as the mechanisms of resistance to it were largely based on biochemical and structural information available on CAM binding to CAT_{III} and to the bacterial ribosome.[4] The present structural study augments this knowledge by filling in the gap in our understanding of the recognition of both CAM and FA by CAT_I. CAM has been largely removed from the clinic in the Western world due to its safety concerns, even though cases of extreme toxicity are exceedingly rare. CAM has remained a popular drug in underdeveloped areas due to its low cost and effectiveness against a variety of pathogens. However, as with other antibiotics, development of resistance against CAM is a major obstacle to its power in saving lives. The detailed picture of CAT_I structure is expected to aid in design of inhibitors of CAT enzymes that could re-sensitize CAM-resistant strains. In addition, structure-guided design of CAM analogs could lead to new antibiotics of this class that would be less toxic and more refractory to inactivation by CAT.

5.5. Materials and Methods

5.5.1. Expression and purification of CAT_I

CAT_I was expressed in BL21 (DE3)/RIL cells (Stratagene), which harbor a plasmid containing a constitutively expressed CAM resistance gene *camR* encoding untagged CAT_I protein. The cells were grown in LB medium (200 rpm, 37 °C) containing CAM

(25 μg/mL) until the culture reached the attenuance of 0.4 at 600 nm. The cells were harvested after an additional 3 h growth. Pelleted cells (centrifugation at 5,000 g, 10 min, 4 °C) were resuspended in the lysis buffer [MES pH 6.5 (40 mM), NaCl (200 mM), glycerol (5%), β-mercaptoethanol (2 mM), and EDTA (0.1 mM)] and lysed by sonication. The lysate was clarified by centrifugation at 35,000 × g for 45 min at 4 °C. We took advantage of the thermostability of CAT proteins[50] in purifying CAT_I without an affinity tag. The clarified lysate was heated (75 °C, 20 min) and subsequently centrifuged (35,000 × g, 45 min, 4 °C) to remove unfolded precipitated proteins. The CAT_I in the soluble fraction was further purified by size-exclusion chromatography on an S-200 column (GE Healthcare) equilibrated with buffer [Tris pH 8.0 (40 mM) and NaCl (100 mM)]. The fractions containing pure CAT_I, as determined by SDS-PAGE, were concentrated to 5 mg/mL by using an Amicon Ultra centrifugal filter device (Millipore) and used for crystallization.

5.5.2. Crystallization of CAT_I alone and in complex with CAM

Crystals of CAT_I alone and a complex of CAT_I with CAM (CAT_I-CAM) were grown by vapor diffusion in hanging drops containing 1 μL of protein and 1 μL of the reservoir solution [HEPES (100 mM) pH 7.5 (pH of 1 M stock of HEPES acid was adjusted by adding NaOH), PEG 4,000 (20% w/v), isopropanol (10% v/v)] or 1 μL of the reservoir solution containing CAM (1 mM), respectively. Irregularly shaped crystals, 40-60 mm in each of the three dimensions were formed in 7-10 days when incubated at 22 °C against the respective reservoir solutions. The crystals were gradually transferred into the reservoir solution containing glycerol (15% v/v) and flash frozen in liquid nitrogen.

5.5.3. Data collection and structure determination

X-ray diffraction data were collected at 100 K at the X25 beamline of the National Light Source at the Brookhaven National Laboratory. The data were processed with HKL2000.[51] The crystals of apo-CAT_I and CAT_I-CAM complex were in the $P2_1$ and P1 space groups, respectively. The structures of both apo-CAT_I and CAT_I-CAM complex were determined by molecular replacement with MOLREP[52] as described in Results. The locations of the CAM molecules in the active sites of CAT_I were clearly identified and

positioned in the omit Fo-Fc density and then refined. The structures were iteratively manually built and refined using programs Coot[53] and REFMAC,[54] respectively. The data collection and refinement statistics are given in Table 5.1. The structures of apo-CAT_I and CAT_I-CAM complex were deposited in the Protein Data Bank with accession codes 3U9B and 3U9F, respectively.

5.6. References

(1) Carter, H. E.; Gottlieb, D.; Anderson, H. W. *Science* **1948**, *107*, 113.
(2) Skolimowski, I. M.; Knight, R. C.; Edwards, D. I. *J Antimicrob Chemother* **1983**, *12*, 535.
(3) Nitzan, O.; Suponitzky, U.; Kennes, Y.; Chazan, B.; Raul, R.; Colodner, R. *Isr Med Assoc J* **2010**, *12*, 371.
(4) Dunkle, J. A.; Xiong, L.; Mankin, A. S.; Cate, J. H. *Proc Natl Acad Sci U S A* **2010**, *107*, 17152.
(5) Bulkley, D.; Innis, C. A.; Blaha, G.; Steitz, T. A. *Proc Natl Acad Sci U S A* **2010**, *107*, 17158.
(6) Shaw, W. V. *J Biol Chem* **1967**, *242*, 687.
(7) Kleanthous, C.; Shaw, W. V. *Biochem J* **1984**, *223*, 211.
(8) Thibault, G.; Guitard, M.; Daigneault, R. *Biochim Biophys Acta* **1980**, *614*, 339.
(9) Shaw, W. V.; Unowsky, J. *J Bacteriol* **1968**, *95*, 1976.
(10) Murray, I. A.; Martinez-Suarez, J. V.; Close, T. J.; Shaw, W. V. *Biochem J* **1990**, *272*, 505.
(11) Lewendon, A.; Shaw, W. V. *Biochem J* **1990**, *272*, 499.
(12) Bennett, A. D.; Shaw, W. V. *Biochem J* **1983**, *215*, 29.
(13) Corpet, F. *Nucleic acids research* **1988**, *16*, 10881.
(14) Gatignol, A.; Durand, H.; Tiraby, G. *FEBS Lett* **1988**, *230*, 171.
(15) Dumas, P.; Bergdoll, M.; Cagnon, C.; Masson, J. M. *EMBO J* **1994**, *13*, 2483.
(16) Kawano, Y.; Kumagai, T.; Muta, K.; Matoba, Y.; Davies, J.; Sugiyama, M. *J Mol Biol* **2000**, *295*, 915.
(17) Maruyama, M.; Kumagai, T.; Matoba, Y.; Hayashida, M.; Fujii, T.; Hata, Y.; Sugiyama, M. *J Biol Chem* **2001**, *276*, 9992.
(18) Biswas, T.; Zolova, O. E.; Lombo, F.; de la Calle, F.; Salas, J. A.; Tsodikov, O. V.; Garneau-Tsodikova, S. *J Mol Biol* **2010**, *397*, 495.
(19) Proctor, G. N.; McKell, J.; Rownd, R. H. *J Bacteriol* **1983**, *155*, 937.
(20) Tanaka, H.; Izaki, K.; Takahashi, H. *J Biochem* **1974**, *76*, 1009.
(21) Volker, T. A.; Iida, S.; Bickle, T. A. *J Mol Biol* **1982**, *154*, 417.
(22) Russ, W. P.; Engelman, D. M. *Proc Natl Acad Sci U S A* **1999**, *96*, 863.
(23) Li, Z.; He, L.; He, N.; Deng, Y.; Shi, Z.; Wang, H.; Li, S.; Liu, H.; Wang, Z.; Wang, D. *J Nanosci Nanotechnol* **2011**, *11*, 1074.
(24) King, D. A.; Hall, B. E.; Iwamoto, M. A.; Win, K. Z.; Chang, J. F.; Ellenberger, T. *J Biol Chem* **2006**, *281*, 20107.
(25) Speck, J.; Stebel, S. C.; Arndt, K. M.; Muller, K. M. *Methods Mol Biol* **2011**, *687*, 333.
(26) Li, W.; Ruf, S.; Bock, R. *Plant Mol Biol* **2010**.
(27) Van der Schueren, J.; Robben, J.; Goossens, K.; Heremans, K.; Volckaert, G. *J Mol Biol* **1996**, *256*, 878.
(28) Leslie, A. G. *J Mol Biol* **1990**, *213*, 167.
(29) Leslie, A. G.; Moody, P. C.; Shaw, W. V. *Proc Natl Acad Sci U S A* **1988**, *85*, 4133.
(30) Day, P. J.; Shaw, W. V.; Gibbs, M. R.; Leslie, A. G. *Biochemistry* **1992**, *31*, 4198.

(31) Barsukov, I. L.; Lian, L. Y.; Ellis, J.; Sze, K. H.; Shaw, W. V.; Roberts, G. C. *J Mol Biol* **1996**, *262*, 543.
(32) Ellis, J.; Bagshaw, C. R.; Shaw, W. V. *Biochemistry* **1995**, *34*, 16852.
(33) Gibbs, M. R.; Moody, P. C.; Leslie, A. G. *Biochemistry* **1990**, *29*, 11261.
(34) Day, P. J.; Shaw, W. V. *The Journal of biological chemistry* **1992**, *267*, 5122.
(35) Berman, H. M.; Westbrook, J.; Feng, Z.; Gilliland, G.; Bhat, T. N.; Weissig, H.; Shindyalov, I. N.; Bourne, P. E. *Nucleic Acids Res* **2000**, *28*, 235.
(36) Crane, B. R.; Arvai, A. S.; Gachhui, R.; Wu, C.; Ghosh, D. K.; Getzoff, E. D.; Stuehr, D. J.; Tainer, J. A. *Science* **1997**, *278*, 425.
(37) Laskowski, R. A.; Macarthur, M. W.; Moss, D. S.; Thornton, J. M. *Journal of Applied Crystallography* **1993**, *26*, 283.
(38) Shaw, W. V.; Bentley, D. W.; Sands, L. *J Bacteriol* **1970**, *104*, 1095.
(39) Kleanthous, C.; Cullis, P. M.; Shaw, W. V. *Biochemistry* **1985**, *24*, 5307.
(40) Murray, I. A.; Lewendon, A.; Shaw, W. V. *J Biol Chem* **1991**, *266*, 11695.
(41) Lewendon, A.; Murray, I. A.; Kleanthous, C.; Cullis, P. M.; Shaw, W. V. *Biochemistry* **1988**, *27*, 7385.
(42) Lewendon, A.; Murray, I. A.; Shaw, W. V.; Gibbs, M. R.; Leslie, A. G. *Biochemistry* **1990**, *29*, 2075.
(43) Murray, I. A.; Cann, P. A.; Day, P. J.; Derrick, J. P.; Sutcliffe, M. J.; Shaw, W. V.; Leslie, A. G. *J Mol Biol* **1995**, *254*, 993.
(44) Murray, I. A.; Lewendon, A.; Williams, J. A.; Cullis, P. M.; Lashford, A. G.; Shaw, W. V. *Nucleic acids research* **1991**, *19*, 6648.
(45) Patel, M. S.; Roche, T. E. *FASEB J* **1990**, *4*, 3224.
(46) de Kok, A.; Hengeveld, A. F.; Martin, A.; Westphal, A. H. *Biochim Biophys Acta* **1998**, *1385*, 353.
(47) Meng, M.; Chuang, D. T. *Biochemistry* **1994**, *33*, 12879.
(48) Langley, D.; Guest, J. R. *J Gen Microbiol* **1978**, *106*, 103.
(49) Burns, D. K.; Crowl, R. M. *Protein structure, folding and design 2, UCLA Symposium of molecular and cellular biology*; A.R. Liss & Co. : New York, 1987; Vol. 69.
(50) Shaw, W. V.; Brodsky, R. F. *J Bacteriol* **1968**, *95*, 28.
(51) Otwinowski, Z.; Minor, W. In *Methods in Enzymology, Macromolecular Crystallography, part A*; C.W. Carter, J. R. M. S., Eds. , Ed.; Academic Press: New York, 1997; Vol. 276, p 307.
(52) Vagin, A.; Teplyakov, A. *Journal of Applied Crystallography* **1997**, *30*, 1022.
(53) Emsley, P.; Cowtan, K. *Acta Crystallogr D Biol Crystallogr* **2004**, *60*, 2126.
(54) Murshudov, G. N.; Vagin, A. A.; Dodson, E. J. *Acta Crystallogr D Biol Crystallogr* **1997**, *53*, 240.

Note:
This chapter is adapted from a published article: Biswas, T.; **Houghton, J. L.**; Tsodikov, O. V.; Garneau-Tsodikova, S. *Protein Sci* **2012**, *21*, 520.

Authors' contribution:
OVT purified CAT_I and OVT and TB determined its structure in the apo form and in complex with CAM.
JLH, TB, OVT, and SGT analyzed the data and wrote the manuscript.

Chapter 6

Future directions

It has been shown that Eis from *Mtb* demonstrates unprecedented activity as an AAC, performing multiple acetylations of numerous AGs. During my time studying Eis in the Garneau-Tsodikova laboratory, we have described several new surprising findings with respect to Eis: (1) the multiple acetylations by Eis may occur in a sequential or non-sequential manner, depending on the AG, (2) Eis acetylates AGs at positions not acetylated by other AACs, including the AHB and 3"-position, and (3) Eis is capable of acetylating non-AG drugs, such as CAP. Further research towards understanding Eis could follow any number of courses, as there is still relatively little known about this important protein from *Mtb*.

First, the structural characteristics that lend Eis its vast substrate promiscuity should be investigated, with the aim to understand and overcome the resistance conferred against AGs. Further developing our NMR methodology so that we can follow the reaction progress of the non-sequentially modified AGs in real time by NMR could provide crucial information about Eis' interaction with the various, diverse scaffolds comprising this important family of antibiotics. In the cases of reactions that do not occur sequentially, quantitative kinetics experiments to compare the rate of reaction at each amine using our current biochemical assays would be impossible. However, NMR experiments would allow us to follow the modification of each specific amine in real time. These studies of the acetylation of AGs by Eis_*Mtb* could help in the development of novel AG analogs that avoid modification, by providing a type of structure activity relationship. This could be aided by expanding our knowledge of the positions acetylated by Eis on all its known AG substrates, all of which are acetylated at multiple positions.

We have developed methodology that allows us to utilize the cosubstrate promiscuity of AACs to generate libraries of compounds to test the activity of AGs with functionalized acyl groups that have been incorporated at specific positions. Extending this methodology to the novel positions that may be acetylated by Eis_*Mtb* would be very useful in determining if additional positions may be modified with functionalized acyl groups to improve antibacterial activity while avoiding the deactivation by AMEs. Since Eis may non-sequentially acetylate multiple positions of a given AG, the investigation of multiply acetylated compounds would also be possible, perhaps without reliance on the sequential application of multiple AACs. Similarly, the application of an AAC other than Eis that may acylate a single position with reliable regio-selectivity followed by acylation by Eis using either the same or a different functionalized acyl group would allow us to generate extremely diverse libraries of acylated AGs to screen for activity. We have reported that Eis_*Mtb* is, when compared to the AACs used in our previous experiments, not highly cosubstrate promiscuous, so, before this strategy may realize its full potential, it will be necessary to expand Eis' cosubstrate promiscuity *via* site-directed mutagenesis. Studies to this affect are currently underway in our laboratory.

There are a number of homologous Eis proteins identified in species of mycobacteria, and our laboratory has reported preliminary studies of the Eis from *Msm*. The systematic characterization of these Eis homologs is currently underway in our laboratory. Efforts should focus on the identification of Eis enzymes that show increased cosubstrate promiscuity for two reasons. First, we could apply them in our efforts to chemoenzymatically generate novel AGs for antibacterial activity screening. Second, we could use the differences in the binding pockets to identify which amino acid residues may be mutated to retain activity while expanding on the cosubstrate promiscuity.

Additional investigations with CAP, including studies of the Eis catalyzed acetylation of the β-lysine side chain, could provide valuable information. It was noted, in Chapter 2, that previous studies of the Eis proteins from *Mtb* and *Msm* have shown that the Eis from each strain modifies a different amine on the Lys55 of DUSP16/MPK-7. The activity of Eis_*Msm* towards CAP has not been thoroughly studied, and it would be interesting to

see if the terminal amine of the β-lysine side chain is modified or if it is the β-amine that is acetylated. Furthermore, since the ability of Eis_*Mtb* to confer resistance to CAP *via* acetylation has not been conclusively disproved, the synthesis and determination of the MIC values of Ac-CAP compounds (separately mono-acetylated at either amine) against strains of mycobacteria could provide a more definitive answer.

The synthesis of AGs with functionalized acyl groups, particularly those modified with a glycinyl or AHB group, has shown to be a very promising strategy in our ability to combat the rapid development of resistance described herein. These problems are in no way specific to AGs and CAM and it is certain that as long as antibacterial treatments are used, resistance will develop. The screening methodology described above will aid in the rapid identification of novel, active compounds; however, once identified, those compounds will need to be synthesized on a larger scale for testing against numerous bacterial strains. Strategies for the facile protection and deprotection of amines other than the 6'- and 1-position on the various AG scaffold should be the primary focus of these efforts.

Although CAM is not currently used for the treatment of systemic infections in the United States, it remains an important drug in many other countries because it is relatively cheap and extremely effective. The need for effective drugs is being amplified by the rapid development of resistance, so the development of novel CAM analogs is still a worthwhile endeavor. Significant research into CAM analogs was performed in the past, yet advances in drug development technology and our increased understanding of structure and function of CAM resistance proteins, should allow this process to be more expedient and precise than was previously possible. Structure activity relationships could now be predicted with some accuracy based on crystallographic data of CAM with its ribosomal target as well as with resistance enzymes. Furthermore, understanding of the genetic predisposition that leads to CAM toxicity is more easily identified than when CAM was withdrawn from many markets, meaning some of the serious toxicity issues could likely be avoided *ab initio*.